The University of Maine
DigitalCommons@UMaine

Electronic Theses and Dissertations | Fogler Library

Summer 8-16-2024

# Modeling the Innate Immune Response to Influenza a Virus Infection Using the Zebrafish

Brandy-Lee Soos
*University of Maine*, brandylee.dennis@maine.edu

Follow this and additional works at: https://digitalcommons.library.umaine.edu/etd

Part of the Immunology and Infectious Disease Commons

## Recommended Citation

Soos, Brandy-Lee, "Modeling the Innate Immune Response to Influenza a Virus Infection Using the Zebrafish" (2024). *Electronic Theses and Dissertations*. 4064.
https://digitalcommons.library.umaine.edu/etd/4064

This Open-Access Dissertation is brought to you for free and open access by DigitalCommons@UMaine. It has been accepted for inclusion in Electronic Theses and Dissertations by an authorized administrator of DigitalCommons@UMaine. For more information, please contact um.library.technical.services@maine.edu.

# MODELING THE INNATE IMMUNE RESPONSE TO INFLUENZA A VIRUS INFECTION USING THE ZEBRAFISH

By

Brandy-Lee A. Soos

B.S. Rochester Institute of Technology, 2012

A DISSERTATION

Submitted in Partial Fulfillment of the

Requirements for Degree of Doctor of Philosophy

(in Molecular and Biomedical Sciences)

The Graduate School

The University of Maine

August 2024

Advisory Committee:

Benjamin L. King, Associate Professor of Bioinformatics, Advisor

Melody N. Neely, Associate Professor and Chair, Molecular and Biomedical Sciences

Deborah Bouchard, Associate Extension Professor, Director, Aquaculture Research Institute,

Clarissa Henry, Professor of Biological Sciences

Joshua Kelley, Associate Professor of Biochemistry

© 2024 Brandy-Lee A. Soos

# MODELING THE INNATE IMMUNE RESPONSE TO INFLUENZA A VIRUS INFECTION USING THE ZEBRAFISH

By Brandy-Lee A. Soos

Dissertation Advisor: Dr. Benjamin L. King

An Abstract of the Dissertation Presented
in Partial Fulfillment of the Requirements for the
Degree of Doctor of Philosophy
(in Molecular and Biomedical Sciences)
August 2024

## ABSTRACT

Influenza causes 9-41 million illnesses yearly in the U.S. Our research explores innate immune responses to the virus, leveraging zebrafish larvae as models due to their immature adaptive immunity. We developed the Color-flu model, allowing real-time visualization of IAV infections and immune responses. Neutrophils, crucial for innate immunity, exhibit complex roles in antiviral responses; infection triggers inflammation and reactive oxygen species (ROS) production, which can lead to hyperinflammation if dysregulated. We hypothesize that optimizing neutrophil ROS can enhance IAV clearance while minimizing tissue damage. Our study uses genetic and pharmacological methods to assess the effects on survival, viral burden, and neutrophil behavior. Chapter 2 reviews IAV, ROS, and zebrafish models. Chapter 3 introduces Color-flu, enabling in vivo drug influence studies. Chapter 4 examines neutrophils' dual roles, finding that altering their levels is harmful. Chapter 5 focuses on ROS modulation, identifying it as key to managing hyperinflammation. Chapter 6 discusses future Color-flu projects and concludes the thesis.

# ACKNOWLEDGEMENTS

I want to thank Dr. Ben King, my advisor, for his support, guidance, coffee, and crazy brain-storming sessions throughout my doctoral research. You kept your promise after Carol left, so thank you. I would also like to thank my dissertation committee members, Drs. Debbie Bouchard, Clarissa Henry, Josh Kelley, and Melody Neely for their input on my research, ability to answer my incessant questions, and patience regarding the writing process. I would like to thank current and past members of the King Lab for their help, friendship, and support: Kodey Silknitter, Emily Robinson, Lily Charpentier, James Seuch, Grace Smith, Julianna Grampone, Sarah Foust, Haley Foreman, Liz Saavedra Perez, Kayla Barton, Steven Allers, Michael Babcock, Alec Ballinger, Riley Grindle, Sam Weafer, Mykayla Weinstein, Wyatt Cannell, Connor Aylesworth, Benjamin Curtis, Jason Hart, Daniela Chavez de Paz Solis, and Hanna Jordan. The Graduate School of Molecular and Biomedical Sciences at the University of Maine, especially Drs. Julie Gosse, Samuel Hess, Edward Bernard, and Robert Wheeler. I would like to thank administrative assistants Doreen Sanborn and Tammy Gosselin. I would also like to thank Mark Nilan, Jess Majors, and Lexi Rutherford for taking wonderful care of the zebrafish and me. I thank my sister Candy Blanchette, my aunt Gina Hoagland, and three great friends, Amanda Berryman, Michal Mudd, and Tess Fresquez. Finally, I thank my husband, Matt Soos, for the late-night coffees and never-ending support. None of this would have been possible without you.

## TABLE OF CONTENTS

ACKNOWLEDGEMENTS……iii

LIST OF TABLES……xii

LIST OF FIGURES……xiii

LIST OF ABBREVIATIONS……xvii

Chapter

1. INTRODUCTION……1

2. IAV, VIRUSES, AND IMMUNITY……4

  2.1. Influenza Viruses……4

    2.1.1. Introduction……4

    2.1.2. History of Influenza Virus……5

    2.1.3. Influenza Virus Disease in Humans……8

    2.1.4. Influenza Virus Replication and Expression……10

  2.2. Antiviral immunity……18

    2.2.1. Introduction……18

    2.2.2. Adaptive Immunity……20

    2.2.3. Innate immunity……24

        - 2.2.3.1. Antiviral pattern recognition and chemokine signaling ….…..…24
        - 2.2.3.2. Cytokine and chemokine signaling and regulation…...…………..27
        - 2.2.3.3. Influenza evades the innate immune system…………………….....35
    - 2.2.4. Hyperinflammation in Antiviral Immunity………………………………..39
        - 2.2.4.1. Respiratory viruses that can cause hyperinflammation…………40
        - 2.2.4.2. Cell types that cause antiviral-induced hyperinflammation….….48
        - 2.2.4.3. Non-coding RNAs that induce hyperinflammation ……………53
    - 2.2.5. Current therapies for IAV…………………………………………………54
- 2.3 NEUTROPHILS………………………………………………………………..57
    - 2.3.1. Introduction………………………………………………………………..57
    - 2.3.2. Role of phagocytes in pathogen response……………………………....58
        - 2.3.2.1. Methods of pathogen clearance by neutrophils…………………59
        - 2.3.2.2. Respiratory burst response………………………………………62
        - 2.3.2.3. Neutrophils diseases…………………………….……….....65
        - 2.3.3. Neutrophil hyperinflammatory tissue damage………….………..69
        - 2.3.4. Non-coding RNA regulation of neutrophils……………….......71
- 2.4. REACTIVE OXYGEN SPECIES (ROS)……………………………………..72

2.4.1. ROS types……………………………………………………………72

2.4.2. Antioxidants/ redox signaling…………………………………………73

2.4.3. Sources of ROS…………………………………………………………76

2.4.4. ROS in disease……………..…………………………………………...78

2.4.5.  ROS in innate immunity………………………………………………80

2.4.6. Viral ROS response………………..…………………………………82

2.5. ZEBRAFISH AS A MODEL ORGANISM…………………………………...…88

2.5.2. Genetic manipulation of zebrafish……………………………………...88

2.5.3. Zebrafish as a model of viral infections…………………….……………89

2.5.4. The zebrafish innate immune system……………………………………92

2.6. Necroptosis……………………………………………………………..…….101

2.7. Drug Discovery……………………………………………..……………..104

2.7.1. Animal models in biomedical research…………………………………107

3. COLOR-FLU IS A NOVEL ZEBRAFISH MODEL TO VISUALIZE IAV INFECTIONS *IN VIVO*………...……………………………………………………....111

3.1. Abstract………………………………………………………………….…113

3.2. Introduction……………………………………………………………...113

3.3. Materials and Methods……………………………………………………………….117

3.3.1. Zebrafish Care and Maintenance………………………………………..117

3.3.2. MDCK/London Cell Culture……………………………………………117

3.3.3. Influenza Virus…………………………………………………..…118

3.3.4. Microinjection…………….…………………………………………….119

3.3.5. Drug Exposures………………………………………………………….120

3.3.6. Survival Studies………………………………………………………….120

3.3.7. Viral Burden Assays……………………………………………………..121

3.3.7. Respiratory Burst Assays………………………………………………..122

3.3.8. Confocal Imaging…………….…………………………………………122

3.3.9. Imaging analysis…………………………………………………………123

3.3.10. qRT-PCRAssays……………………………………………..………123

3.3.11. Statistical Analysis……………………………………………………...124

3.4. Results……………………………………………………………………………...125

3.4.1. IAV Infection decreases survival and replicates in zebrafish……………125

3.4.2. Color-flu infection decreases survival and replicates in zebrafish………127

3.4.3. Color-flu infection increases proinflammatory gene expression...………129

3.4.4. Zebrafish lines respond differently to influenza infections……………...131

3.4.5. Live confocal imaging of zebrafish infected with Color-flu…………..…136

3.4.6. Evaluating small molecules that alter the response to IAV infection……138

3.5. Discussion………………………………………………………………….152

3.6. Conclusion..……………………………………………………………….157

4. NEUTROPHIL TRAFFICKING REGULATION IS ESSENTIAL FOR SURVIVAL IN A ZEBRAFISH MODEL OF INFLUENZA A INFECTION……........……………158

4.1. Abstract……………………………………………………………………158

4.2. Introduction……………………………………………………………..158

4.3. Materials and Methods……………………………………………………160

4.3.1. Zebrafish Care and Maintenance………………………………………..160

4.3.2. MDCK/London Cell Culture……………………………………………161

4.3.3. Influenza Virus……………………………………………………...…162

4.3.4. Microinjection…………….……………………………………………162

4.3.5. Drug Exposures…………………………………………………………162

4.3.6. Survival Studies…………………………………………………………163

4.3.7. Viral Burden Assays……………………………………………………..163

4.3.8. Respiratory Burst Assays…………………………………………………...163

4.3.9. Confocal Imaging…………..……………………………………………163

4.3.10. Imaging analysis……………………………………………………..163

4.3.11. Statistical Analysis…………………………………………………...163

4.4. Results……………………………………………………………………...…164

4.4.1. AT7519 recapitulates neutropenia and decreases survival in IAV infection……………………………………………………………….164

4.4.2. Cxcl8b morphants display decreased survival after IAV infection…..….168

4.4.3. Cxcr4b WHIM mutants decrease survival in IAV infection………...….170

4.4.4. miR-199 overexpression mutants decrease survival in IAV infection….177

4.4.5. miR-722 overexpression mutants decrease survival and in IAV infection…………………………………………………………...182

4.4.6. miR-199 and WHIM overexpression mutants display different neutrophil profiles…………………….……………….……………..184

4.5. Discussion………………………………………………………………………186

4.6. Conclusion....……………………………………………………………...188

5. ROS MODULATION IMPROVES OUTCOME IN A ZEBRAFISH MODEL OF INFLUENZA A INFECTION…..……………………………………………………189

5.1. Abstract……………………………………………………………………….189

5.2. Introduction…………………………………………………………………...190

5.3. Materials and Methods………………………………………………………..193

5.3.1. Zebrafish Care and Maintenance……………………………………..193

5.3.2. MDCK/London Cell Culture…………………………………………194

5.3.3. Influenza Virus…………………………………………………..…194

5.3.4. Microinjection…………..……………………………………………194

5.3.5. Drug Exposures………………………………………………………194

5.3.6. Survival Studies………………………………………………………195

5.3.7. Viral Burden Assays…………………………………………………..195

5.3.8. Respiratory Burst Assays……………………………………………..195

5.3.9. Reactive Oxygen Species Staining……………………………………195

5.3.10. Confocal Imaging…..……….………………………………………196

5.3.11. Imaging analysis……..………………………………………………196

5.4. Results………………………………………………………………………..196

5.4.1. Spotless mutants exhibit improved survival, reduced viral burden, and altered ROS profiles compared to wild-type controls…………………..196

5.4.2. Diverse ROS inhibitors alter IAV infection response and rescue IAV infection…………………….…………….…………………………204

5.5. Discussion………………………………………………………………………213

5.6. Conclusion..……………………………………………………………………..220

6. CONCLUSION AND FUTURE DIRECTIONS………………………………………221

6.1. Color-flu zebrafish are a tool for the influenza community to study………………221

6.2. Neutrophils are required to clear IAV infection………………….……………….223

6.3. Not all ROS are created equal in influenza infections……………………………..226

6.4. Color-flu's future resides in small molecules, toxins, autophagy, and the neuromuscular system……………………………………………………………….230

REFERNCES……………………………………………………………………………...238

APPENDICES…………………………………….………………………………………276

APPENDIX A. WHIM Genes to Investigate for Chapter 4……….……….....………………276

APPENDIX B. Spotless Genes to Investigate for Chapter 5…….……………….………………277

BIOGRAPHY……………………………………………………………………………..278

# LIST OF TABLES

Table 2.1 mRNA and Protein Data for IAV…………………………………………………..13

Table 2.2 Common interleukin cytokines and their receptors…………………………………...27

Table 2.3 Interferon cytokines and their receptors……………………………………………30

Table 2.4 Tumor necrosis factors and their receptors…………………………………………31

Table 2.5 Chemokines and their receptors……………………………………………………33

Table 2.6 Respiratory virus proteins that activate inflammasomes……………………………...47

Table 2.7 List of viruses that have been studied in zebrafish models……………………………90

Table 2.8 Proinflammatory genes affiliated with antiviral immunity in zebrafish………………95

Table 2.9 Antiviral genes affiliated with antiviral immunity in zebrafish……………………....97

Table 2.10 Autophagy genes affiliated with antiviral immunity in zebrafish…………………...99

Table 2.11 Animal models used for antiviral efficacy during influenza infection……………..108

Table 6.1 Compounds to study in IAV infections……………………………………………...231

Table A.1 WHIM Genes……………………………………………………………………….276

Table B.1 Spotless Genes………………………………………………………………………277

## LIST OF FIGURES

Figure 2.1 A historical timeline of influenza pandemics spanning the past century……………...6

Figure 2.2 Influenza A Virus……………………………………………………………….12

Figure 2.3 Influenza virus entry, replication, and release process……………………………17

Figure 2.4 Lymphocyte classes……………………………………………………………..21

Figure 2.5 Response times in innate and adaptive immunity…………………………………25

Figure 2.6 Depiction of IAV interference in antiviral immunity……………………………...37

Figure 2.7 Inflammasome activation by respiratory viruses……………………………………46

Figure 2.8 The antimicrobial mechanisms of neutrophils involve a series of protective actions to eliminate microbial pathogens……………………………………………...60

Figure 2.9 The neutrophil NADPH oxidase complex…………………………………………64

Figure 2.10 Neutrophil response to infection in WHIM disorder……………………………..67

Figure 2.11 KEAP1-NRF2 redox signaling network in cellular homeostasis and oxidative stress………………………………………………………………………….………..76

Figure 2.12 Sources of ROS generation……………………………………………………77

Figure 2.13 The zebrafish antiviral response to IAV…………………………………………...100

Figure 2.14 Signal transduction events that lead to necroptosis……………………………..103

Figure 2.15 Animal models for influenza antiviral evaluation………………………………109

Figure 3.1 Characterization of PR8 and Color-flu systemically infected AB zebrafish………..126

Figure 3.2 Control infections to characterize PR8 and Color-flu systemically infected AB Zebrafish…………………………………………………………………..128

Figure 3.3 Expression of candidate genes at 24 hpi…………………………………………130

Figure 3.4 Characterization of PR8 and Color-flu systemic infection across zebrafish lines….132

Figure 3.5 Swimbladder infections with PR8 or mVenus-PR8 of zebrafish with varying genetic backgrounds……………………………………………………………….135

Figure 3.6 Confocal imaging of Color-flu-infected zebrafish………………………………….137

Figure 3.7 Ramipril and MDIVI-1 increase survival in systemically infected PR8 and Color-flu-infected 3 dpf zebrafish…………………………………………………...139

Figure 3.8 Ramipril concentrations at 2 dpf and 3 dpf are used to determine toxicity…………141

Figure 3.9 MDIVI-1 concentrations at 2 dpf and 3 dpf are used to determine toxicity………...143

Figure 3.10 Ramipril and MDIVI-1 treatments lower viral burden in IAV-infected zebrafish....................................................................................................145

Figure 3.11 Ramipril and MDIVI-1 treatment alters the respiratory burst response in IAV systemically infected zebrafish at 48 hpi……………………………………………147

Figure 3.12 Quantification of the number of neutrophils………………………………………150

Figure 3.13 Quantification of virus, neutrophils, and macrophages by fluorescent confocal imaging of Tg*(mpeg1:*eGF*P;lyz:*dsRed*)* larvae at 48 hours post-injection by eCFP-PR8 or HBSS following treatment by DMSO, ramipril, and MDIVI-1..………..152

Figure 4.1 Survival rates of AT7519 infected zebrafish compared to DMSO control…………165

Figure 4.2 Functional changes in antiviral response of AT7519 infected zebrafish compared to DMSO control………………………………………………………….167

Figure 4.3 Survival rates of *cxcl8b* morphants compared to control morphants……………….169

Figure 4.4 Survival rates of WHIM compared to WHIM hets and WHIM control……………172

Figure 4.5 Functional assessment of antiviral response of WHIM mutants compared to WHIM sibling control………………………………………………………………..174

Figure 4.6 Survival rates of WHIM *mpx*$^{(-/-)}$ compared to WHIM *mpx*$^{(+/+)}$ with therapeutic rescue…………………………………………………………………………...176

Figure 4.7 Survival rates of *tg(LyzC: miR-199: Dendra2)* compared to control with therapeutic rescue……………………………………..……………………………179

Figure 4.8 Survival rates of overexpressed *tg(LyzC: miR-199: Dendra2)* compared to control with therapeutic rescue…………………………..……………181

Figure 4.9 Survival and antiviral response assessment of overexpressed *tg(LyzC: miR-722: Dendra2)* compared to control……………………………………..183

Figure 4.10 miR-199 and WHIM overexpression mutants display different neutrophil profiles……………………………………………………………………………185

Figure 5.1 Survival rates of Spotless *(mpx*$^{NL144/NL144}$*)* zebrafish compared to Spotless heterozygotes heterozygotes and AB wild-type controls.. ……………………………………………198

Figure 5.2 Survival rates of Spotless *(mpx*$^{NL144/NL144}$*)* zebrafish treated with ROS inhibitors……...200

Figure 5.3 Spotless *(mpx*$^{NL144/NL144}$*)* zebrafish reveal decreased viral burden and neutrophil respiratory fitness……………………………………………………………………202

Figure 5.4 Spotless *(mpx*$^{NL144/NL144}$*)* alters the profile of ROS species……………………………...203

Figure 5.5 Survival rates of AB zebrafish treated with various ROS inhibitors………………..206

Figure 5.6 Survival rates of AB zebrafish treated with unsuccessful concentrations of the various ROS inhibitors……………………………………………………………….208

Figure 5.7 The viral burden of ROS inhibitor treatments compared to DMSO controls……….210

Figure 5.8 Respiratory burst assay of ROS inhibitor treatments compared to DMSO control zebrafish…………………………………………………………………...211

Figure 5.9. CellROX profiles of ROS therapeutic targets……………………………………212

Figure 6.1. Neutrophils robustly clear infection while preventing tissue-damaging hyperinflammation from excessive ROS levels……………………………………………229

# ABBREVIATIONS

| | |
|---|---|
| HA | Hemagglutinin |
| NA | Neuraminidase |
| IAV | Influenza A virus |
| RNA | Ribonucleic acid |
| ICU | Intensive care unit |
| RSV | Respiratory syncytial virus |
| COVID | SARS-CoV-2 |
| IFN | Interferon |
| ISG | Interferon-stimulated gene |
| CTLs | Cytotoxic T lymphocytes |
| DC | Dendritic cell |
| TNF | Tumor necrosis factor |
| IL | Interleukin |
| Th1 | Type 1 T helper |
| Treg | Regulatory T cells |
| Tfh | Follicular helper T cells |
| Th2 | T helper 2 |
| Th17 | T helper 17 |
| NK | Natural killer |
| ILC | Innate lymphoid cells |
| PAMPs | Pathogen-associated molecular patterns |

| | |
|---|---|
| PRRs | Pathogen recognition receptors |
| RIG-I | Retinoic acid-inducible gene-I protein |
| TLR | Toll-like receptor |
| dsRNA | Double-stranded RNA |
| ssRNA | Single-stranded RNA |
| MDA5 | Melanoma differentiation-associated gene 5 |
| CARD | Caspase activation and recruitment domains |
| TRIM | Tripartite motif containing |
| TBK-1 | Tank-binding kinase |
| IKK-ε | IκB kinase-ε |
| IRF | Interferon regulatory factor |
| NF-κB | Nuclear factor kappa-light-chain-enhancer |
| pDCs | Plasmacytoid dendritic cells |
| IFN-β | Interferon beta |
| NOD | Nucleotide oligomerization domain |
| LRR | Leucine-rich repeat |
| NLR | NOD-like, LRR, containing protein receptor |
| G-CSF | Granulocyte colony-stimulating factor |
| GM-CSF | Granulocyte-macrophage colony-stimulating factor (GM-CSF) |
| LIF | Leukemia inhibitory factor |
| OSM | Oncostatin M |
| INFAR | Interferon-α/β receptor |
| INFGR | Interferon-gamma receptor |

| | |
|---|---|
| IRAK1 | IL-1R-associated kinase-1 |
| TRAF6 | TNF receptor-associated factor 6 |
| MAPKs | Mitogen-activated kinases |
| TRIF | TIR-domain-containing adapter-inducing interferon-β |
| IRF3 | Interferon regulatory factor 3 |
| RD | Repressor domain |
| Tyk2 | Tyrosine kinase 2 |
| JAK1 | Janus kinase 1 |
| STAT | Signal transducer and activators of transcription |
| SOCS | Suppressor of cytokine signaling |
| MMP-9 | Matrix metalloproteinase-9 |
| MPO/MPX | Myeloperoxidase |
| NE | Neutrophil elastase |
| MIP-2 | Macrophage-inflammatory protein 2 |
| ECM | Extracellular matrix |
| ROS | Reactive oxygen species |
| NETs | Neutrophil extracellular traps |
| C/EBPβ | CCAAT/enhancer-binding protein-β |
| LAIV | Live attenuated influenza vaccine |
| TIV | Trivalent inactivated vaccine |
| lncRNAs | Long non-coding RNAs |
| NEAT1 | Nuclear-enriched abundant transcript 1 |
| MALAT1 | Metastasis-associated lung adenocarcinoma transcript-1 |

| | |
|---|---|
| miRNAs | Micro RNAs |
| ncRNAs | Non-coding RNAs |
| NK | Natural killer cells |
| DENV | Dengue virus |
| BALF | Bronchoalveolar fluid |
| HBoV | Human bocavirus |
| HRV | Human rhinovirus |
| LDH | Lactate dehydrogenase |
| ARDS | Acute respiratory distress syndrome |
| SH | Small hydrophobic |
| RSV | Respiratory syncytial virus |
| HMPV | Human metapneumovirus |
| HPIV | Human parainfluenza virus |
| ASC | Apoptosis-associated speck-like proteins |
| LRTIs | Lower respiratory tract infections |
| SOCS | Suppressor of cytokine signaling |
| PKR | Protein kinase R |
| ACKRs | Atypical chemokine receptors |
| cCKRs | Chemokine-bound chemokine receptors |
| BCRs | B cell receptors |
| GAGs | Glycosaminoglycans |
| PMNs | Polymorphonuclear neutrophils |
| Rac | Rho family GTPases |

| | |
|---|---|
| HPI | Hours post infection/ injection |
| DPI | Days post infection |
| MDIVI-1 | Mitochondria division inhibitor |
| MPX | Myeloperoxidase |
| WHIM | Warts, hypogammaglobulinemia, immunodeficiency, myelokathexis syndrome |
| NOX2 | NADPH oxidase 2 |
| UA | Urolithin A |
| NAC | N-acetyl cysteine |

# CHAPTER 1 INTRODUCTION

This dissertation investigates the roles of neutrophils in antiviral immunity in response to influenza type A virus (IAV) and the delicate balance between viral clearance and hyperinflammation. This was accomplished by developing a new model of the human innate immune response to IAV infection using zebrafish, where the progression of infection and the response of immune cells in the host can be visualized in vivo using the fluorescent reporter strains, Color-flu. Using characteristics of the zebrafish model, neutrophil function can be teased out to ascertain their role in antiviral immunity. Is the presence of neutrophils required in a viral infection? Is their ability to traffic a necessary function in response to influenza infection? What role does the production of reactive oxygen species play in antiviral immunity and hyperinflammation? These are the imperative biological questions we ask in the research presented in this dissertation. A combination of experimental methods, including genetics, live fluorescent confocal imaging, and assays to measure the response to IAV, are used to answer these questions. This research is a major contribution to the field as the response to IAV can be monitored in real-time.

Chapter 2 comprehensively reviews current knowledge about the biological systems and processes relevant to this dissertation. It details influenza virus replication, virus infection, host antiviral immunity, and current models used to study influenza. This chapter also describes the roles of neutrophils and reactive oxygen species (ROS) have in responding to infections and how zebrafish are used to study them.

Chapter 3 provides a detailed description of the new zebrafish model of IAV infection that uses Color-flu. We describe the response of zebrafish larvae to infection by different strains of Color-flu using several assays and confocal microscopy. The utility of the Color-flu zebrafish model to advance our understanding of response to IAV infection is showcased through a real-time investigation into innate immune function and how it was used to demonstrate how two drugs could be repurposed as novel antiviral therapies. This model holds immense potential for future research and advancements in antiviral immunity.

Chapter 4 describes a comprehensive study of the role of neutrophils in antiviral immunity. We establish the need for sufficient neutrophils to generate a robust enough response to clear infections. Zebrafish are instrumental in visualizing the innate immune response to IAV infection as a model organism. They can be used to investigate the role of neutrophil trafficking in response to virus infection through confocal imaging, survival, viral burden, and gene expression studies. By studying the response to IAV infection in different zebrafish mutants, we observed reduced trafficking and enhanced abundance of neutrophils. Moreover, we demonstrate the necessity of neutrophils in antiviral immunity through pharmacological ablation, a finding of significant importance.

Chapter 5 investigates the role that ROS plays in antiviral immunity and hyperinflammation. We show how reducing ROS, either overall, mitochondrial-specific, or neutrophil-specific, alters the response to IAV infection. Genetic models and novel pharmacological therapies are used to tease out ROS's roles in neutrophil function to clear the infection while preventing hyperinflammation. Utilizing the zebrafish Color-flu model, confocal imaging, and MATLAB image analysis scripts, *in vivo* ROS levels following infection were quantified. Additionally, how the ROS therapeutics impact genetics and phagocytes are identified. These studies are innovative as equivalent studies cannot be performed in other vertebrate models of IAV infection in vivo.

Chapter 6 discusses the scientific merit of these studies and their contribution to the field. We also outline additional lines of investigation that fully utilize the Color-flu model. These include screening for novel antiviral drug therapies, examining how environmental toxicants alter antiviral immunity, and tissue damage following IAV infection.

# CHAPTER 2 IAV, VIRUSES, AND IMMUNITY

## 2.1 Influenza Virus

Influenza viruses have existed for an extensive period of time. Over the past century, they have been the cause of six significant pandemics. Since the first identification of influenza in the 1930s, our society has made significant progress in understanding this virus. It is well known that infections can be particularly severe for children, older individuals, and those with compromised immune systems. The entry and replication mechanisms of the virus within the cell have been partially elucidated, as well as its ability to mutate rapidly into new variants.

Fortunately, antiviral treatments are available to address severe infections, and annual vaccines are administered to mitigate the impact of extreme cases. However, despite these advancements, millions of individuals still fall ill with influenza each year, with a significant portion requiring hospitalization. This burdens the patients and their caregivers and leads to substantial economic repercussions. We must continue to stay ahead of this virus as the potential for another pandemic looms on the horizon.

### 2.1.1. Introduction

Influenza is a segmented, negative-sense RNA virus surrounded by an outer envelope. It is part of the Orthomyxoviridae family, consisting of seven genera, with A, B, and C most commonly recognized (Abbas, 2022). The classification of these viruses is based on their hemagglutinin (HA) and hemagglutinin (NA) viral membrane proteins. Influenza viruses do not have a mechanism for proofreading during replication, which allows small changes to accumulate over time, leading to surface protein alterations known as antigenic drift. Influenza A viruses are the most extensively studied as they have caused five pandemics since 1900 (Webster, 2013).

Influenza A viruses (IAV), originating from avian species acting as reservoirs, can spread among diverse zoonotic species, including humans, horses, pigs, poultry, and sea mammals. IAV can occasionally cross species boundaries to infect whales, pigs, humans, cats, and dogs. Zoonotic transmission of viruses can result in new worldwide human infections like the 2009 pandemic flu (Webster, 2013) . The global impact of influenza is extensive, causing significant respiratory illness, substantial economic costs, and, in severe cases, death. Recognizing the complexity involved in controlling the spread of these infections is crucial. As human interaction with animals becomes more frequent due to expanding territories and increased human activity, the risk of cross-species transmission and viral adaptation rises. This presents a significant challenge and underscores the importance of ongoing research and surveillance efforts (Howley, 2020).

Research on influenza has been ongoing since the 1930s (Webster, 2013). In more recent times, such as in 2009, a pandemic caused by an H1N1 variant highlighted our continued vulnerability to this infectious disease (Howley, 2020). The persistence of influenza, a malady first described by Hippocrates, reminds us of its insidious nature and resilience (Webster, 2013). Despite advances in modern medicine, complete eradication of the influenza virus remains elusive. Our focus as individuals is to deepen our understanding of this illness through research to enhance treatment options for those affected (Krammer, 2018a). This literature review will briefly overview current knowledge and areas that warrant further exploration concerning influenza infections.

### 2.1.2. History of Influenza Virus

Influenza, a disease historically documented by Hippocrates in 412 B.C., possesses a complex and fascinating past. Ancient global health crises caused by influenza are distinguished by their significant impact on the elderly population and occurred sporadically and varied in severity. The initial scientific documentation of historical influenza pandemics has been accomplished through seroarchaeology (Francis, 1960). Detailed epidemiological data from six pandemics from 1889 to 2009 can be found in Figure 2.1 (Webster, 2013; Howley, 2020). The specific strain of the original virus responsible for the 1889 pandemic remains unidentified; however, analysis of serum samples suggests a potential H2 or H3 subtype of the Influenza A virus, believed to have originated in Russia and resulted in a relatively mild disease outbreak.

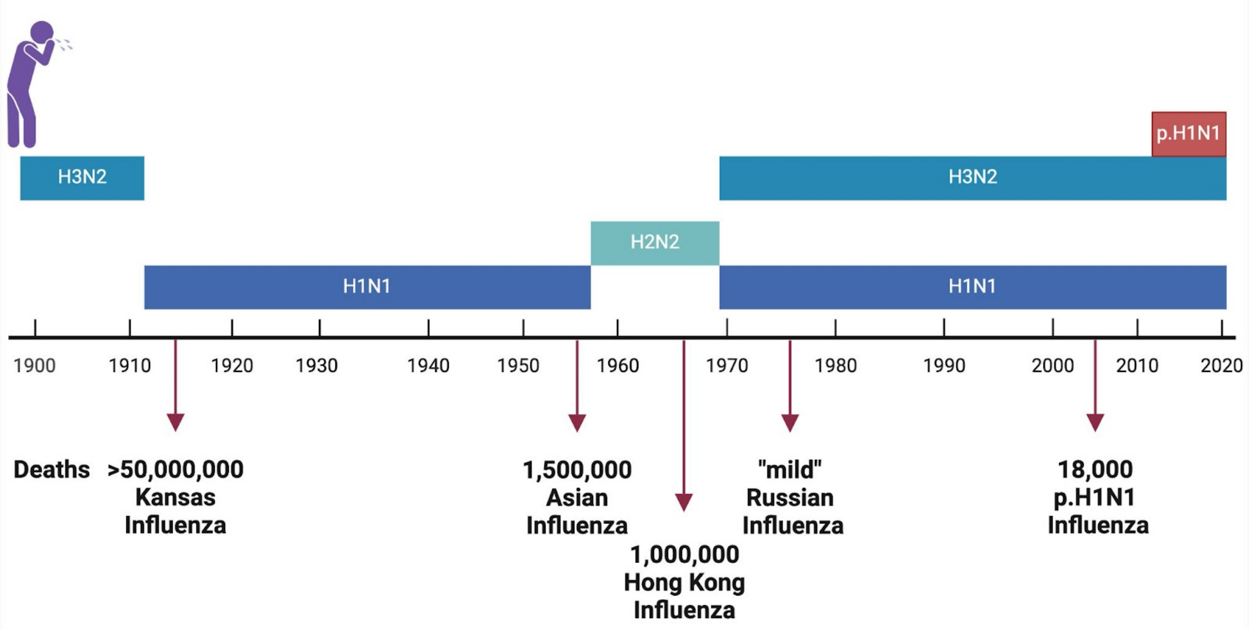

**Figure 2.1 A historical timeline of influenza pandemics spanning the past century.** This timeline depicts the duration of influenza subtype circulation and the emergence of pandemic strains. In the late 1800s, either the H3N2 or H2N2 strain was prevalent. By 1918, the H1N1 strain had become the predominant variant. From 1957 to 1968, the H2N2 strain held dominance until it was eventually replaced by the H3N2 strain in 1968. Subsequently, the H1N1 strain resurfaced in 1977, and following an antigenic shift event, the p.H1N1 strain emerged in 2008. To this day, both H1N1 and H3N2 remain in circulation. *This information has been adapted from Robert G. Webster's authoritative work, Textbook of Influenza (2nd edition).*

The renowned 1918 influenza pandemic, known as the Spanish Flu, was first characterized as a mild respiratory illness in Fort Funston, Kansas (Howley, 2020). It is believed to have swept across the world in three successive waves (Olson, 2005). This devastating event was caused by the H1N1 subtype of the Influenza A virus, with complications compounded by co-infections of *Haemophilus influenzae, Streptococcus pneumoniae,* and *Streptococcus pyogenes* (Morens, 2008).

Initial estimates suggested a death toll of 20 million, but subsequent research revealed that the actual number was closer to 50 million when considering fatalities in developing nations like India (Jordan, 1927) and Madagascar (Rasolofonirina, 2003). One of the distinctive features of this pandemic was its impact on healthy adults in their prime (Webster, 2013). The H1N1 strain remained predominant until the emergence of the 1957 pandemic.

The pandemics of 1957 and 1968 originated in China and were first documented in Hong Kong. The 1957 pandemic saw the emergence of a new H2N2 subtype through an antigenic shift caused by genetic components from avian influenza virus coding elements of hemagglutinin, neuraminidase, and PB1. This new subtype became dominant until 1968, when H3N2 became the predominant strain following another antigenic shift where the influenza virus acquired a PB1 gene and an H3 gene from an avian strain. These strains primarily affected the elderly, young individuals, and those with specific underlying medical conditions (Kawaoka, 1989).

In 1977, the H1N1 strain reemerged, resulting in a relatively mild infection. People over 25 were less affected due to similarities with a strain from the 1950s. Notably, both H1N1 and H3N2 strains began circulating concurrently, a phenomenon that has persisted to the present day (Gregg, 1978).

The first pandemic of the modern era was initiated in 2009 when a circulating H1N1 strain likely recombined with a strain in the avian reservoir to produce a milder version of the 1918 strain called p.H1N1. The 2009 strain once again targeted younger children and healthy adults at higher-than-average rates. A surveillance program initiated in China identified that this strain had been in circulation in swine for 9-17 years before the onset of the pandemic (Smith, 2009). This oversight enhanced the surveillance of intermediary species, such as swine and bats.

Richard Shope was credited with first isolating swine influenza in 1930 (Shope, 1931), while the first human influenza virus was isolated in 1933 from ferrets (Smith, 1933). These viruses were subsequently modified to propagate in chicken eggs, leading to the development of the inaugural influenza vaccine in 1943 (Kilbourne, 2002). Subsequently, seasonal vaccines have been produced to combat infection. In response to the reemergence of the 1977 H1N1 strain, bivalent influenza vaccines now contain H1N1, H3N2, and Type B components. Aside from a select few antivirals, vaccinations are the most successful method for preventing influenza infections (Webster, 2013).

### 2.1.3. Influenza Virus Disease in Humans

The influenza virus attaches to specific receptors known as α-2,6-sialic acid or α-2,3-sialic acid receptors found on the surface of ciliated epithelial or mucus secreting cells within the nasal cavity (Weis, 1988). It is commonly transmitted through small-particle aerosols, larger droplets, or through indirect contact with contaminated surfaces. Human influenza viruses typically reproduce in the lining of the respiratory tract. The highest levels of viral replication usually occur 2-3 days after infection. Viral shedding normally lasts 5-7 days, but in children, it can extend up to 14 days. Symptoms of influenza may include fever, headache, fatigue, muscle aches, and nausea. Elderly individuals are at a higher risk of experiencing severe complications from the virus, although those with cardiovascular issues, compromised immune systems, or metabolic disorders can also face severe consequences. In rare instances, such as during the 1918 and 2009 pandemics, even healthy young adults can be at risk of serious complications (Webster, 2013).

The influenza virus typically targets ciliated and nonciliated secretory cells found in the epithelia of the upper respiratory tract, including the nose, trachea, and bronchi. However, once the virus infects the alveolar cells in the lungs, there is an increased risk of developing pneumonia due to compromised gas exchange, which can result in severe respiratory complications and extreme cases, even death (Tomashefski, 2008; Kuiken, 2008). The specific cells and tissues the virus targets can significantly influence the severity and outcome of influenza infection (Matrosovich, 2008). Additionally, factors such as the rate of viral spread, viral load, and the effectiveness of the host's immune response play crucial roles in determining the progression of the infection (Webster, 2013).

In addition to causing infection, severe disease outcomes drastically increase when influenza coinfects with other pathogens. With the recent COVID-19 pandemic, coinfection with influenza was reported at 2.45% in COVID-19 patients. Coinfection was more common in cases of death and intensive care unit (ICU) admission, as coinfection with IAV led to severe disease outcomes in COVID-19 patients (Steponavičienė, 2023; Sweets, 2022; Yan, 2023). A recent meta-analysis by Qiao et al. demonstrated that bacterial co-infection is correlated with a mortality risk of approximately 2.6 times greater than that of a single influenza infection. Further, there is a roughly two-fold increased risk of ICU admission and mechanical ventilation requirement for bacterial coinfection compared to those with influenza single-infection. Similarly, it was observed that approximately 20% of influenza-related deaths could be attributed to bacterial coinfection (Qiao, 2023).

Respiratory viruses exhibit a common preference for the human respiratory system and are responsible for a significant disease burden. While growing evidence suggests that interactions, such as coinfections, between viruses play a key role in virus dynamics and transmission, much of our understanding of virus biology and pathogenesis comes from a simplified research approach that focuses on studying each virus independently. Current research has shown that interactions between respiratory viruses can have measurable effects at separate levels, including people and tissue types. However, there are few studies directly examining how viruses interact within cells. One such study indicates prior exposure to rhinovirus can impede IAV infection by triggering the activation of antiviral defenses within the human airway epithelium, which serves as the target tissue for both viruses (Pang, 2017). Treatment with interferon or a history of rhinovirus infection can effectively hinder the replication of IAV. Furthermore, it has been noted that prior exposure to rhinovirus significantly boosts the expression of Interferon-Stimulated Genes (ISGs) during the early stages of IAV infection. In addition, the prevention of ISG induction has been shown to alleviate the replication of IAV following rhinovirus infection. This was even confirmed in human cases (Anchi, 2020). Another study indicated that in cases of coinfection between IAV and respiratory syncytial virus (RSV), IAV replicates at similar or slightly higher levels than when it infects alone. At the same time, RSV replication is reduced (Haney, 2022). This counters coinfection concerning rhinovirus, where IAV replication is stymied. These findings suggest that the outcomes of coinfections depend extensively on the specific viruses implicated in infection.

### 2.1.4. Influenza virus replication and expression

IAV is a zoonotic virus group that infects various species, including birds, humans, and pigs (Webster, 2013). Genetic and antigenic differences in the glycoproteins HA and NA determine host adaptation. IAVs are subject to constant negative selection due to viral proteins' functional needs and genome limitations (Dou, 2018). 18 HA and 11 NA subtypes are currently in the wild (Hao, 2020). All IAV strains express eight structural proteins essential for infection, replication, and budding. IAV expresses various NSPs like M42, NS1, NS3, PA-N155, PA-N182, PA-X, PB1-F2, and PB1-N40, which play important roles in host defense suppression, virulence, and pathogenicity (Dou, 2018). These NSPs are derived from splicing, frame-shifting, and truncating structural protein-coding regions (Hao, 2020).

The genome of the IAV consists of single-stranded RNA divided into eight segments known as viral RNA (vRNA) segments (Figure 2.2). These segments encode ten crucial proteins and six strain-specific varieties (Dou, 2018; Hao, 2020; McGeoch, 1976; Palese, 1976;). The first three segments encode the largest polymerase proteins: PA, PB1, and PB2. Segment 2 also encodes two other proteins, PB1-F2 and PB1-N40 (Jagger, 2012), while segment 3 produces three additional proteins (PA-N155, PA-N182, and PA-X) through translational frameshifting (Hao, 2020). Segments 4-6 encode one essential protein: HA, NP, and NA. Segments 7 and 8 encode mRNAs N and M (Webster, 2013), which are subject to splicing before being translated into additional proteins (see Table 2.1).

Polymerase proteins PB2, PB1, and PA are crucial in the viral lifecycle (Webster, 2013). PA-X exhibits endonucleolytic activity and RNA degradation capabilities (Desmet, 2012; Jaegger, 2012). Mutant strains lacking PA-N182 and PA-N155 show reduced replication and pathogenicity, but their function remains unknown (Muramoto, 2013). PB1-F2 acts as a proapoptotic virulence factor, impacting various cellular processes to enhance viral pathogenicity (Hao, 2020; McAuley, 2010). PB1-N40 is dispensable for virus replication, but its absence negatively affects viral growth (Wise, 2009). HA binds to host cell receptors, creating a tight fusion with the host cell. NP plays a role in vRNA replication by binding to integrins to import into the nucleus (Dou, 2018). NA facilitates virus release by cleaving sialic acid from the cell surface (Watanabe, 2010). M1 and M2 proteins are essential for virus uncoating (Dou, 2018; Webster, 2013). NS1 and NS2 inhibit host defenses and are vital for virus replication (Bullido, 2001; Burgui, 2003; Gack, 2009; Gao, 2012; Garcia-Sastre, 1998; Rajsbaum, 2012; Robb, 2009; Zhao, 2017). NS1 has many additional roles, which will be discussed later in the chapter. NS3, a truncated form of NS1, has limited research available (Hao, 2020).

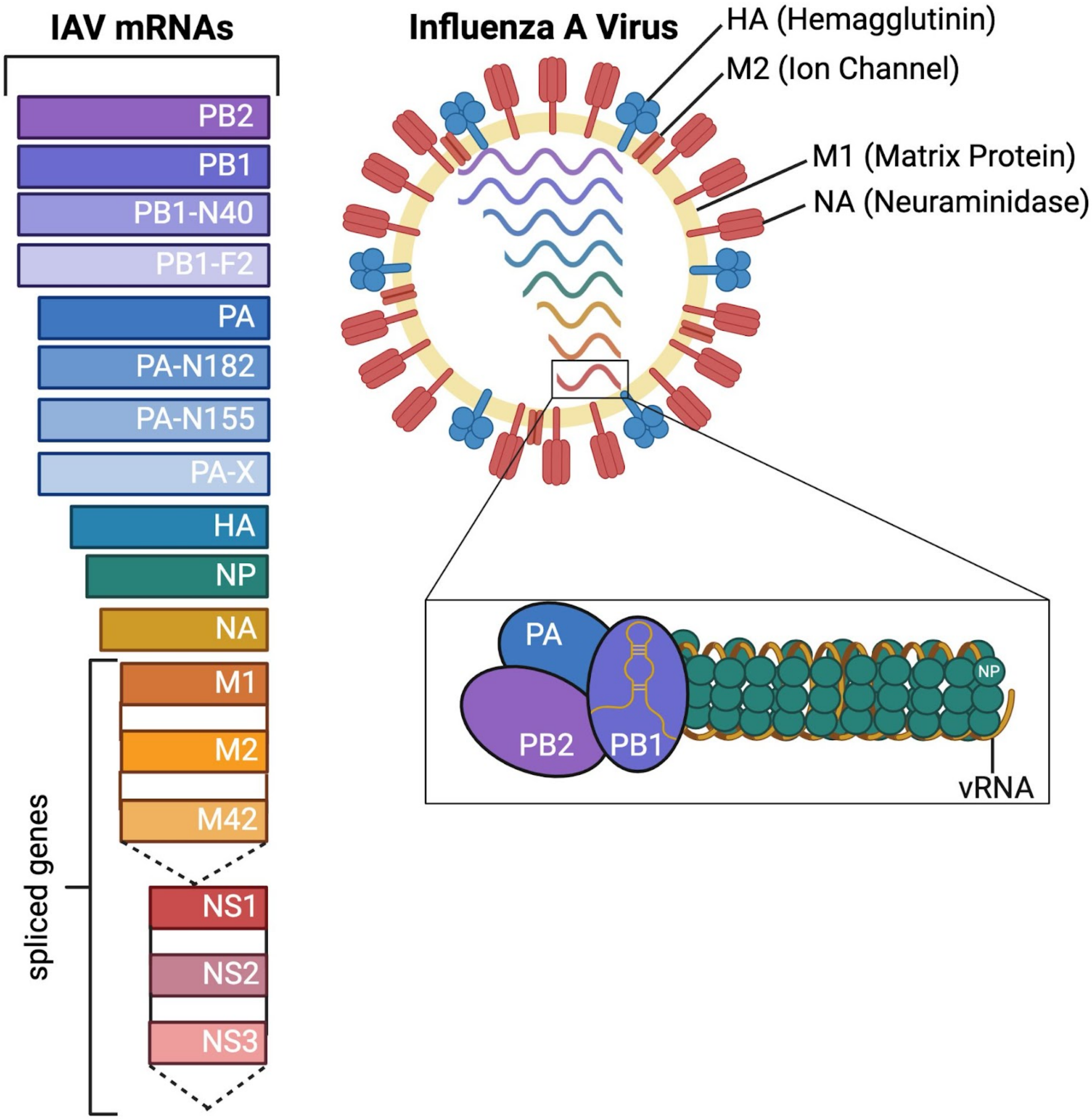
IAV mRNAs
PB2
PB1
PB1-N40
PB1-F2
PA
PA-N182
PA-N155
PA-X
HA
NP
NA
M1
M2
M42
NS1
NS2
NS3
spliced genes
Influenza A Virus
HA (Hemagglutinin)
M2 (Ion Channel)
M1 (Matrix Protein)
NA (Neuraminidase)
PA
PB2
PB1
NP
vRNA

**Figure 2.2 Influenza A Virus.** Diagram of the viral mRNAs (left) transcribed from the IAV vRNA templates. Boxes indicate the viral gene product encoded by each mRNA, and the dashed lines show the alternative splicing of the IAV M and NS transcripts. Cross-section of an influenza virus (right) with viral membrane proteins HA, NA, and M2 on the envelope, along with the eight viral ribonucleoproteins (vRNPs) and the matrix protein M1 that supports the viral envelope. A vRNA gene segment is wrapped around multiple nucleoprotein (NP) copies. The conserved promoter regions in the 5′ and 3′ UTRs form a helical hairpin bound by a single heterotrimeric viral RNA-dependent RNA polymerase. *The image was adapted from Dou D, Revol R, Östbye H, Wang H, and Daniels R (2018) Influenza A Virus Cell Entry, Replication, Virion Assembly and Movement. Front. Immunol. 9:1581. doi: 10.3389/fimmu.2018.01581.*

**Table 2.1 mRNA and Protein Data for IAV**

| Segment | Nucleotides | Protein Name | Amino Acids | Function |
|---|---|---|---|---|
| 1 | 2341 bp | PB2 | 759 | Polymerase, cap-binding |
| 2 | 2341 bp | PB1 | 757 | Polymerase, nucleotide addition |
| 2 | 2341 bp | N40 | 718 | Affects virulence; more studies are needed |
| 2 | 2341 bp | PB1-F2 | 87 | Apoptotic regulation, host immune evasion |
| 3 | 2233 bp | PA | 716 | Polymerase, endonuclease |
| 3 | 2233 bp | PA-N182 | 535 | Unknown function, maybe virulence |
| 3 | 2233 bp | PA-N155 | 562 | Unknown function, maybe virulence |
| 3 | 2233 bp | PA-X | 252 | Disrupts host RNA generation |
| 4 | 1778 bp | HA | 566 | A surface glycoprotein and receptor binding trigger endocytosis, proteolytic activity, and fusion of viral and host components |
| 5 | 1565 bp | NP | 498 | Nuclear localization |
| 6 | 1413 bp | NA | 454 | Surface glycoprotein facilitates virus release from the host cell |
| 7 | 1027 | M1 | 252 | Matrix protein |

table continued

| | | | | |
|---|---|---|---|---|
| 7 | 1027 | M2 | 97 | Ion channel |
| 7 | 1027 | M42 | 99 | Possible M2 alternative |
| 8 | 890 | NS1 | 237 | Multifunctional protein involved in virulence, host immune evasion, etc |
| 8 | 890 | NS2 | 121 | Protein involved in virulence, host immune evasion, etc |
| 8 | 890 | NS3 | 194 | Unknown function |

The interaction between HA and the receptor initiates the process of internalizing the virion (Figure 2.3). This can occur either through a mechanism dependent on clathrin, involving dynamin and the adaptor protein Epsin-1, or through macropinocytosis (Chen, 2008; Rust, 2004; de Vries, 2011). Once the virion is inside the cell, it is transported to the endosome, where the acidic environment activates the M2 ion channel, leading to a significant structural change in HA that exposes the fusion peptide (Pinto, 2006). Activation of the M2 ion channel results in rapid acidification inside the viral particle, allowing the release of the packaged vRNPs from M1 (Bui, 1996; Yoshimura, 1984). This facilitates the transfer of the vRNPs into the host cytoplasm through HA-mediated fusion (Martin, 1991). The process of transporting viral ribonucleoprotein complexes (vRNPs) to the nucleus is thought to involve the utilization of the importin-α–importin-β nuclear import pathway for gaining access to the host cell nucleoplasm (Kemler, 1994; O'Neil, 1995). vRNPs employ nuclear localization sequences on multiple NP molecules to attract the adapter protein importin-α (Wang, 1997). Importin-α is then recognized by the importin-β transport receptor, facilitating the translocation of vRNPs to the nuclear pore complex (Chou, 2013).

Within the nucleus, the heterotrimeric viral RNA-dependent RNA polymerase transcribes and replicates the viral RNAs (Plufg, 2017). This process involves two key steps: the transcription of complimentary RNA (cRNA) and the subsequent transcription of new vRNA copies using the cRNAs as templates (Newcomb, 2009). The production of cRNAs occurs through an unprimed process that relies on the precise complementation of free ribonucleoside triphosphates (primarily GTP and ATP) with the 3' end of the vRNA template (York, 2013b). This complementation securely locks the vRNA template into the polymerase active site within the PB1 subunit, forming an A-G dinucleotide from which the cRNA is extended (Robb, 2016). York et al. (2013) concluded that once the cRNA is released from the polymerase, it interacts with newly synthesized NP molecules and a single copy of the viral polymerase to form a cRNP (ribonucleoprotein complex).

Viral mRNA transcription involves priming from vRNA templates, where the viral polymerase acquires primers through a mechanism known as cap snatching. The association with the cellular RNA polymerase II C-terminal domain facilitates this process (Reich, 2014). During cap snatching, the viral polymerase utilizes the PB2 subunit to bind to 5′ caps of host transcripts and the PA subunit endonuclease domain to cleave nucleotides downstream of the 5′ cap (Dias, 2009; Guilligay, 2008). The PB2 cap-binding domain then positions the newly acquired capped primer into the PB1 catalytic center for extension using the vRNA template (Reich, 2014). Subsequently, each transcript undergoes polyadenylation through a "reiterative stuttering" process, which occurs when the polymerase encounters a short poly-U sequence at the vRNA 5′ end (Poon, 1999). The IAV protein synthesis process relies entirely on the translation machinery within the host cell (Dou, 2018). Once exported from the nucleus, viral mRNA translation occurs with the assistance of cytosolic ribosomes (for PB1, PB2, PA, NP, NS1, NS2, and M1) and endoplasmic reticulum (ER)-associated ribosomes for the membrane proteins HA, NA, and M2. Nuclear localization sequences on the newly synthesized NP proteins and polymerase subunits (PB1, PB2, and PA) facilitate their transport into the nucleus through the importin-α-importin-β pathway (York, 2013a). While NP and PB2 are imported individually, PB1 and PA are imported as heterodimers (Fodor, 2013). These proteins aid in viral mRNA transcription and vRNA replication inside the nucleus (York, 2013a). NP monomers bind to 12 nucleotide stretches with a partial bias towards G in vRNAs. The heterotrimeric polymerase then assembles and binds to the newly formed cRNPs to transcribe vRNAs, generating additional viral mRNA or cRNA transcripts (Reich, 2017). In the cytoplasm, Rab11 plays a crucial role in transporting viral ribonucleoproteins (vRNPs) towards the plasma membrane to assemble viruses. Rab11 aids in this process by forming associations with the polymerase PB2 subunit of the virus (Eisfeld, 2011).

The influenza A virus (IAV) membrane proteins are produced by ribosomes attached to the endoplasmic reticulum (ER) membrane (Dou, 2018). Like regular cellular secretory proteins, ribosome-nascent chain complexes containing viral proteins such as NA, HA, or M2 are directed to the ER during their synthesis by interacting with the signal recognition particle (SRP). The translocation mechanism allows the nascent NA, HA, and M2 polypeptides to enter the ER lumen (Daniels, 2003; Dou, 2014). It helps insert their transmembrane domains into the ER membrane through a specific gate (Bowie, 2005). HA is initially transported from the ER as an inactive form, which needs to be cleaved into HA1 and HA2 subunits to become functional for viral fusion. This cleavage process can occur at single or multiple basic sites (Huang, 1981).

IAV coordinates the organization of the appropriate viral components in the upper budding location; IAVs must modify the membrane to initiate bud formation and, ultimately, separate the viral covering from the cell membrane (Dou, 2018). The upregulation and downregulation of HA and NA expression play key roles in initiating viral budding. The efficiency and consistency of the budding process are enhanced by the presence of M1 protein (Chen, 2007). The ion channel M2 also defines the budding site boundary. It contributes to the separation of IAV particles by acting as a protein that alters the shape of the membrane (Rossman, 2013). Following the budding process, the release of newly formed IAVs heavily relies on the enzymatic activity of NA. NA functions by breaking down the glycosidic linkage and attaching Sialic Acid (SA) to neighboring sugar molecules. Through this enzymatic action, NA prevents the binding of HA to the cell surface, thus facilitating the successful virus release (Rossman, 2013).

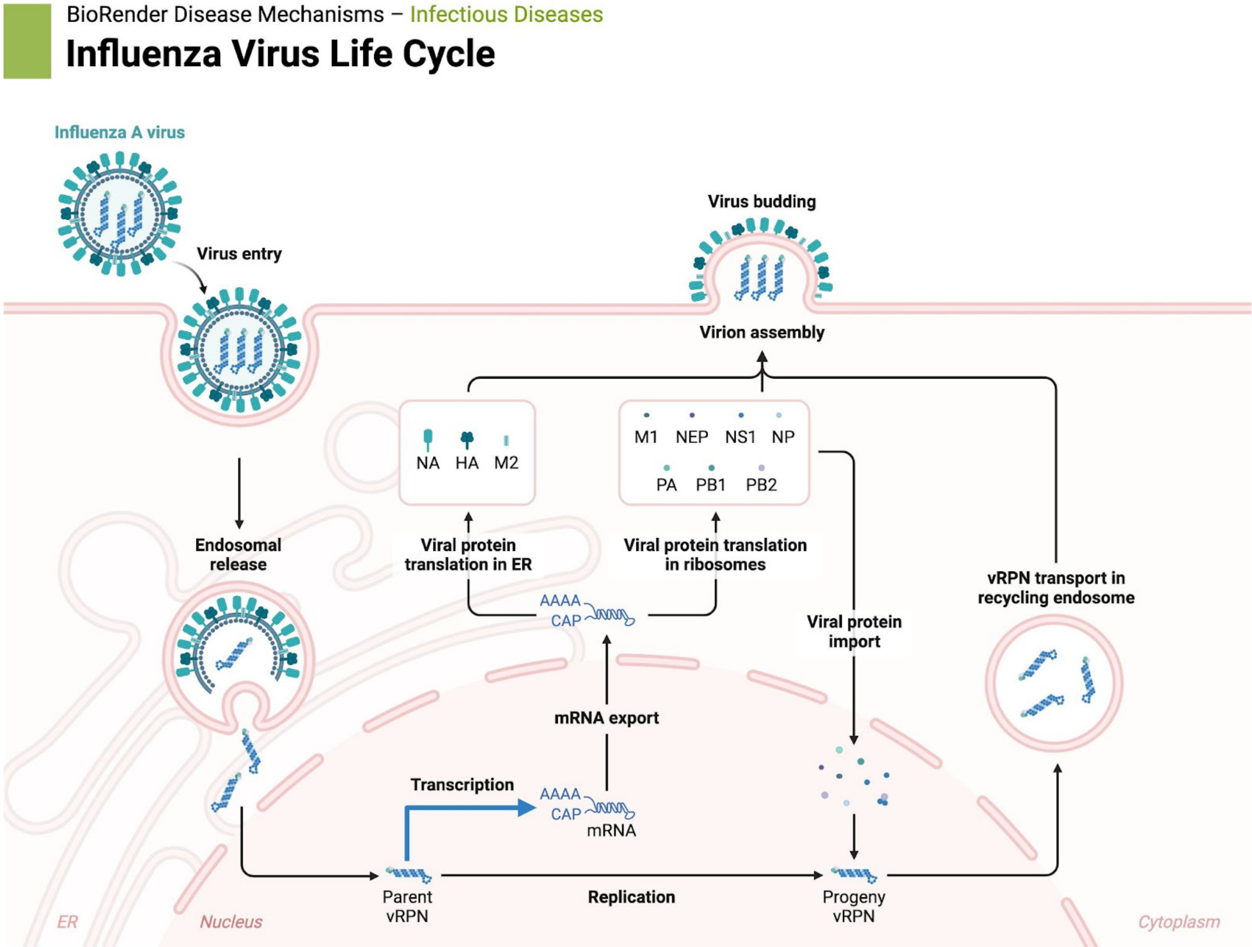
BioRender Disease Mechanisms – Infectious Diseases
Influenza Virus Life Cycle
Influenza A virus
Virus entry
Virus budding
Virion assembly
NA
HA
M2
M1
NEP
NS1
NP
PA
PB1
PB2
Endosomal release
Viral protein translation in ER
Viral protein translation in ribosomes
vRPN transport in recycling endosome
AAAA
CAP
Viral protein import
mRNA export
Transcription
AAAA
CAP
mRNA
Parent vRPN
Replication
Progeny vRPN
ER
Nucleus
Cytoplasm

**Figure 2.3 Influenza virus entry, replication, and release process.** The attachment, entry, replication, and release stages of influenza virus infection are outlined. Attachment occurs through the interaction of HA protein (shown in light green) with sialic acid receptors on the host cell. Subsequently, the virus enters the cell via endocytosis. The fusion of viral and endosomal membranes, facilitated by HA, occurs under acidic conditions within the endosome, releasing vRNP. The transported vRNP enters the cell nucleus, initiating mRNA synthesis and cRNA and

vRNA replication. Additionally, the process of budding, whereby new virus particles are released from the host cell, is depicted. The neck region where budding occurs is characterized by a membrane lacking lipid rafts and HA, NA spikes, and M1 protein presence. M2 protein may also be present in this region. *Taken from BioRender Templates, created by (Gaia Lugano who referenced Krammer, F., Smith, G. J. D., Fouchier, R. A. M., Peiris, M., Kedzierska, K., Doherty, P. C., Palese, P., Shaw, M. L., Treanor, J., Webster, R. G., & García-Sastre, A. (2018). Influenza. Nature Reviews Disease Primers.*

## 2.2 Antiviral Immunity

Recent technological advances such as genome-wide RNAi screens provide additional avenues to discovering new host antiviral factors, as exemplified by the recent success in identifying many host proteins and non-coding RNAs (e.g., microRNA) that either permit or impede the replication of viruses. As we gain experience and develop new tools to differentiate true-positive hits from false-negative or false-positive hits, large-scale screening approaches will be applied to more viruses with better success rates. The next challenge will be to investigate the function of novel antiviral factors and elucidate their mechanisms of action. Knowledge gained from these studies will be a potent tool for designing future antiviral therapies.

### 2.2.1. Introduction

The field of immunology has advanced from establishing fundamental principles of immune response mechanisms to applying these principles to develop therapies for human diseases. The progress in immunological therapies over the past decade has been remarkable, with some of the most innovative and effective immunotherapies emerging from advancing fundamental science and the explicit understanding of immune activation and regulation. The development of the COVID-19 vaccine, a process that typically takes over a decade, was completed in just 16 months, serving as a compelling case study. This achievement not only demonstrates the potential for rapid advancements in other viral diseases but also instills a sense of hope and optimism in the field of immunology.

Understanding the three stages of antiviral immunity is crucial. The first stage focuses on the production of interferons and natural killer cells. In the second stage, CD4+ and CD8+ T cells play pivotal roles. CD8+ T-cytotoxic lymphocytes and natural killer cells can destroy infected cells, aiding in viral clearance. In contrast, activation of the interferon (IFN) system can enhance the expression of interferon-stimulated genes (ISGs), which directly hinders viral replication. The final stage involves antiviral antibody production and release. This comprehensive view of the immune response helps us to appreciate the complexity and effectiveness of the antiviral immune defense.

In light of recent advancements in basic science, clinical translation, and antiviral immunity, it is crucial to recognize vital steps in a rush to generate a completed product. During the initial phase, phagocytic cells such as neutrophils and macrophages are sometimes not given due consideration for their role in combating viral infections. Additionally, the vital function of dendritic cells in priming naive T cells may be unintentionally omitted between the initial and subsequent phases. Furthermore, there is a need for more emphasis on how other cell types could contribute to priming the adaptive immune response. This oversight is concerning, particularly considering that neutrophils and macrophages constitute a significant portion of circulating white blood cells, accounting for approximately 60-85% of the total. Moving forward, it will be imperative to investigate strategies for harnessing the potential of these cells to combat viruses and stimulate the adaptive immune response effectively. Disregarding these cells underscores the need for caution and awareness in the research process, drawing attention to the importance of these cell types in the immune response.

### 2.2.2. Adaptive Immunity

Adaptive immune responses take longer to launch than innate immunity but offer greater specificity in pathogen targeting. Adaptive immune reactions primarily aim to eliminate foreign pathogens and their associated toxins. It is essential that these responses specifically target non-host molecules to avoid harmful effects on the host. The adaptive immune system can differentiate between closely related antigens, such as proteins with minor variations or identical molecules with different spatial arrangements (Alberts, 2002). In cell-mediated immune responses, a subset of adaptive immune reactions, activated T cells, directly target foreign antigens displayed on host cell surfaces (Figure 2.4). For instance, T cells may eliminate virus-infected cells by recognizing viral antigens on their surfaces, thus preventing viral replication. Sometimes, T cells release signaling molecules that stimulate macrophages to eliminate phagocytosed invading microbes (Abbas, 2022).

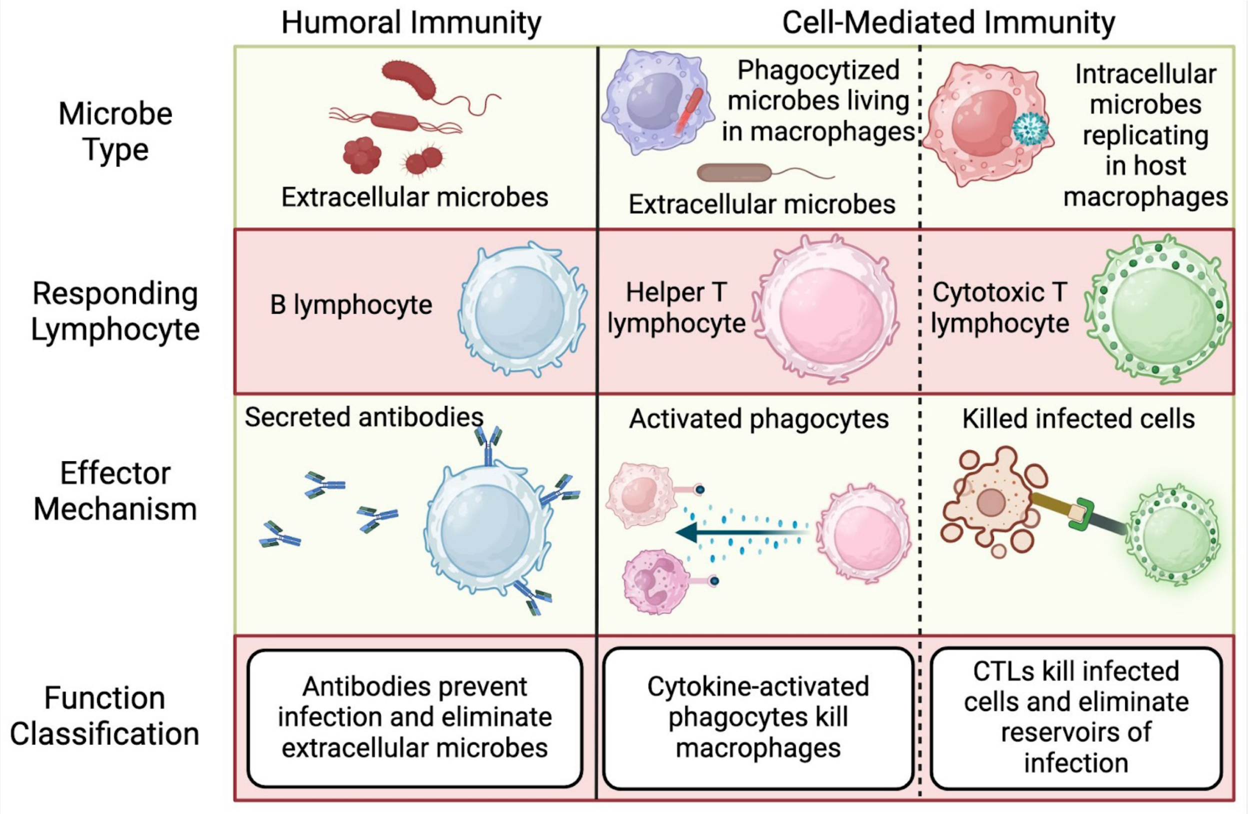
Humoral Immunity
Cell-Mediated Immunity
Microbe Type
Extracellular microbes
Phagocytized microbes living in macrophages
Extracellular microbes
Intracellular microbes replicating in host macrophages
Responding Lymphocyte
B lymphocyte
Helper T lymphocyte
Cytotoxic T lymphocyte
Effector Mechanism
Secreted antibodies
Activated phagocytes
Killed infected cells
Function Classification
Antibodies prevent infection and eliminate extracellular microbes
Cytokine-activated phagocytes kill macrophages
CTLs kill infected cells and eliminate reservoirs of infection

**Figure 2.4 Lymphocyte classes.** The various forms of adaptive immunity include humoral immunity, where B lymphocytes produce antibodies to prevent infections and eliminate extracellular microbes, and cell-mediated immunity, where helper T lymphocytes activate macrophages and neutrophils to destroy phagocytosed microbes or cytotoxic T lymphocytes directly target and eliminate infected cells. CTLs are cytotoxic T lymphocytes. *The image was retrieved from Abbas, A.K., Lichtman, A.H. and Pillai, S. (2022) Cellular and molecular immunology, 10th ed. The image was generated in BioRender.*

Lymphocytes, a type of white blood cell, orchestrate adaptive immune responses. Two main categories of responses from adaptive immunity are antibody responses and cell-mediated immune responses. The humoral immune response is facilitated by molecules in the bloodstream and mucosal secretions, known as antibodies. This type of immunity is the primary defense mechanism against microbes and their toxins outside cells (Cyster, 2019). On the other hand, cell-mediated immunity, also called cellular immunity, protects against microbes phagocytized by phagocytes but capable of surviving within them.

Additionally, some microbes, like viruses, can infect and reproduce in various host cells, thus making them immune to antibodies. Cell-mediated immunity aids in eradicating microbes inside phagocytes and eliminating infected cells to prevent the spread of infection (Mueller, 2016). Different subsets of lymphocytes can be identified based on the presence of specific membrane proteins, many of which are labeled with CD numbers. These surface molecules also play a role in the functions of lymphocytes (Kumar, 2018).

Antibodies are produced by B cells that specifically bind to foreign antigens, while T cells target infected host cells. The combined immune responses of B and T cells neutralize pathogens, mark them for destruction, and enhance phagocytic clearance (Au, 2020). Antibodies are effective against extracellular viruses, hindering initial infection and intercellular transmission. The most potent antibodies are high-affinity antibodies generated through T-dependent germinal center reactions. By binding to viral proteins, antibodies prevent attachment and entry into host cells (Abbas, 2022). Specifically, antibodies are crucial in neutralizing viruses in the respiratory and intestinal tracts, promoting phagocytic clearance, and activating complement to enhance antiviral immunity (Galani, 2021).

Cytotoxic T lymphocytes (CTLs) are a subset of CD8+ T cells that recognize and target intracellular viral peptides presented by class I MHC molecules (Whitmire, 2005). When infected cells present viral antigens, dendritic cells (DCs) can process and present these antigens to naive CD8+ T cells, initiating an antiviral T cell response (Krejitz, 2011). The CD4+ T cell is critical in the adaptive immune response against viral infection. Upon activation by DCs, CD4+ T cells differentiate into Th1 cells in response to various stimuli, including antigens, co-stimulatory molecules, and cytokines released by DCs, epithelial cells, and inflammatory cells (Ho, 2011). Th1 effector CD4+ T cells produce antiviral cytokines such as IFN-γ, TNF, and IL-2, activating alveolar macrophages (Pipkin, 2010). The cytokines IL-2 and IFN-γ produced by Th1 cells also regulate the differentiation of CD8+ T cells to combat viral infection (Grant, 2016). CD4+ T cells can differentiate into subsets such as Th2, Th17, regulatory T cells (Treg cells), and follicular helper T cells (Tfh) and occasionally exhibit cytotoxic activity (Szabo, 2000). Th2 cells interact with virus-associated peptides presented by antigen-presenting cells and secrete IL-4 and IL-13 to enhance B cell responses (Lamb, 1982). Additionally, Th17 and Treg cells have been implicated in modulating the cellular immune response during viral infection (Chen, 2018). The noteworthy aspect of the adaptive immune system lies in the retention of information for future defense against the same pathogen. The adaptive immune system is characterized by the development of immune memory (Figure 2.5), showcasing the impressive ability of lymphocytes to efficiently and accurately react to a previously encountered pathogen-derived antigen, leading to enhanced (or total) immunity against reinfection (Chi, 2024). Although it may not eliminate infections, it can significantly lower their occurrence.

Additionally, Follicular CD4+ T cells migrate to the B cell zone, engaging with antigen-specific B cells within the germinal center. Recognition of intact antigens by B cells via B cell receptors (BCRs) induces B cell activation and presentation of antigens to CD4+ T cells, which in turn signal the activation of B cells through interactions such as CD40L-CD40 binding and secretion of cytokines (e.g., IL-4 and IL-21). *Image 2.5 is from Abbas, A.K., Lichtman, A.H. and Pillai, S. (2022) Cellular and molecular immunology, 10th ed.*

### 2.2.3. Innate Immunity

The innate immune responses serve as the primary defense mechanism against invading pathogens. They are also necessary for triggering specific adaptive immune responses. Intrinsic immune responses rely on the body's ability to identify standard features of pathogens that are absent in a healthy individual. These responses are not tailored to a specific pathogen like adaptive immune responses are. They rely on a group of proteins and phagocytic cells that identify standard features of pathogens and rapidly activate to assist in eliminating invaders. While the adaptive immune system emerged less than 500 million years ago and is only present in vertebrates, intrinsic immune responses have been observed in both vertebrates and invertebrates and plants, and the fundamental mechanisms that regulate them remain consistent. The nonspecific response consists of various barriers, such as epithelial surfaces, pathogen-associated immunostimulants, abundant phagocytic cells, and other protective physiological processes (Alberts, 2002). These barriers shield the host from invading pathogens before they can establish an infection.

#### 2.2.3.1. Antiviral pattern recognition and signaling

The innate immune system is our primary defense mechanism against infections, providing vital protection against microbes and tissue damage. The innate immune system responds within 6 hours to pathogen invasion (Figure 2.6). Critical components of this system include barrier epithelia, which prevent the entry of microbes; tissue-resident sentinel cells such as macrophages, mast cells, and dendritic cells, which recognize invading pathogens and trigger immune responses; white blood cells like neutrophils, monocytes, natural killer (NK) cells, and others, that migrate from the circulation to eliminate pathogens and damaged cells; and various plasma proteins that target and neutralize microbes in both blood and tissues (Abbas, 2022).

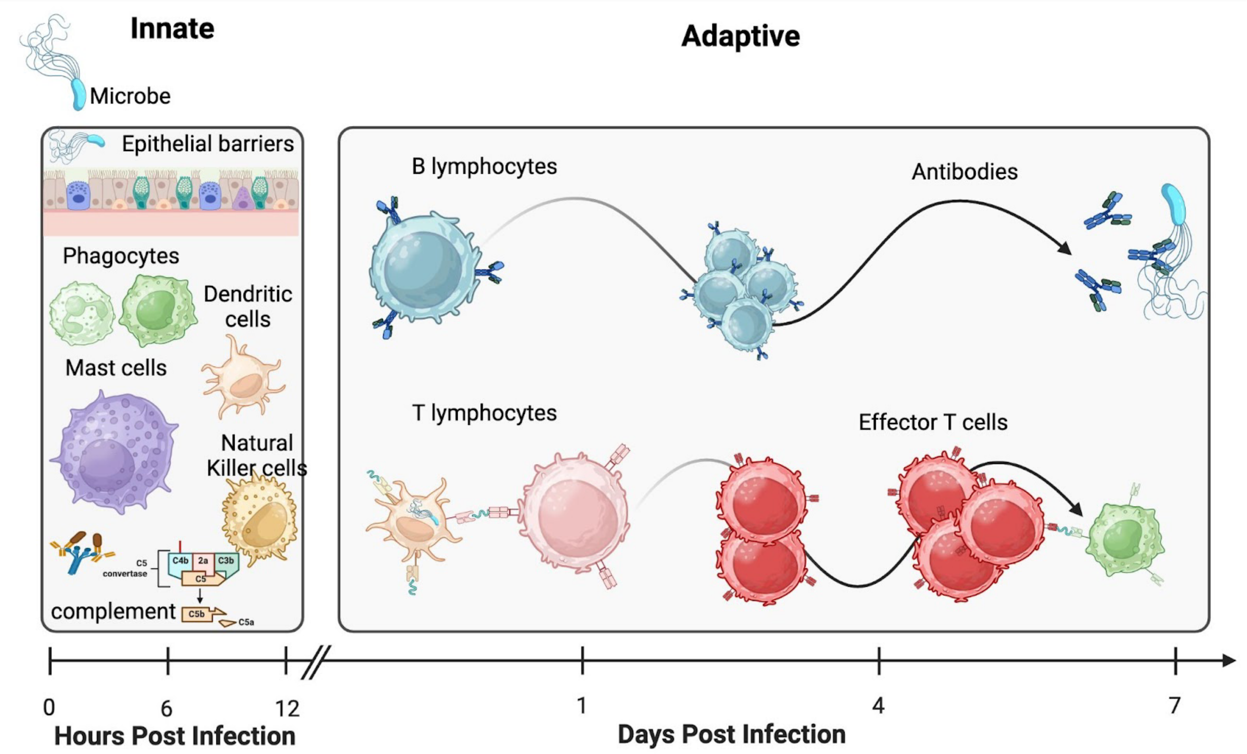
Innate
Microbe
Adaptive
Epithelial barriers
Phagocytes
Dendritic cells
Mast cells
Natural Killer cells
C5 convertase
C4b
2a
C3b
C5
complement
C5b
C5a
B lymphocytes
Antibodies
T lymphocytes
Effector T cells
0
6
12
Hours Post Infection
1
4
7
Days Post Infection

**Figure 2.5 Response times in innate and adaptive immunity.** Innate immunity mechanisms provide an initial defense against infections within hours of the start of the disease. In contrast, adaptive immunity requires lymphocyte activation and takes longer to respond to infection. The phagocytes shown are neutrophils (with the kidney-shaped nucleus) and macrophages. ILCs are innate lymphoid cells. *The image was retrieved from Abbas, A.K., Lichtman, A.H. and Pillai, S. (2022) Cellular and molecular immunology, 10th ed. The image was generated in BioRender.*

During a viral infection, host cells recognize viral conserved components known as pathogen-associated molecular patterns (PAMPs) through pathogen recognition receptors (PRRs) like retinoic acid-inducible gene-I protein (RIG-I) and toll-like receptor (TLR). This recognition triggers innate immune signaling, producing various cytokines and antiviral molecules (Cao, 2016). These PAMPs exhibit distinct features of viral RNA that set them apart from cellular RNAs, such as regions of double-stranded RNA (dsRNA) and a 5'-triphosphate group (Rehwinkel, 2010).

PRRs are capable of distinguishing between self and non-self molecules within infected cells. RIG-I plays a crucial role in recognizing intracellular single-stranded RNA (ssRNA) and transcriptional intermediates of ssRNAs. Non-self RNA and transcriptional products of ssRNA viruses in the cytoplasm are also sensed by melanoma differentiation-associated gene 5 (MDA5) (Piclmar, 2006). Upon PAMP recognition, RIG-I becomes activated and exposes its caspase activation and recruitment domains (CARDs). E3 ligases, like tripartite motif-containing protein 25 (TRIM25), modulate the CARD through dephosphorylation or ubiquitination (Munir, 2010). This triggers the association of RIG-I and MAVS, initiating downstream signaling at the outer mitochondrial membrane. As a result, Tank-binding kinase (TBK-1) and IκB kinase-ε (IKK-ε) phosphorylate transcription factors such as interferon regulatory factor 3 (IRF3), IRF7, and nuclear factor kappa-light-chain-enhancer (NF-κB) of activated B cells are activated, leading to the expression of various IFNs and cytokines (Kawai, 2005; Hiscott, 2006).

Toll-like receptors are essential as pattern recognition receptors, detecting pathogens on the cell membrane and within endosomes and lysosomes. TLRs such as TLR1, 2, 4, 5, and 6 on the cell membrane identify PAMPs from various microorganisms (Iwasaki, 2010; Kawai, 2010; Kumar, 2011). At the same time, TLR3, 7, 8, and 9 within endosomes and lysosomes specifically recognize nucleic acid PAMPs from viruses, including IAVs. TLR3, TLR7, and TLR8 are vital players in detecting components of IAVs during viral replication. In plasmacytoid dendritic cells (pDCs), TLR7 recognizes single-stranded RNA from influenza viruses, prompting downstream signaling that activates the expression of pro-inflammatory cytokines and type I interferons (Goubau, 2014; Lund, 2004). TLR3 interacts with adapter proteins to regulate interferon beta (IFN-β) expression, a potent antiviral cytokine in other immune cells like macrophages and dendritic cells (Fitzgerald, 2020). Furthermore, specific nucleotide oligomerization domain (NOD)-like, leucine-rich repeat (LRR)-containing proteins (NLR) receptors, such as NLRP3 and NLR apoptosis inhibitory protein 5, are activated in response to viral infections (Swanson, 2019). These receptors trigger the production of inflammatory cytokines through a multi-step process involving pathogen detection, ion channel activity, and lysosomal accumulation of viral proteins.

#### 2.2.3.2. Cytokine and chemokine signaling and regulation

The host's response to microbial pathogens requires coordinated efforts from the immune system's innate and adaptive components (Abbas, 2022). This communication network between cells is facilitated, in part, by cytokines (see Tables 2.2 through 2.6) and chemokines (see Table 2.7) in response to viral infections (Aakanksha, 2017; Alberts, 2002). Cytokines are small, soluble proteins that regulate various immune functions upon stimulation by different triggers, such as bacterial or viral elements (Chen, 2018). They are produced by multiple cells, including immune cells like leukocytes and nonimmune cells like fibroblasts and endothelial cells (Murphy, 2012). Cytokines are important in controlling the immune response by influencing cell activation, proliferation, differentiation, and the production of antibodies and other cytokines (Abbas, 2022).

**Table 2.2 Common interleukin cytokines and their receptors**

| Name | Amino Acids | Receptors | Function |
|---|---|---|---|
| IL-1α | 271 | IL1R and IL1RAP | Involved in immune responses, inflammation, and hematopoiesis |
| IL-1β | 269 | IL1R and IL1RAP | Mediates inflammation, cell proliferation, and apoptosis |
| IL-1RA | 177 | ILR1 | Inhibits IL-1α and IL-1β activation to modulate immunity and inflammation |
| IL-18 | 193 | IL18R1 | Stimulates IFN-ɣ production and regulation of Th1 and Th2 responses |

table continued

| | | | |
|---|---|---|---|
| IL-33 | 270 | ST2 and IL1RAP | Maturation of Th2 cells, activation of basophils, eosinophils, plus mast and natural killer cells |
| IL-36Ra | 155 | IL1RL2 | Inhibits NF-κB produced by IL-6 |
| IL-36α | 158 | IL1RL2 and IL1RAP | Activates NF-κB and MAPK signaling |
| IL-36β | 164 | IL1RL2 and IL1RAP | Activates NF-κB and MAPK signaling |
| IL-36ɣ | 169 | IL1RL2 and IL1RAP | Activates NF-κB and MAPK signaling |
| IL-37 | 218 | IL18R1 and ILR8 | Suppresses innate immunity and inflammation |
| IL-38 | 152 | IIL1RL2 | Immunomodulation |
| IL-2 | 153 | IL2R | Activates immune responses and tolerance |
| IL-4 | 153 | IL4R | Mediates and regulates allergic reactions, wound repairs, anti-parasitic reactions, and inflammation |
| IL-7 | 177 | IL7R | Aids in development, proliferation, and expansion of naive T-cells and memory B cells |
| IL-9 | 144 | IL9R | Involved in the immune response against parasites |
| IL-13 | 146 | IL4R and IL13R | Regulates allergic reactions, anti-parasitic reactions, and inflammation |
| IL-15 | 162 | IL15R | Modulates innate and adaptive immune cells |
| IL-21 | 153 | IL21R | Promotes transition between innate to adaptive immunity |
| IL-3 | 152 | IL3 | Promotes proliferation of hematopoietic progenitor cells |
| IL-5 | 133 | IL5R | Promotes growth and differentiation of B cells and eosinophils |
| GM-CSF | 144 | CSF2R | Promotes growth and differentiation of hematopoietic progenitor cells |
| IL-6 | 212 | IL6R | Regulates inflammation and B cell maturation |
| IL-11 | 199 | IL11R | Promotes megakaryocyte progenitor cell proliferation leading to an increase in platelet production |
| G-CSF | 207 | CSF3R | Regulates hematopoiesis of granulocytes and monocyte-macrophages |
| IL-12 | IL12A (253) and IL12B (328) | IL12R | Regulates T and natural killer cell responses and links innate and adaptive immunity |

table continued

| | | | |
|---|---|---|---|
| IL-23 | IL23A (189) and IL12B (328) | IL23R | Activates JAK and TYK, aids in intracellular bacterial clearance and promotes expansion/ survival of Th17 cells |
| IL-27 | IL30 (243) and IL27B (229) | IL27R | Regulates T-helper development, suppresses T-cell proliferation, stimulates CD8+ T cells, and stimulates innate immune activity |
| IL-30 | 243 | IL27R | Regulates T-helper development, stimulates CD8+ T-cells and naive CD4+ T-cells. Stimulates innate immune activity |
| IL-35 | IL12A (253) and IL27B (229) | IL35R | Functions in innate immunity along with IL-27 |
| LIF | 202 | LIFR | Pleiotropic cytokine involved in immunity, nervous system and kidney development, and interfaces at the maternal-fetal-line |
| OSM | 252 | OSMR | Growth regulator and regulation of cytokine production from endothelial cells |
| IL-10 | 178 | IL10R | Pleiotropic effects in inflammation and immune regulation |
| IL-19 | 177 | IL20R | Regulates Th2 helper T-cells to turn on anti-inflammation |
| IL-20 | 176 | IL20R | Involved in immunity, hemopoiesis, and epidermal/ keratinocyte differentiation |
| IL-22 | 179 | CRF2-4 and IL-22R | Modulates tissue responses during inflammation |
| IL-24 | 207 | IL20R and IL22R | Regulates immune responses, tissue homeostasis, oncogenesis, and host defense |
| IL-26 | 171 | IL10R | Recently discovered, may play a role in mucosal immunity |
| IL-14 | 546 | IL4R | Recently discovered, may play a role in exocytosis |
| IL-16 | 1332 | CD4 and CD9 | Modulates T cell activation and inhibits HIV replication |
| IL-17 | 155 | IL17R | Tissue integrity and microbial host defense |

The cytokines in green are all classified as IL-1l-like. The cytokines in pale cyan have common CD132 g chains. In light cornflower blue, the cytokines have common CD131 b chains. CM-CSF is related to the CD131 b chain cytokines in the darker shade of cornflower blue. In light blue, the cytokines are IL-6-like. Those cytokines are associated with the IL-6-like cytokines in the darker shade of light blue. The cytokines highlighted in light purple are IL-10-like. Granulocyte colony-stimulating factor (G-CSF), Granulocyte-macrophage colony-stimulating factor (GM-CSF), Leukemia inhibitory factor (LIF), Oncostatin M (OSM). *Table created from data obtained by*

table continued

Dembic, Z. (2015) *The cytokines of the immune system: The role of cytokines in disease related to immune response*.

**Table 2.3 Interferon cytokines and their receptors**

| **Name** | **Amino Acids** | **Receptors** | **Function** |
|---|---|---|---|
| IFN-α1/ 13 | 189 | INFAR | Antiviral response to modulate the innate immune response |
| IFN-α2 | 188 | INFAR | Mediates platelet adhesion and other cell types through the extracellular matrix |
| IFN-α4 | 189 | INFAR | Antiviral activities and stimulates oligoadenylate synthetase |
| IFN-α5 | 189 | INFAR | Antiviral activities and stimulates oligoadenylate synthetase |
| IFN-α6 | 1130 | INFAR | Antiviral activities and stimulates oligoadenylate synthetase |
| IFN-α7 | 502 | INFAR | Antiviral activities and stimulates oligoadenylate synthetase |
| IFN-α8 | 189 | INFAR | Antiviral activities and stimulates oligoadenylate synthetase |
| IFN-α10 | 189 | INFAR | Antiviral activities and stimulates oligoadenylate synthetase |
| IFN-α14 | 189 | INFAR | Antiviral activities and stimulates oligoadenylate synthetase |
| IFN-α16 | 785 | INFAR | Antiviral activities and stimulates oligoadenylate synthetase |
| IFN-α17 | 189 | INFAR | Antiviral activities and stimulates oligoadenylate synthetase |
| IFN-α21 | 189 | INFAR | Antiviral activities and stimulates oligoadenylate synthetase |
| IFN-β | 187 | INFAR | Responds to infection, tumor development, and inflammatory stimuli through innate immunity |
| IFN-ω | 195 | INFAR | Possesses antiviral activity |
| IFN-ε | 208 | INFAR | Predicted to activate B-cells in response to invading organisms |
| IFN-κ | 207 | INFAR | Predicted to regulate immune cell function against viruses |
| IFN-ɣ | 166 | IFNGR | Triggers a cellular response to microbial and viral infections |
| IFNλ1/ IL-29 | 200 | IFNLR | Antiviral, immune regulation, and anti-tumor activities |
| IFNλ2/ IL-28A | 200 | IFNLR | Antiviral, immune regulation, and anti-tumor activities |
| IFNλ3/ IL-28B | 196 | IFNLR | Antiviral, immune regulation, and anti-tumor activities |

table continued

| | | | |
|---|---|---|---|
| IFNλ4 | 179 | IFNLR | Antiviral response that activates JAK/STAT and ISGs |

The interferons highlighted in blue belong to Type I interferons. IFN-ɣ is the only Type II interferon in light red. In the light purple rows are Type III interferons. Interferon-α/ β receptor (INFAR), interferon-gamma receptor (IFNGR), interferon lambda receptor (IFNLR). *Table created from data obtained by* Dembic, Z. (2015) *The cytokines of the immune system: The role of cytokines in disease related to immune response*.

**Table 2.4 Tumor necrosis factors and their receptors**

| **Name** | **Amino Acids** | **Receptors** | **Function** |
|---|---|---|---|
| TNFα | 233 | TNFR1/ TNFR2 | A major regulator of inflammation |
| TNFβ | 205 | TNFR1/ TNFR2/ HVEM | Involved in cytotoxicity signaling |
| TNFɣ | 205 | LTβR | A major regulator of immune responses |
| CD70 | 193 | CD27 | Regulator of immune system activation |
| CD134L | 183 | CD134 | Stimulator of T and B cell activation |
| CD137L | 254 | CD137 | Enhancer of immune responses |
| CD153 | 234 | CD30 | Anti-mycobacterium immune response |
| CD154 | 261 | CD40 | Maintains immune responses |
| CD178 | 281 | FAS | Activation of apoptosis and termination of immune responses |
| CD253 | 281 | DR4/ DR5/ TRAILR3/ TRAILR5 | Apoptotic function and MAK8/ JNK signaling |
| CD254 | 317 | RANK/ TR1 | Enhances dendritic stimulation of T cells |
| CD256 | 250 | CD267/ CD268/ CD269 | Involved in B cell development |
| CD257 | 285 | CD267/ CD268/ CD269 | B cell activation, proliferation, and differentiation |
| EDA | 391 | EDAR/ EDAR2/ NGFR/ TROY | Activation of NF-κb and JNK pathways |

table continued

| | | | |
|---|---|---|---|
| LIGHT | 240 | LTβR/ HVEM | Lymphoid organ development, antiviral response amplification, and various innate/ adaptive functions |
| TWEAK | 249 | Fn14 | Tissue regeneration regulation, inflammation |
| VEGI | 251 | DR3 | Costimulation of T-cells and inflammation, inhibits vascular endothelial growth and angiogenesis |

Ligands and receptors related to the tumor necrosis superfamily. *Table created from data obtained by* Dembic, Z. (2015) *The cytokines of the immune system: The role of cytokines in disease related to immune response. * EDA data obtained from Cai et al. Ectodysplasin A/Ectodysplasin A Receptor System and Their Roles in Multiple Diseases. Front Physiol. 2021*

Chemokines are another type of secreted cytokine with a broad range of functions. While housekeeping chemokines are constantly expressed under normal conditions and contribute to development and tissue balance, inducible inflammatory chemokines aid in directing immune cells to infected or inflamed areas. These chemokines are vital for the body's defense against pathogens (Chemokine, 2009). Both cytokines and chemokines are essential in orchestrating the immune response to viral infections. The specific cytokine and chemokine profiles induced by pathogens determine the type of immune cells activated and the overall immune response in infected tissues (Hughes, 2018).

Chemokines are categorized based on their structural properties, specifically the number and arrangement of conserved cysteines. There are four subclasses: CC (β-chemokines), CXC (α-chemokines), CX3C, and C chemokines. CC, CXC, and CX3C chemokines each have four conserved cysteines, with varying numbers of amino acids between the first two cysteines (Monneau, 2016). On the other hand, XC chemokines only have the second and fourth cysteines present. In addition to structural classification, chemokines can be grouped by function into homeostatic and inflammatory groups (Chemokine, 2009; Hughes, 2018). While most chemokine receptors can bind multiple chemokine ligands with high affinity, these ligands tend to belong to the same structural subclass. Moreover, most chemokines can bind to multiple receptor subtypes (vonHundelshausen, 2017). Receptors for inflammatory chemokines exhibit high promiscuity in ligand specificity, often lacking a specific endogenous ligand (Hughes, 2018).

**Table 2.5 Chemokines and their receptors.**

| **Receptors** | **Chemokines** |
|---|---|
| CCR1 | CCL3, CCL3L, CCL4, CCL5, CCL6, CCL8, CCL9, CCL10, CCL12 , CCL13, CCL14, CCL15, CCL16, CCL23 |
| CCR2 | CCL2, CCL7, CCL8, CCL1,1 CCL13, CCL15, CCL16, CCL26 |
| CCR3 | CCL3L1, CCL4, CCL7, CCL11, CCL13, CCL15, CCL18, CCL23, CCL26, CCL28, CXCl9, CXCLl0, CXCL11 |
| CCR4 | CCL17, CCL22 |
| CCR5 | CCL3, CCL3L, CCL4, CCL4L, CCL7, CCL11, CCL14, CCL16, CCL26, CXCL11, ACKR1, CXCR4 |
| CCR6 | CCL20 |
| CCR7 | CCL19, CCL21, CCL21Ser, CXCR4 |
| CCR8 | CCL1, CCL8, CCL18 |
| CCR9 | CCL25 |
| CCR10 | CCL27, CCL28 |
| CXCR1 | CXCL5, CXCL6, CXCL8 |
| CXCR2 | CXCL1, CXCL2, CXCL3, CXCL5, CXCL6, CXCL7, CXCL8 |
| CXCR3 | CCL11, CXCL4, CXCL4L, CXCL9, CXCL10, CXCL11, CXCR4 |
| CXCR4 | CXCL112, CXCL14, CCR2, CCR5 |
| CXCR5 | CXCL13 |
| CXCR6 | CXCL16 |
| CXCR8/ Gpr35 | CXCL17 |
| Xcr1 | XCL1, XCL2 |

table continued

| | |
|---|---|
| Cx3cr1 | Cx3cr1 |
| Ackr1 | CCL5, CCL7, CCL11, CCL13, CCL14, CXCL1, CXCL2, CXCL3, CXCL6, CXCL8, CXCL11 CCR5 |
| Ackr2 | CCL2, CCL3, CCL3L1, CCL4, CCL4L1, CCL5, CCL7, CCL11, CCL13, CCL14, CCL17, CCL22 |
| Ackr3 | CXCL11, CXCL12 |
| Ackr4 | CCL19, CCL21, CCL21Ser, CCL25, CXCL14 |

List of chemokines, receptors, and general functions. *This table was generated with data from two papers. First, Cai Z, Deng X, Jia J, Wang D, Yuan G. Ectodysplasin A/Ectodysplasin A Receptor System and Their Roles in Multiple Diseases. Second, Hughes CE, Nibbs RJB. A guide to chemokines and their receptors.*

The functionality and distribution of chemokines post-secretion greatly depend on their immobilization on cell surfaces and extracellular matrix (Lohman, 2017). Glycosaminoglycans (GAGs) play a crucial role in this process by influencing chemokine binding, receptor interactions, half-life, and cellular responses in various tissues (Proudfoot, 2003). Chemokines can exist as monomers or form dimers, aggregates, or complexes with other chemokine species, influenced by interactions with GAGs (Dyer, 2016). They are also subject to post-translational modifications, such as citrullination, nitration, and cleavage by various proteases, which can significantly impact their biological activity (Metzemakers, 2016).

Chemokine-bound chemokine receptors (cCKRs) typically initiate signaling cascades through G-proteins and beta-arrestins, leading to cell migration, adhesion, and other biological responses (Hughes, 2018). Chemokines can induce other biological processes, including proliferation, differentiation, and antimicrobial activity in different cell types (López-Cotarelo, 2017). Some of the other biological processes can be seen in the CXCL12/CXCR4/ACKR3 node that is essential for life, as it is vital for organ development and function (Bolajipour, 2008; Dambly-Chaudière, 2007; Gerrits, 2008; Sànchez-Alcañiz, 2011; Yu, 2011). Chemokines produced in response to infection or inflammation play a key role in leukocyte recruitment to damaged tissues, thereby controlling immune responses (Eash, 2010; Griffith, 2014; Lancaster, 2018; Ueno, 2002). Changes in cCKR expression affect leukocyte function, particularly during T-cell activation and differentiation (Hughes, 2018).

The chemokine network comprises 18 cCKRs, crucial in combatting microbial subversion by enhancing leukocyte responses during infection (Kufareva, 2015). Atypical chemokine receptors (ACKRs) regulate chemokine localization and abundance without initiating signal transduction pathways, indirectly influencing chemokine-cCKR interactions (Bachelerie, 2014). The chemokine network is pivotal in development, immunity, inflammation, tissue repair, and disease pathogenesis. While significant progress has been made since the discovery of chemokines in 1987 (Yoshimura, 1987), there is still much to learn and explore in this field.

#### 2.2.3.3. Influenza evades the immune system

The innate and adaptive immune responses are activated upon infection with an influenza A virus. Influenza A viruses have developed various strategies to evade the immune system's antiviral response. These strategies may hinder the recognition by immune response components, potentially leading to a reduced ability to clear the virus and infected cells (van de Sandt, 2012). One key player in immune evasion is the NS1 protein, as seen in Figure 2.7, which actively works against the antiviral innate immune response (Fernandez-Sesma, 2006). Studies have shown that genetically modified influenza viruses with non-functional NS1 genes trigger more robust IFN responses than wild-type viruses (Ferko, 2004). Viruses with defective NS1 genes also exhibit reduced virulence in animal models after infection (Staskova, 2005). NS1 hinders the signaling of the RIG-I receptor through various mechanisms, ultimately blocking the recognition of viral RNA and inhibiting downstream signaling pathways (Takeuchi, 2008).

The influenza polymerase complex, consisting of viral proteins PB2, PB1, and PA, plays a significant role in viral RNA synthesis (Dias, 2009; Plotch, 1981; Sugiyama, 2009). Additionally, this complex interferes with the host cell gene expression, including the production of IFN-β by cap-snatching the host's mRNAs(Conenello, 2011). Another viral protein, PA-X, can suppress the expression of genes involved in initiating the cellular immune response (Jagger, 2012).

Influenza A virus infection triggers the production of antiviral protein kinase R (PKR) [Garcia, 2006]. The cellular protein p58IPK regulates PKR activity, with the influenza NP and M2 proteins modulating this regulation to their advantage (Guan, 2010; Sharma, 2011). The NP protein also reduces the formation of double-stranded RNA, which activates immune signaling pathways (van de Sandt, 2012). Ultimately, these interactions may lead to host cell apoptosis, enhancing viral release (Guan, 2010).

To further evade the immune response, influenza A viruses disrupt type I interferon receptor signaling by inducing the expression of suppressor of cytokine signaling (SOCS) proteins, causing disruption of JAK/STAT activity (Pothlichet, 2008). These proteins inhibit the activation of crucial immune signaling pathways, aiding the virus in immune evasion (Boliar, 2010; Mao, 2009).

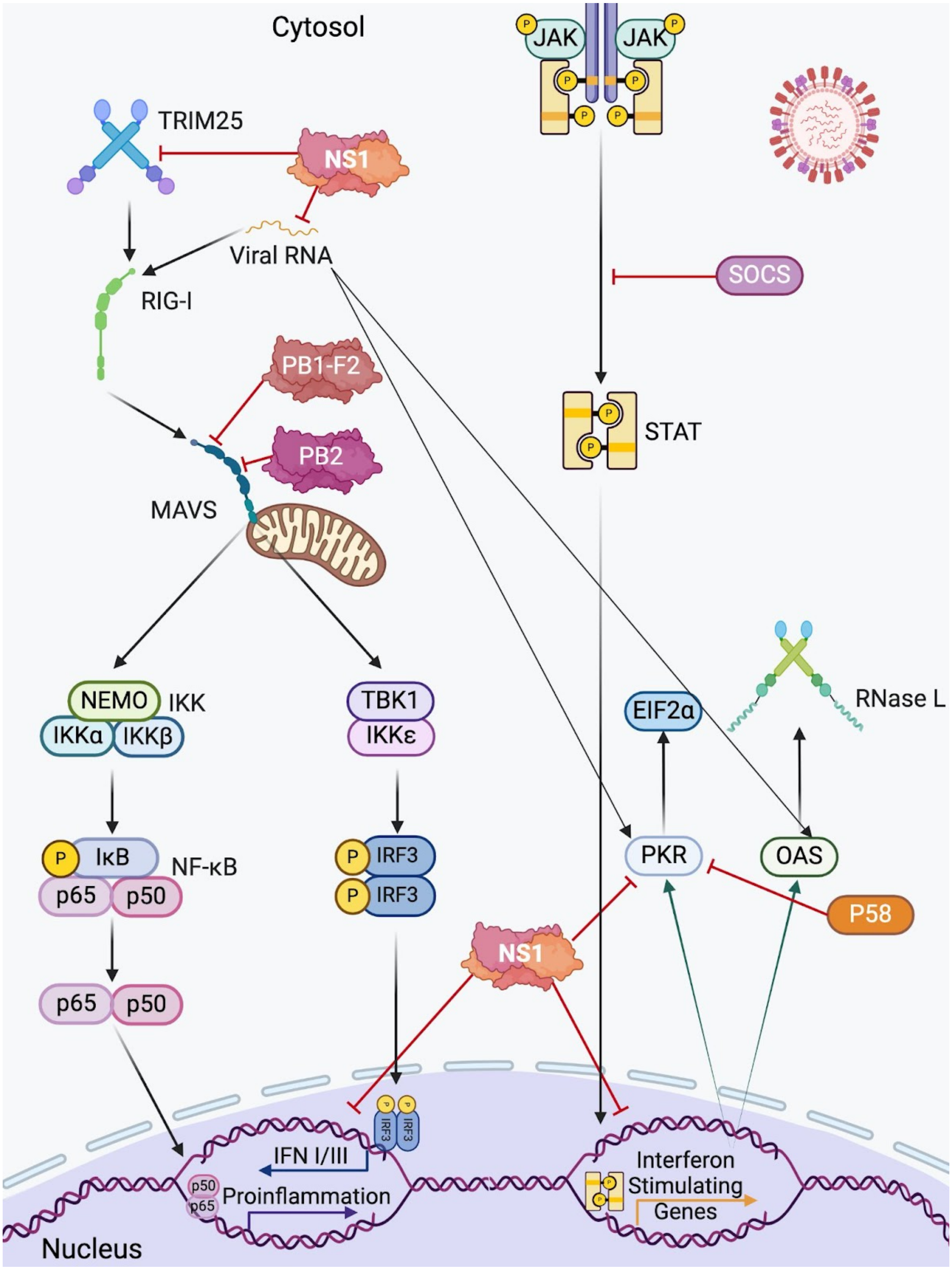
Cytosol
JAK
JAK
P
TRIM25
NS1
Viral RNA
RIG-I
SOCS
PB1-F2
PB2
MAVS
STAT
NEMO
IKK
IKKα
IKKβ
TBK1
IKKε
EIF2α
RNase L
P
IκB
NF-κB
p65
p50
IRF3
IRF3
PKR
OAS
P58
NS1
p65
p50
IFN I/III
p50
p65
Proinflammation
Interferon Stimulating Genes
Nucleus

**Figure 2.6 Depiction of IAV interference in antiviral immunity.** Detailed examination of the functions of NS1 protein within the cytoplasm and nuclei of infected cells reveals its crucial role as an interferon antagonist against the influenza virus. NS1 functions by inhibiting the induction of interferons at both pre-transcriptional and post-translational stages. This inhibition occurs through the blocking of RIG-I activation and the repression of antiviral properties of PKR and OAS/RNase L. During viral replication, the production of 5'-triphosphates ssRNA and dsRNA triggers conformational changes in the RIG-I receptor, leading to the exposure of CARDS that TRIM25 then ubiquitinates. Subsequently, RIG-I associates with MAVS, initiating a signaling cascade that activates transcription factors IRF3 and NF-κB, resulting in the transcription of IFN-β mRNA. The interference of NS1 in the transcription of ISGs prompts SOCS to intervene in STAT dimerization. Additionally, NS1 disrupts the processing and nuclear export of cellular mRNAs. The areas where IAV disrupts this pathway are highlighted with red lines for further clarification. *Adapted from García-Sastre A. Induction and evasion of type I interferon responses by influenza viruses. Virus Research 2011, Ji ZX, Wang XQ, Liu XF. NS1: A Key Protein in the "Game" Between Influenza A Virus and Host in Innate Immunity. Front Cell Infect Microbiol. 2021, and Kim HJ, Jeong MS, Jang SB. Structure and Activities of the NS1 Influenza Protein and Progress in the Development of Small-Molecule Drugs. International Journal of Molecular Sciences. 2021.*

Numerous factors contribute to the evasion of adaptive immune responses by influenza A viruses (van de Sandt, 2012). The lack of proofreading activity during viral RNA transcription by the RNA polymerase leads to errors and the incorporation of incorrect nucleotides (Smith, 2004), creating quasi-species with random mutations in the viral genome (De Jong, 2000). Antibodies developed in response to previous infections or vaccinations exert selective pressure on these quasi-species, favoring variants with amino acid substitutions in regions of the viral HA protein targeted by neutralizing antibodies (De Jong, 2000: Rambaut, 2008; Smith, 2004). This process, known as antigenic drift, enables the virus to avoid detection by antibodies and causes annual influenza epidemics (De Jong, 2000: Rambaut, 2008).

RNA viruses, including influenza, have small genomes and limited coding capacity but can evade T-cell recognition through high mutation rates and selective pressure from virus-specific T cells (Horst, 2011; van de Sandt, 2012). Mutations are more frequently found in CTL epitope regions of the influenza NP protein, indicating immune pressure on these sites (Berkhoff, 2007a; Berkhoff, 2007b; Rimmelzwaan, 2004; Voten, 2000).

Our understanding of how influenza viruses evade immune responses has greatly advanced, leading to the development of effective seasonal vaccines that reduce morbidity and mortality (van de Sandt, 2012). However, gaps remain in our knowledge, leaving room for improvement in developing vaccines with broader protection against diverse influenza strains.

### 2.2.4 Hyperinflammation in Antiviral Immunity

An endless battle ensues between cells and viruses within the biological realm. Viruses must infiltrate cells and take control of their processes to replicate, while cells possess an immune response tool to identify and eradicate viruses and other harmful pathogens. The initial defense against viruses is the innate immune response, which acts without bias towards any particular pathogen. A critical player in initiating the innate immune response is the type-I interferon (IFN-I) signaling pathway. This pathway begins with detecting viruses by internal sensors like PAMPS and PRRs within the cells and culminates in the production of IFNs. Respiratory viral infections like severe acute respiratory syndrome coronavirus 2 (SARS-CoV-2) and IAV result in distinct clinical outcomes determined by immunity-driven viral clearance or disease characterized by excessive and prolonged inflammation.

#### 2.2.4.1 Respiratory viruses that can cause hyperinflammation

Respiratory viruses encompass numerous viruses that target upper and lower respiratory tract cells. While most cases of mild respiratory virus infections are typically contained in the upper respiratory tract, individuals such as children, the elderly, those with weakened immune systems, and individuals with chronic illnesses are more susceptible to developing severe lower respiratory tract infections (LRTIs) compared to healthy individuals (Cerato, 2023). The most common respiratory viruses that lead to severe LRTIs include adenovirus, rhinovirus, IAV, respiratory syncytial virus (RSV), parainfluenza, and coronaviruses (Cerato, 2023; Schneider, 2014). Once these viruses reach the lower respiratory tract, they are identified by epithelial cells and resident alveolar macrophages through PRRs, activating the inflammasome (Pribul, 2008).

The inflammasome is a complex comprising multiple proteins, including a sensor, an adaptor, and an effector molecule (Cerato, 2023). Two signals are required to activate inflammasomes (Agostini, 2004; Mariathasan, 2004). The first signal, known as priming, is triggered by TLR activation or cytokine receptor signaling, leading to the activation of NF-κB and the production of inactive pro-IL-1β and inflammasome components (Agostini, 2004). The second activation signal is provided by various stimuli such as extracellular ATP, pore-forming toxins, and RNA viruses (Mariathasan, 2004).

Numerous respiratory viruses have been found to significantly activate inflammasomes. For instance, NLRP3 is activated in response to RSV, influenza, adenovirus, and coronavirus infections. Some viruses, like IAV, adenoviruses, and rhinoviruses, can be detected by multiple inflammasomes (Cerato, 2023). Research suggests that the activation of inflammasomes by respiratory viruses has both positive and negative effects. It plays a significant role in clearing the virus from the body but can also lead to severe disease (Malinczak, 2021; Thomas, 2009).

IAV is widely recognized as a primary stimulator of the NLRP3 inflammasome (Allen, 2009). Studies have demonstrated that infection with IAV triggers the NLRP3/caspase 1 pathway, leading to the secretion of IL-1β and IL-18 in bone marrow-derived macrophages (Kanneganti, 2006). Moreover, IAV activates the NLRP3 inflammasome in non-immune cells, such as lung fibroblasts and primary bronchial epithelial cells (Allen, 2009; Thomas, 2009). Research has revealed that NLRP3 can detect viral RNA during IAV infection in mice. It was observed that IAV infection resulted in elevated levels of IL-1β in the bronchoalveolar lavage (BAL) fluid of wild-type mice, while deficient mice lacking NLRP3, caspase 1, or apoptosis-associated speck-like proteins (ASC) showed decreased levels of this cytokine (Tate, 2016). This suggests the significant role of inflammasome proteins in the immune response against IAV (Cerato, 2023). Studies also indicated that mice lacking inflammasome proteins were more vulnerable to IAV infection than their wild-type counterparts, with increased morbidity attributed to reduced levels of inflammatory cytokines in BAL fluid, such as TNF and IL-6 (Allen, 2009).

Interestingly, the activation of NLRP3 can have beneficial or detrimental effects depending on the phase of IAV infection (Cerato, 2023). Additionally, the expression and activation of the AIM2 inflammasome has been reported in response to IAV. The AIM2 inflammasome is activated during infection and is crucial in IAV-induced lung damage and mortality (Zhang, 2017). Furthermore, persistent activation of NLRP3 following IAV infection led to excessive recruitment of inflammatory monocytes and lung pathology (Cerato, 2023). NLRP3-deficient mice also exhibited lung injury and decreased IL-1β production following IAV infection (Eicholz, 2016), suggesting secondary mechanisms at work.

The Human parainfluenza virus (HPIV) is a member of the paramyxovirus family and is known for causing severe respiratory illnesses such as bronchiolitis, pneumonia, and croup, particularly in young children (Fox, 2014). Similarly, the Human metapneumovirus (HMPV) belongs to the Pneumoviridae family and can lead to recurrent infections throughout life, with initial infections typically occurring before age 5. HMPV is a significant infectious agent responsible for respiratory illnesses, mainly posing a greater risk to young children and the elderly population (Schuster, 2014). Despite their impact, limited literature is available on these viruses, and their precise mechanisms remain largely unknown. Current knowledge suggests they target inflammasomes for activation (Cerasto, 2023; Lê, 2019; Shil, 2018).

RSV is responsible for a significant health burden in infants, individuals with compromised immune systems, and the elderly globally. RSV is the primary cause of hospital admissions due to viral bronchiolitis and pneumonia among children under the age of 5 (Nair, 2010). The progression of RSV infection involves a shift in the immune response towards a Th2 phenotype and the production of IL-1β (Tabarani, 2013). Activating the NLRP3 inflammasome and caspase 1 by RSV is essential for producing IL-1β, IL-33, and IL-18 during infection (Shim, 2015). Mechanistically, the inflammasome activation by RSV in human lung epithelial cells requires TLR4 as the initial signal, with the RSV small hydrophobic (SH) protein acting as the second trigger (Yoo, 2013). This protein, classified as a viroporin, may create pores or channels on the cell membrane (Triantafilou, 2013). In mouse bone marrow-derived macrophages infected with RSV, the assembly of the NLRP3/ASC inflammasome is mediated by reactive oxygen species (ROS) and the TLR2/MyD88/NF-κB pathway, leading to caspase-1 activation and IL-1β release (Lukacs, 2010: Stoppelenburg, 2014). These findings indicate that inflammasome activation can harm Th17 responses during RSV infection in both human and mouse models, contributing to airway immunopathology (Cerato, 2023).

Betacoronavirus viruses, specifically SARS-CoV and SARS-CoV-2, were responsible for the 2003 and 2019 pandemic outbreaks, respectively (de Almeida, 2022). These viruses can affect various tissues, such as the lungs, kidneys, and liver, potentially leading to multi-organ failure (Yan, 2020). It is suggested that the overactivity of inflammasomes and the excessive production of inflammatory cytokines, referred to as a cytokine storm, may contribute to acute respiratory distress syndrome (ARDS) in individuals infected with SARS-CoV-2 (Xian, 2021). Research indicates that the severity of COVID-19 outcomes is directly correlated with the extent of inflammasome activation (Rodrigues, 2019).

Severe COVID-19 patients have been found to have elevated levels of IL-1β, Casp1p20, IL-1RA, IL-18, and lactate dehydrogenase (LDH) in their plasma (Junquiera, 2022; Rodrigues, 2019). LDH, a cell death marker, may be released due to various cell death processes like necroptosis and NLRP3-mediated pyroptosis (Rodrigues, 2019). While some studies show inflammasome activation, others suggest that SARS-CoV-2 and its components may inhibit the expression and function of inflammasome-related proteins (Cerato, 2023). Recent research indicates that targeting inflammasome pathways could offer new therapeutic approaches for treating COVID-19, potentially reducing viral replication, lung damage, immune cell infiltration, and inflammatory cytokines in mouse models (Zeng, 2022).

Human rhinoviruses (HRVs) belong to the Picornaviridae family and Enterovirus genus members (Cerato, 2023). They are positive-stranded RNA viruses known to be the causative agents in 80% of cases of the common cold (Johnston, 1995). Additionally, HRVs have been linked to exacerbations of asthma and chronic obstructive pulmonary disease (COPD) throughout a person's lifetime (Cerato, 2023). In individuals with asthma, HRV infection has been associated with increased levels of caspase 1 and the upregulation of the AIM2 inflammasome (Menzel, 2017; Robinson, 2020). Furthermore, the HRV 2B protein functions as a calcium ion channel, activating the NLRP3 and NLRC5 inflammasomes (Liu, 2019). There is conflicting data regarding the effects of the inflammasome-derived cytokine IL-18, and further research is needed to clarify this issue (Cerato, 2023; Han, 2019; Han, 2020).

Adenoviruses are double-stranded DNA, nonenveloped viruses that typically cause mild infections of the respiratory tract, gastrointestinal tract, or conjunctiva (Lynch, 2016). More than 50 serotypes of adenoviruses are classified into seven species from A to G (Cerato, 2023). While children and adults can contract adenovirus infections, the disease tends to be more severe in individuals with compromised immune systems (Lynch, 2016). Through genetic manipulation, adenoviruses can induce pro-inflammatory cell death, specifically necroptosis and, to a lesser extent, pyroptosis (Barlan, 2011b; Ma, 2020). This unique ability has led to the exploration of adenoviruses as vectors for delivering various treatments and vaccines, prompting extensive research on the interaction between the virus and the innate immune system (Ma, 2020).

Studies have shown that adenoviruses can activate the NLRP3 inflammasome in a manner dependent on TLR9. The efficient activation of the inflammasome by adenoviruses requires the release of cathepsin B from the late endosome into the cytoplasm, with higher levels of lysosomal cathepsin B correlating with more robust NLRP3 activation. (Barlan, 2011b) Additionally, the production of reactive oxygen species is essential for the inflammasome activation induced by adenoviruses (Barlan, 2011a).

The human bocavirus (HBoV) is classified within the genus Bocaparvovirus in the family Parvoviridae and encompasses several serotypes (Kapoor, 2010). HBoV is commonly identified in young children experiencing acute respiratory tract illnesses (Cotmore, 2014). Symptoms of HBoV infection may range from typical cold symptoms to more severe conditions such as pneumonia and bronchiolitis (Uršič, 2011). An important challenge in studying HBoV is the absence of an animal model for infection, prompting researchers to utilize polarized human airway epithelium in an air-liquid interface in vitro (Deng, 2013; Dijkman, 2009). Consequently, the assessment of host immune factors involved in the pathogenesis of the disease is constrained due to the lack of an animal model (Deng, 2013).

Infection with HBoV1 triggers pyroptotic cell death in human airway epithelial cells by activating NLRP3 and caspase-1. Knockdown of NLRP3 or caspase-1, rather than caspase-3, significantly reduced the cell death induced by HBoV1 (Deng, 2017). Additionally, HBoV1 infection substantially increases the expression of IL-1α and IL-18. Notably, HBoV1 also upregulates anti-apoptotic genes, the silencing of which causes infected cells to undergo apoptosis (Deng, 2017). The authors propose that HBoV1 alters the mode of cell death from apoptosis to pyroptosis to promote persistent infection (Cerato, 2023).

Multiple outbreaks of respiratory tract infections occur annually. When individuals experience respiratory virus infections, inflammasomes detect the acute infection and trigger a robust pro-inflammatory response to contain the infection and prevent the further spread of the virus (Cerato, 2023). Also, inflammasome activation plays a role in repairing lung tissue damage and restoring balance in the body after infection-induced injury, as seen in Figure 2.8. However, excessive inflammasome activity can contribute to disease development and worsen outcomes following viral infections (Cerato, 2023). Recent research indicates that inflammasomes are time-dependent in respiratory viral infections. Early inflammasome activation is essential for clearing the virus, but uncontrolled activation later in the infection process can lead to harmful immune reactions (Cerato, 2023). Therefore, investigating the relationship between respiratory viruses and inflammasomes could pave the way for new research opportunities and the development of innovative therapies for these infections.

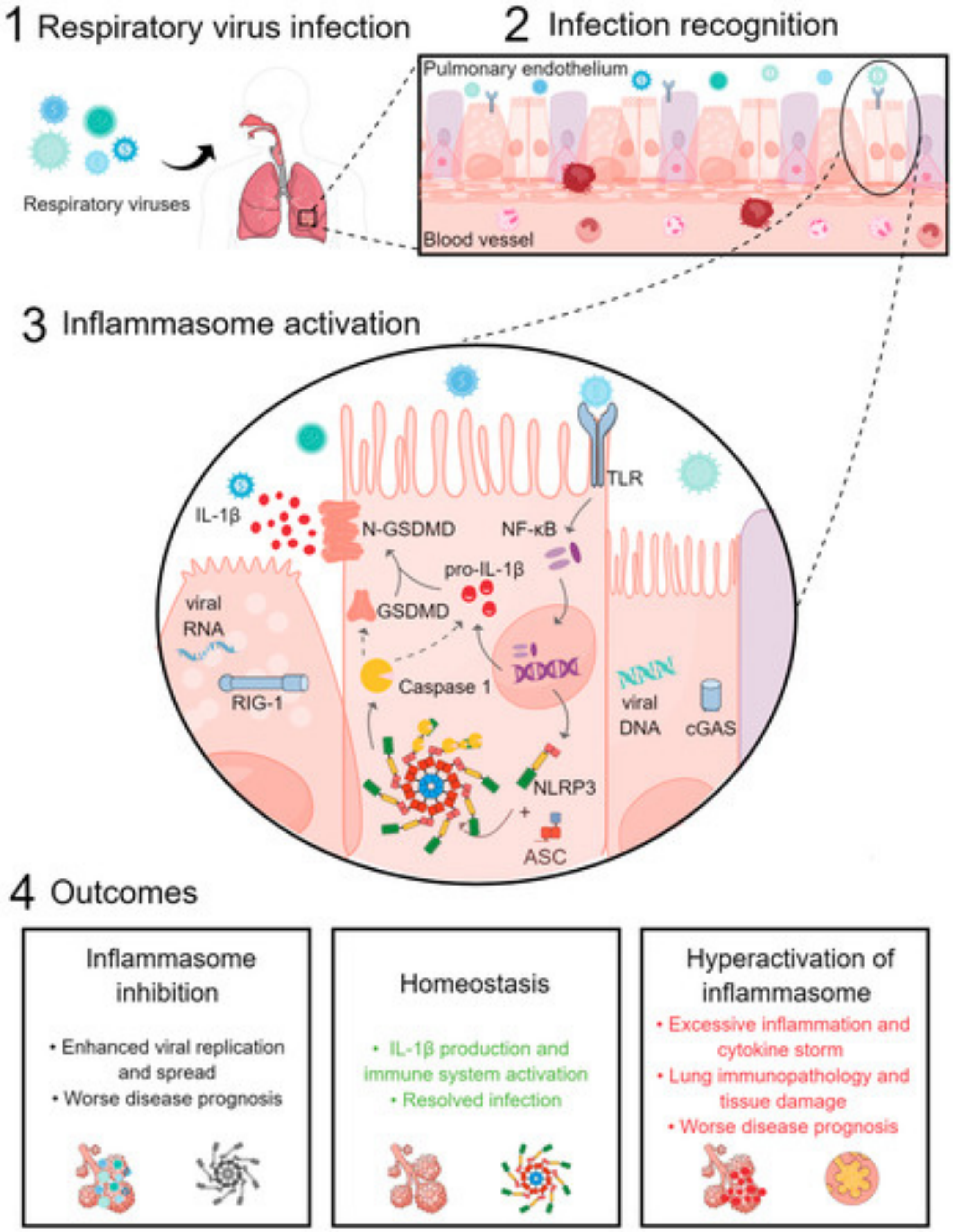
1 Respiratory virus infection
Respiratory viruses
2 Infection recognition
Pulmonary endothelium
Blood vessel
3 Inflammasome activation
TLR
IL-1β
N-GSDMD
NF-κB
pro-IL-1β
GSDMD
viral
RNA
RIG-1
Caspase 1
viral
DNA
cGAS
NLRP3
+
ASC
4 Outcomes
Inflammasome inhibition
• Enhanced viral replication and spread
• Worse disease prognosis
Homeostasis
• IL-1β production and immune system activation
• Resolved infection
Hyperactivation of inflammasome
• Excessive inflammation and cytokine storm
• Lung immunopathology and tissue damage
• Worse disease prognosis

**Figure 2.7. Inflammasome activation by respiratory viruses.** 1) Upon entry into the airways, these viruses interact with respiratory 2) epithelial cells and alveolar macrophages, triggering recognition of pathogen-associated molecular patterns by innate sensors. 3) This recognition leads to activation of the NF-kB pathway via TLR receptors, resulting in the up-regulation of NLRP3 and pro-IL-1β. Subsequent formation of the inflammasome complex, through binding to ASC and cleavage of caspase-1, leads to the release of IL-1β through membrane pores formed by cleaved GSDMD. Further, inflammasome activation can occur through cGAS and RIG-1 receptors, which recognize viral DNA and RNA. 4) The outcomes of inflammasome activation vary, with inhibition by the virus resulting in unchecked replication and disease progression in the host. Conversely, proper activation leads to IL-1 β production and activation of an immune response, aiding in infection resolution and restoration of lung homeostasis. However, hyperactivation of the inflammasome can lead to excessive inflammation, cytokine storm, lung immunopathology, tissue damage, and worsened disease outcomes. *The image was taken from Cerato JA, da Silva EF, and Porto BN. Breaking Bad: Inflammasome Activation by Respiratory Viruses. Biology (Basel). 2023 Jul 1;12(7):943.*

**Table 2.6 Respiratory virus proteins that activate inflammasomes**

| **Virus** | **Serotype** | **Activator** | **Inflammasome** |
|---|---|---|---|
| Adenovirus | Ad5 | Protein VI | AIM2 |
| | | dsRNA | NLRP3 |
| | | dsRNA | cGas/ STING-NLRP3 |
| | | vRNA | NLRP3 |
| Bocavirus | N/A | vRNA | NLRP3 |
| Influenza | IAV | dsRNA | AIM2 |

table continued

| | | | |
|---|---|---|---|
| | IAV | M2 protein | NLRP3 |
| Parainfluenza | N/A | Viral particle | TLR2/ NLRP3 |
| Metapneumovirus | N/A | HMPV SH | NLRP3 |
| Respiratory syncytial virus | N/A | Viroporin SH | NLRP3 |
| Coronavirus | SARS-CoV | Spike | NLRP3 |
| | | ORF3a | NLRP3/ RIPK3 |
| | | ORF8b | NLRP3 |
| | SARS-CoV-2 | Envelope | NLRP3 |
| | | ORF3a | NLRP3 |
| | | Nucleocapsid | NLRP3 |
| | | NS6 | NLRP3 |
| | | Spike | NLRP3 |
| | | NS5 | NLRP3 |
| Rhinovirus | HRV | 2B | NLRP3/ NLRC5 |
| | | 3C | NLRP1 |

HMPV SH: small hydrophobic protein; NS: non-structural protein; ORF: open reading frame. *The table was adapted from Cerato JA, da Silva EF, and Porto BN. Breaking Bad: Inflammasome Activation by Respiratory Viruses. Biology (Basel). 2023 Jul 1;12(7):943.*

### 2.2.4.2 Cells that can cause antiviral induced hyperinflammation

Various types of cells have been shown to respond to viral infections. However, some go beyond the normal response and produce a tissue-damaging response known as hyperinflammation or, recently, a cytokine storm. This section will focus on these cell types, the mechanisms, and viruses that cause these seemingly normal cell responses to go haywire.

Monocytes and macrophages are susceptible to causing hyperinflammation in coronavirus infections. The bronchoalveolar fluid (BALF) obtained from individuals suffering from severe cases of COVID-19 revealed an abundance of CCL2 and CCL7 chemokines, known for their efficacy in attracting monocytes expressing CCR2 (Zhou, 2020). Macrophages harboring SARS-CoV-2 viral components were found to exhibit interleukin-6 (IL-6) expression, with the presence of IL-6+ macrophages correlating with a significant reduction in lymphocytes within the spleen and lymph nodes (Channappanavar, 2017). In patients with COVID-19, CD68+NP+ macrophages were also observed in the kidneys, with acute tubular damage linked to notable accumulation of monocytes and macrophages (Hadjadj, 2020). Post-mortem examination of lung tissues from these patients revealed substantial infiltration by macrophages (Xu, 2020).

A comparable disease progression to that observed in SARS-CoV-2 infection has been documented in cases involving other extremely pathogenic coronaviruses like SARS-CoV and MERS-CoV, wherein 20% of patients eventually develop acute respiratory distress syndrome (ARDS) leading to fatality (Merad, 2020). Similar to findings in SARS-CoV-2 cases, elevated levels of interferon-γ (IFNγ), IL-6, IL-12, transforming growth factor-β (TGFβ), CCL2, CXCL10, CXCL9, and IL-8 were reported in individuals infected with SARS-CoV (Guan, 2020; Merad, 2020).

Neutrophils comprise a diverse population that significantly impacts the host immune response through their interactions with pathogens and other immune cells (Rawat, 2021). Neutrophils can be found throughout the host in blood and tissues. They can travel to where they are needed when required. Often, they can be found combating severe respiratory viruses (Ma, 2021). Neutrophils in the lungs can aid in combating infections and elicit antiviral immune responses during acute viral infections (Tate, 2009). However, excessive neutrophil infiltration can have detrimental effects, such as increased mucus production and edema, potentially leading to airway obstruction and severe clinical consequences (Wang, 2019).

Studies have shown that neutrophils recruited to the lungs within two days of IAV infection are crucial in clearing the virus, recruiting effector CD8+ T cells, and mitigating disease severity (Lim, 2015; Tate, 2009). Interestingly, the extent of neutrophil infiltration in response to IAV varies based on the virus's pathogenicity and the infection dose (Tate, 2011). Additionally, elevated lung neutrophil levels are associated with severe RSV disease in both animal models and humans (Goritzka, 2015). Although neutrophils respond to many different types of viruses, there is insufficient evidence to suggest a correlation between specific neutrophil functions and the type of virus involved. The activation of neutrophils and the complications associated with neutrophil extracellular traps (NETs) may vary depending on the virus, the primary site of infection, and the host's immune response (Rawat, 2021).

Natural killer (NK) cells are part of the adaptive immune response from the same lymphoid progenitor cells that give rise to B and T-cells. NK cells are known to respond to infections quickly to prevent disease spreading. Flaviviruses, such as dengue virus (DENV), West Nile virus, Japanese encephalitis virus, tick-borne encephalitis virus, yellow fever virus, and Zika virus, are significant emerging human pathogens that impact millions globally. These viruses can cause hemorrhagic fever-like syndromes and diseases of the central nervous system in infected individuals (Gould, 2008). NK cells respond to these infections to limit their spread. Despite this knowledge, there remains a lack of information regarding which flaviviruses in humans target specific host cells and whether they are susceptible to NK cell responses (Björkström, 2022).

Research on innate immune responses to flaviviruses has primarily been conducted in animal models, focusing on infections like DENV and Zika virus (Nelmans, 2019). Several studies have indicated that $CD56^{bright}$ NK cells and certain subpopulations of less differentiated $CD56^{dim}$ NK cells have shown robust responses to various flavivirus infections (Marquardt, 2015; Zimmer, 2019). Type I and type III interferons are believed to contribute to the NK cell responses observed in infections such as yellow fever virus. Despite these findings, there is a noticeable gap in research specifically dedicated to understanding the role of NK cells in acute flavivirus infections (Marquardt, 2015). Further exploration and study in this area could provide valuable insights into how NK cells contribute to the immune response against these viral pathogens.

Similarly, during IAV infection, a complex interplay of immune responses can lead to excessive inflammation and tissue damage (Björkström, 2022). NK cells are implicated in this process, as evidenced by their increased presence in the lungs following infection with IAV in mice. The recruitment of NK cells to the lungs and airways during IAV infection relies on specific chemokine receptors, namely CXCR3 and CCR5 (Carlin, 2018). Additionally, certain natural cytotoxicity receptors on NK cells are thought to be involved in their functional activation upon encountering IAV particles (Luczo, 2021). Nevertheless, the precise extent of NK cell involvement in eliminating influenza virus remains to be fully elucidated. Overall, the complex interactions between NK cells flavivirus/ IAV highlight the importance of further research to understand better the role of NK cells in host defense mechanisms against viral infections, including influenza (Björkström, 2022).

T-cells have evolved to have many functions in a host’s antiviral response. Memory T-cells are one such cell type that can be generated through natural infection or vaccination (Wherry, 2022). The T-cell bystander population generates another function; they can self-activate (Shim, 2022). Numerous well-characterized proinflammatory signals known to induce T-cell bystander activation include cytokines such as type I IFN, IL-12, IL-15, and IL-18, TLRs, particularly TLR2, and recently reported complement proteins (Yunnis, 2022). Xie et al. identified a potential role for IL-2 and CD25 in supporting the development and/or expansion of bystander-activated CD8+ T cells. Their study observed higher frequencies of CD38+KI67+PD-1+ CD8+ T cells expressing CD25 in bronchoalveolar lavage fluid from severe COVID-19 patients compared to those with mild infection (Xie, 2021).

Research by Kedzierska and team focused on mouse models of A/H9N2, A/H7N9, and A/H3N2 infection. They found that influenza-specific immunodominant DbNP366+CD8+ T cells and non-IAV-specific CD8+ T cells, both detected by tetramers, exhibited CD38+MHC-II+ or CD38+PD-1+ markers in bronchoalveolar lavage and lymphoid tissues. These CD8+ T cell populations expanded early during infection, and their frequency increased in a dose-dependent manner. They contributed to severe disease and premature death in mice (Jia, 2021). In H7N9 infections in humans, patients with early induction of CD38+HLA-DR+PD-1+ CD8+ T cells survived, whereas patients with persistent expansion of this population suffered from severe disease and succumbed to the infection (Wang, 2018).

It is essential to note that pathogen-activated and bystander-activated T cells may exhibit different functions in respiratory virus infections. While Type I IFN can effectively trigger bystander CD8+ T-cell activation, the activation and expansion are antigen-independent, whereas cytotoxicity is antigen-dependent (Kohlmeir, 2010). This suggests activating bystander T-cells could heighten inflammation (Yunis, 2023). However, there is currently insufficient conclusive evidence to determine the extent to which bystander-activated T cells contribute to mortality in individuals infected with SARS-CoV-2 or IAV.

#### 2.2.4.3 Non-coding RNAs involved in antiviral hyperinflammation

Non-coding RNAs (ncRNAs) refer to a class of RNAs that do not undergo translation into proteins or peptides (Menon, 2020). There are many types of RNAs, but the focus will be on ncRNAs involved in hyperinflammation. Research has indicated that certain microRNAs (miRNAs) can impede NLRP3 activation (Feng, 2021; Zhou, 2016). However, there is conflicting information in the scientific literature regarding the expression of miRNAs during respiratory virus infections (Cerato, 2023). For example, the increased expression of miR-7 during influenza A virus infection has been linked to the suppression of inflammatory and antiviral proteins, with potential implications for impeding NLRP3 inflammasome assembly (Głobińska, 2014; Zhou, 2016). Conversely, the downregulation of miR-22 in critically ill influenza A/H1N1 virus patients, as compared to those with mild illness, may lead to heightened NLRP3 activity and an increase in pro-inflammatory cytokines, ultimately contributing to severe lung damage and illness severity (Feng, 2021; Morán, 2015).

Long non-coding RNAs (lncRNAs) are crucial in regulating RNA transduction, gene expression, chromatin remodeling, and post-transcriptional processes (Menon, 2020). Two specific lncRNAs, nuclear-enriched abundant transcript 1 (NEAT1) and metastasis-associated lung adenocarcinoma transcript-1 (MALAT1), have been associated with respiratory diseases. Both NEAT1 and MALAT1 exhibit overexpression in severe cases of COVID-19 (Huang, 2022). Functionally, NEAT1 can be found in the cytoplasm, where it interacts with ASC to stabilize caspase 1, facilitating inflammasome complex formation and fostering a pro-inflammatory environment (Hirose, 2014; Menon, 2020; Zhang, 2019). NEAT-1 has also been shown to activate NLRC4 and AIM2 inflammasomes (Zhang, 2019). On the other hand, MALAT-1 acts as a competing endogenous RNA, inhibiting certain miRNAs that have been implicated in suppressing

NLRP3. Consequently, it is feasible to suggest that by antagonizing these miRNAs, MALAT-1 indirectly promotes NLRP3 activation. Despite limited research on the impact of ncRNAs on inflammasome pathways during respiratory virus infections, it presents a promising area for future investigation.

#### 2.2.4.4. Current treatments and vaccines for IAV

Influenza is a highly transmissible respiratory illness caused by influenza viruses that poses a significant public health challenge. Complications like bacterial pneumonia and cytokine storms can complicate treatment (Li, 2024). Vaccinating before the flu season and/ or promptly addressing influenza infections is essential to prevent the development of new strains or pandemics, especially in severely ill patients (Li, 2024; Wong, 2013). Various FDA-approved antiviral drugs for influenza are categorized based on their mechanisms of action (Li, 2024). These drugs, including entry inhibitors like HA and M2 inhibitors, target different aspects of the virus to inhibit replication (Jing, 2008; Zeng, 2017). While some older drugs like amantadine are no longer recommended due to resistance issues, newer options like Baloxavir marboxil, which targets the PA subunit preventing viral mRNA transcription, offer innovative ways to combat the virus (CDC, 2024; O’Hanlan, 2019).

NA inhibitors, such as zanamivir, oseltamivir, and peramivir, target the neuraminidase enzyme to prevent viral replication and spread (Babu, 2000; Kim, 1997). These drugs are effective when taken within the first two days of infection (Li, 2024). While each drug has its own administration method and considerations, they all play a crucial role in treating and preventing influenza infections. The current FDA-approved drugs require timely usage in managing influenza infections and reducing the risk of severe complications (Li, 2024). Proper utilization of these drugs can help mitigate the impact of influenza on individuals and communities (WHO, 2023).

In humans, the seasonal influenza vaccine is designed to protect against endemic H1N1, H3N2, and B strains that are circulating worldwide (Wong, 2013). The objectives of influenza vaccination can be broadly defined into two main categories: (i) preventing infection and disease and (ii) promoting herd immunity to reduce virus transmission within the population (Salk, 1997). Due to the short-lived antibody response generated by influenza vaccines, annual vaccination before the onset of winter seasons is recommended (Song, 2010). This presents challenges for tropical regions where influenza seasons are less defined (Cheong, 2009).

The most commonly used seasonal influenza vaccine is the trivalent inactivated vaccine (TIV). This traditional vaccine contains the three current seasonal influenza virus strains: two influenza A viruses (H3N2 and H1N1) and a B type (Wong, 2013). The vaccine is available in whole-virus, split, or subunit. These vaccines are typically produced using embryonated chicken eggs, with each virus type inoculated separately (Wong, 2013). The manufacturing process involves chemical inactivation, concentration, and purification to remove nonviral protein contaminants (Duxbury, 1968). In split-virus vaccines, an additional step with detergent is employed to expose all viral proteins and subviral elements (Laver, 1976). Subunit vaccines undergo further purification to enrich the HA protein (Bachmayer, 1976).

The live attenuated influenza vaccine (LAIV) was developed to mimic natural infection, potentially inducing cellular and humoral immunity (Wong, 2013). Attenuated influenza viruses were created in the 1960s through serial passage in eggs under suboptimal conditions (Massab, 1967). These viruses, known as master donor strains, were adapted to grow at nasal passage temperature but not at respiratory tract temperature (Massab, 1999). Master donor strains contribute internal genes to generate vaccine strains with desired HA and NA genes through classical reassortment or reverse genetics (Massab,1990). Various strategies have been developed to generate attenuated viruses through molecular manipulations of internal genes (Talon, 2000). However, due to the risk of immunizing with live viruses, LAIV is not recommended for immunocompromised individuals or close contacts (Wong, 2013).

For conventional influenza vaccines to be most effective, the vaccine viruses must be antigenically matched to circulating influenza viruses (Wong, 2013). The most suitable vaccine strains are identified through global surveillance led by the World Health Organization (WHO) via its Global Influenza Surveillance and Response System (GISRS) network (Barr, 2010). The selection of vaccine strains is a critical step in manufacturing, and they are susceptible to challenges such as continuous egg supply, virus growth, and regulatory compliance (Gerdil, 2003). Manufacturers must also meet strict biosafety and sterility requirements to ensure vaccine quality (Wong, 2013). The success of influenza vaccination campaigns relies on extensive surveillance and manufacturing resources for timely vaccine delivery (Barr, 2010). Given that vaccine components are updated every 2 to 3 years on average, occasional issues may arise (Wong, 2013).

Despite science's best efforts, IAV can adapt to drug therapeutics. Tang et al. described a drug-resistant strain of IAV that was difficult to treat. Additionally, taking an antiviral is only helpful if it is done two days post-infection (Lempejo, 2020). Many people don’t go to the doctor in the US unless they have to, meaning they often miss out on that time frame. Vaccination is also a major challenge due to the lottery of IV strains, low vaccination rates, and inherent issues with manufacturing (Wong, 2013). As long as the flu exists, there will need to be treatments for it. The ideal situation would be to increase surveillance to improve vaccines and study the hosts’ response to the flu to develop alternative treatments.

### 2.3. Neutrophils

Neutrophils are recognized as the initial immune cells recruited to inflamed tissues or sites of infection. They are the most abundant white blood cells in the human body and are traditionally known to play a crucial role in acute inflammatory responses. During infections or trauma, inflammation is necessary to protect the host from external pathogens and to facilitate the repair of damaged tissues. In such acute and self-limiting situations, inflammation is viewed as beneficial in restoring tissue balance.

#### 2.3.1. Introduction

The vital immune functions and short lifespan of neutrophils necessitate their continuous production in the bone marrow, known as granulopoiesis (Dancey, 1976). Granulopoiesis heavily relies on the cytokine G-CSF, which operates at various levels to regulate the production of neutrophils (Semerad, 2002). G-CSF stimulates the expression of transcription factors such as PU.1 and CCAAT/enhancer-binding protein-β (C/EBPβ) in myeloid progenitors, promoting differentiation towards the granulocytic lineage (Soehnlein, 2017). Additionally, G-CSF controls the release of neutrophils into the bloodstream, particularly during acute demand (Semerad, 2002). By inhibiting the CXCR4-CXCL12 axis, G-CSF facilitates the mobilization of neutrophils from the bone marrow into the blood (Köhler, 2011). Furthermore, G-CSF enhances neutrophil mobilization by stimulating the production of CXCL1 by megakaryocytes and endothelial cells, which attracts neutrophils through CXCR2 signaling (Bajrami, 2016).

Recent research has discovered a reservoir of neutrophils naturally harbored in the microvasculature of the mouse lung, which can be mobilized into circulation by inhibiting CXCR4 (Devi, 2013). Furthermore, hematopoietic progenitors present in the bloodstream of healthy mice can accumulate in infected tissues and differentiate into fully functional neutrophils, expediting the response to infections by providing a local supply of precursors or mature neutrophils (Swirski, 2009).

Neutrophils are known for their diverse functions, including their capacity to interact with other cells through various mediators. They maintain close interactions with platelets, monocytes, dendritic cells, and different subsets of lymphocytes in circulation, at sites of inflammation, and in lymphatic tissues (Soehnlein, 2017). Neutrophils and platelets are rapidly activated upon the onset of inflammation through coordinated processes that regulate inflammation within the blood vessels and surrounding tissues (Abdulnour, 2014). Platelets activate neutrophils by releasing soluble mediators, with chemokines like CCL5 and CXCL4 playing essential roles in the bloodstream. The release of soluble mediators, combined with neutrophil integrin ligation, leads to luminal NETs to combat pathogens (Rossaint, 2014).

Recent studies have shed light on mechanisms by which neutrophils contribute to the shift from neutrophilic to monocytic recruitment (Mokart, 2006). During their movement from the bloodstream into tissues, neutrophils deposit granule proteins that attract monocytes (Ortega-Gomez, 2016). The collaboration between neutrophils, monocytes, and platelets has been highlighted, particularly in promoting communication between innate and adaptive immune cells in specialized environments like secondary lymphoid organs (Hampton, 2015). Studies have demonstrated the infiltration of neutrophils into lymph nodes through different pathways, providing them access to the adaptive immune system cells (Gorlino, 2014; Hampton, 2015).

### 2.3.2. Roles of neutrophils in pathogen response

Upon entry into tissues, neutrophils navigate chemoattractant gradients to reach areas of infection or inflammation. Chemokines, such as CXCL8 (IL-8 in humans) or its mouse analog CXCL1, CXCL2 (macrophage-inflammatory protein 2 [MIP-2]), and CXCL5, serve as attractants for neutrophils (Selders, 2017). As neutrophils travel toward affected sites, they must maneuver through the extracellular matrix (ECM), interacting with proteins like collagen, laminin, fibronectin, and fibrinogen, which provide regulatory signals to the cells (Köhler, 2011).

Neutrophils migrate from the bloodstream to infection sites, deploying various antimicrobial strategies against a wide range of pathogens, including bacteria, fungi, and protozoa (Abbas, 2022). These mechanisms include degranulation, reactive oxygen species (ROS) production, phagocytosis, and NET formation (Rosales, 2020).

#### 2.3.2.1. Methods of pathogen clearance by neutrophils

Upon encountering microorganisms, neutrophils must mount a swift defense (Selders, 2017). They rely on four antimicrobial mechanisms (Figure 2.9) to mount a defense: degranulation, NETosis, phagocytosis, and ROS (Rosales, 2020). The degranulation process relies on pre-existing effector molecules stored in their intracellular granules, which fall into four categories: primary (azurophil) granules containing proteins like myeloperoxidase (MPO), neutrophil elastase (NE), azuracidin, and defensins; secondary (specific) granules containing lactoferrin, cathelicidin, and metalloproteinases; tertiary (gelatinase) granules containing matrix metalloproteinase 9 (MMP9) for ECM protein degradation; and secretory granules containing serum albumin and cytokines (Lacy, 2008; Soehnlein, 2009). Neutrophil degranulation is a tightly regulated process involving different types of granules released in a specific order (Rosales, 2020).

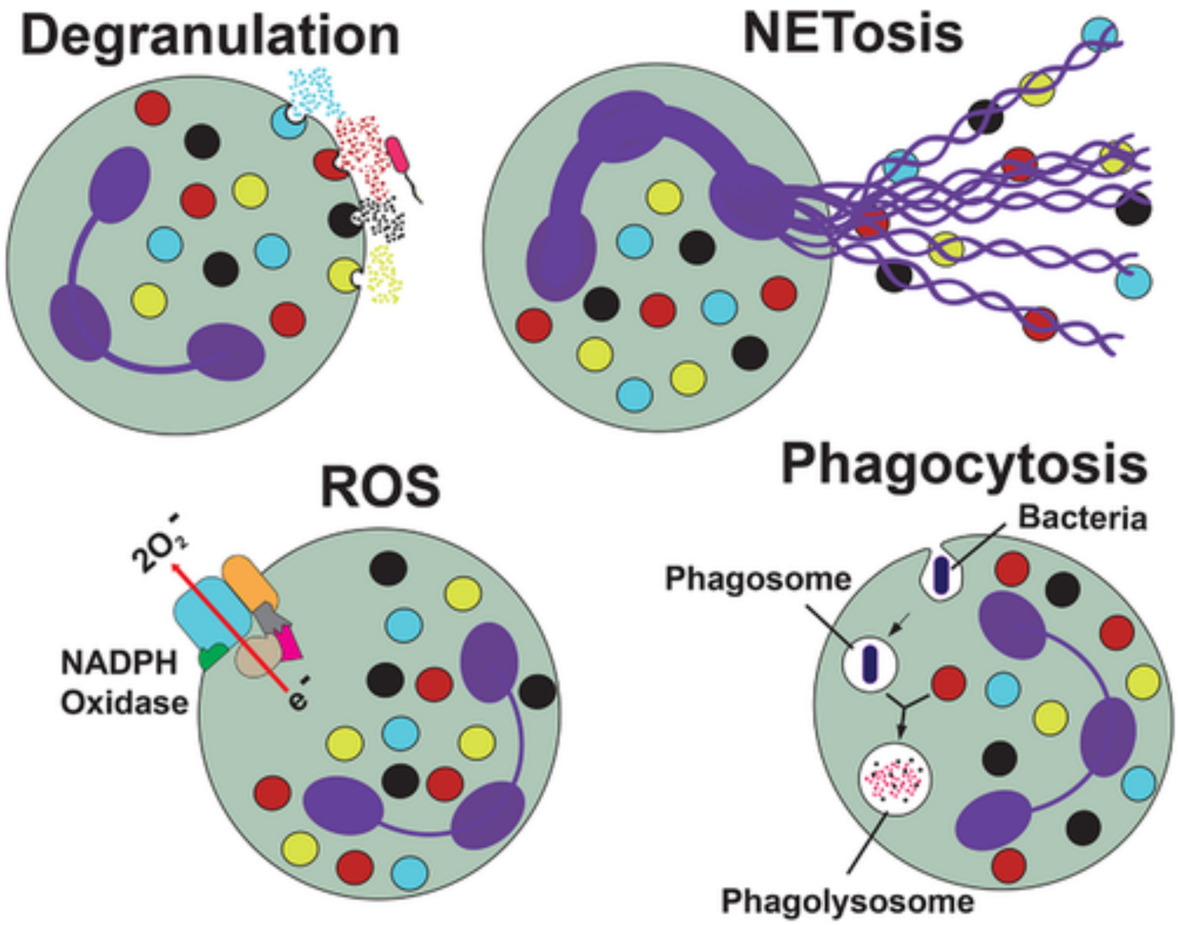

**Figure 2.8. The antimicrobial mechanisms of neutrophils involve a series of protective actions to eliminate microbial pathogens.** When neutrophils detect such threats, they utilize various functions to neutralize them. One such function is degranulation, where neutrophils release the contents of their granules into the surrounding environment. These substances are predominantly microbicidal in nature. Additionally, neutrophils can activate the enzymatic complex known as NADPH oxidase, enabling them to generate high levels of ROS like hydrogen peroxide ($O_2^-$), which are extremely harmful to many microorganisms. Another mechanism neutrophil employs is phagocytosis, where the microorganism is engulfed and enclosed within a phagocytic vacuole that later matures into a phagolysosome. The microorganism is efficiently eradicated within this specialized organelle through low pH levels and powerful degrading enzymes. When the microorganism is too large to be engulfed through phagocytosis, neutrophils

can undergo an alternative process known as NETosis. This produces extracellular traps of DNA fibers and proteins originating from the neutrophil's granules. *Image taken from Rosales C. Neutrophils at the crossroads of innate and adaptive immunity. J Leukoc Biol. 2020 Jul;108(1):377-396.*

While secretory vesicles and tertiary granules degranulate swiftly, azurophilic granules require the priming of neutrophils. Neutrophils in circulation are typically resting to prevent accidental release of granule contents and tissue damage. Priming involves transitioning a neutrophil from this resting state to a state of heightened readiness for efficient responses to activating stimuli, such as exposure to proinflammatory cytokines, chemokines, or microbial products. Primed neutrophils exhibit increased generation of ROS by the NADPH oxidase, which is essential for regulating degranulation and preventing excessive release of granule contents.

An additional method for eliminating microorganisms involves the production of Reactive Oxygen Species (ROS). Neutrophils activate the NADPH oxidase to produce large quantities of superoxide, a precursor to other forms of ROS with strong antimicrobial properties. ROS can permeate the membranes of bacterial pathogens and damage their nucleic acids, proteins, and cell membranes. Section 2.3.2.1 will provide further discussion on neutrophil ROS.

Phagocytosis is a receptor-mediated process in which the cell internalizes a particle larger than 0.5 μm into a vacuole known as the phagosome. Neutrophils identify pathogens through PAMPs or opsonins (antibodies or complement components). Activation of phagocytic receptors triggers signaling cascades that alter the actin cytoskeleton and induce lipid modifications in the cell membrane to envelop the particle and form the phagosome. The early phagosome later fuses with vesicles from the Golgi complex or the endoplasmic reticulum to create an intermediary phagosome, which merges with endocytic vesicles and releases secretory vesicles. This dynamic process remodels the membrane composition, reduces the pH of the phagosome, and eventually leads to the formation of the microbicidal phagolysosome. The NADPH oxidase is then recruited to the phagosomal membrane to initiate ROS production, while the pH inside the phagosome drops to 4.5–5. Furthermore, potassium ions are pumped into the phagolysosome to facilitate the release of serine proteases, and $H_2O_2$ is transformed into HOCl by MPX, which exhibits potent bactericidal properties. The interior of the phagolysosome becomes a hostile environment for the ingested pathogen.

Neutrophils also combat the spread of infections by forming Neutrophil Extracellular Traps (NET). NETosis is a programmed cell death process in neutrophils that is responsible for generating NET. Once deployed, NETs act as a physical barrier to trap pathogens, allowing their extracellular elimination independent of phagocytosis. Various microbes, including bacteria, fungi, protozoan parasites, and even viruses, have been found to induce NET formation. Therefore, NET is considered a beneficial neutrophil response that aids in controlling the dissemination of infectious microorganisms.

#### 2.3.2.2. Respiratory burst response

ROS generated by NADPH oxidase plays a crucial role in the host's defense against microbes and inflammation. The targeted release of ROS in phagosomes containing pathogens helps eliminate invading bacteria while minimizing tissue damage. Immune cells, such as neutrophils (PMNs), release significant amounts of ROS at infection sites upon activation of surface receptors. Priming these cells with ligands for G-protein-coupled receptors, toll-like receptors, and cytokine receptors can enhance their response to subsequent signals. Moreover, activation of Fc and integrin receptors directly stimulates high levels of ROS production. Neutrophil chemoattractant GPCRs binding to bacterial-peptide analog fMLP can prime cells for a robust response and trigger low levels of ROS production. Activation of these receptors initiates intracellular signaling pathways that activate downstream effector proteins, assemble the NADPH oxidase complex, and ultimately produce ROS.

Inactive in resting cells, NADPH components become activated in response to pro-inflammatory mediators, microbial presence, phagocytosis, or pattern recognition receptor activation. The phox complex comprising five subunits (Figure 2.10) - gp91phox, p22phox, p40phox, p47phox, and p67phox - generates superoxide by transferring electrons from NADPH across the membrane to $O_2$. Neutrophils express various receptors recognizing pathogens and inflammatory signals upon infection, triggering intracellular signaling pathways supporting antimicrobial responses and inflammation. Fc receptors enable antibody-opsonized pathogen recognition and phagocytosis, while integrin receptors contribute to ROS production.

NADPH oxidase activation leads to the complex's assembly and activation, involving translocation of cytosolic components and phosphorylation. Small G proteins, particularly Rac proteins (Rac1, Rac2, Rac3), regulate NADPH oxidase activity. Rac2 interaction with cytb558 is crucial for electron transfer, and Rac1/Rac2 binding to p67phox facilitates oxidative burst. The respiratory burst response involves superoxide dismutation to hydrogen peroxide, which can then form hydroxyl radicals through the Fenton reaction. Myeloperoxidase in neutrophils converts hydrogen peroxide to hypochlorous acid, potentially enhancing pathogen clearance.

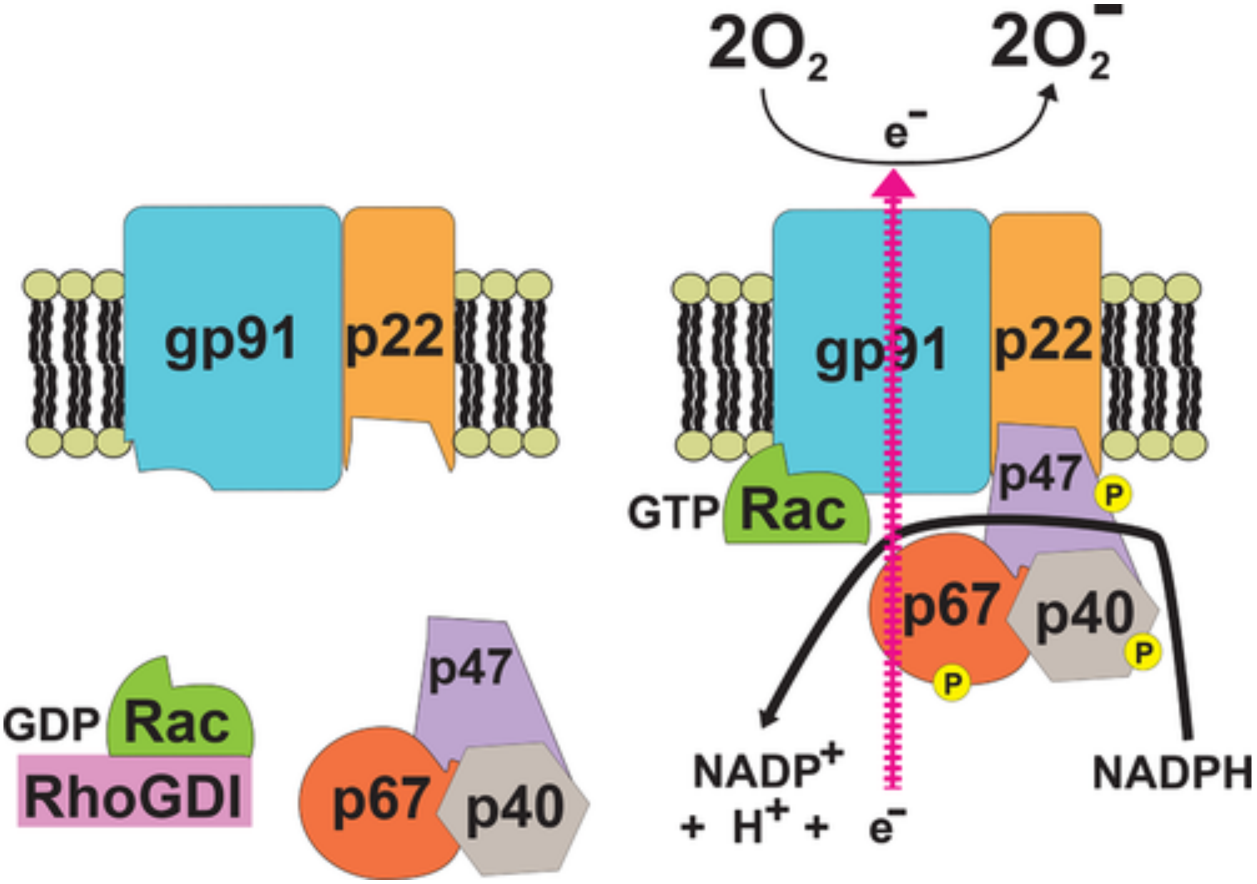

**Figure 2.9. The neutrophil NADPH oxidase complex.** The NADPH oxidase complex found in neutrophils is a critical component that generates superoxide to aid the immune response. This complex consists of two membrane-bound subunits, gp91phox, and p22phox, along with three cytosolic regulatory subunits - p67phox, p47phox, and p40phox. The three regulatory subunits form a trimer within the cytosol of resting neutrophils. The membrane-bound heterodimer is known as flavocytochromeb558. Also, when activated, the GTPase Rac plays a role in the oxidase complex. Prior to activation, Rac is localized in the cytosol bound to Rho GDP-dissociation inhibitor. Upon activation, cellular kinases trigger the phosphorylation of the cytosolic subunits, allowing them to move to the membrane along with the activated form of Rac, bound to GTP. This assembly forms an active enzymatic complex, transferring electrons derived from NADPH to

oxygen, producing superoxide. *Image taken from Rosales C. Neutrophils at the crossroads of innate and adaptive immunity. J Leukoc Biol. 2020 Jul;108(1):377-396.*

### 2.3.2.3. Neutrophil diseases

Immunodeficiency diseases offer a unique perspective on both typical physiological functions and pathogenic mechanisms. Regarding aberrant neutrophil function in humans, immunodeficiency resulting from abnormalities in neutrophil quantity or function is quite prevalent, affecting roughly 20% of individuals with congenital primary immunodeficiency disorders (Leiding, 2017). Disorders affecting neutrophils can be categorized into four types: neutrophil numbers, neutrophil granules, neutrophil movement towards chemical signals, and neutrophil ability to eliminate pathogens (Bousfiha, 2015).

One category of neutrophil disorders is neutropenia, a medical condition characterized by an abnormally low count of neutrophils. Neutrophils are granulated leukocytes essential for the initial immune response to inflammation and infection (Leidig, 2017). Neutropenia can be categorized as primary, resulting from decreased production or ineffective neutrophils, or secondary, caused by the consumption or destruction of neutrophils. The potential causes for neutropenia include primary bone marrow production disorders, genetic, and cyclical deficiencies (Bousfiha, 2015). Mutations in ELANE can lead to Severe Congenital Neutropenia (SCN) type 1, a chronic form of neutropenia resulting from an aberrant stress response in neutrophils, causing premature cell death (Dale, 2000). GFI1 mutations underlie (SCN) type 2, affecting normal neutrophil creation and impacting lymphoid and myeloid cell lines (Hock, 2003). HAX1 deficiency (SCN type 3) results in marked neutropenia and a heightened risk of life-threatening bacterial infections (Klein, 2007). G6PC3 mutations cause Severe Congenital Neutropenia type 4, impacting myeloid maturation and leading to additional congenital defects

(Boztug, 2012). Wiskott–Aldrich syndrome (WAS) is an X-linked disorder. WAS protein mutations lead to infection susceptibility, thrombocytopenia with bleeding tendencies, and eczema (Buchbinder, 2014).

Compared to SCN diseases, myelokathexis restricts neutrophils from leaving the bone marrow, contributing to severe congenital neutropenia (Leidig, 2017). The Warts, hypogammaglobulinemia, infections, and myelokathexis (WHIM) syndrome (Figure 2.11) is an immune disorder characterized by B cell lymphopenia, hypogammaglobulinemia, and neutropenia (Kawai, 2009). WHIM syndrome mostly arises from CXCR4 mutations (Martin, 2003). CXCR4, similar to other G protein-coupled receptors (GPCRs), comprises seven transmembrane helices, an extracellular N-terminal domain, and an intracellular C-terminal domain. In the classic desensitization process, a GPCR kinase (GRK) phosphorylates specific serine and threonine residues on the C-terminal domain of CXCR4, leading to the recruitment of β-arrestin for receptor internalization (Heusinkveld, 2019). WHIM syndrome is often diagnosed as severe congenital neutropenia despite affecting multiple types of white blood cells in most patients (Tassone, 2009). Mutations in CXCR4 associated with WHIM syndrome introduce premature stop codons, resulting in a truncation of the receptor's cytoplasmic C-terminal region (Heusinkveld, 2019). Patients present with neutropenia, hypogammaglobulinemia, and warts (Kawai, 2009). Stromal cell-derived growth factor-1 (SDF1) and CXCR4 receptor function are crucial in bone marrow retention of neutrophils (Suratt, 2004). Individuals with CXCR4 mutations have an accumulation of apoptotic neutrophils in the bone marrow, resulting in neutropenia (Kawai, 2009).

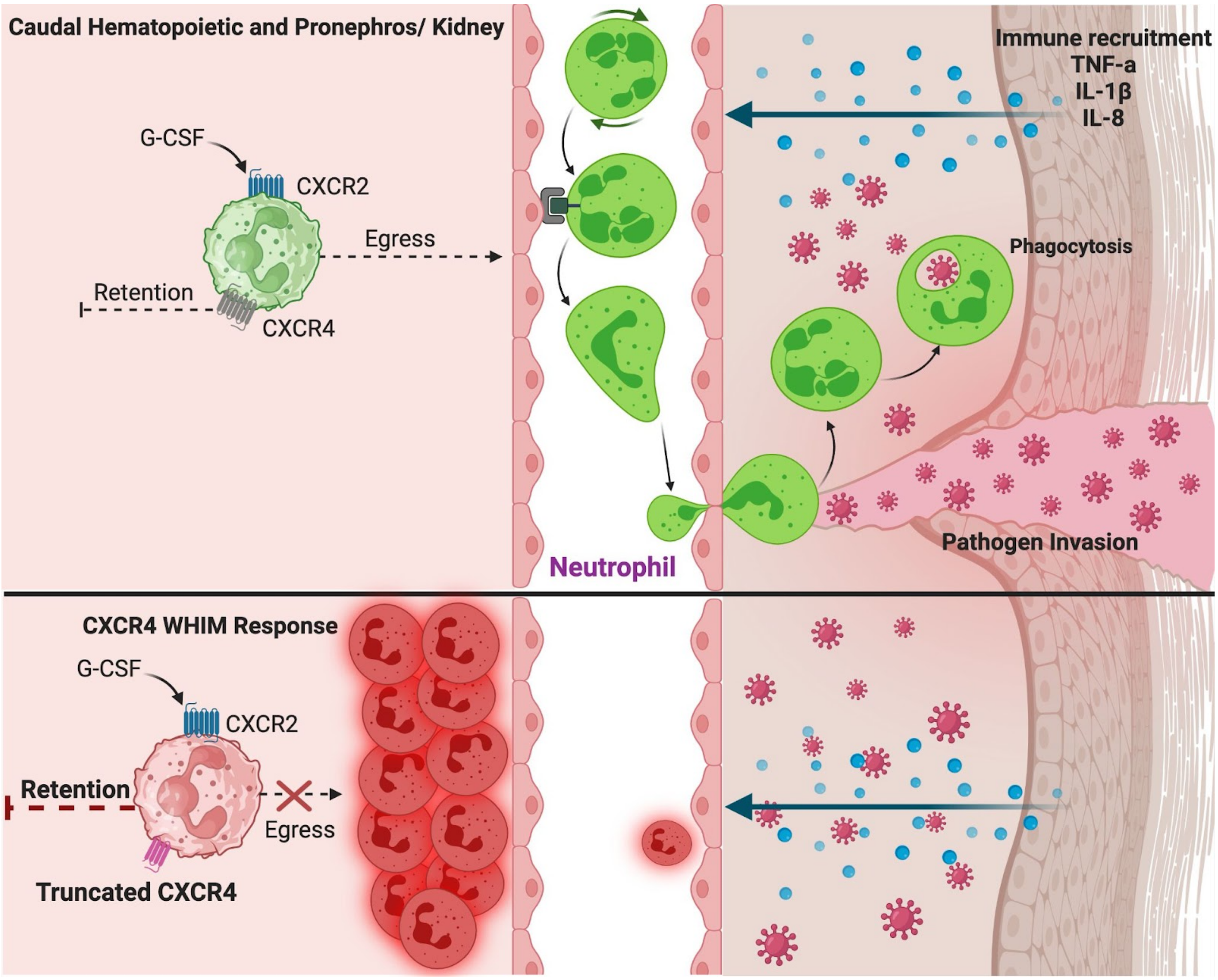
Caudal Hematopoietic and Pronephros/ Kidney
G-CSF
CXCR2
Egress
Retention
CXCR4
Immune recruitment
TNF-a
IL-1β
IL-8
Phagocytosis
Pathogen Invasion
Neutrophil
CXCR4 WHIM Response
G-CSF
CXCR2
Retention
Egress
Truncated CXCR4

**Figure 2.10. Neutrophil response to infection in WHIM disorder.** Neutrophil adhesion to endothelial cells involves multiple sequential steps, commencing with attachment to activated endothelial cells. This is followed by migration within blood vessels, passage through the blood vessel wall, and movement within the tissue spaces. In tissue infection or inflammation areas, endothelial cells become activated and increase the expression of adhesion receptors such as E- and P-selectins. Neutrophils adhere to these selectins through specific ligands, such as PSG-1, initiating a rolling motion along the endothelial cells. Subsequently, neutrophils become activated by chemokines, leading to the activation of integrins, which bind to adhesion molecules like ICAM on endothelial cells. This interaction promotes a stable adhesion, halting the neutrophils'

movement. The neutrophils then traverse the endothelial barrier, navigating along the basement membrane until they locate a small opening between pericytes, ultimately transmigrating into the affected tissues. In individuals with WHIM syndrome, neutrophils exhibit C-terminal truncations of the CXCR4 protein. The prevailing theory regarding WHIM syndrome attributes the abnormal functioning of the mutated CXCR4 protein to the retention of fully developed neutrophils within the bone marrow, delaying their release into circulation. Neutrophils with reduced levels of CXCR4 respond more efficiently to CXCR2 signaling for egress from the bone marrow but at a delayed pace. As these neutrophils age in the periphery, their CXCR4 levels elevate, prompting their return to the CXCL12-rich bone marrow environment. Subsequently, these neutrophils undergo apoptosis and are cleared by macrophages (Heusinkveld 2019). *The image was generated in BioRender.*

Neutrophil chemotaxis disorders stem from dysfunction in neutrophil integrins, specifically LFA-1 and Mac-1. This affects their ability to engage with intracellular adhesion molecules on endothelial cells (Leidig, 2015). Various clinical syndromes arise from deficiencies in these adhesion molecules. Leukocyte adhesion deficiency-I is an autosomal recessive disorder resulting from CD18 defects, leading to bacterial infections, prolonged umbilical cord attachment, poor wound healing, and neutrophilia (Hanna, 2012). Leukocyte adhesion deficiency-II, a rare AR disorder, occurs due to deficiencies in the SLC35C1 gene, manifesting susceptibility to infections with additional symptoms such as intellectual disability and physical abnormalities. Leukocyte adhesion deficiency-III, caused by Kindlin 3 mutations, presents similar symptoms to LAD-I but with milder manifestations (Hanna, 2012).

Phagocytosis involves the fusion of phagosome membranes and neutrophil granules, releasing contents for microbial killing (Borregaard, 1997). Chediak–Higashi syndrome, caused by LYST defects, impacts granule structure and degranulation. Albinism, neurologic issues, immunodeficiency, and mild bleeding tendencies mark this syndrome (Introne, 1993). Neutrophil-specific granule deficiency (SGD) results in neutrophils lacking lactoferrin production, rendering individuals susceptible to bacterial infections (McIlwaine, 2013). Mutations in PHOX subunits may lead to chronic granulomatous disease (CGD), characterized by inflammation and heightened infection vulnerability (Kuhns, 2010). CGD typically presents in childhood with severe or recurrent infections in various body areas (Leidig, 1993). Neutrophils play a crucial role in defending against invasive pathogens, with deficiencies in neutrophil function posing a significant health risk, emphasizing their importance in the immune system (Leidig, 2017). Studying the molecular mechanisms behind neutrophil disorders provides valuable insights into how the innate immune system responds to pathogenic threats.

### 2.3.3. Neutrophil hyperinflammation tissue damage

As previously stated, neutrophils exhibit antiviral properties through various mechanisms to restrict viral replication and spread. However, the broad-spectrum antiviral activity of neutrophils may result in tissue damage due to the non-specificity and abundance of their antimicrobial substances, potentially eliciting a counterproductive response in the host's antiviral defense (Ma, 2021). Neutrophil granules contain an array of enzymes; excessive release of these granules can lead to vascular leakage, pulmonary edema, and hypoxemia (Narasaraju, 2011). The release of MMP9 by neutrophils can worsen pathological effects in a mouse model of influenza virus infection (Bradley, 2012). In children suffering from RSV-induced bronchiolitis, the extent of neutrophilic inflammation correlates with disease severity (Geerdink, 2015). The pathogenic mechanism involves neutrophil elastase breaking down elastin fibers and disrupting the structure of lung tissue. Furthermore, cathepsin G, elastase, and protease 3 secreted by neutrophils also contribute to vascular leakage, inflammation, and pathological alterations (Yasui, 2005).

Previous studies have demonstrated that the clearance of neutrophils can diminish lung inflammation during RSV infection (Wang, 2000). Subsequent investigations have shed light on the underlying pathological processes (Ma, 2021). Neutrophils within the lungs undergo oxidative burst and generate high levels of reactive oxygen species (ROS), which can oxidize biomolecules, harm host cellular structures, and induce lung damage (Geerdink, 2015). Similarly, in cases of influenza infection, excessive neutrophil activity produces ROS that can impair the epithelial-endothelial barrier, impede the clearance of the influenza A virus, and provoke harmful inflammation and increased morbidity in mice (Agraz-Cibrian, 2017).

While NETs play a constructive role in defending against viral infections, an overabundance of NETs can lead to unintended harm. The release of NETs by neutrophils can directly harm neighboring cells, such as endothelial cells and hepatocytes in the liver (Schönrich,  2016). The detrimental effects of NETs are primarily attributed to their constituents, including proteases that serve as autoantigens, triggering and perpetuating inflammation (Mantovani, 2011). Histones and myeloperoxidase (MPO) found in NETs are key substances that mediate cytotoxicity and damage lung tissues (Saffarzedah, 2012). Various enzymes like elastase, cathepsin, and serine protease present in neutrophils also contribute to host injury (Narasaraju, 2011). Furthermore, the accumulation of NETs can incite autoimmune responses, resulting in localized tissue damage and organ dysfunction (Ma, 2021). Since the components of NETs can act as antigens for autoimmune conditions, they may prompt the production of autoantibodies. These autoantibodies form immune complexes with NETs that deposit in the kidneys, leading to tissue damage Raftery, 2014). NETs in the alveoli, histones, and MMP9 can induce pulmonary capillary damage and obstruct small blood vessels, ultimately causing lung injury (Cortjens, 2018). In mice infected with IAV, heightened neutrophil infiltration and elevated levels of NETs are linked to damage in alveolar structures (Dienz, 2012).

### 2.3.4. Non-coding RNAs that induce hyperinflammation

An important discovery in genomics from the early 2000s revealed that protein-coding exons comprise less than 2% of mammalian DNA (Lander, 2001). Further research in transcriptomics has shown that a large portion of the genome is transcribed into RNA, revealing new layers of genetic regulation (Carninci, 2005). Previously dismissed as "junk DNA," noncoding RNAs (ncRNAs) have now been found to play a significant role in genetic regulation across different species (Paralkar, 2013). Studies on microRNAs and lncRNAs have provided valuable insights into various biological processes, including immune response regulation (Ireland, 2020).

MicroRNAs are crucial for gene expression regulation in immune function, development, and tissue repair. For example, miR-722 and miR-199 have been shown to play a role in neutrophil migration in zebrafish with infections (Hsu, 2019a; Hsu, 2019b). On the other hand, lncRNAs do not encode proteins but are involved in important regulatory processes such as transcription and mRNA regulation (Ireland, 2020). In oncology research, lncRNAs have been found to impact immune responses in the context of cancer, including the regulation of neutrophil extracellular traps (NETs) in lung and breast cancer (Ireland, 2020; Jiang, 2023; Wang, 2022).

Overall, these studies highlight ncRNAs' intricate neutrophil regulatory roles in various biological processes and diseases, providing new avenues for research and potential therapeutic interventions.

## 2.4. Reactive oxygen species (ROS)

ROS is a common term frequently referenced within biology and medicine. This term encompasses a collection of oxygen-containing reactive elements, including superoxide ($O_2^-$), hydrogen peroxide ($H_2O_2$), hydroxyl radical (OH), singlet oxygen ($^1O_2$), peroxyl radical (ROO), alkoxyl radical (RO), lipid hydroperoxide (ROOH), peroxynitrite ($ONOO^-$), hypochlorous acid (HOCl), and ozone ($O_3$), among others (Halliwell, 1996). While ROS is the preferred terminology in the scientific community, alternative terms like reactive oxygen metabolites (ROMs), reactive oxygen intermediates (ROIs), and oxygen radicals exist in the literature. ROS is widely accepted and most commonly utilized out of these various terms (Li, 2016).

### 2.4.1. ROS types

Some ROS consist of unpaired electrons and, consequently, fall into the category of free radicals. They are called oxygen radicals or free radicals (Halliwell, 2007). Free radicals are chemical species capable of existing independently and containing one or more unpaired electrons (Genestra, 2007). An unpaired electron occupies an atomic or molecular orbital on its own. Examples of oxygen radicals include superoxide, hydroxyl, peroxyl, and alkoxyl radicals (Halliwell, 2007). Conversely, certain ROS do not contain unpaired electrons and are thus not classified as free radicals. Examples of non-radical ROS include hydrogen peroxide, peroxynitrite, hypochlorous acid, and ozone (Li, 2016).

Similarly, Reactive Nitrogen Species (RNS) has been formulated to encompass nitric oxide, peroxynitrite, nitrogen dioxide radical, and other nitrogen oxides or nitrogen-containing reactive species. Since RNS mainly consist of oxygen, they may also be categorized as ROS (Pham-Huy, 2008). Reactive Chlorine Species (RCS) refers to chlorine-containing reactive species, with hypochlorous acid (HOCl) as a notable example. Compared to ROS and RNS, RCS is not frequently used in biology and medicine (Li, 2016).

### 2.4.2. Antioxidant/ redox signaling

The human body has various mechanisms to combat oxidative stress by producing antioxidants, which can be either naturally generated within the body (endogenous antioxidants) or obtained from outside sources such as food (exogenous antioxidants). Antioxidants are crucial in neutralizing excess free radicals, protecting cells from their harmful effects, and aiding in disease prevention (Droge, 2002).

Key antioxidant enzymes involved in neutralizing reactive oxygen species (ROS) and reactive nitrogen species (RNS) include superoxide dismutase (SOD), catalase (CAT), glutathione peroxidase (GPx), and glutathione reductase (GRx) (Genestra, 2007). SOD serves as the primary defense against free radicals by converting superoxide anion radicals into hydrogen peroxide, which is then metabolized into water and oxygen by CAT or GPx. GPx utilizes hydrogen peroxide to oxidize glutathione, which GRx then regenerates with the help of NADPH (Pham-Huy, 2008).

Different members of the GPx family have antioxidant functions in various cellular components, with GPx1 found in the cytosol and mitochondria, GPx2 in the cytosol and nucleus, GPx3 in the plasma, and GPx4 protecting cellular membranes (Liu, 2014). The thioredoxin (Trx) antioxidant system, consisting of NADPH, thioredoxin reductase (TrxR), and Trx, is also critical in combating oxidative stress and repairing DNA and proteins (Lu, 2014).

The antioxidant process can operate through chain-breaking or prevention methods, where antioxidants like vitamins C, E, and carotenoids stabilize free radicals or cause them to disintegrate harmlessly (Pham-Huy, 2008). Maintaining a balance of antioxidants in the body is important, as their efficacy can vary depending on the system and circumstances (Pham-Huy, 2008). Some antioxidants potentially act as pro-oxidants under certain conditions. Constant replenishment of antioxidant resources is essential to ensure optimal antioxidant function and combat oxidative stress effectively (Young, 2001).

Electron flow is significant in biological studies (Zuo, 2020). Nobel laureate and esteemed biochemist Albert Szent-Györgyi noted that life can be likened to an electron seeking a stable resting place. While life is undoubtedly multifaceted beyond the realm of electrons, electron transfer remains crucial. This process entails converting energy from a state of excitation (characterized by high-energy electrons) to a state of equilibrium (comprised of low-energy resting electrons)  (Herrmann, 2012).

The transfer of electrons from donor molecules to acceptor molecules activates oxidative and reductive processes, known as redox reactions. These reactions generate intracellular energy by moving electrons from one reductant to another oxidant (Sies, 2024). The high-energy electrons transfer to a final acceptor, typically molecular oxygen in aerobic organisms, to produce water (Zuo, 2020). In humans, enzymes within cells reduce oxygen, enabling ATP production. However, under specific conditions, such as redox control, oxygen reduction may be obstructed at an intermediate stage, like hydrogen peroxide, which acts as an active oxidant to regulate various physiological and pathological redox signaling pathways based on oxidant levels (Sies, 2017). Various crucial intermediary proteins are involved in linking electron flow to cellular responses. These functional proteins are critical in governing cellular biological processes and determining cell destiny (Seis, 2024). Essentially, the primary objective of redox biology is to uncover the coordination and communication between electron gradients and cellular responses (Zuo, 2020).

The presence of intracellular hydrogen peroxide is naturally occurring. It can be derived from various sources within the cell, such as NOX complexes, mitochondrial oxidative phosphorylation (mtOXPHOS)—which refers to the electron transport chain (ETC) of mitochondria—and other cellular compartments like peroxisomes and the endoplasmic reticulum (ER) (Seis, 2017; Zuo, 2020). Hydrogen peroxide can also be externally introduced into the cell due to environmental stressors, such as ultraviolet radiation, ionizing radiation, and exposure to toxic substances (Parvez, 2018).

The imbalance in redox signaling between oxidants and antioxidants, particularly in oxidative stress, is associated with numerous health conditions, including neurological, immune system, cardiovascular, and skeletal disorders (Zuo, 2020). It should be noted, however, that not all redox-related disorders stem from an overproduction of ROS. Various pathological states may also arise from the influence of other reactive species, such as reactive nitrogen and sulfur species, or small signaling molecules like hydrogen, ammonia, and carbon monoxide, all of which can contribute to an imbalance in redox signaling (Zuo, 2020).

One important gene involved in redox signaling is nuclear erythroid 2-related factor 2 (NRF2), a transcription factor that directly controls the expression of antioxidant proteins (Yamamoto, 2018). The Kelch-like ECH-associated protein 1 (Keap1)-Nrf2 pathway is a crucial mechanism in eukaryotes that helps maintain redox balance in response to oxidative stress, as seen in Figure 2.12 (Schieber, 2014). Keap1 acts as a sensor, normally inhibiting Nrf2 activity by marking it for degradation. However, when cells are under oxidative stress, Nrf2 is freed from Keap1 (Yamamoto, 2018). It is a key regulator in activating genes such as cysteine uptake transporter and heme oxygenase 1, which are crucial for cell protection and survival (Niture, 2014).

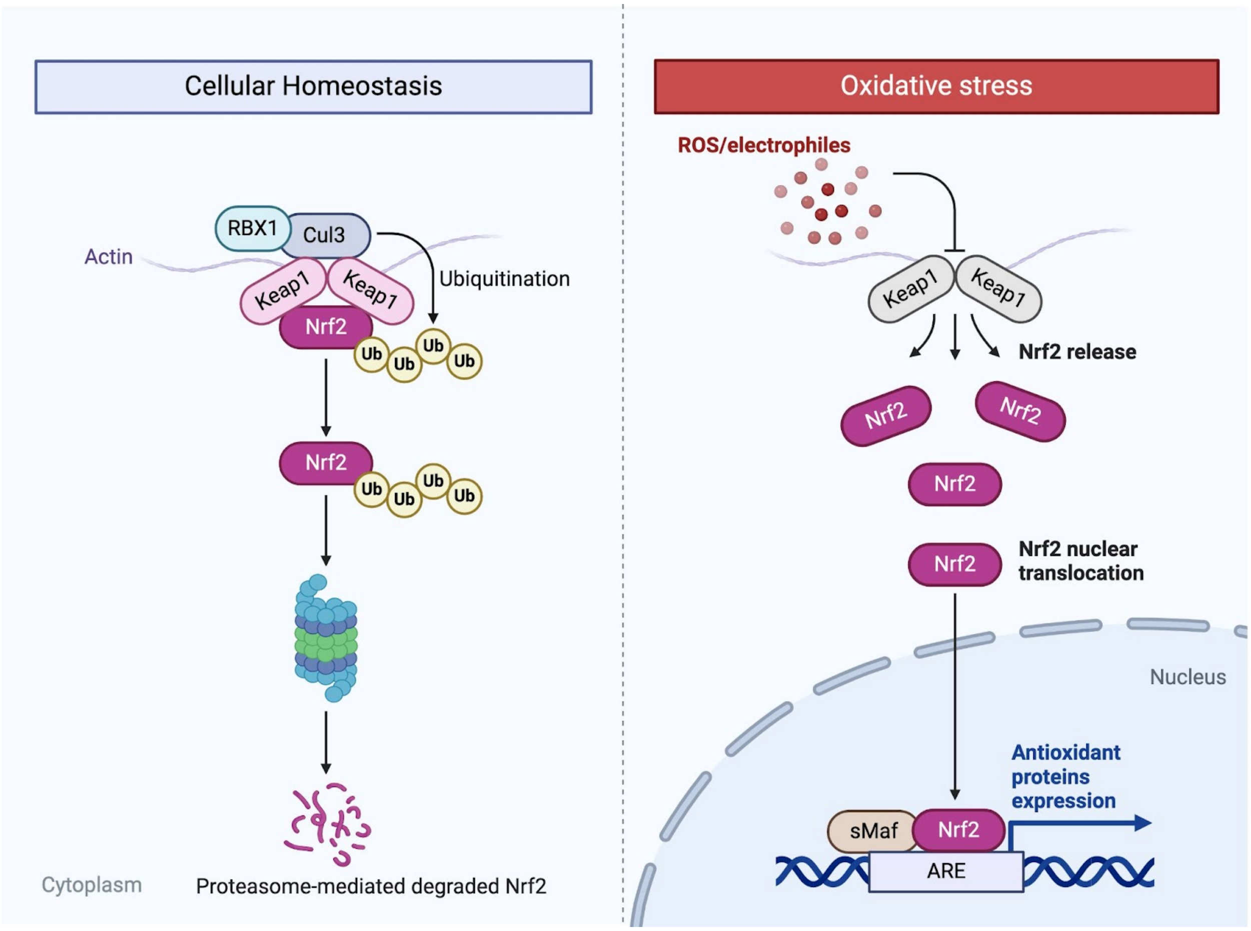
Cellular Homeostasis
Actin
RBX1
Cul3
Keap1
Keap1
Nrf2
Ubiquitination
Ub
Nrf2
Ub
Cytoplasm
Proteasome-mediated degraded Nrf2
Oxidative stress
ROS/electrophiles
Keap1
Keap1
Nrf2 release
Nrf2
Nrf2
Nrf2
Nrf2
Nrf2 nuclear translocation
Nucleus
Antioxidant proteins expression
sMaf
Nrf2
ARE

**Figure 2.11. KEAP1-NRF2 redox signaling network in cellular homeostasis and oxidative stress.** In normal conditions, NRF2 interacts with KEAP1. When ROS levels rise, KEAP1 oxidizes, releasing NRF2 to translocate to the nucleus. There, NRF2 forms a complex with small MAF proteins to bind to the DNA's antioxidant-responsive elements (AREs) and regulate the expression of multiple antioxidant genes (Zuo, 2020). *Figure generated in BioRender.*

### 2.4.3. Sources of ROS

Reactive oxygen species (ROS) can be generated from internal or external cellular sources, see Figure 2.13. Internally, ROS are produced in cellular organelles such as mitochondria, peroxisomes, and endoplasmic reticulum, where high oxygen consumption levels occur.

Mitochondria, in particular, are the main source of intracellular ROS, with superoxide radicals being generated at key sites within the electron transport chain (Bhattacharyya, 2014).

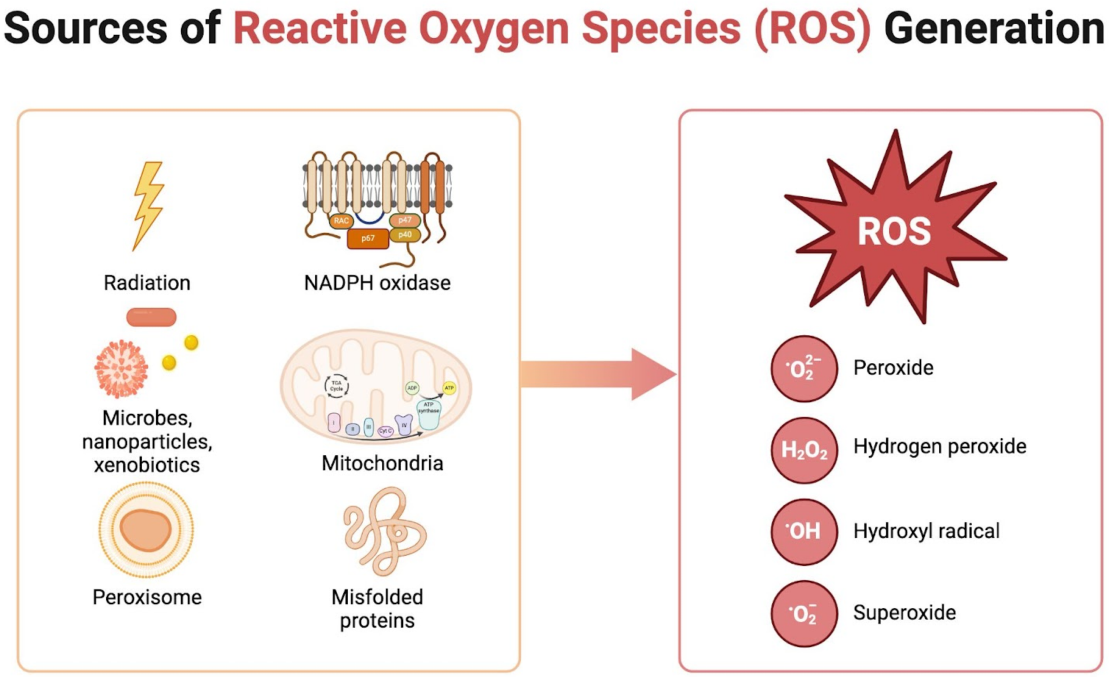
Sources of Reactive Oxygen Species (ROS) Generation
Radiation
NADPH oxidase
RAC
p47
p67
p40
Microbes, nanoparticles, xenobiotics
Mitochondria
TCA Cycle
ADP
ATP
ATP synthase
Cyt C
Peroxisome
Misfolded proteins
ROS
·O2 2−
Peroxide
H2O2
Hydrogen peroxide
·OH
Hydroxyl radical
·O2−
Superoxide

**Figure 2.12. Sources of ROS generation.** The figure demonstrates endogenous (NOX, mitochondria, peroxisome, misfolded protein) and exogenous (pathogens, drugs, radiation) that can produce common ROS species peroxide, hydrogen peroxide, hydroxide, and superoxide ( Phaniendra, 2015). *The image was generated by BioRender.*

In peroxisomes, the respiratory pathway converts various metabolites to oxygen, forming hydrogen peroxide (De Duve, 1966). Unlike mitochondria, this process does not produce ATP but releases energy in the form of heat (Schrader, 2006). Other free radicals, such as dioxygen, hydroxide, and nitric oxide, are also produced in peroxisomes, primarily through the beta-oxidation of fatty acids (Phaniendra, 2015). The enzymes within the endoplasmic reticulum, including cytochrome p-450 and b5 enzymes, play a role in ROS formation (Cheeseman, 1993). The thiol oxidase enzyme Erop1p facilitates electron transfer to oxygen, producing hydrogen peroxide (Gross, 2006). Other internal sources of ROS include prostaglandin synthesis, auto-oxidation of adrenaline, phagocytic cells, and various metabolic processes (Phaniendra, 2015).

Externally, ROS can be generated by air pollutants, tobacco smoke, radiation, certain foods, drugs, and xenobiotics (Yildirim, 2000). Chemical agents like quinones and heavy metals like lead, arsenic, mercury, chromium, and cadmium are common sources of exogenous ROS (Bolton, 2020). Ionizing radiation from X-rays and UV rays can also produce ROS (Bhattacharyya, 2014).

While ROS plays a role as signaling molecules in biological systems, excessive ROS can disrupt bodily homeostasis and result in oxidative damage to tissues (Zuo, 2020). However, it's not all doom and gloom. Natural antioxidant pathways, our body's built-in defense system, help mitigate ROS's effects, offering a glimmer of hope in this complex biological process. But, it's important to note that oxidative stressors can elevate ROS levels and contribute to tissue damage over time.

### 2.4.4. ROS in disease

Diabetes mellitus is a diverse group of chronic conditions marked by elevated blood glucose levels (hyperglycemia) stemming from inadequate insulin secretion (type I diabetes), resistance to insulin (type II diabetes), or a combination of both (He, 2017). The condition is linked to an uptick in free radicals or a decline in antioxidant systems' effectiveness, leading to the development of oxidative stress. Both mitochondrial and non-mitochondrial sources of reactive oxygen species contribute to diabetes-related oxidative stress (Phaniendra, 2015).

The central nervous system (CNS is highly vulnerable to oxidative stress due to its high lipid content, elevated oxygen consumption, and limited levels of antioxidant enzymes. For instance, SOD is predominantly found in neurons, while glutathione (GSH) and GPx are primarily located in astrocytes (Pollack, 1999). Parkinson's disease involves the degeneration of dopaminergic neurons (which play a role in learning, memory, and motor control), particularly in the substantia nigra region of the midbrain, alongside the formation of Lewy bodies containing α-synuclein (Santiago-López, 2010). A disruption in redox balance leads to oxidative harm to these neurons, altering dopamine synthesis and metabolism pathways, thereby heightening oxidative stress due to quinone generation (Santiago-López, 2010). Alzheimer's disease is marked by the buildup of amyloid protein plaques (formed through incorrect folding and processing of amyloid β precursor protein - ABPP) and intracellular neurofibrillary tangles made up of abnormal and hyperphosphorylated tau protein (Butterfield, 2006; Phaniendra, 2015). The aggregation of hyperphosphorylated tau protein binds to Fe3+, forming neurofibrillary tangles (Butterfield, 2006). Amyloid-β peptide can generate hydrogen peroxide through chelation (Uttara, 2009). Lipid peroxidation is also extensive in Alzheimer's patients, potentially leading to neuronal death through various mechanisms like the impairment of ion pumps, glucose transporters, and glutamate transporters (Butterfield, 2006). Multiple sclerosis is an autoimmune neurological disorder characterized by compromised nerve conduction due to demyelination of the central nervous system (CNS). The activation of microglia/macrophages sets off multiple sclerosis by generating reactive oxygen species that can induce lipid peroxidation, resulting in demyelination and neuronal damage (Gonsette, 2008).

The presence of free radicals is a significant contributor to health issues in individuals. Free radicals can induce mutagenic effects through chemical alterations in DNA, potentially playing a role in the development of cancer (Dreher, 1996). It has been observed that cancer cells, as opposed to normal cells, exhibit heightened levels of ROS and are more prone to mitochondrial dysfunction due to their increased metabolic activity (Acuna, 2012). The elevated oxidative stress in cancer cells is attributed to the activation of oncogenes and the suppression of tumor suppressors. Changes in gene expression and growth signals induced by ROS contribute to the uncontrolled proliferation of cancer cells (Phaniendra, 2015). Furthermore, ROS can cause damage to DNA by triggering various modifications such as base alterations, deletions, strand breakages, chromosomal rearrangements, and hyper- and hypo-methylation of DNA (Valko, 2004).

ROS plays a complex role in human health, with evidence pointing to positive and negative effects dependent on various factors influencing their impact. For instance, a controlled level of hydrogen peroxide can activate important physiological pathways by oxidizing specific protein targets regulating cellular activities like growth and movement (He, 2017). On the other hand, excessive hydrogen peroxide production can lead to oxidative stress and trigger various physiological and pathological processes like protein damage, inflammation, and cell death (Phaniendra, 2015). Research has linked oxidative stress to conditions such as inflammatory bowel disease (IBD), diabetes, heart disease, neurological disorders, and cancer. ROS has been implicated in many other diseases as well (Bhattacharyya, 2014; Phaniendra, 2015; Zuo, 2020).

### 2.4.5. ROS in innate immunity

The innate immune response serves as the primary defense mechanism against invading pathogens. ROS and RNS are key players in various innate immune system functions, including respiratory bursts and inflammasome activation (Manoharan, 2024). These reactive species, found throughout the cell environment, are short-lived intermediates crucial for cellular signaling and proliferation, with their impact depending on where they are formed within the cell (Phaniendra, 2015). When immune cells are activated in response to pathogens, they release inflammatory mediators that increase vascular permeability and guide white blood cell migration to the injury site. ROS helps regulate the expression of certain cell adhesion molecules that facilitate the interaction between white blood cells and the endothelium (Muri, 2020). Conversely, increased expression of superoxide dismutase can reduce this interaction (Manoharan, 2024). Additionally, hydrogen peroxide plays a role in early white blood cell recruitment to the injured tissue (Nguyen, 2017).

Macrophages are a diverse group of immune cells that contribute to tissue homeostasis and respond to infections by engulfing pathogens and aiding in tissue repair (Manoharan, 2024). These cells can switch between pro-inflammatory (M1) and anti-inflammatory (M2) states to promote inflammation or wound healing (Viola, 2019). The production of NADPH through the pentose phosphate pathway influences the inflammatory response of M1 macrophages by regulating the production of ROS and nitric oxide, essential for killing pathogens (Nguyen, 2017). Studies have shown that deleting the TRX1 system can impair the activation of certain immune pathways in macrophages, leading to decreased production of inflammatory cytokines and increased ROS levels (Canton, 2021).

Neutrophils use glycolysis and the pentose phosphate pathway to produce NADPH, which fuels the production of free oxygen radicals essential for their functions, such as phagocytosis and the formation of neutrophil extracellular traps (NETs) to combat invading pathogens (Nguyen, 2017). The process of NETosis, facilitated by ROS, involves the release of certain enzymes and histones from neutrophils to trap and kill pathogens (Mullen, 2020). The production of secondary oxidants like hypochlorous acid during NETosis depends on the activity of specific enzymes in neutrophils (Papayannopoulos, 2010).

The cellular redox status, including the balance between ROS production and antioxidant systems, plays a crucial role in neutrophil function (Mullen, 2020). Chronic elevation of ROS levels can lead to dysregulated immune responses, affecting processes such as phagocytosis, oxidative bursts, and cytokine production (Nguyen, 2017). Ultimately, the balance of ROS levels dictates how neutrophils detect and respond to pathogens, influencing their migration and activation.

### 2.4.6. Viral ROS response

Peterhans published the initial evidence indicating that a virus can induce oxidative stress by elevating levels of ROS (Peterhans, 1987). Through experimentation, it was shown that infecting mouse splenocytes with Sendai virus, a paramyxovirus, increased chemiluminescence levels due to the oxidation of luminol by ROS (Peterhans, 1979). Furthermore, it was observed that UV-light-inactivated viruses could still generate ROS. In contrast, heat-inactivated viruses did not exhibit this ability, indicating that the structure of the viral particle plays a role in mediating this phenomenon (Peterhans, 1979).

ROS may facilitate or enhance viral replication in cellular activation, depending on the specific cell type and virus involved (Laforge, 2020). The impact of ROS on cellular functions is influenced by the quantity of ROS present and the duration of exposure (Nguyen, 2017). While the production of ROS varies among different viruses, they collectively contribute to a common pathogenic pathway characterized by increased ROS production and depletion of antioxidants (Angostinelli, 2010).

Viruses are identified, engulfed, and phagocytosed during infection by inflammatory cells like macrophages, neutrophils, and dendritic cells (Abbas, 2022). This process triggers the expression of NADPH oxidase complex and nitric oxide synthase in phagocytic cells, leading to heightened ROS production (Nguyen, 2017). The activation of phagocytes by viruses is linked to oxidative stress due to ROS release and the release of pro-oxidant cytokines by activated phagocytes (He, 2017). Pro-oxidant cytokines such as TNF and IL-1 promote iron absorption by the reticuloendothelial system, which can accumulate and generate the hydroxyl radical OH via the Fenton and Haber Weiss reactions (Laforge, 2020).

In cases of dengue fever, patients exhibit higher levels of peroxidation potential, lipid peroxidation products, and superoxide dismutase activity, along with lower levels of glutathione peroxidase and total hydroperoxides (Klassen, 2004). This suggests a disturbance in redox status due to oxidative stress, potentially impacting the disease's progression (Laforge, 2020). Research has shown that oxidative stress levels vary across different clinical stages of DENV infection, most severe in dengue shock syndrome (Soundravally, 2008). DENV infection can induce endothelial cell production of reactive oxygen species and apoptotic cell death, with inflammation playing a crucial role in disease severity. Animal studies have demonstrated the importance of reactive nitrogen and oxygen species in DENV-related hemorrhaging (Yen, 2008).

Numerous studies have indicated that oxidative stress may play a role in developing lung injury and inflammation following influenza A infection (Laforge, 2020). ROS, such as superoxide and nitric oxide, are secreted by inflammatory and airway epithelial cells, potentially exacerbating lung damage post-influenza virus pneumonia (Suliman, 2001). Studies have shown that lung tissue damage results from both virus-induced cytopathic and cytotoxic effects of excessive inflammation. In one study, mice infected with a lethal dose of influenza A/PR8/34 virus exhibited increased levels of oxide and hydrogen peroxide in bronchoalveolar lavage fluid (BALF) cells and lung tissue at the early stages of infection, indicating the presence of oxidative stress (Buffington, 1992). Another study revealed a reduction in antioxidant concentrations, such as glutathione and vitamins C and E, during the initial stages of infection, suggesting a potential increase in susceptibility to other pathogens (Hennet, 1992). Furthermore, research has shown that H5N1 virus infection in lung cells led to decreased expression of the SOD1 enzyme, which reduces RS production (Lin, 2016). Overexpression of SOD1 in these cells inhibited RS production, reduced inflammation, and hindered viral replication. Notably, H5N1 infection resulted in higher RS production and a decreased GSH/GSSG ratio compared to H1N1 infections and control cells (Lin, 2016).

Oxidative stress plays a significant role in the development of pulmonary inflammation triggered by RSV (Laforge, 2020). In a study by Mochizuki et al., alterations in the intracellular glutathione redox status were examined in cultured human airway epithelial cells (A549) and normal human bronchial epithelial cells (NHBE) infected with RSV (Mochizuki, 2009). The results indicated that RSV infection led to oxidative stress, which could provoke airway inflammation (Hosakote, 2009). RSV infection in airway epithelial cells generated ROS, increased lipid peroxidation products, and reduced the expression of antioxidant enzymes such as SOD1, SOD3, CAT, and GST. However, there was a slight rise in SOD2. Additionally, there was a noted escalation in SOD activity and declines in CAT, GPx, and GST levels (Casola, 2001; Hosakote, 2009). Studies on infected mice revealed that RSV induced oxidative stress in the lungs, with clinical symptoms and pulmonary inflammation being mitigated by antioxidant treatment (Castro, 2006; Hosakote, 2011). Huang et al. demonstrated that mice infected with RSV displayed elevated levels of oxidative stress markers such as NO, MDA, and OH, along with reduced GSH and SOD activity (Huang, 2010). Children suffering from acute bronchiolitis caused by RSV also exhibited increased oxidative stress induced by the virus. As a result, concentrations of GSSG and GPx were boosted, and there was a positive association between GSSG levels and disease severity (Moreno-Solís, 2015).

Dhanwani et al. demonstrated that neonatal mice infected with CHIKV experience alterations in their apoptotic, inflammatory, and stress pathways (Dhanwani, 2011). This includes an elevation of inflammatory cytokines such as IL-6, TNF-α, and IL-1 and a decrease in antioxidant enzymes CAT and peroxiredoxin-6. The infection also leads to changes in the urea cycle and energy metabolism in the liver and brain (Dhanwani, 2011). This study suggests that the stress response plays a crucial role in the pathogenesis and inflammation caused by CHIKV, with tissue injury and apoptosis being key events Laforge, 2020).

Moreover, another study conducted on the neuroblastoma cell line SH-SY5Y infected with CHIKV revealed a reduction in glutathione expression, decreased levels of enzymes SOD, CAT, GPx, GR, and GST, and an increase in MDA levels post-infection (Dhanwani, 2012). Additionally, there was a rise in inflammatory cytokine levels (IL-6, TNF-α, and IL-1), indicating inflammation in CHIKV-induced neuronal infection (Dhanwani, 2012). Patil et al. observed alterations in oxidative homeostasis in mice infected with CHIKV. These mice exhibited elevated levels of inflammatory cytokines iNOS, TNF-α, IL-1α, and IL-1β, along with increased levels of COX-2 and CCL-3 proteins during the symptomatic phase of the disease, which normalized during the recovery phase (Patil, 2012). Furthermore, Joubert et al. found that CHIKV infection in cells and mice resulted in heightened reactive species (RS) production, leading to the endoplasmic reticulum and oxidative stress (Joubert, 2012). These processes trigger autophagy independently during CHIKV infection (Laforge, 2020).

The prevalence of oxidative stress in individuals with HIV infection has been extensively documented in the available literature, with numerous research articles reporting various alterations in experimental models (Laforge, 2020). It has been observed that oxidative stress, alongside other viral infections, may facilitate the replication of HIV and the activation of NF-kB, a crucial element for both viral replication and the activation of immune system inflammatory cytokines (Staal, 1990). Patients who are HIV-positive or have progressed to AIDS typically exhibit elevated levels of serum hydroperoxide and MDA (Favier, 1994). Studies concerning HIV frequently report a decline in antioxidant enzyme levels and heightened levels of oxidants. Research by Malvy et al., Dröge et al., and Fuchs et al. has revealed significant reductions in GSH, cysteine, vitamin C, GPx, and SOD levels in the plasma and leukocytes of individuals with HIV infections, accompanied by increased lipid peroxidation and elevated MDA levels in the plasma (Dröge, 1994; Fuchs, 1995; Malvy, 1994). Overall, HIV infection is associated with a depletion of antioxidants, leading to compromised immune function (Laforge, 2020). Immune cells demand higher antioxidants than other cells to uphold their redox balance, integrity, and functionality (De La Fuente, 2002). Consequently, oxidative stress plays a critical role in HIV infection, as a reduction in antioxidants like CAT and glutathione can result in an overabundance of hydrogen peroxide, leading to the generation of hydroxide radicals that trigger programmed cell death (Leff, 1992). Excessive reactive species are believed to contribute to AIDS progression through various mechanisms, such as the apoptosis of CD4 cells and disruptions in other immune system components (Reishi, 2014).

COVID-19, caused by the betacoronavirus SARS-CoV-2, has a high neutrophil-to-lymphocyte ratio in critically ill patients and is linked to in-hospital mortality. Autopsies of deceased patients have shown neutrophil infiltration in pulmonary capillaries, extravasation into alveolar spaces, and neutrophilic mucositis (Fu, 2020). Circulating neutrophil extracellular traps (NETs), indicating neutrophil activation, have also been observed (Barnes, 2020).

Oxidative stress, resulting from an imbalance between oxidant production and antioxidant mechanisms, leads to oxidative damage, such as lipid peroxidation and DNA oxidation (Laforge, 2020). In patients with COVID-19, there is an increase in neutrophil infiltration and release of ROS, along with a decrease in antioxidant defenses (Golonka, 2020). This exposure to pro-oxidants typically triggers nuclear translocation of the redox-sensitive transcription factor NRF2 to activate antioxidant defenses. However, respiratory viral infections like SARS-CoV-2 inhibit NRF2-mediated pathways and activate NF-κB signaling, promoting inflammation and oxidative damage (Komaravelli, 2014).

Moreover, decreased expression of the antioxidant enzyme superoxide dismutase 3 (SOD3) has been observed in the lungs of elderly COVID-19 patients with severe disease (Abouhashem, 2020). Interestingly, children who have less reactive and adherent neutrophils and maintain redox balance are less susceptible to severe forms of COVID-19. The cascade of events initiated by oxidative stress in SARS-CoV-2 infection likely plays a significant role in disease severity (Laforge, 2020).

Evidence suggests that oxidative stress plays a multifaceted role in viral diseases, impacting host cell function and viral replication. Even cells that react to infection may generate reactive oxygen species (ROS), with neutrophils being the most common source. Neutrophils respond vigorously to hazardous signals, swiftly migrating to infected tissues, releasing NETs, and generating ROS through an oxidative burst. Targeted administration of antioxidants in treating viral diseases may be a valuable tactic, capable of modulating neutrophil responses at various stages of viral infection. Furthermore, managing ROS generation and oxidative stress could offer a promising pharmaceutical approach to mitigate the effects of viral pathogenesis.

### 2.5. Zebrafish as a model organism

Due to numerous notable attributes, the zebrafish (*Danio rerio*) is highly regarded as an ideal model organism for a wide array of scientific studies. These include reaching sexual maturity by 6 months, with females capable of producing approximately 100-200 embryos per mating. The rapid development and transparent nature of early-stage zebrafish make them well-suited for developmental studies and observing host-pathogen interactions i*n vivo*. Zebrafish also have 84% gene synteny compared to humans (Howe, 2013). Despite the numerous advantages of using zebrafish as a model organism, limitations such as possessing a swimbladder instead of a lung, lacking an adaptive immune system during the first 7 days post fertilization (dpf), and the absence of antibodies for protein-protein interactions should be considered.

#### 2.5.1. Genetic manipulation of zebrafish

In reverse genetics, targeted gene knockdown is a valuable tool used in zebrafish research to investigate the function and significance of specific proteins concerning various disorders or traits. While CRISPR-Cas9 has gained popularity, its practicality is diminished when examining mutations that result in mortality (Li, 2016). However, the presence of two copies of genes in zebrafish and the nature of morpholinos still allow for investigative possibilities. Morpholino antisense oligonucleotides (MO) are synthetic molecules containing a morpholino ring, inhibiting translation or altering targeted genes' splicing events (Meeker and Trede, 2008). They are injected into a 1-2 cell embryo and can last up to 10 days with a 50% waning effect occurring at days 3-4.

Furthermore, gene expression can be manipulated by introducing DNA or mRNA variants of wild-type, mutant, or dominant negative forms of a selected gene into zebrafish embryos. Creating transgenic zebrafish lines has significantly enhanced their utility as a model organism, accomplished through the microinjection of DNA plasmids encoding fluorescent proteins into newly fertilized embryos. The Tol2 transposon system has improved this process, leading to high integration rates for genes of interest (Abe, 2011).

Various zebrafish transgenic approaches have been applied to model acquired diseases by labeling cells involved in infection and inflammation, aiding in studying disease progression *in vivo* (Niethammer, 2009; Soos, 2024). Moreover, bioinformatics tools such as Ensembl and NCBI websites play a crucial role in genetic studies of zebrafish, enabling researchers to access sequence databases and gene annotations for comparative analyses with mammalian models. Notably, the genetic conservation between the zebrafish and human genomes highlights their relevance in disease-related research.

### 2.5.1. Zebrafish as a model of viral infections

The zebrafish model system demonstrates significant potential for elucidating the innate immune response to viral infection. Zebrafish possess a limited adaptive immune response in the initial 4-6 weeks of their development, relying predominantly on their innate immune system to combat various forms of infection. As outlined in section 2.5.4, numerous innate immune system components are functionally preserved in zebrafish. This allows for a valuable expression of how physiological inflammatory reactions to viral infections can escalate to a severe and fatal extent. Zebrafish have been used as an infectious model for over two decades. In Table 2.8, the viruses that are studied in zebrafish are outlined. Also outlined, is the virus family, classification, receptor, the viruses' preferred host, and the method used to cause zebrafish infection.

## Table 2.7 List of viruses that have been studied in zebrafish models

| **Virus Family** | **Virus Type** | **Virus** | **Preferred Host** | **Method(s) of Infection** | **Receptor** |
|---|---|---|---|---|---|
| *Adenoviridae* | dsDNA viruses | Adenovirus | Human<br>Fish<br>Mice | CHO cells transfected with zebrafish CAR receptor, | CAR* (5) |
| *Alloherpesviridae* | dsRNA | Cyprinid herpesvirus 1 | Fish | ZF4 cell infected with virus | Unknown |
| | | Cyprinid herpesvirus 3 | Fish | Intraperitoneal injection, immersion, ZF4 cell infected with virus | Unknown |
| *Amnooviridae* | (-) ssRNA viruses | Tilapia lake vi rus | Tilapia | Intraperitoneal injection | Unknown |
| *Birnaviridae* | dsRNA viruses | Common carp birnavirus* | Fish | ZF4 cell infection | Unknown |
| | | Infectious hematopoietic necrosis virus | Fish | Intraperitoneal injection, immersion, caudal vein, aorta | Unknown |
| | | Infectious pancreatic necrosis virus | Fish | Vertical transfer (female),<br>natural occurrence,<br>immersion,<br>intraperitoneal injection | Unknown |
| *Calciviridae* | (+) ssRNA viruses | Norovirus | Human | Yolk sac injection, immersion | Unknown |
| *Coronaviridae* | (+) ssRNA viruses | Severe acute respiratory syndrome2 | Human<br>Bats | Swimbladder and coelomic cavity | ACE2 |
| *Flaviviridae* | (+) ssRNA viruses | Zika virus | Mosquito<br>Human | Xenograft | AXL* (3) |
| *Hepeadnaviridae* | dsDNA viruses | Hepatitis b virus | Human | One-cell stage injection with transgenic plasmid | NTCP* (4) |
| | | Hepatitis c virus | Human | One-cell stage injection with transgenic plasmid | scavenger receptor class B type I*, CD81*, claudin-1*, occluding* (2) |

table continued

| | | | | | |
|---|---|---|---|---|---|
| *Herpesviridae* | dsDNA viruses | Cytomegalovirus | Human | One-cell stage injection with pUL97 plasmid | ORF14l1 (6) |
| | | Herpes simplex virus type 1 | Human | Inoculation by injection in the dorsal telencephalon or olfactory bulb, CHO-K1 cells transfected with 3-*O* sulfotransferases | Heparin sulfate proteoglycan*, nectin-1*, and herpes virus entry mediator (1) |
| | | Kaposi's sarcoma associated - herpesvirus | Human | Xenograft | DC-SIGN, ephrin receptor A2, ephrin receptor A4, integrins (α3β1, αVβ3, and αVβ5), ICAM-3, xCT (7) |
| *Iridoviridae* | dsDNA viruses | Epizootic hematopoietic necrosis virus | Fish | EPC cells transfected with zebrafish ISG15 | Unknown |
| | | European sheatfish virus | Fish | Immersion | Unknown |
| | | Infectious spleen and kidney necrosis virus | Fish | Intraperitoneal injection, natural occurrence | Unknown |
| | | Lymphocystis disease virus | Fish | Intraperitoneal injection | Unknown |
| *Nodaviridae* | (+) ssRNA viruses | Betanodavirus (nervous necrosis virus) | Fish | Intraperitoneal injection, natural occurrence, immersion | GHSC70* (8) |
| *Orthomyxoviridae* | (-) ssRNA viruses | Common carp orthomyxovirus | Fish | ZF4 cell infected with virus | Unknown |
| | | Influenza | Human | Duct of Cuvier, swimbladder | Sialic acid* (9) |
| *Paramyxoviridae* | (-) ssRNA viruses | Common carp paramyxovirus | Fish | ZF4 cell infected with virus | Unknown |
| *Picornaviridae* | (+) ssRNA viruses | Coxsackie B virus | Human | CHO cells transfected with zebrafish CAR receptor, | CAR* (10) |
| | | Cyprivirus | Zebrafish | Natural occurrence | Unknown |
| *Poxviridae* | dsDNA viruses | Carp oedema virus | Fish | ZF4 cell infected with virus | Unknown |

table continued

| | | | | | |
|---|---|---|---|---|---|
| *Reoviridae* | dsRNA viruses | Chum salmon reovirus | Fish | Intraperitoneal injection, immersion, ZF4 cell infected with virus | Unknown |
| | | Grass carp reovirus | Carp | ZBE3 cells infected with virus, immersion | Laminin* (11) |
| *Retroviridae* | (+) ssRNA viruses | Zebrafish endogenous retrovirus | Zebrafish | Natural occurrence | Unknown |
| *Rhabdoviridae* | (-) ssRNA viruses | Infectious hematopoietic necrosis virus | Fish | Z4 cells infected with virus | Unknown |
| | | Spring viraemia of carp virus | Fish | Immersion, intraperitoneal injection, duct of Cuvier, ZF4 cell infected with virus | Unknown |
| | | Snakehead rhabdovirus | Fish | Immersion, intraperitoneal injection | Unknown |
| | | Viral haemorrhagic septicaemia virus | Fish | Immersion, intraperitoneal injection | Unknown |
| *Togaviridae* | (+) ssRNA viruses | Chikungunya virus | Mosquito<br>Human | Caudal vein, aorta | Unknown |

*The table was modified from Sullivan C., Soos B.L., Millard P.J., Kim C.H., King B.L. Modeling Virus-Induced Inflammation in Zebrafish: A Balance Between Infection Control and Excessive Inflammation. Front. Immunol. 2021;12:636623.*

### 2.5.1. The zebrafish innate immune system

## Section Forward

This section was previously published in Frontiers in Immunology on May 7, 2021. (Sullivan et al., 2021). CS and BK developed the overall outline of the manuscript. B-LS created all tables and Figures 1, 2 and 4. BK created Figure 3. CS, B-LS, CK, PM and BK wrote the manuscript. All authors contributed to the article and approved the submitted version. *Parts of the paper were modified for this section.*

The immune system's innate and adaptive components influence defense against viral infection. While the adaptive immune system offers protection through B and T lymphocytes, this section focuses on the initial response provided by the innate immune system. The immune system includes physical barriers, phagocytic cells, PRRs, interferons and ISGs, cytokines, and chemokines (Alberts, 2002). Physical barriers such as the mucus barrier, which consists of polymeric-secreted mucins, play a role in preventing viral entry. Phagocytes like neutrophils and macrophages can eliminate virus particles and recruit additional phagocytes to infection sites (Abbas, 2022). A key function of phagocytes is the respiratory burst response, which releases ROS to destroy viruses and attract more phagocytes. The innate immune response activation relies heavily on PRRs, which recognize PAMPs and DAMPs (Abbas, 2022). This recognition leads to the expression of interferons and cytokines through NF-kB and IRF transcription factors. Interferons are critical in combating viral infections by activating a range of ISGs. Additionally, inflammatory cytokines and chemokines aid in recruiting phagocytes to infection sites (Abbas, 2022).

Multiple types of nucleotides, including double-stranded RNA, single-stranded RNA, and CpG-deoxynucleotides (CpG-DNA), are acknowledged by Toll-like receptors TLR3, TLR7, TLR8, and TLR9, respectively (42). Zebrafish possess conserved homologs tlr340, tlr741, tlr8a41, tlr8b41, and tlr942 corresponding to TLR3, TLR7, TLR8, and TLR9 (40-42). Additionally, a distinct antiviral Toll-like receptor, tlr21, specific for CpG-DNA42, is identified in zebrafish but not in mammalian genomes, with conservation in avian species (43). The TLR signaling cascade in zebrafish involves adaptor proteins Myd88, Tirap, Ticam1, and Sarm1 for downstream communication (26). Ticam2, the mammalian adaptor protein gene, is absent in zebrafish. Myd88 interacts with all TLRs except TLR3 (26). TLR signaling is orchestrated by TRAF6 and IRAK4, activating various transcription factor families, including NFκB, IRF, STAT, ATF, and AP-1. Also, zebrafish feature TLR4 paralogs tlr4ba and tlr4bb (Sullivan, 2021).

In the realm of zebrafish biology, it has been observed that while some elements of inflammasome signaling are shared with other species, distinct differences are also present. Zebrafish possess an impressive array of over 400 NLR genes (47), yet only two, namely nlrp3 and nlrp6, have been linked to inflammasome activity, with nlrp6 displaying functionality akin to NLRP1 (48). Furthermore, an additional inflammasome adaptor known as *caiap* has been identified as playing a role in regulating inflammasome activation in zebrafish in response to *Salmonella typhimurium* infection (49). While the pro-inflammatory cytokine, il1b, is indeed conserved in zebrafish, no equivalent to IL18 has been pinpointed thus far.

Regarding antiviral responses, studies have shown that Mavs, a key regulator in the IFN pathway, is crucial in combating CHIV infection in zebrafish. Research has demonstrated that the IFN response and overall survival rate significantly declined in Mavs morphants infected with CHIV (52). Moreover, zebrafish analogues of DDX58, IFIH1, and DHX58 have been identified as *ddx58, ifih1*, and *dhx58*, respectively.

Early zebrafish studies uncovered that IFN expression is induced in zebrafish liver cells upon infection by SHRV (59). Alongside the originally characterized IFN gene, now designated *ifnph1*, zebrafish possess three additional IFN genes, *ifnphi2, ifnphi3*, and *ifnphi4*, which activate in response to viral intrusion (60-61). Furthermore, zebrafish harbor two paralogs of type II IFN, IFNG, known as *ifng1* (interferon gamma 1) and *ifng1r* (interferon gamma 1 related) (63).

In the zebrafish immune system, the IFN receptor complex comprises two distinct Crfb heterodimers (Crfb1/ Crfb5 and Crfb2/ Crfb5) (61, 64). Interestingly, the knockdown of caveolin 1 (Cav1) in zebrafish has been shown to disrupt Crfb1 IFN receptor clusters, subsequently diminishing antiviral immune responses (65). These receptor clusters initiate signaling through the Jak/STAT pathway, activating IFN-stimulated genes (ISGs) that share a common IFN-stimulated response element (ISRE) (66). A list of studied proinflammatory, antiviral, and viral-associated autophagy genes will be listed below in Tables 2.9 and 2.10. Another critical aspect of the immune response in zebrafish involves the role of macrophages and neutrophils in executing a respiratory burst response during infection and injury. This response attracts additional phagocytes and breaks down pathogens. The PHOX complex responsible for this burst is notably conserved between humans and zebrafish.

The zebrafish's NADPH oxidase (Nox) gene family encompasses nox1, cybb, nox4, nox5, and the dual oxidases duox and duox2 (72). While Nox1 and Cybb are involved in the PHOX complex and regulated by cytosolic factors, Nox5, Duox, and Duox2 are activated by calcium (Ca2+) due to helix-loop-helix EF-hand domains (72). Nox4 differs in that it is stabilized by p22phox and remains active at all times. Additionally, the expression patterns and functions of Nox family members vary across different tissues. Zebrafish Duox has been identified as essential for peripheral axon regeneration, highlighting its significance in the process (79). A proposed model of antiviral immunity is demonstrated in Figure 2.14.

**Table 2.8. Proinflammatory genes affiliated with antiviral immunity in zebrafish**

| Gene Symbol | Gene Name | Virus(es) |
|---|---|---|
| *Asc (pycard)* | *PYD and CARD domain containing* | Spring viremia carp virus |

table continued

| | | |
|---|---|---|
| *caspa* | *Caspase a* | Spring viremia carp virus |
| *ifn- γ* | *Interferon gamma 1* | Spring viremia carp virus<br>Tilapia lake virus |
| *ifnφ1* | *Interferon phi 1* | Grass carp reovirus<br>Infectious hematopoietic necrosis virus<br>Infectious pancreatic necrosis virus Spring viremia carp virus<br>Tilapia lake virus<br>Viral haemorrhagic septicaemia virus |
| *ifnφ2* | *Interferon phi 2* | Spring viremia carp virus |
| *ifnφ3* | *Interferon phi 3* | Grass carp reovirus<br>Spring viremia carp virus<br>Tilapia lake virus |
| *il-1ß* | *Interleukin 1, beta* | Spring viremia carp virus<br>Tilapia lake virus |
| *il-8* | *chemokine (C-X-C motif) ligand 8a* | Tilapia lake virus |
| *il-10* | *Interleukin 10* | Tilapia lake virus |
| *irf1* | *Interferon regulatory factor 1* | Spring viremia carp virus |
| *irf3* | *Interferon regulatory factor 3* | Grass carp reovirus<br>Spring viremia carp virus<br>Tilapia lake virus |
| *irf7* | *Interferon regulatory factor 7* | Tilapia lake virus |
| *isre* | *Interferon-stimulated response* | Grass carp reovirus<br>Spring viremia carp virus |
| *lta* | *Lymphotoxin alpha (TNF superfamily, member 1)* | Grass carp reovirus<br>Spring viremia carp virus |
| *mita* | *F3 activation* | Spring viremia carp virus |
| *rarres3* | *Retinoic acid receptor responder 3* | Spring viremia carp virus |
| *tnfα* | *Tumor necrosis factor a (TNF superfamily, member 2)* | Spring viremia carp virus<br>Tilapia lake virus |
| *tnf1* | *Tumor necrosis factor 1* | Spring viremia carp virus |
| *tnf2* | *Tumor necrosis factor 2* | Spring viremia carp virus |

## **Table 2.9. Antiviral genes affiliated with antiviral immunity in zebrafish**

| Gene Symbol | Gene Name | Virus(es) |
|---|---|---|
| *defbl2* | *Defensin, beta-like 2* | Spring viremia carp virus |
| *foxo3b* | *Forkhead box O 3* | Spring viremia carp virus |
| *ifit13a* | *Interferon-induced protein with tetratricopeptide repeats 8* | Spring viremia carp virus |
| *ifit17a* | *Interferon-induced protein with tetratricopeptide repeats 14* | Spring viremia carp virus |
| *isg15* | *ISG15 ubiquitin like modifier* | Infectious hematopoietic necrosis virus<br>Infectious pancreatic necrosis virus<br>Spring viremia carp virus<br>Viral haemorrhagic septicaemia virus |
| *mavs* | *Mitochondrial antiviral signaling protein* | Spring viremia carp virus |
| *mda5* | *Interferon induced with helicase C domain 1* | Spring viremia carp virus |
| *mxa* | *Myxovirus (influenza virus) resistance A* | Chum salmon reovirus<br>Cyprinid carp herpesvirus 3<br>Influenza<br>Spring viremia carp virus Tilapia lake virus |
| *mxb* | *Myxovirus (influenza virus) resistance B* | Spring viremia carp virus |
| *mxc* | *Myxovirus (influenza virus) resistance C* | Grass carp reovirus<br>Spring viremia carp virus |
| *nod2* | *Nucleotide oligomerization domain 2* | Spring viremia carp virus |
| *pkz* | *Protein kinase containing Z-DNA binding domains* | Grass carp reovirus<br>Spring viremia carp virus |
| *prmt3* | *Protein arginine methyltransferases 3* | Grass carp reovirus<br>Spring viremia carp virus |
| *rela (NF-kB p65)* | *V-rel avian reticuloendotheliosis viral oncogene homolog A* | Spring viremia carp virus |

table continued

| | | |
|---|---|---|
| *rig-1* | *DEAD (Asp-Glu-Ala-Asp) box polypeptide 58* | Infectious hematopoietic necrosis virus<br>Infectious pancreatic necrosis virus<br>Spring viremia carp virus<br>Tilapia lake virus<br>Viral haemorrhagic septicaemia virus |
| *ripk2* | *Receptor-interacting serine-threonine kinase 2* | Spring viremia carp virus |
| *serpine1* | *Serpin peptidase inhibitor, clade E (nexin, plasminogen activator inhibitor type 1), member 1* | Infectious hematopoietic necrosis virus<br>Spring viremia carp virus<br>Viral haemorrhagic septicemia virus |
| *tbk1* | *TANK-binding kinase 1* | Spring viremia carp virus |
| *tlr3* | *Toll-like receptor 3* | Spring viremia carp virus<br>Tilapia lake virus |
| *tlr7* | *Toll-like receptor 7* | Spring viremia carp virus |
| *tlr8a* | *Toll-like receptor 8a* | Spring viremia carp virus |
| *tlr22* | *Toll-like receptor 22* | Spring viremia carp virus<br>Tilapia lake virus |
| *trim25* | *Tripartite motif containing 25* | Infectious hematopoietic necrosis virus<br>Infectious pancreatic necrosis virus<br>Spring viremia carp virus<br>Viral haemorrhagic septicaemia virus |
| *vig-1 (rsad2)* | *Radical S-adenosyl methionine domain containing 2* | Chum salmon reovirus<br>Cyprinid carp herpesvirus 3<br>Infectious hematopoietic necrosis virus<br>Infectious pancreatic necrosis virus<br>Spring viremia carp virus<br>Viral haemorrhagic septicaemia virus |
| *vtg3 (Pv)* | *Vitellogenin 3* | Lymphocystis disease virus |

**Table 2.10. Autophagy genes affiliated with antiviral immunity in zebrafish**

| Gene Symbol | Gene Name | Virus(es) |
|---|---|---|

table continued

| | | |
|---|---|---|
| *ambra1a (beclin-1)* | *Autophagy/beclin-1 regulator 1a* | Spring viremia carp virus |
| *atg4b* | *Autophagy related 4B, cysteine peptidase* | Spring viremia carp virus<br>Viral haemorrhagic septicaemia virus |
| *atg4c* | *Autophagy related 4C, cysteine peptidase* | Spring viremia carp virus<br>Viral haemorrhagic septicaemia virus |
| *atg5* | *ATG5 autophagy related 5 homolog* | Spring viremia carp virus<br>Viral haemorrhagic septicaemia virus |
| *atg7* | *ATG7 autophagy related 7 homolog* | Spring viremia carp virus<br>Viral haemorrhagic septicaemia virus |
| *atg10* | *ATG10 autophagy related 10 homolog* | Heptaitis C virus<br>Spring viremia carp virus<br>Viral haemorrhagic septicaemia virus |
| *atg12* | *ATG12 autophagy related 12 homolog* | Spring viremia carp virus<br>Viral haemorrhagic septicaemia virus |
| *erk1* | *Mitogen-activated protein kinase 3* | Spring viremia carp virus |
| *erk2* | *Mitogen-activated protein kinase 1* | Spring viremia carp virus |
| *gabarapa* | *GABA(A) receptor-associated protein a* | Heptaitis C virus<br>Spring viremia carp virus<br>Viral haemorrhagic septicaemia virus |
| *gabarapl2* | *GABA(A) receptor-associated protein like 2* | Spring viremia carp virus<br>Viral haemorrhagic septicaemia virus |
| *lamp1* | *Lysosomal associated membrane protein 1a* | Spring viremia carp virus<br>Viral haemorrhagic septicaemia virus |
| *lc3a* | *Microtubule-associated protein 1 light chain 3 alpha* | Spring viremia carp virus |
| *mTOR* | *Mechanistic target of rapamycin kinase* | Spring viremia carp virus |
| *pik3c3* | *Phosphatidylinositol 3-kinase, catalytic subunit type 3* | Spring viremia carp virus |

table continued

| | | |
|---|---|---|
| | | Viral haemorrhagic septicaemia virus |
| *sqstm1 (p62)* | *Sequestosome 1* | Spring viremia carp virus |
| *ulk1* | *Unc-51 like autophagy activating kinase 1a* | Heptaitis C virus<br>Spring viremia carp virus<br>Viral haemorrhagic septicaemia virus |
| *wipi1* | *WD repeat domain, phosphoinositide interacting 1* | Spring viremia carp virus<br>Viral haemorrhagic septicaemia virus |

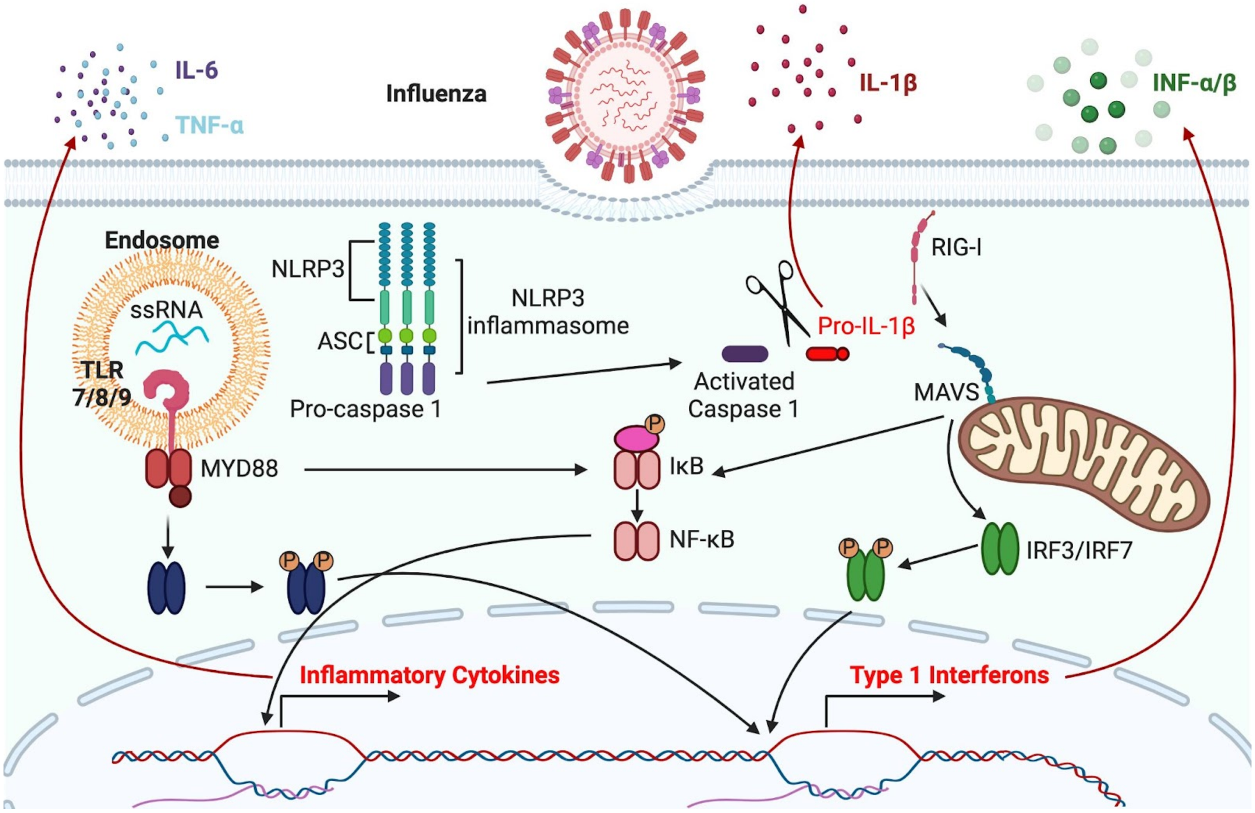
IL-6
TNF-α
Influenza
IL-1β
INF-α/β
Endosome
NLRP3
ssRNA
NLRP3 inflammasome
ASC
TLR 7/8/9
Pro-caspase 1
Activated Caspase 1
Pro-IL-1β
RIG-I
MAVS
MYD88
P
IκB
NF-κB
P
P
P
P
IRF3/IRF7
Inflammatory Cytokines
Type 1 Interferons

**Figure 2.13. The zebrafish antiviral response to IAV.** After the entry and infiltration of the Influenza A Virus (IAV), the single-stranded RNA (ssRNA) that is taken up by endosomes triggers a response from Toll-like receptors 3, 7, 8, and 9. The Toll-like receptor adaptor known as MYD88

then activates the NF-kB transcription factor via IkB. NF-kB, in turn, prompts the transcription of inflammatory cytokines such as IL-6, IL-1B, and TNFA. Interestingly, Damage-associated molecular patterns (DAMPs) and Pathogen-associated molecular patterns (PAMPs) have the ability to activate the NLRP3 inflammasome through the activation of caspase 1 (CASP1). Furthermore, the activation of the RIG-I (DDX58) receptor by cytosolic viral RNA leads to the activation of the IRF3 and IRF7 transcription factors through the MAVS pathway. These transcription factors then trigger the expression of type 1 interferons, which play a crucial role in further enhancing the innate immune response to viral infection. *The image was generated in BioRender.*

## 2.6. Necroptosis

In the past 20 years, there have been significant advancements in our understanding of cell death. Previously, it was thought that apoptosis and necrosis were distinct types of cell death, with apoptosis being controlled and necrosis being accidental. However, recent research has shown that this is an oversimplified view. It is now clear that some forms of necrosis also involve regulatory processes, such as membrane receptors and intracellular signaling molecules. One well-studied type of regulated necrosis is necroptosis, which plays a key role in various diseases.

Apoptosis and necroptosis exhibit distinct morphological characteristics and signaling pathways. Cells undergoing apoptosis maintain cell membrane integrity, while cells undergoing necroptosis experience membrane disruption, resembling necrosis (Gupta, 2018). Despite sharing common triggers, the intracellular pathways leading to apoptosis and necroptosis are different. Caspases mediate apoptosis, while receptor-interacting protein kinases (RIPKs) play a key role in necroptosis (Gupta, 2018). Both cell death processes intersect at various points, with caspase-8 known to counter necroptosis by cleaving necroptosis mediators as one of the best examples (Feng, 2007).

Necroptosis is a cellular response to environmental stressors such as injury, inflammation, or infection (Khoury, 2020). Current research on necroptosis is mainly focused on the TNF-α receptor system. TNF-α can initiate different responses (see Figure 2.15), including survival, apoptosis, or necroptosis depending on the cellular context (Mandal, 2014). The formation of various cell death complexes, such as complex I, complex IIa, and necrosome (complex IIb), dictates the outcome (Mandal, 2014). The necrosome, comprising RIPK1, RIPK3, and Fas-associated protein with death domain, triggers necroptosis through MLKL phosphorylation, leading to plasma membrane rupture and cell death (Sun, 2012). Other downstream effectors of RIPK3, such as mitochondrial serine/threonine-protein phosphatase and Ca2+/calmodulin–dependent protein kinase-II, contribute to necroptosis (Mandal, 2014).

Cell death and inflammation have been found to be intricately intertwined in biological processes. Numerous proinflammatory cytokines, such as TNF-α and IL-1β, along with inflammatory cells possess the capability to induce cell death (Mandal, 2014). The manner in which cells perish, whether through apoptosis or necroptosis, can have varying impacts on the inflammatory response. Apoptosis typically elicits a milder inflammatory reaction by preserving the integrity of the plasma membrane and preventing the release of intracellular contents (Sun, 2010). In contrast, necroptosis has the potential to directly trigger and modulate inflammatory responses by releasing intracellular components through a ruptured plasma membrane (Pasparakis, 2015).

The connection between necroptosis and inflammation has been observed in various pathological conditions, serving as a pivotal aspect in the development of necroptosis-related diseases (Khoury, 2020). Furthermore, key regulators of necroptosis, such as RIPK1 and RIPK3, have demonstrated roles in inflammation independent of their involvement in cell death processes (Khoury, 2020). Further research is ongoing to identify additional effectors in this processes.

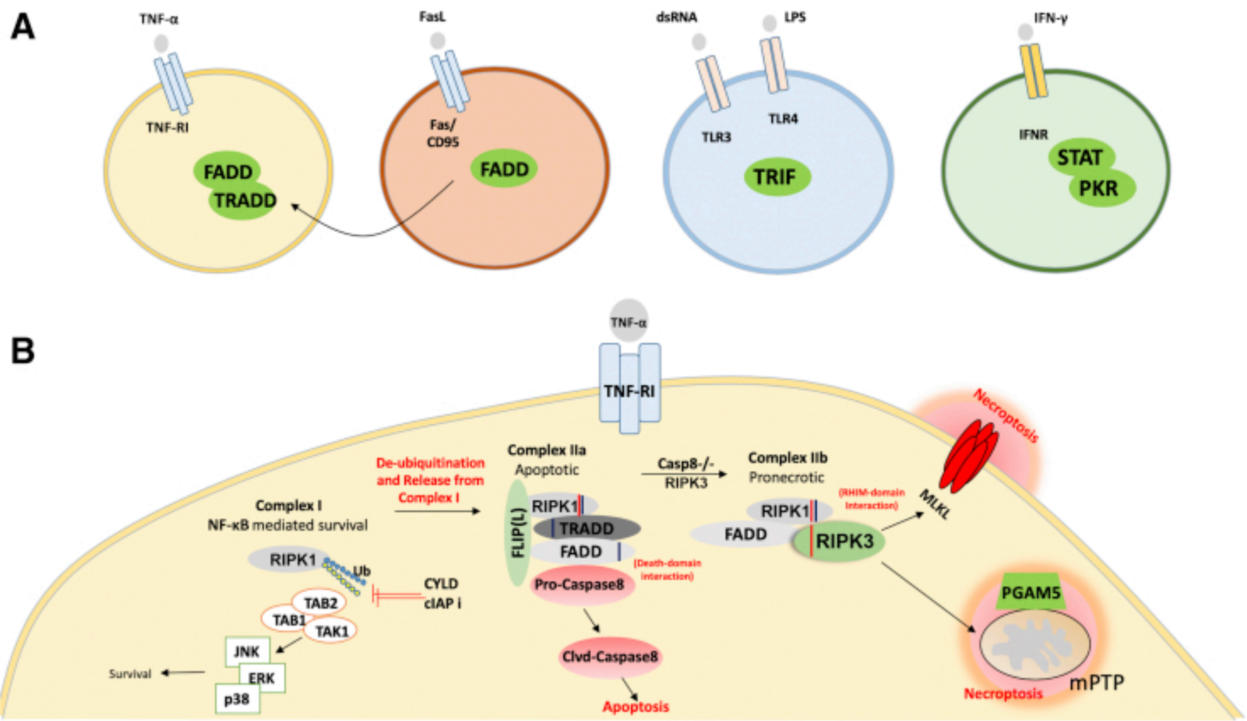
A
TNF-α
TNF-RI
FADD
TRADD
FasL
Fas/
CD95
FADD
dsRNA
LPS
TLR3
TLR4
TRIF
IFN-γ
IFNR
STAT
PKR
B
TNF-α
TNF-RI
Complex I
NF-κB mediated survival
RIPK1
Ub
TAB2
TAB1
TAK1
JNK
ERK
p38
Survival
CYLD
cIAP i
De-ubiquitination
and Release from
Complex I
Complex IIa
Apoptotic
FLIP(L)
RIPK1
TRADD
FADD
Pro-Caspase8
(Death-domain
interaction)
Clvd-Caspase8
Apoptosis
Casp8-/-
RIPK3
Complex IIb
Pronecrotic
RIPK1
FADD
RIPK3
(RHIM-domain
interaction)
MLKL
Necroptosis
PGAM5
Necroptosis
mPTP

**Figure 2.14. Signal transduction events that lead to necroptosis.** Signal transduction events downstream of tumor necrosis factor receptor 1 (TNF-RI) that cause necroptosis. A: Overall schematic highlighting the unique receptors and intracellular signal-transduction components that activate necroptosis by binding to their ligands. The receptors include the TNF-receptor superfamily (TNF-RI and Fas/CD95), the Toll-like-receptor superfamily (TLR3/4), and the interferon receptor (IFNR). The signal transducers are in green circles. Note: all signaling components converge on RIP3 for the execution of necroptosis, and an example of the downstream events is shown in B. B: Signal transduction events downstream of TNF-RI that cause necroptosis. Activation of the TNF-RI, by engagement of TNF-α, can trigger the formation of a prosurvival complex (Complex I), which contains receptor-interacting protein kinase-1 (RIPK1). When

Complex I is ubiquitinated, this leads to NF-κB mediated survival. Alternately, de-ubiquitination of RIPK1 by either ubiquitin carboxyl-terminal hydrolase (CYLD) or pharmacologic targeting of cellular inhibitors of apoptosis (cIAPs) can activate complex IIa. Complex IIa is a protein ensemble consisting of tumor necrosis factor receptor type 1 associated death domain protein (TRADD), Fas-associated protein with death domain (FADD), and RIP1. In the presence of caspase 8, complex II preferentially drives toward IIa, leading to apoptosis. However, in the absence of caspase 8 and the presence of RIP3, complex II switches to IIb, which is pro-necroptotic. Complex IIb then leads to necroptosis via the phosphorylation of mixed-lineage kinase domain-like pseudokinase (MLKL) by RIPK3 or its association of phosphoglycerate mutase family member (PGAM)-5 with RIPK3 that causes the opening of the mitochondrial permeability transition pore complexes (mPTPs). *This figure was taken from Khoury MK, Gupta K, Franco SR, Liu B. Necroptosis in the Pathophysiology of Disease. Am J Pathol. 2020 Feb;190(2):272-285.*

## 2.7. Drug discovery

The drug discovery process encompasses multiple stages that necessitate a diverse range of skills and the utilization of sophisticated technological platforms, often involving a blend of computational and experimental methodologies, to validate targets and identify potential therapeutic agents (Singh, 2023). Once initial experimental compounds have undergone rigorous optimization to achieve selectivity, potency, and safety in early in vitro studies and animal models, they may be identified as promising drug candidates. This pivotal juncture marks a transition from drug discovery to drug development, facilitating the progression of the candidate molecules into human clinical trials. Upon successfully passing through all phases of clinical testing, the therapeutic agent undergoes regulatory registration, paving the way for market release of the drug product (Singh, 2023).

The process typically commences by targeting disease and identifying potential targets, often proteins, that can be influenced by small compounds (Hughes et al., 2011). These compounds are anticipated to disrupt or prevent the disease, or at the very least, mitigate the progression of symptoms (Singh, 2023). Identification of these targets can be achieved through various methods such as cellular assays, genomic studies, proteomic studies, among others. Subsequently, a multitude of small molecules need to undergo testing using diverse types of assays. Promising molecules are then evaluated in animal models that simulate human diseases. It is important to note that findings from animal models can sometimes be inconclusive (Pognan et al., 2023).

Simultaneously, absorption, distribution, and elimination studies (ADME) are carried out. Following years of research, a select few compounds may prove to be safe and effective enough to progress to trials involving human subjects (Singh, 2023). These various stages may go by different designations in the scientific realm, often referred to as the pre-discovery and basic research phase (approximately 5-6 years), during which targets and modulating small molecules are explored in silico (i.e., computer-based), in vitro (i.e., test tube experiments), ex vivo (e.g., tissues or organs), and in vivo using rudimentary animal models (i.e., living organisms, typically rats or mice) (Singh, 2023).

Subsequently, there is the preclinical stage (2-3 years), where the most promising small molecules are selected through a series of in silico, in vitro, and in vivo experiments (Singh, 2023). Following a thorough evaluation, only a handful of compounds typically advance to the subsequent stage. Additional investigation into toxicity is conducted on at least two animal models (one rodent – such as a rat, and one non-rodent – for example, dogs or mini-pigs), often utilizing diverse routes of administration (Singh, 2023). Should the small molecules successfully pass this stage, the compounds are deemed as nominated clinical candidates and granted regulatory approval to proceed to human clinical trials (Singh, 2023). Before initiating clinical trials, an Investigational New Drug (IND) application must be submitted to regulatory bodies. Upon approval of the IND application, clinical trials commence (lasting 4-7 years) (Kandi and Vadakedath, 2023).

Phase I involves testing the safety and tolerability of the therapeutic agent (initially with a single dose, followed by short-term multiple-dose studies) in a small group of healthy individuals (e.g., 20-80 participants). This phase also evaluates various parameters including dosing levels (Singh, 2023). Phase II typically enrolls 100-500 patients and may span multiple hospitals across different countries. This phase aims to determine if the therapeutic agent delivers the intended therapeutic results. The initial segment of phase II, referred to as phase IIa, aims to fine-tune the dosage necessary further to achieve the desired therapeutic effect or monitored endpoints for the clinical candidate (Singh, 2023). Following determining appropriate dosage levels, phase IIb studies commence, focused on assessing the overall efficacy of the candidate drugs in a restricted subject population. Numerous drug candidates fail during phase IIb due to safety concerns or lack of effectiveness (Singh, 2023). Phase III evaluates the drug candidate's efficacy in a larger patient cohort. These studies typically involve 1,000-5,000 patients across multiple clinical trial sites. They are constructed to ascertain the efficacy of the candidate compound in comparison to the current standard of care or a placebo, potential interactions with other medications, and reassessing different dosage levels (Singh, 2023).

Drug repurposing, or drug repositioning, involves taking a drug that has already been approved or is in advanced clinical stages, or even a drug that has been withdrawn from the market, and using it for a different indication (Singh, 2023). This strategy typically involves small molecules. Drug repurposing can be particularly valuable in emergency situations, such as during a pandemic, as well as for rare and neglected diseases where specific drug development may be lacking (Singh, 2023). This approach is seen as cost- and time-effective for providing new medicines, with claims that it can be faster, more economical, less risky, and have higher success rates compared to traditional drug development approaches (Singh, 2023).While drug repurposing offers many advantages, it also comes with challenges. For instance, optimizing a therapeutic molecule for a new indication can be difficult without losing the repurposing potential (Singh, 2023). Identifying the optimal dosage and formulation for a new disease indication may also be time-consuming and require further investigations. Additionally, side effects may arise with a new indication, requiring dosage adjustments (Singh, 2023). Despite these challenges, investigating the molecular mechanisms behind drug repurposing can be valuable in identifying novel targets and potentially serving as a starting point for developing new compounds (Singh, 2023). Overall, drug repurposing is an appealing strategy for faster drug development. Combining approved drugs, possibly with newer drugs, could also enhance effectiveness in some instances (Singh, 2023).

## 2.6. Animal models in biomedical research

Animal research is widely recognized as vital for advancing biomedical science. Despite the ethical debates surrounding its use, animal models play a crucial role in enhancing our understanding of diseases and developing innovative treatment options for animals and humans. Studies involving animals, such as primates, rodents, and pigs, have been instrumental in identifying infection pathways and formulating effective therapeutic strategies for recent global health crises like COVID-19. However, choosing the correct animal model for the job can pose a challenge. The question to ask when choosing an animal model is do the benefits outweigh the costs of using this animal (physical discomfort, reproducibility, financial) ? The remainder of this section will be focused on demonstrating how these animal models can be used for diverse studies..

In medicine, the shift from an artistic approach to a more scientific methodology can largely be attributed to the utilization of diverse animal models (Hobson, 2018). These models are carefully selected based on their genetic and functional attributes to align with specific research objectives (Domínguez-Oliva, 2023). They make significant contributions to the field by deepening our knowledge of biological and pathological processes and aiding in developing and testing medical interventions like drugs, vaccines, and surgical procedures applicable in both human and veterinary practices (Smith, 2019).

Rodents, in particular, are considered prime candidates for research due to their physiological similarities to humans (Domínguez-Oliva, 2023). This makes them valuable subjects for studying various conditions such as sepsis, obesity, cancer, and organ transplants (Jota, 2021). Other animal species like monkeys, pigs, rats, mice, guinea pigs, dogs, rabbits, birds, cows, sheep, fruit flies, nematodes, sea slugs, bees, squid, horses, fish, frogs, cats, reptiles, chimpanzees, hamsters, and zebrafish are also enlisted for specific research purposes, ranging from neurological disorders to metabolic diseases (Babac, 2021; Lasko, 2021; Zang, 2018). In Table 2.12 and Figure 2.15 animal models used for antiviral studies against IAV are revealed.

**Table 2.11 Animal models used for antiviral efficacy during influenza infection**

| Animal Model | Presence of clinical signs | Transmission |
|---|---|---|
| Mice (*Mus musculus*) | Yes | No |
| Golden Syrian Hamster (*Mesocricetus auratus*) | No | Yes |
| Cotton rats (*Sigmodon hispidus*) | Yes | No |
| Guinea pigs (*Cavia porcellus*) | No | Yes |
| Ferret (*Mustela furo*) | Yes | Yes |
| Chicken (*Gallus gallus*) | Yes | Yes |

table continued

| | | |
|---|---|---|
| Non-human primates | Yes | N/R |
| Horses (*Mus musculus*) | Yes | N/R |
| Zebrafish (*Danio rerio*) | Yes | No |

*The table was modified from Caceres CJ, Seibert B, Cargnin Faccin F, Cardenas-Garcia S, Rajao DS, Perez DR. Influenza antivirals and animal models. FEBS Open Bio. 2022 Jun;12(6):1142-1165.*

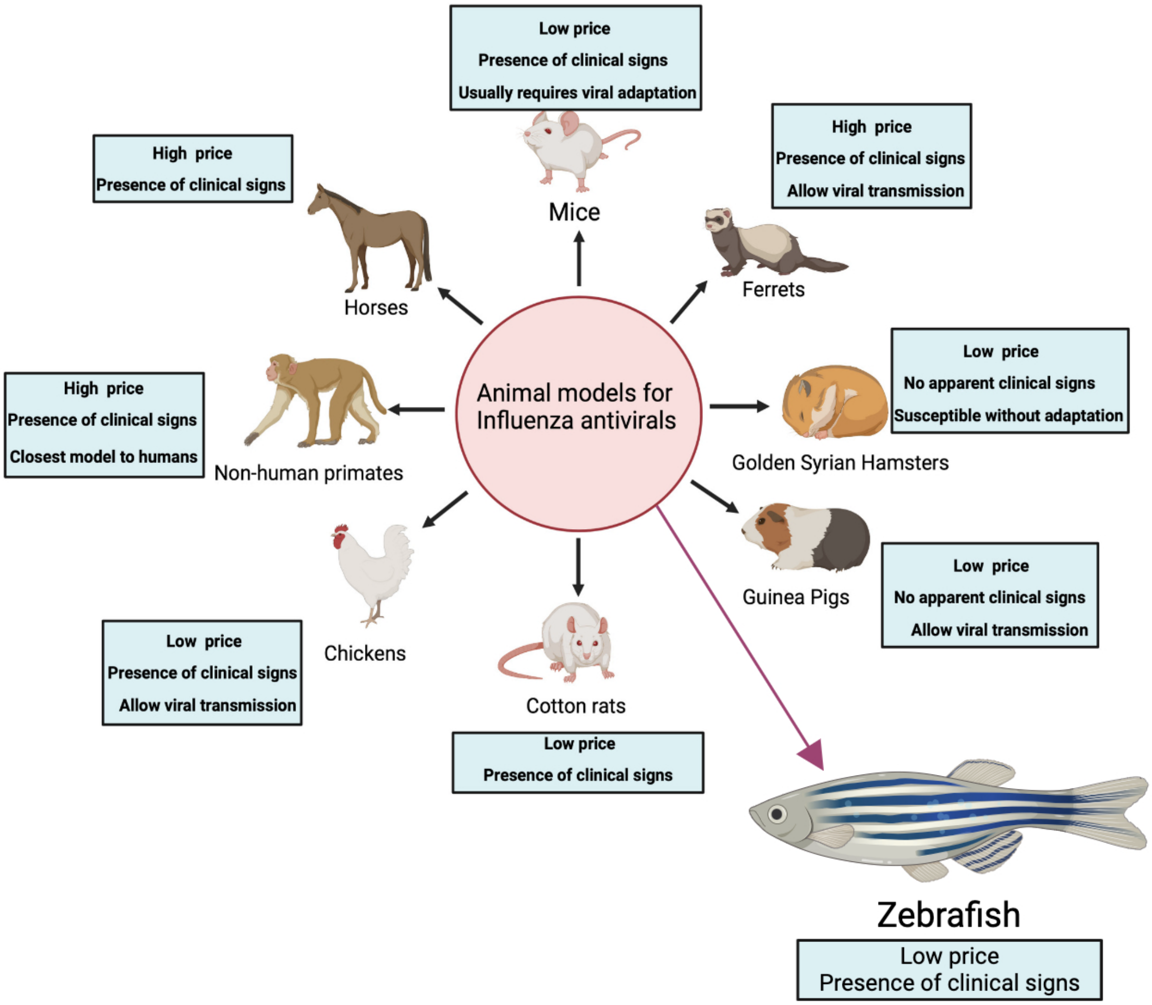
Animal models for Influenza antivirals
Mice
Low price
Presence of clinical signs
Usually requires viral adaptation
Ferrets
High price
Presence of clinical signs
Allow viral transmission
Golden Syrian Hamsters
Low price
No apparent clinical signs
Susceptible without adaptation
Guinea Pigs
Low price
No apparent clinical signs
Allow viral transmission
Cotton rats
Low price
Presence of clinical signs
Chickens
Low price
Presence of clinical signs
Allow viral transmission
Non-human primates
High price
Presence of clinical signs
Closest model to humans
Horses
High price
Presence of clinical signs
Zebrafish
Low price
Presence of clinical signs

**Figure 2.15. Animal models for influenza antiviral evaluation.** Pictorial summary of animal models currently utilized in antiviral research against influenza viruses. *The image was generated in BioRender. The image was modified from Table was modified from Caceres CJ, Seibert B, Cargnin Faccin F, Cardenas-Garcia S, Rajao DS, Perez DR. Influenza antivirals and animal models. FEBS Open Bio. 2022 Jun;12(6):1142-1165.*

In experimental settings, animals may be utilized entirely, or specific components like cells, tissues, organs, genes, or other biological elements to simulate pathological processes (Smith, 2019). Each species offers unique insights into different aspects of disease processes, contributing to the advancement of biomedical science and ultimately paving the way for innovative medical solutions (Domínguez-Oliva, 2023).

# CHAPTER 3

# COLOR-FLU FLUORESCENT REPORTER INFLUENZA A VIRUSES ALLOW FOR IN VIVO STUDIES OF INNATE IMMUNE FUNCTION IN ZEBRAFISH

## Chapter Forward

This chapter was previously published in Viruses on January 20, 2024 (Soos et al., 2024). Brandy-Lee Soos and Benjamin L. King designed the experiments. Brandy-Lee Soos performed experiments with assistance from Alec Ballinger (respiratory burst assays), Mykayla Weinstein (respiratory burst assays), Haley Foreman (RNA extraction, cDNA synthesis, and qRT-PCR), Julianna Grampone (qRT-PCR), Sam Weafer (imaging), Connor Aylesworth (qRT-PCR), and Benjamin L. King (resources, supervision, and validation. Brandy-Lee Soos conducted RNA extraction, cDNA synthesis, qRT-PCR, confocal imaging, survival curves, TCID50 assays, respiratory burst, and drug assays. Brandy-Lee Soos grew up the strains of the four color-flu IAV viruses. Brandy-Lee Soos developed the standardized models of wild-type IAV and color-flu IAV. Brandy-Lee Soos and Benjamin L. King wrote and edited the manuscript. Brandy-Lee Soos and Benjamin L. King conducted data analysis. Brandy-Lee Soos and Mark Nilan maintained and bred the zebrafish lines used in this paper. The animal study protocol was approved by the Institutional Animal Care and Use Committee (IACUC) at the University of Maine under protocol number: A2021-02-02 and was approved on June 25, 2021. This work was supported by the National Institute of Allergy and Infectious Diseases of the National Institutes of Health, under grant number R15 AI131202 awarded to Benjamin L. King, and the Institutional Development Award (IDeA) from the National Institute of General Medical Sciences of the National Institutes of Health under grant numbers P20 GM144265 awarded to Benjamin L. King and P20 GM103423 also awarded to Benjamin L. King.

We thank Yoshihiro Kawaoka of the University of Wisconsin for sharing the Color-flu IAV strains, and Mark Nilan at the University of Maine's Zebrafish Facility for providing excellent zebrafish care.

### 3.1. Abstract

Influenza virus infection can cause severe respiratory disease and is estimated to cause millions of illnesses annually. Studies on the contribution of the innate immune response to influenza A virus (IAV) to viral pathogenesis may yield new antiviral strategies. Zebrafish larvae are useful models for studying the innate immune response to pathogens, including IAV, in vivo. Here, we demonstrate how Color-flu, four fluorescent IAV strains originally developed for mice, can be used to study the host response to infection by simultaneously monitoring infected cells, neutrophils, and macrophages in vivo. Using this model, we show how the angiotensin-converting enzyme inhibitor, ramipril, and mitophagy inhibitor, MDIVI-1, improved survival, decreased viral burden, and improved the respiratory burst response to IAV infection. The Color-flu zebrafish larvae model of IAV infection is complementary to other models where the dynamics of infection and the response of innate immune cells can be visualized in a transparent host in vivo.

### 3.2. Introduction

Influenza A virus (IAV) infection can result in acute respiratory inflammation that requires hospital care, and in severe cases, can lead to death. An estimated 10–37 million influenza infections occur each year in the US, with 114,000–624,000 needing hospital care for associated respiratory and heart symptoms (Tokars, 2018). Between 5000 and 27,000 deaths occur each year in the US from influenza infections (Reed, 2015). While vaccines have been widely used, they have only been between 19 and 60% effective in preventing influenza because of antigenic variation in strains circulating in different populations and the difficulty of formulating vaccines against those strains (Treanor, 2012; Zimmerman, 2016). Outbreaks of new influenza strains can become pandemic, such as the 2009 A(H1N1)pdm09 strain that resulted in an estimated 60.8

million infections, 274,000 hospitalizations, and 12,000 deaths in the US (Shrestha, 2011). Antiviral therapies, such as oseltamivir (Tamiflu®), are valuable tools for treating influenza, but the potential risks that drug-resistant strains pose make it necessary to develop new therapies that target alternative mechanisms.

One roadblock to understanding the pathogenesis of influenza infection is the fact that the relative contributions of the virus and host factors have not been well characterized in vivo. Mammalian influenza virus infections originate in respiratory epithelial cells and alveolar macrophages (Yu, 2011). The innate immune response to influenza infection includes type I interferons (IFNs) and proinflammatory cytokines and chemokines that activate neutrophils and macrophages. The innate antiviral immune response is activated in response to influenza infection and initiates a feed-forward loop that leads to the recruitment of excess neutrophils characterized with a dysregulation of IFN expression and reactive oxidative species (ROS) production (Brandes, 2013). Characterizing the complex dynamics of host immune cells during their response to influenza virus infection requires simultaneous monitoring of multiple cell types along with the virus. Biopsy studies in human, primate, or mammalian models cannot show the temporal dynamics of viral invasion and subsequent neutrophil and macrophage recruitment.

Influenza viruses that express fluorescent proteins are powerful tools for understanding viral pathogenesis in vivo. For example, Manicassamy et al. created a green fluorescent protein (GFP) reporter strain of A/Puerto Rico/8/34 (PR8; H1N1) that was used to study antigen presentation during IAV infection (Manicassamy, 2010). Fukuyama et al. generated four different mouse-adapted PR8 strains that express different fluorescent reporter proteins (Fukuyama, 2015). These “Color-flu” strains express either Venus (mVenus-PR8), a GFP with improved chromophore formation and brightness, enhanced cyan fluorescent protein (eCFP-PR8), enhanced

GFP (eGFP-PR8), or mCherry (mCherry-PR8). For each strain, coding sequences for the fluorescent tags were fused to the end of the open reading frame for non-structural protein 1 (NS1) in the PR8 genome, allowing for the expression of NS1 fluorescent chimeric proteins during viral replication. Importantly, the development of these mouse-adapted strains included serial passaging and selecting for strains that had an increased pathogenicity and strong fluorescent protein expression to overcome the attenuation observed with viruses expressing reporter proteins (Kittel, 2004; Shinya, 2004). Moreover, Color-flu strains were used to detect virus-infected cells in mouse bronchial tissue via imaging fluorescence in (Fukuyama, 2015). Simultaneous co-infections with the four strains allowed for areas of local virus propagation in the bronchial epithelium using multispectral imaging.

Zebrafish are powerful animal models for studying host responses to virus infection, as there are several genetic and pharmacological approaches that can be used to screen pathways and genes in combination with in vivo imaging of transparent embryos (Sullivan, 2021). Major human immune signaling pathways that respond to viral infection are conserved in zebrafish (Sullivan, 2021). Gabor et al. established the zebrafish model of IAV infection Gabor, 2014). In their study, it was demonstrated that: (1) zebrafish embryos express α-2,6-linked sialic acid receptors; (2) embryos have reduced survival following IAV disseminated infection; (3) IAV replicates in embryos; (4) interferon phi 1 (*ifnphi1*) and myxovirus (influenza) resistance A (*mxa*) had upregulated expression with IAV infection; (5) disseminated IAV infection resulted in necrosis of the liver, gills, and head kidney tissue along with pericardial edema; and (6) pathological phenotypes from IAV infection were reduced in embryos treated with the neuraminidase inhibitor Zanamivir. Their study also showed how neutrophils are recruited to the site of localized infection in the swimbladder using fluorescent confocal imaging of zebrafish embryos infected with NS1-

GFP PR8 IAV (Manicassamy, 2010) These initial studies demonstrated that in vivo imaging of fluorescent influenza strains in a vertebrate is possible. Goody et al. used the zebrafish IAV model to study how IAV infection exacerbated skeletal muscle damage in *sapje* zebrafish mutants (Goody, 2017). The zebrafish IAV model was also recently used to demonstrate how cetylpyridinium chloride exposure increased survival and decreased viral burden following IAV infection compared to controls (Raut, 2022).

In this study, we demonstrate the application of Color-flu in zebrafish embryos to study host responses to IAV infection in vivo. We first compared the survival and viral burden of embryos to systemic infection by H1N1 PR8 with Color-flu. Next, we show how microinjecting Color-flu into the circulatory system results in disseminated infection throughout the embryo. We also show how Color-flu can be simultaneously imaged with neutrophil and macrophage reporter lines. As genetic background can influence phenotypes, we examined the survival of two wild-type zebrafish strains, AB and Ekkwill (EK), along with the pigment mutant, *casper* (*mitfaw2/w2; mpv17a9/a9*) (D'Agati, 2017; White, 2008), with disseminated infection. Next, we demonstrate how Color-flu can be used to test for the efficacy of two small molecules, ramipril and mitochondrial division inhibitor 1 (MDIVI-1), which were found to increase survival following systemic infection. Ramipril is an inhibitor of the angiotensin-converting enzyme (ACE) (Witte, 1984), and a recent study found that individuals who have prescriptions for ACE inhibitors had a lower risk of influenza (Chung, 2020). MDIVI-1 inhibits dynamin 1-like protein (DNM1L) and blocks apoptosis by preventing mitochondrial and peroxisomal division (Cassidy-Stone, 2008). Together, these studies demonstrate the utility of using Color-flu in a zebrafish model of IAV infection to study the host response and screen small molecules in vivo.

## 3.3. Materials and Methods

### 3.3.1. Zebrafish care and maintenance

The zebrafish used in this study were housed and maintained in the Zebrafish Facility at the University of Maine in accordance with the recommendations and standards in the *Guide for the Care and Use of Laboratory Animals* of the National Institutes of Health and the Institutional Animal Care and Use Committee (IACUC) at the University of Maine. Protocols utilized in this study were approved by the IACUC at the University of Maine (Protocol Number: A2021-02-02). Zebrafish were housed in recirculating tanks following standard procedures of a 14 h light, 10 h dark cycle at 28 °C [21]. The zebrafish lines used in this study were AB, Ekkwill (EK), *casper* (*mitfaw2/w2; mpv17a9/a9*) (Whitte, 2008), and Tg(*mpeg1*:eGFP;*lyz*:dsRed). The Tg(*mpeg1*:eGFP;*lyz*:dsRed) line was created by crossing the Tg(*mpeg1*:eGFP) (Renshaw, 2006) and Tg(*lyz*:dsRed) (Hall, 2007) zebrafish lines. Embryos were obtained by spawning adult zebrafish using varying sets of females. Embryos were kept at 33 °C in 50 mL of sterilized egg water (60 µg/mL Instant Ocean Sea Salts; Aquarium Systems, Mentor, OH, USA) in 100 mm × 25 mm Petri dishes (catalog number 89220-696, VWR, Radnor, PA, USA), with water changes every 2 days.

### 3.3.2. MDCK/ London cell culture

Madin–Dardy canine kidney/London (MDCK/London; Influenza Reagent Resource) cells (passage 3–4) were cultured using a modified protocol originally developed by Eisfield et al. [24]. Cells were grown at 37 °C with 5% CO2 in T-175 flasks (CELLSTAR Flasks; USA Scientific, Ocala, FL, USA), in minimal essential medium (MEM; catalog number 11090073, Gibco, Thermo Fisher Scientific, Waltham, MA, USA) containing final percentages/concentrations as follows: 5% heat-inactivated newborn calf serum (NCS; catalog number 26010074, Gibco), 2% heat-inactivated fetal bovine serum (FBS; catalog number 16140071, Gibco), 0.23% sodium bicarbonate solution (catalog number 25080094, Gibco), 2% MEM amino acids (from 50× stock; catalog number 11130051, Gibco), 1% MEM vitamin solution (from 100× stock; catalog number 11120052, Gibco), 4 mM L-glutamine (catalog number 25030081, Gibco), and 1% antibiotic–antimycotic (from 100× stock; catalog number 15240062, Gibco). The cells were maintained by washing twice with 1× Dulbecco's phosphate-buffered saline (PBS, pH 7.4), trypsinized with 0.25% trypsin-EDTA with phenol red (catalog number 25300054, Gibco), and passaged in a 1:10 dilution every 2–3 days up to passage eight. Virus-infected cells were grown in MEM-BSA-TPCK media (Eisfeld, 2014), which were prepared similarly to the MEM media described above but supplemented with 1 µg/mL Tosyl phenylalanyl chloromethyl ketone (TPCK) trypsin (Worthington Chemical Corporation, Lakewood, NJ, USA) and Bovine Albumin Fraction V (7.5% solution; catalog number 15260037, Gibco) instead of NCS and FBS.

### 3.3.3. Influenza virus

PR8 influenza virus (A/PR/8/34 (H1N1) Purified Antigen; catalog number 10100374) was purchased from Charles River Laboratories (now AVS Bio in Norwich, CT, USA). Upon arrival, the virus was defrosted on ice, aliquoted into microcentrifuge tubes, and stored at −80°. Prior to use, virus aliquots were thawed on ice and diluted in cold sterile Hank's buffered salt solution (HBSS) using a ratio of 87% virus to 13% diluent.

Color-flu (Fukuyama, 2015) influenza virus strains MA-mVenus-PR8 (mVenus-PR8), MA-eCFP-PR8 (eCFP-PR8), MA-eGFP-PR8 (eGFP-PR8), and MA-mCherry-PR8 (mCherry-PR8) were kindly provided by Dr. Yoshihiro Kawaoka's laboratory and stored at −80 °C. Color-flu virus strains were propagated in separated T-25 flasks (CELLSTAR Flasks; USA Scientific) using MDCK/London cells using MEM-BSA-TPCK as outlined in Eisfeld et al. [24] (see

MDCK/London Cell Culture section). Color-flu strains were grown for 4 days before being collected, filter sterilized using 0.45 μm tube top vacuum filters (VWR), aliquoted, and stored at −80 °C until use.

### 3.3.4. Microinjection

Microinjection was used to inject either vehicle (HBSS) controls or influenza virus to introduce a disseminated or localized infection in our zebrafish larvae. First, influenza virus strains were thawed on ice for 30 min. The virus strains were diluted in cold, sterile HBSS (catalog number 14170120, Gibco) at a solution of 87% virus and 13% HBSS. Next, the larvae were anesthetized in sodium bicarbonate-buffered MS-222 (tricaine methanesulfonate) solution (200 mg/L) (Syndel, Ferndale, WA, USA) at 2 or 3 dpf for disseminated infection experiments, or 4 dpf for localized infection experiments. The larvae were then lined up on a 2% agarose gel in a Petri dish coated with 3% methylcellulose. Microinjections of the virus or HBSS were conducted using pulled microcapillary needles (1.2 mm outside diameter, 0.94 mm inside diameter; Sutter Instruments, Novato, CA, USA) controlled with an MPPI-3 pressure microinjector (Applied Scientific Instruments, Eugene, OR, USA). For disseminated infection experiments of PR8 virus, 1 or 2 nL of virus (~$2.8 \times 10^8$ EID50 for lot 1, ~$4.4 \times 10^7$ EID50 for lot 2, ~$1.7 \times 10^6$ EID50 for lot 3) or HBSS was injected into the duct of Cuvier (DC) at 2 or 3 dpf, respectively. A total of 6 nL of Color-flu virus (~$7.44 \times 10^5$ TCID50/mL for mVenus-PR8, ~$5.04 \times 10^5$ TCID50/mL for eCFP-PR8, ~$4.80 \times 10^5$ TCID50/mL for eGFP-PR8, and ~$4.56 \times 10^5$ TCID50/mL for mCherry-PR8) or HBSS was injected into the DC at 3 dpf for disseminated Color-flu infection experiments. For localized infection experiments with PR8 virus, 4 nL (~$4.4 \times 10^7$ EID50 for lot 2, ~$1.7 \times 10^6$ EID50 for lot 3) of virus or HBSS was injected into the swimbladder of the larvae at 4 dpf. For localized Color-flu infection experiments, 10 nL of Color-flu or HBSS was injected into the swimbladder at

4 dpf. For the control experiments, the larvae were also injected with heat-inactivated or UV-inactivated virus. Virus aliquots were either heat-inactivated at 80 °C for 5 min, or UV-inactivated with 254 nm light exposure for 60 min on ice (UV CrossLinker, VWR). For virus infections, microcapillary needles were changed hourly to keep the virus viable. For disseminated infection experiments, zebrafish were sorted into Petri dishes at a density of ~50 larvae/dish and maintained in embryo water at 33 °C (see Zebrafish Care and Maintenance section). For localized infection experiments, zebrafish were kept at a density of ~45 larvae/dish.

### 3.3.5. Drug exposures

For all of our small molecule drug studies, virus-infected or HBSS-injected larvae were exposed to either dimethyl sulfoxide (DMSO; Sigma-Aldrich, St. Louis, MO, USA), DMSO-solubilized ramipril (Cayman Chemical Company, Ann Arbor, MI, USA), or DMSO-solubilized MDIVI-1 (Cayman Chemical Company, Ann Arbor, MI, USA) by adding these solutions into the embryo water at 24 hpi. The larvae were exposed to DMSO, ramipril, or MDIVI-1 for one hour at 33 °C in a dark incubator. After exposure, zebrafish were transferred to 50 mL of fresh embryo water twice to rinse away the DMSO or DMSO-solubilized drugs. The final concentrations used were 0.2 nM for ramipril (Vishnolia, 2020) and 7 nM for MDIVI-1 (Vargo, 2017).

### 3.3.6. Survival studies

For survival studies, mortality was monitored and counted daily in infected and control-injected larvae for up to 7 dpf. Larvae were maintained in dishes (~50 larvae/dish) at 33 °C with embryo water changes every two days.

### 3.3.7. Viral burden assays

Tissue culture infectious dose 50 (TCID50) end-point dilution assays using MDCK/London cells were used to measure the viral burden of influenza virus in zebrafish. Cohorts of 200 zebrafish per experimental group were used (see Zebrafish Care and Maintenance section), infected (see Microinjections section), and maintained in embryo water at 33 °C in dishes (~50 larvae/dish) with water changes every other day. Zebrafish were collected at 0, 24, 48, 72 and 96 hpi for the larvae infected at 2 dpf, and 0, 24, 48 and 72 hpi for the larvae infected at 3 dpf. At the appropriate timepoint, 25 larvae per group were collected and euthanized with an overdose (300 mg/L) of MS-222 for 10 min. Next, the larvae were transferred into 500 µL of RNAlater (Invitrogen, Thermo Fisher Scientific), flash-frozen with liquid nitrogen, and stored at −80 °C.

The MDCK/London cells were plated into 96-well plates (PlateOne; catalog number 1837-9600, USA Scientific) the evening before the TCID50 assay at a cell density of ~15,000 cells per well to achieve 90–95% confluency the next day. After thawing the frozen samples on ice, the RNAlater was replaced with 500 µL of MEM-BSA-TPCK (see MDCK/London Cell Culture section). Samples were homogenized with a Bullet Blender tissue homogenizer (Next Advance, Troy, NY, USA) using a sterile metal bead at setting #3 for 5 min at 4 °C and centrifuged at 8000× *g* for 1 min. Next, eight 1-to-8.5 serial dilutions ($10^{-0.9}$ to $10^{-7.4}$) for each sample were prepared in MEM-BSA-TPCK. Cells were washed twice with PBS prior to adding the serial dilutions. After removing the second PBS wash, 50 µL serial dilutions for each sample were plated using triplicate wells (24 wells/sample), with 4 control wells per plate; 50 µL of MEM-BSA-TPCK was added to the control wells. Plates were centrifuged at 2000× *g* for 10 min at 4 °C and then incubated at 37 °C for two hours with 5% $CO_2$. Cell media were removed from all wells and 105 µL of MEM-BSA-TPCK was added to each well. Plates were then incubated at 37 °C for 72 h with 5% $CO_2$.

Next, cytopathic effects were observed, and the cells were counted using a Bio-Rad TC20 Automated Cell Counter (Bio-Rad, Hercules, CA, USA). TCID50/mL was calculated using the Spearman–Kärber method (Hierholzer, 1996).

### 3.3.8. Respiratory burst assays

The capacity of zebrafish to generate ROS in vivo was quantified using a respiratory burst assay. Virus-infected and HBSS-injected zebrafish were collected at 24 and 48 hpi, anesthetized in sodium bicarbonate-buffered MS-222 (200 mg/L), and placed into black, flat-bottom 96-well plates (Fluotrac 600, Greiner-Bio., Monroe, NC, USA) with 100 µL of embryo water. The HBSS-injected zebrafish were placed into the wells in the first 6 columns of the plate, and the virus-infected zebrafish were placed into the remaining wells. The first 2 columns were treated with 5 µL of 1 mM protein kinase C inhibitor, bisindolylmaleimide I (BisI, Cayman Chemical Company), in DMSO. The BisI-treated embryos were incubated for 30 min at 28 °C. Zebrafish in columns 1, 3–4, and 7–9 were treated with 100 µL of embryo water plus 1 µg/mL 2′,7′-dichlorofluorescein diacetate (H2DCFDA) (Sigma-Aldrich) in 0.4% DMSO. Zebrafish in columns 2, 5–6, and 10–12 were treated with 100 µL of embryo water plus 1 µg/mL H2DCFDA and 400 ng/mL phorbol 12-myristate 13-acetate (PMA, Sigma-Aldrich). The plates were then covered with aluminum foil and incubated at 28 °C for 2.5 h. Fluorescence was read using a plate reader (BioTek Synergy, Agilent Technologies, Santa Clara, CA, USA). Assays were repeated three times.

### 3.3.9. Confocal imaging

Zebrafish were anesthetized in sodium bicarbonate-buffered MS-222 (200 mg/L) and placed in 24-well glass-bottom imaging plates (MatTek, Ashland, MA, USA) with embryo water with 0.7% agarose. An Olympus Fluoview IX-81 inverted microscope with an FV1000 confocal system with 405, 458, 488, 514, and 543 nm laser lines was used for fluorescence and brightfield imaging of the zebrafish. Images were obtained using ×4 or ×10 objectives. Ten zebrafish were scanned per group and one was randomly chosen to visualize Color-flu infected AB larvae. Twelve zebrafish were scanned per group and one was randomly selected to visualize eCFP-PR8 infected Tg(*mpeg1*:eGFP;*lyz*:dsRed) larvae. For quantification of the number of neutrophils, macrophages, and relative abundance of virus infected cells, six Tg(*mpeg1*:eGFP;*lyz*:dsRed) larvae were scanned over two separate trials, and the four healthiest zebrafish from each experiment were selected for analysis. The Z-stack cross sections were 5 microns thick, and five slices were imaged both dorsally and ventrally (50 microns total) from the center of the larvae and then analyzed.

### 3.3.10. Image analysis

Image analyses to count neutrophils and macrophages and quantify virus levels based on fluorescence intensities were conducted using MATLAB (version R2023a; The MathWorks Inc., Natick, MA, USA). Longitudinal images obtained on the confocal were composed of 5 μm-thin sections. Five sections proximal to the center of the zebrafish and five sections distal to the center of the zebrafish were analyzed for a total of 50 μm (approximately 40–50% of the total zebrafish width). Masks were generated to identify dsRed-tagged neutrophils, eGFP-tagged macrophages, and eCFP-PR8 Color-flu virus. Those masks were then used to count both neutrophils and macrophages, and the level of eCFP-PR8 virus infection (pixels).

### 3.3.11. qRT-PCR assays

Four biological replicate total RNA samples were prepared per sample group using 8 larvae per sample. Each set of larvae for a given sample was homogenized using a Next Advance Bullet Blender (Next Advance, Troy, NY, USA) with a single 5 mm sterile, stainless steel metal bead in

360 µL of Trizol (Invitrogen, Waltham, MA, USA) for 3 min. Homogenates were centrifuged for 3 min at 8000× *g* and transferred to new tubes. Total RNA was extracted using the Direct-zol RNA microprep kit (Zymo Research, Irvine, CA, USA) following the manufacturer's protocol. cDNA was synthesized using the ProtoScript II First Strand cDNA synthesis kit (New England Biolabs, Ipswich, MA, USA), following the manufacturer's protocol. qRT-PCR assays were conducted using Bio-Rad SsoAdvance Universal SYBR Green Mastermix (Bio-Rad, Hercules, CA, USA), and oligos (IDT, Coralville, IA, USA), shown in Table S1, and a Bio-Rad CFX96 instrument (Bio-Rad) according to the manufacturer's protocol.

### 3.3.11. Statistical analysis

GraphPad Prism 9.5.1 (GraphPad Software, Boston, MA, USA) was used to generate and analyze survival curves and graphs. The Kaplan–Meier survival analysis method was used to analyze survival curves with 95% confidence intervals. Mantel–Cox test *p*-values <0.05 between the sample groups were considered significant. Two-way ANOVAs followed by Dunnett's multiple comparison tests were used to analyze the Color-flu TCID50/mL values. A Brown–Forsythe one-way ANOVA test was used to analyze the TCID50/mL values from the live PR8, heat-inactivated and UV-inactivated larvae, followed by Dunnett's multiple comparison tests. Statistical analyses of the fold induction from respiratory burst assays were conducted using the Kruskal–Wallis test with the Dunn's multiple comparison test for pairwise comparisons. Pairwise comparisons with an adjusted *p*-value < 0.05 were considered significant.

## 3.4. Results

### 3.4.1. IAV infection decreases survival and replicates in zebrafish

It has previously been shown that zebrafish express α-2,6-linked sialic acid-containing receptors and are susceptible to infection by PR8 H1N1 and X-31 A/Aichi/68 H3N2 IAV (Gabor, 2014). We modified the original zebrafish IAV infection protocol to achieve approximately 50% mortality by 7 days post fertilization (dpf) by infecting embryos with PR8 IAV at either 2 or 3 dpi, by increasing the level of virus infection compared to the original protocol, and by using Hank's buffered salt solution (HBSS) instead of phosphate-buffered saline (PBS) as the diluent. In our protocol, we microinjected a 1 nL solution of 87% PR8 IAV and 13% HBSS ($\sim 1.7 \times 10^{6}$ to $\sim 2.8 \times 10^{8}$ EID50, depending on the virus lot) into the duct of Cuvier (DC) in 2 or 3 dpf anesthetized embryos. This virus concentration was higher than the original study, which used 1.5 nL ($\sim 5 \times 10^{3}$ EID50) of PR8. We found reduced survival in the AB zebrafish systemically infected with three different PR8 virus lots at 2 dpf compared to vehicle (HBSS) controls (Figure 3.1A). The percentage of survival after 5 days was 57.6%, 55.6%, and 57.6% following infection with the three lots. Similar reductions in survival were observed in zebrafish systematically infected with two different PR8 lots at 3 dpf compared to vehicle controls (Figure 3.1B). After 4 days, 55.3% and 56.4% of the larvae survived following injection by the two lots. Injection of heat- and ultraviolet (UV)-inactivated PR8 in 2 dpf AB zebrafish did not alter survival compared to vehicle controls (Figure 3.2A). Increased viral titer was observed at 24 hpi in 2 dpf infected AB zebrafish, but not in heat- and UV-inactivated PR8 (Figure 3.2B).

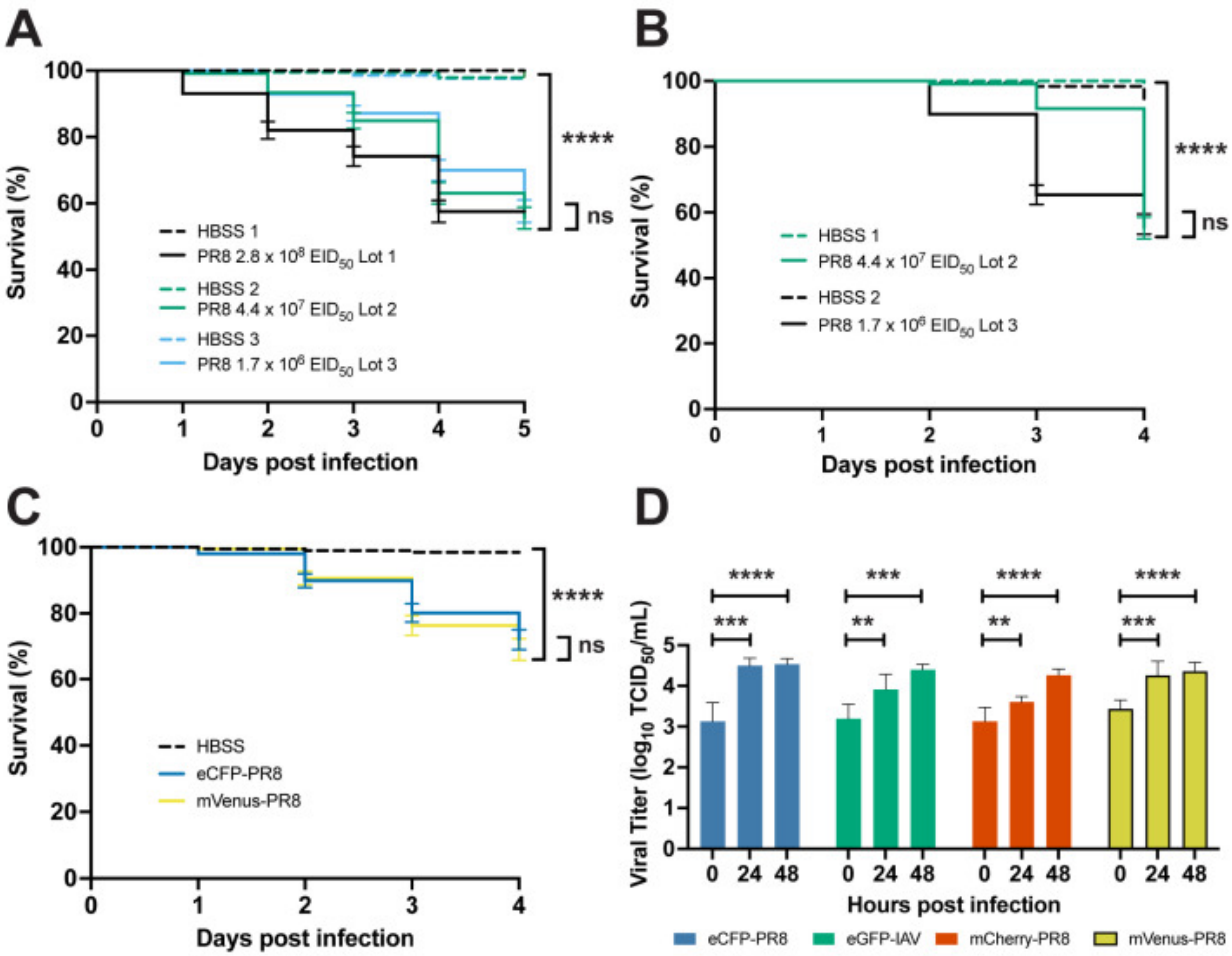

**Figure 3.1. Characterization of PR8 and Color-flu systemically infected AB zebrafish.** (**A**) Decreased survival of AB zebrafish systemically infected with three different lots of PR8 IAV at 2 dpf compared to vehicle (HBSS) controls ($p < 0.0001$ for each lot comparison). Survival rates of PR8-infected embryos were not significantly different between lots ($p = 0.0603$). (**B**) Decreased survival of AB zebrafish systemically infected with two different lots of PR8 IAV at 3 dpf compared to vehicle controls ($p < 0.0001$ for each lot comparison). Survival rates of PR8-infected embryos were not significantly different between lots ($p = 0.1442$). (**C**) Decreased survival of AB zebrafish systemically infected with eCFP-PR8 or Venus-PR8 ($3.2 \times 10^2$ TCID50/mL) compared to vehicle controls ($p < 0.0001$ for each comparison). Survival rates of eCPF-PR8- or Venus-PR8-infected zebrafish were not significantly different strains ($p = 0.5238$). (**D**) Increased TCID50 viral

titer in Color-flu systemically infected AB zebrafish at 24 and 48 hpi compared to 0 hpi. eCFP-PR8-, mCherry-PR8-, and Venus-PR8-infected zebrafish had increased viral titers at 24 and 48 hpi compared to 0 hpi (adjusted *p*-values = 0.0001 and <0.0001, respectively, for eCFP-PR8; 0.0019 and 0.0001, respectively, for eGFP-PR8; 0.0047 and <0.0001, respectively, for mCherry-PR8; and 0.0003 and <0.0001, respectively, for Venus-PR8). Survival studies were conducted with four independent experiments ($n = 4$) and 50 larvae per sample group. TCID50 assays were carried out with three independent experiments ($n = 3$) and 25 larvae per group for each time point. Not significant (ns), $p > 0.05$; ** $p < 0.01$; *** $p < 0.001$; **** $p < 0.0001$.

### 3.4.2. Color-Flu Infection Decreases Survival and Replicates in Zebrafish

Using Color-flu (Fukuyama, 2015) stocks, we examined survival and viral burden in systemically infected zebrafish at 3 dpf (Figure 3.1C, 3.1D and Figure 3.2C, 3.2D). Due to the lower virulence of Color-flu (Fukuyama, 2015), our infection protocol was modified to inject a 6 nL solution of 87% Color-flu (~$7.44 \times 10^5$ TCID50/mL for mVenus-PR8, ~$5.04 \times 10^5$ TCID50/mL for eCFP-PR8, ~$4.80 \times 10^5$ TCID50/mL for eGFP-PR8, and ~$4.56 \times 10^5$ TCID50/mL for mCherry-PR8) and 13% HBSS into the DC, and 6 nL of HBSS for controls. Decreased survival was observed for all four of the strains (Figure 3.2D). Consistent with studies on these Color-flu strains in mice (Fukuyama, 2015), we observed higher survival rates for zebrafish infected with Color-flu than those infected with PR8. The larvae survival rate after 4 days was lowest for the mVenus-PR8 (66.7%) and eCFP-PR8 (69.6%) strains, and higher for the mCherry-PR8 (80.0%) and eGFP-PR8 (80.8%) strains. Consistent with the virulence shown in the survival studies, the zebrafish systemically infected with Venus-PR8 and eCFP-PR8 had higher viral titers at 0 hpi than the other two Color-flu strains (Figure 3.1D). Significant increases in viral titers were observed at 24 hpi and 48 hpi for all Color-flu strains.

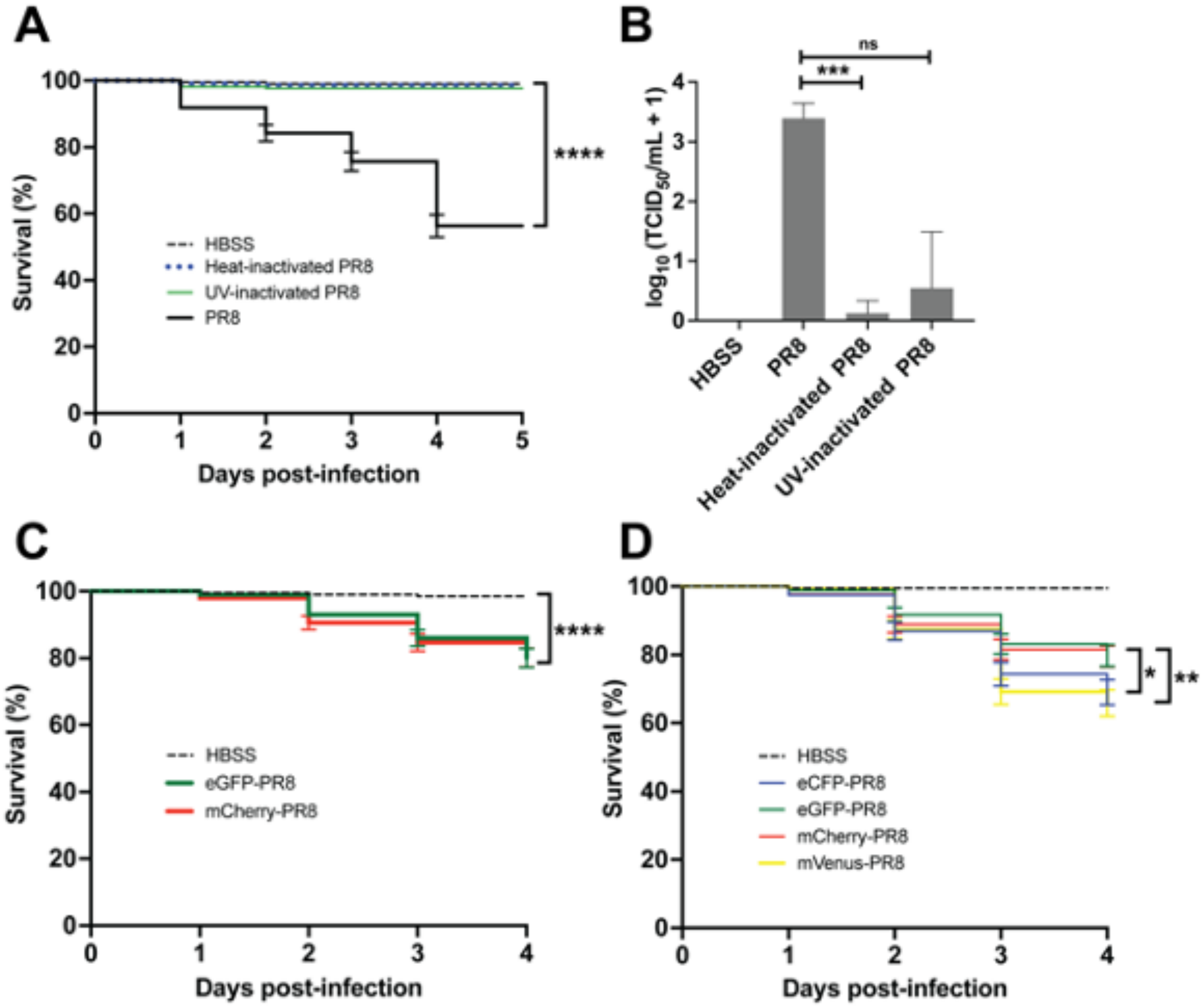

**Figure 3.2. Control infections to characterize PR8 and Color-flu systemically infected AB zebrafish.** : A) Survival with PR8 and heat- and UV-inactivated PR8. Heat and UV-inactivated controls were not significantly different in survival compared to diluent controls (****$p < 0.0001$). B) Viral burden with PR8 and heat- and UV-inactivated PR8 at 24 hpi. Very limited viral titer was picked up in heat and UV-inactivated PR8 compared to wild-type PR8. (***$p<0.0036$) C) eGFP-PR8 and mCherry-PR8 color-flu (systemic infection). Both color-flu strains had ~80% (mCherry-PR8 80.0% and eGFP-PR8 80.8%) survival compared to 99.9% vehicle control. (****$p < 0.0001$) D) Survival comparison of all color-flu strains with systemic infection at 3 dpf. eCFP-PR8 had a survival rate of 69.6%, mVenus-PR8 had a survival rate of 66.7%, mCherry-PR8

infected zebrafish survived at 80.0%, and eGFP-PR8 infected zebrafish survived at an average of 80.8%. Survival studies were conducted with four independent experiments ($n = 4$) and 50 larvae per sample group. TCID50 assays were carried out with three independent experiments ($n = 3$) and 25 larvae per group for each time point. Not significant (ns), *$p > 0.05$; ** $p < 0.01$; *** $p < 0.001$; **** $p < 0.0001$.

### 3.4.3. Color-Flu Infection Induces Proinflammatory Gene Expression

We examined the expression of six proinflammatory genes in response to PR8 and mVenus-PR8 infection at 24 hpi (Figure 3.3.). These genes are known to be activated by major inflammatory response pathways, including type I interferon, Toll-like receptor (TLR), and cytokine signaling, as well as ROS production. IAV infection has previously been shown to induce a type I interferon response in zebrafish larvae (Gabor, 2014) that, in turn, induces inflammation. Interferon regulatory factor 9 (*irf9*) activates the type I interferon response during viral infection (Hernandez, 2018), and this was upregulated with mVenus-PR8 infection. Humans with mutations in *IRF9* have the immunologic disorder Immunodeficiencey-65, and are susceptible to viral infections Bravo, 2019; Hernandez, 2018). Zebrafish receptor (TNFRSF)-interacting serine-threonine kinase 1 (*ripk1l*) is orthologous to human RIPK1, which participates in Toll-like receptor (TLR) and retinoic acid-inducible gene I (RIG-I) signaling following viral infection (Malik, 2020) and which was upregulated with mVenus-PR8 infection. The suppressor of cytokine signaling 3b (*socs3b*) is the zebrafish ortholog of human *SOCS3* and is a negative regulator of cytokine signaling that has been shown to be upregulated following influenza virus infection, resulting in an overexpression of interleukin 6 (Liu, 2019). The expression of neutrophil cytosolic factor 1 (*ncf1*), which encodes a subunit of NADPH oxidase, was decreased at 24 hpi with mVenus-PR8 infection (Figure 3.3.).

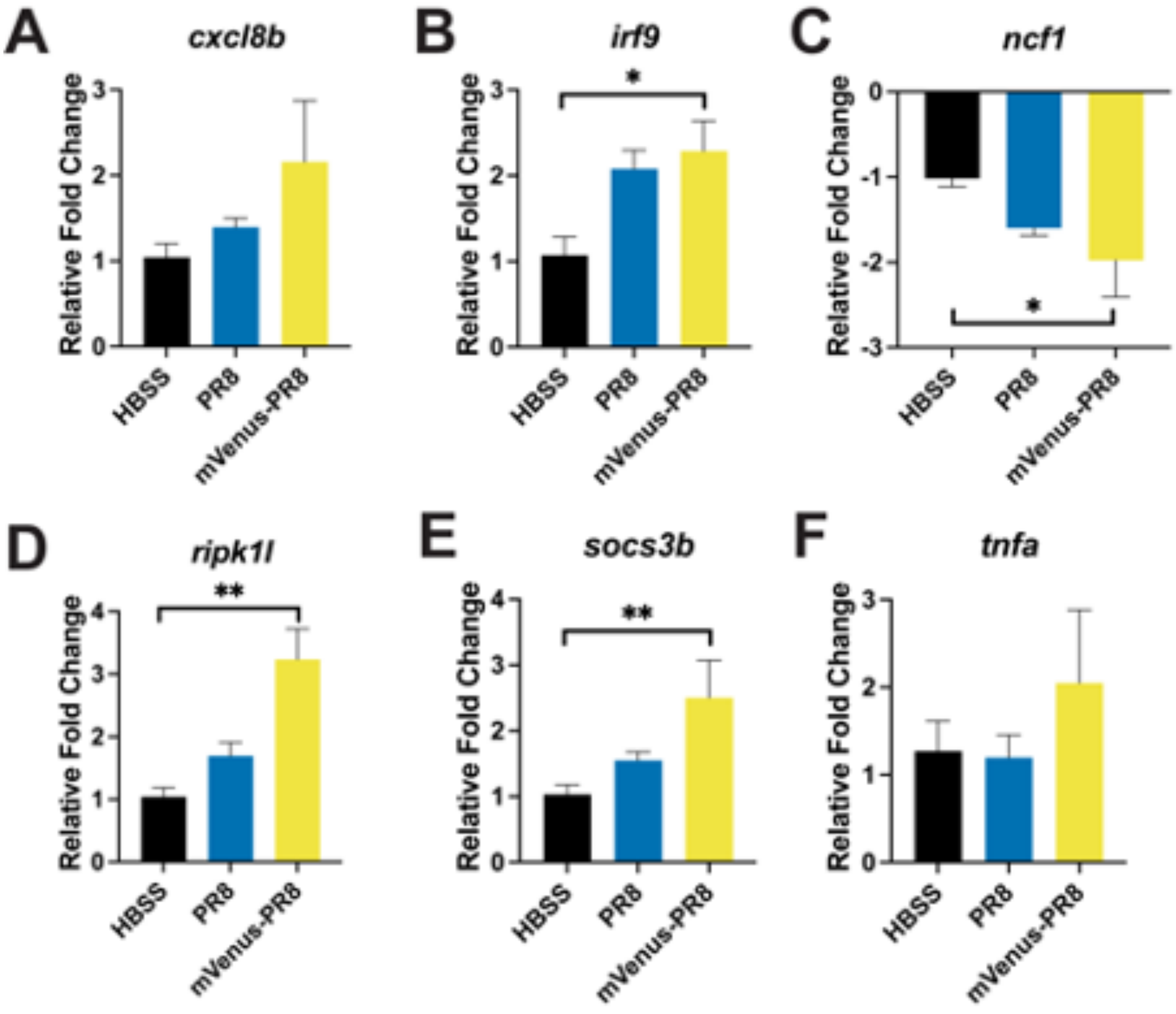

**Figure 3.3. Expression of candidate genes at 24 hpi.** Relative fold change of six genes using qRT-PCR (*n* = 4): A) *cxcl8b*; B) *irf9* had increased exoression with mVenus-PR8 infection (adjusted p-value = 0.0281); (C) *ncf1* had decreased expression with mVenus-PR8 infection (adjusted p-value = 0.0285); (D) *ripk1l* had increased expression with mVenus-PR8 infection (adjusted p-value = 0.0065); (E) *socs3b* had increased expression with mVenus-PR8 infection (adjusted p-value = 0.0088); and (F) *tnfa*.

### 3.4.4. Zebrafish Lines Respond Differently to Influenza Infection

Multiple zebrafish lines have been used to model a wild-type response to injury and infection. To evaluate the consistency of the zebrafish response to IAV infection, we compared the response of three lines to infection: AB, the wild line; EkkWill (EK); and the pigmentation mutant, *casper* (*mitfaw2/w2; mpv17a9/a9*). The AB line was originally used to establish the zebrafish as a model for studying the innate immune response to influenza virus (Gabor, 2014) as well as bacterial (Pressley, 2005) and fungal infection (Brothers, 2011). The EK line has been used to study fin (Yin, 2008) and cardiac (Poss, 2002) tissue regeneration. The *casper* line is optically transparent throughout development into adulthood, allowing for various studies, including research on stem cells and tumor biology (Whitte, 2008). Systemic PR8 infection in 2 dpf embryos resulted in reduced survival for all three lines compared to HBSS vehicle controls (Figure 3.4A). *Casper* larvae had the lowest percentage of survival (44.2%) after 5 days, followed by EK (63.0%) and AB (62.6%). For the embryos infected with PR8 at 3 dpf and followed for 4 days, *casper* larvae also had the lowest survival rate (45.7%) compared with EK (53.7%) and AB (62.7%) (Figure 3.4B).

Viral load was measured at daily intervals following the systemic PR8 infection of 2 dpf embryos from all three lines using tissue culture infectious dose (TCID50) virus titer assays (Figure 3.4C). Viral titers increased by 24 hpi in all three lines, peaked at 48–72 hpi, and then declined by 96 hpi. The AB larvae had their peak viral load at 72 hpi and still had an increased load at 96 hpi. The EK and *casper* larvae had their peak viral loads at 48 hpi, with levels not dissimilar to the 0 hpi controls at 96 hpi. Viral load also increased with systemic PR8 infection in 3 dpf embryos from the three lines by 72 hpi (Figure 3.4D). The *casper* larvae had their peak viral load at 48 hpi, like the 2 dpf infected embryos.

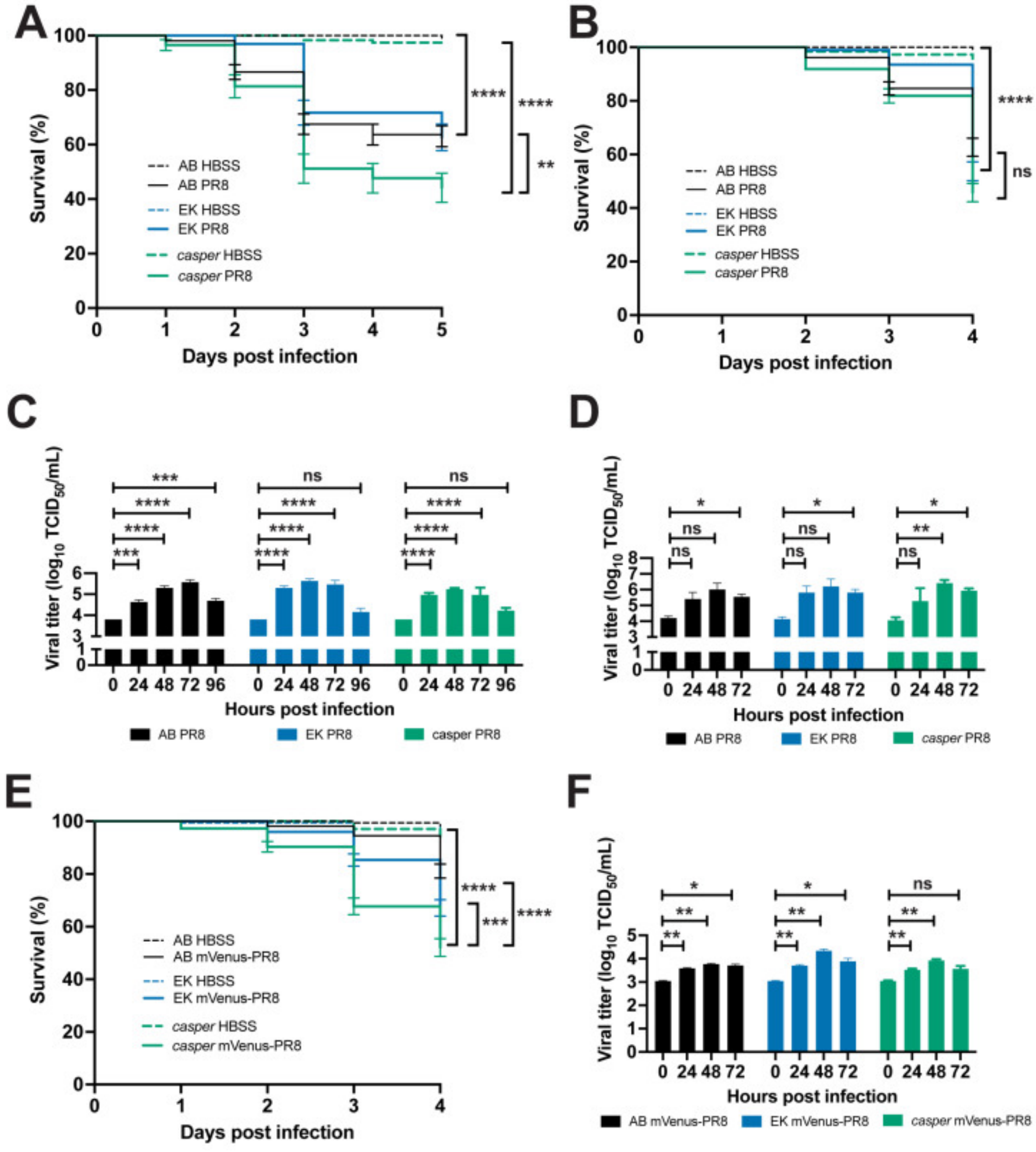

**Figure 3.4. Characterization of PR8 and Color-flu systemic infection across zebrafish lines.** (**A**) Decreased survival was greater in *casper* than AB or EK lines with 2 dpf systemic PR8 infection. PR8-infected zebrafish had a decreased survival rate compared to vehicle (HBSS)

controls ($p < 0.0001$ for all lines). *Casper* zebrafish had a lower survival rate than EK ($p = 0.0024$) and AB ($p = 0.0055$) according to the log-rank Mantel-Cox test. (**B**) Decreased survival rates were observed in AB, EK, and *casper* with 3 dpf PR8 infection compared to controls ($p < 0.0001$ for all lines). No significant (ns) difference in survival rate was detected between PR8-infected AB, EK, and *casper* larvae. (**C**) Increased TCID50 viral titer in 2 dpf PR8-infected AB, EK, and *casper* zebrafish at 24, 48, and 72 hpi compared to 0 hpi (adj. *p*-value < 0.001 for all comparisons except for AB 24 hpi (adj. *p*-value = 0.0006) and AB 96 hpi (adj. *p*-value = 0.0003)). (**D**) Increased TCID50 viral titer in 3 dpf PR8-infected AB, EK, and *casper* zebrafish at 72 hpi compared to 0 hpi (adj. *p*-value = 0.0323, 0.0211, and 0.0452, respectively) and *casper* zebrafish at 48 hpi compared to 0 hpi (adj. *p*-value = 0.0063). (**E**) Decreased survival with 3 dpf mVenus-PR8-infected AB, EK, and *casper* zebrafish compared to HBSS controls ($p < 0.0001$ for all lines). As observed with PR8 infection, *casper* zebrafish had the lowest survival rate (67.7%), which was lower than that of AB (94.5%, $p < 0.0001$) and EK (85.5%, $p < 0.0002$). (**F**) mVenus-PR8-infected AB, EK, and *casper* zebrafish had an increased viral titer at 24 and 48 hpi compared to 0 hpi (adjusted *p*-values = 0.0012 and 0.0022, respectively, for AB; 0.0025 and 0.0027, respectively, for EK; and 0.0045 and 0.0066, respectively, for Venus-PR8). mVenus-PR8-infected AB and EK zebrafish had an increased viral titer at 72 hpi compared to 0 hpi (adjusted *p*-value = 0.0236, and 0.0281, respectively). Survival studies were conducted with four independent ($n = 4$) experiments and 50 larvae per sample group. TCID50 assays were carried out with three independent ($n = 3$) experiments and 25 larvae per group for each time point. Not significant (ns), $p > 0.05$; * $p < 0.05$; ** $p < 0.01$; *** $p < 0.001$; **** $p < 0.0001$.

Localized PR8 infection in the swimbladder of 4 dpf AB, EK, and *casper* larvae also resulted in decreased survival by 3 dpi over the HBSS controls (Figure 3.5A). Like the survival observed with systemic infection, PR8-infected *casper* larvae also had the lowest survival rate (31.5%) compared to EK (54.5%) and AB (61.9%). Likewise, localized Color-flu (mVenus-PR8) infection in the swimbladder of 4 dpf AB, EK, and *casper* larvae also resulted in reduced survival, with *casper* having the lowest percentage of survival (42.3%), followed by EK (67.5%) and AB (74.1%) (Figure 3.5B).

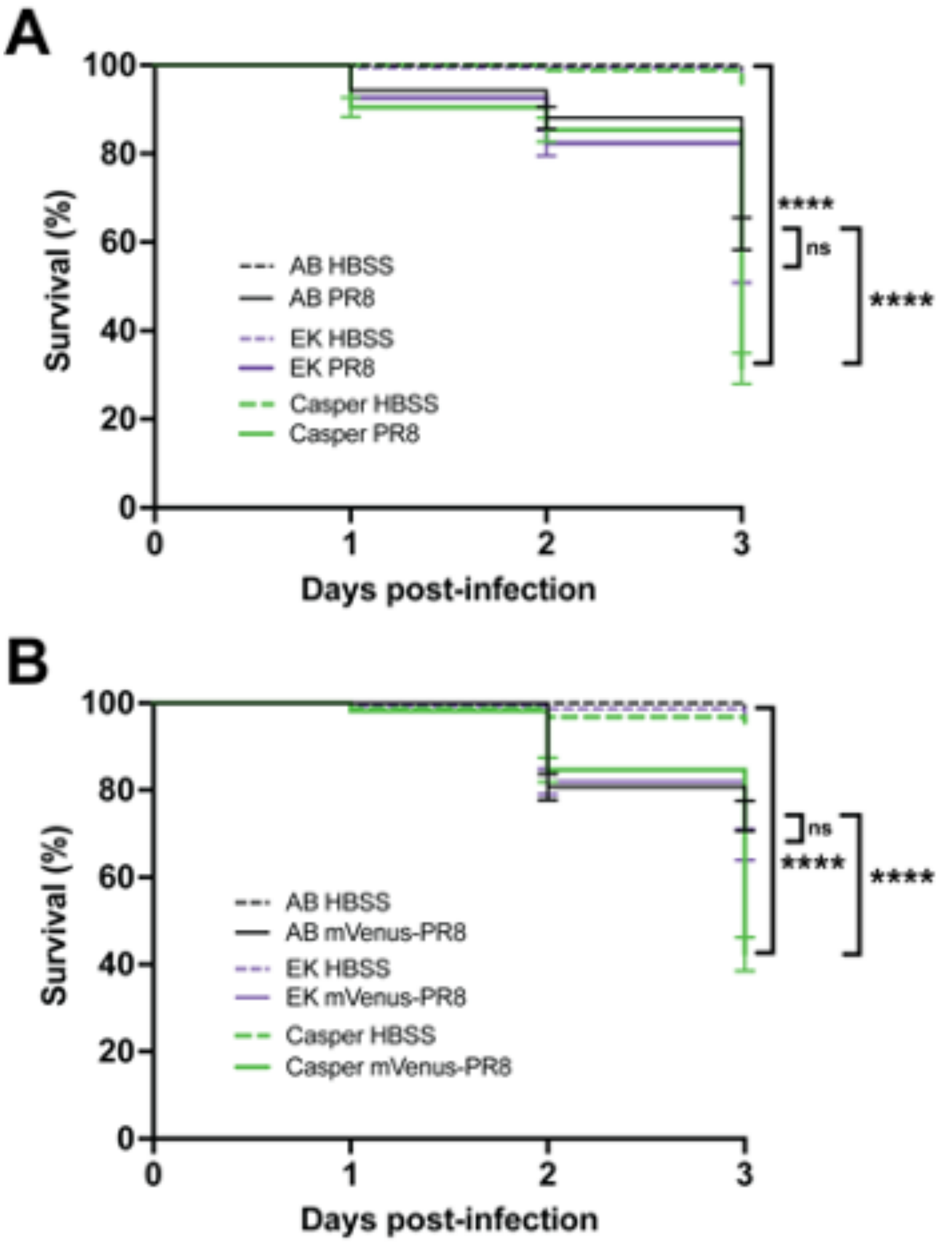

**Figure 3.5. Swimbladder infections with PR8 or mVenus-PR8 of zebrafish with varying genetic backgrounds**: A) Survival with PR8 following swimbladder infection. *Casper* larvae had the lowest survival rate when injected with PR8 at 31.5% compared to EK at 54.5% and AB at 61.9%, (****$p<0.0001$) B) Survival with mVenus-PR8 following swimbladder infection. *Casper* larvae again had the lowest survival rate at 42.3% compared to EK at 67.5% and AB at 74.1%

(****p<0.0001). Swimbladder survival studies were conducted with four independent (*n* = 4) experiments and 40 larvae per sample group at 4 dpf.

### 3.4.5. Live confocal imaging of zebrafish infected with color-flu

The optical transparency of zebrafish embryos and larvae allows for in vivo confocal imaging of Color-flu infection, where the host response can be visualized. With disseminated infection, virus-infected cells were observed throughout the AB larvae for each of the four Color-flu strains (Figure 3.6A). In these whole larvae lateral views at 24 hpi, the highest density of viral infection was in the yolk sac and yolk sac extension. Virus-infected cells were also observed in the skeletal muscle. Several zebrafish transgenic fluorescent reporter strains have been used to visualize cell types, including neutrophils and macrophages. We injected the dual macrophage and neutrophil reporter line Tg(*mpeg1*:eGFP;*lyz*:dsRed) with eCFP-PR8 and a vehicle (HBSS) control at 3 dpf and imaged the larvae at 24 hpi (Figure 3.6B). The control larvae show macrophages and neutrophils in their circulatory system and other tissues including the skeletal muscle. Imaging of the eCFP-PR8-infected larvae allows for the simultaneous visualization of macrophages, neutrophils, and infected cells.

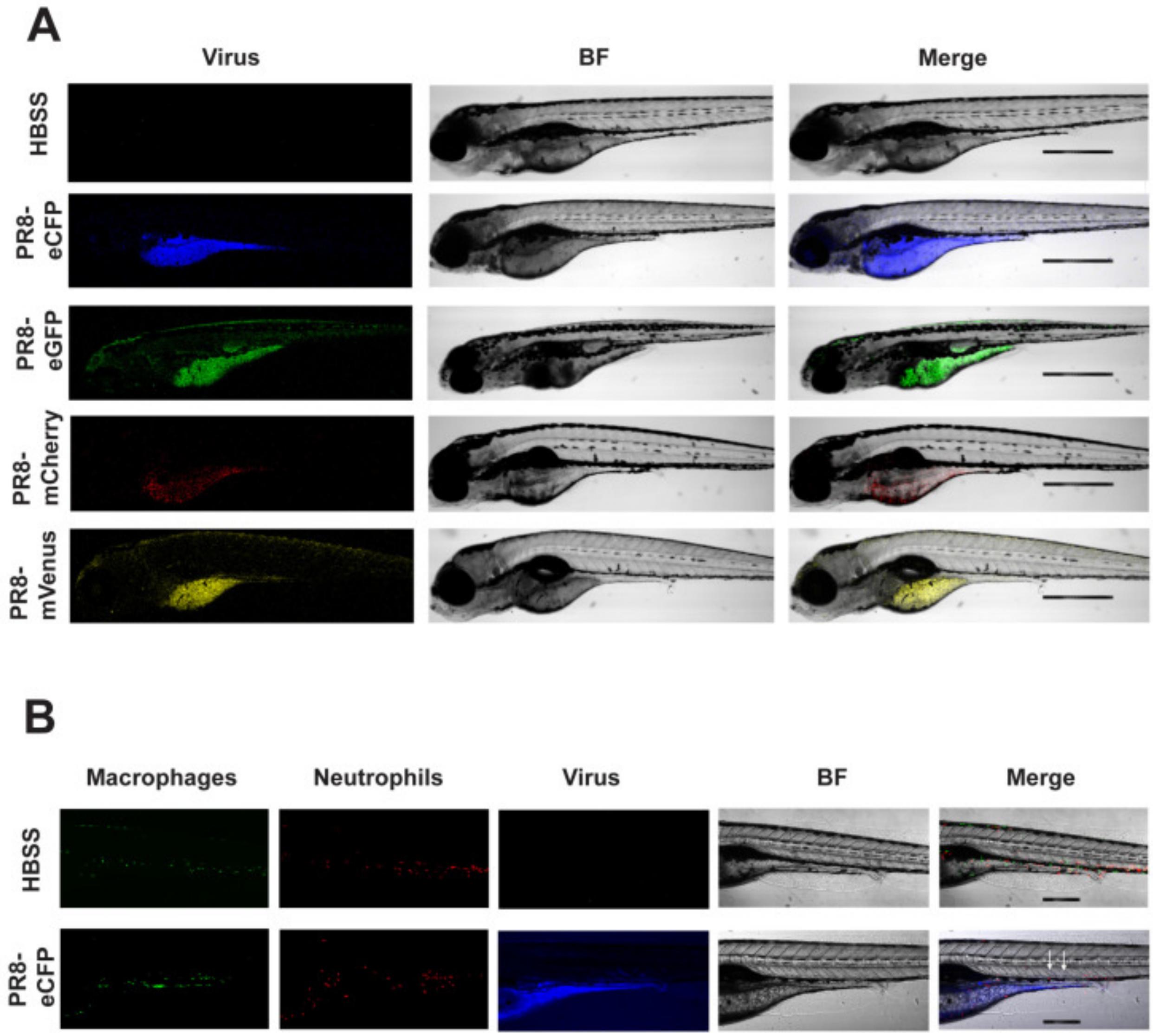
A
Virus
BF
Merge
HBSS
PR8-eCFP
PR8-eGFP
PR8-mCherry
PR8-mVenus
B
Macrophages
Neutrophils
Virus
BF
Merge
HBSS
PR8-eCFP

**Figure 3.6. Confocal imaging of Color-flu-infected zebrafish.** (**A**) Representative images of larvae at 24 h post systemic injection of HBSS, eCFP-PR8, eGFP-PR8, mCherry-PR8, and mVenus-PR8 at 3 dpf, at 4× resolution. Scale bar: 300 mm. BF: brightfield. (**B**) Representative images of Tg(*mpeg1*:eGFP;*lyz*:dsRed) larvae at 24 h post systemic injection of HBSS, eCFP-PR8 at 3 dpf at 10× resolution, showing macrophages (green), neutrophils (red), and eCFP-PR8 (blue). Infected skeletal muscle was detected (white arrowheads). Scale bar: 700 μm.

### 3.4.6. Evaluating Small Molecules That Alter the Response to IAV Infection

Next, we evaluated how two small molecule drugs, ramipril and MDIVI-1, would alter the response to IAV infection. We examined survival, viral burden, and immune capacity via respiratory burst assays. We also used confocal imaging to study the relative abundance of neutrophils and macrophages, and the level of viral infection. To model drug therapies administered after infection, embryos were infected with IAV at 3 dpf, then treated with either DMSO (control), ramipril, or MDIVI-1 at 24 hpi for one hour, and then washed and maintained in clean embryo water for up to 4 days post infection. The ramipril and MDIVI-1 administered to the PR8-infected and vehicle (HBSS) control larvae were at concentrations of 0.2 nM and 7nM, respectively, which increased survival (Figure 3.7). Ramipril increased survival to 90.0% compared to 52.1% in the DMSO controls. MDIVI-1 increased survival to 85.4% compared to 55.4% in DMSO controls. With mVenus-PR8-infected larvae, ramipril or MDIVI-1 treatment increased survival to 87.7% and 85.0%, respectively, compared to 58.9% in DMSO controls. The ramipril and MDIVI-1 concentrations used were selected after evaluating differences in survival due to drug treatment in PR8-infected larvae at 2 and 3 dpf (Figure 3.8 and Figure 3.9). The range of concentrations evaluated for ramipril were 0.1, 0.2, 0.3, and 0.4 nM. For MDIVI-1, the range of concentrations evaluated were 3, 5, 7, and 10 nM. Both the 0.1 and 0.2 ramipril treatments, and only the 7 nM MDIVI-1 treatment, increased survival in larvae infected with PR8 at both 2 and 3 dpf. The highest doses of ramipril (0.4 nM) and MDIVI-1 (10 nM) both decreased survival in the control (HBSS) injected larvae.

**A**

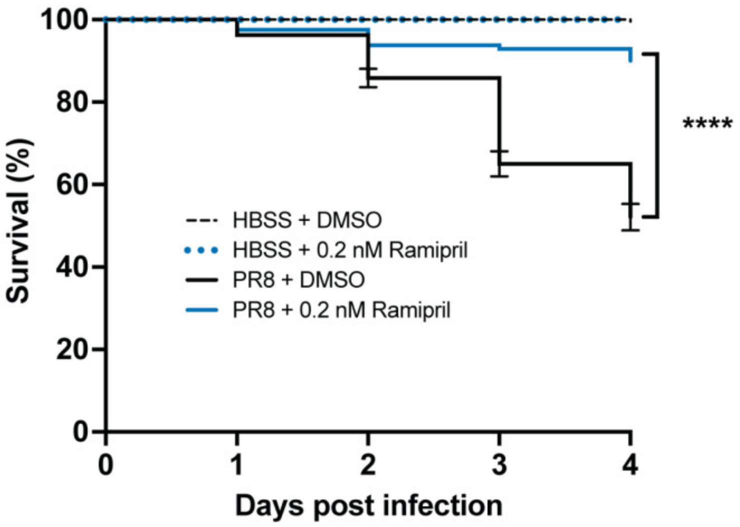

Survival (%)
100
80
60
40
20
0
0
1
2
3
4
Days post infection
****
HBSS + DMSO
HBSS + 0.2 nM Ramipril
PR8 + DMSO
PR8 + 0.2 nM Ramipril

**B**

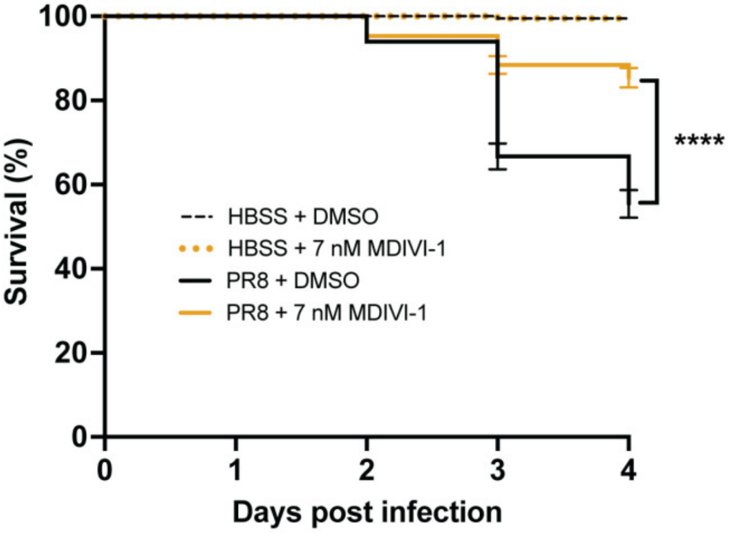

Survival (%)
100
80
60
40
20
0
0
1
2
3
4
Days post infection
****
HBSS + DMSO
HBSS + 7 nM MDIVI-1
PR8 + DMSO
PR8 + 7 nM MDIVI-1

**C**

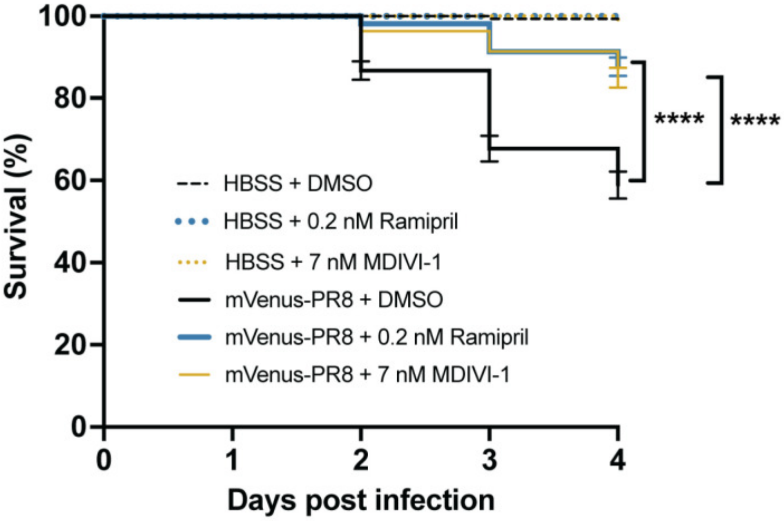

Survival (%)
100
80
60
40
20
0
0
1
2
3
4
Days post infection
****
****
HBSS + DMSO
HBSS + 0.2 nM Ramipril
HBSS + 7 nM MDIVI-1
mVenus-PR8 + DMSO
mVenus-PR8 + 0.2 nM Ramipril
mVenus-PR8 + 7 nM MDIVI-1

**Figure 3.7 Ramipril and MDIVI-1 increase survival in systemically infected PR8 and Color-flu-infected 3 dpf zebrafish.** (**A**) Increased survival in PR8-infected AB zebrafish treated with 0.2 nM ramipril compared to DMSO controls (**** $p < 0.0001$). (**B**) Increased survival in PR8-infected AB zebrafish treated with 7 nM MDIVI-1 compared to DMSO controls ($p < 0.0001$). (**C**) Increased survival in mVenus-PR8-infected AB zebrafish treated with 0.2 nM ramipril or 7 nM MDIVI-1 compared to DMSO controls ($p < 0.0001$). Survival studies were conducted with $n = 4$ and 50 larvae per sample group.

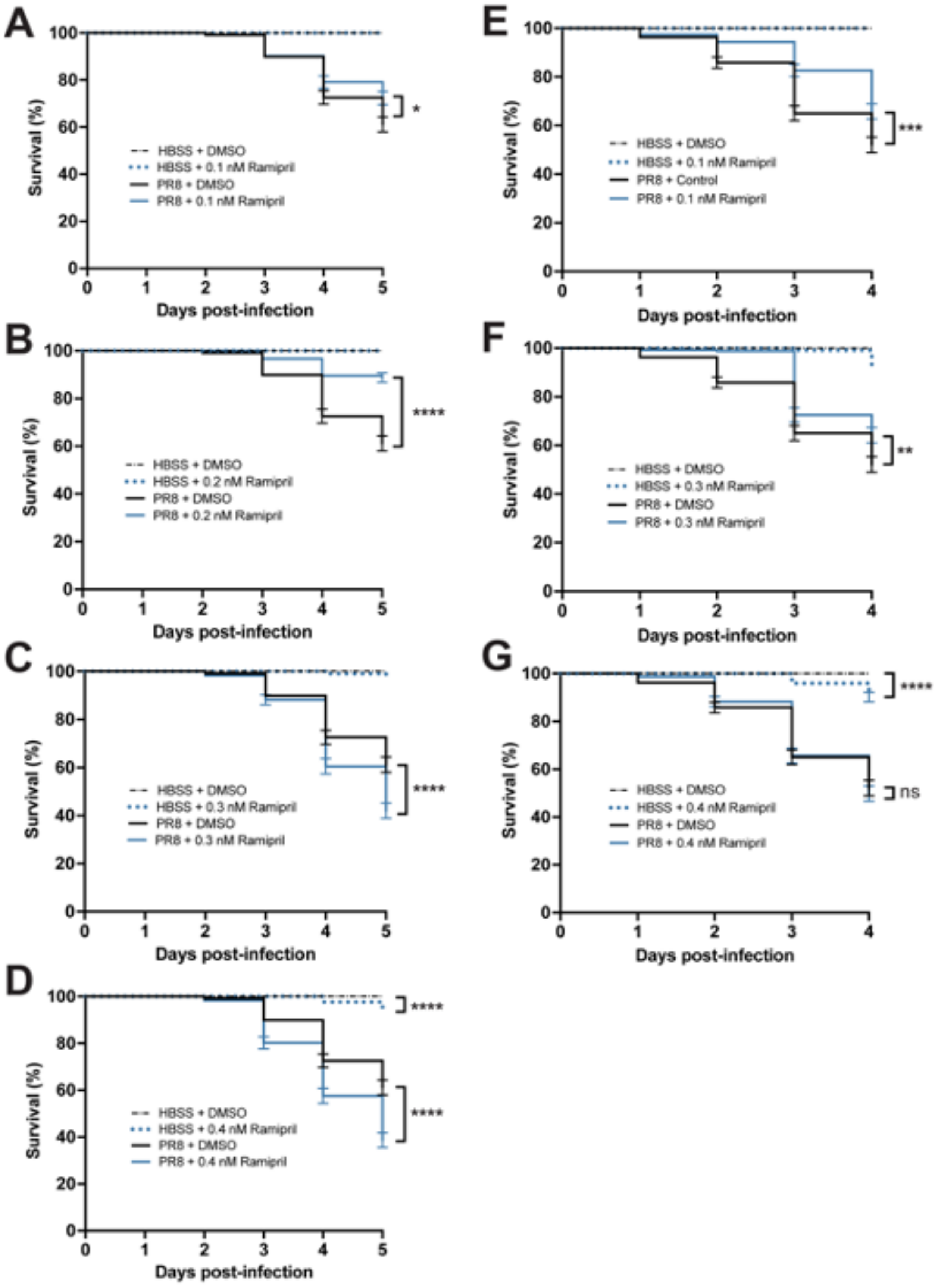

A
B
C
D
E
F
G
Survival (%)
Days post-infection
HBSS + DMSO
HBSS + 0.1 nM Ramipril
PR8 + DMSO
PR8 + 0.1 nM Ramipril
HBSS + 0.2 nM Ramipril
PR8 + 0.2 nM Ramipril
HBSS + 0.3 nM Ramipril
PR8 + 0.3 nM Ramipril
HBSS + 0.4 nM Ramipril
PR8 + 0.4 nM Ramipril
PR8 + Control
*
**
***
****
ns

**Figure 3.8 Ramipril concentrations at 2 dpf and 3 dpf are used to determine toxicity.** A-D) 2 dpf survival curves with increasing doses of ramipril A = 0.1 nM ramipril, B = 0.2 nM ramipril, C = 0.3 nM ramipril, D = 0.4 nM ramipril. 0.2 nM of ramipril was chosen as it significantly increased survival. 0.1 nM of ramipril was not selected as it slightly increased survival. 0.3 and 0.4 nM of ramipril were not selected as they decreased survival. E-F) 3 dpf survival curves with increasing doses of ramipril E = 0.1 nM ramipril, F = 0.3 nM ramipril, and G = 0.4 nM ramipril. 0.2 nM of ramipril was chosen as it significantly increased survival. 0.1 nM and 0.3 nM of ramipril were not selected as it slightly increased survival. 0.4 nM of ramipril was not selected as it decreased survival. Not significant (ns), $p > 0.05$; * $p < 0.05$; ** $p < 0.01$; *** $p < 0.001$; **** $p < 0.0001$. Survival studies were conducted with $n = 4$ and 50 larvae per sample group.

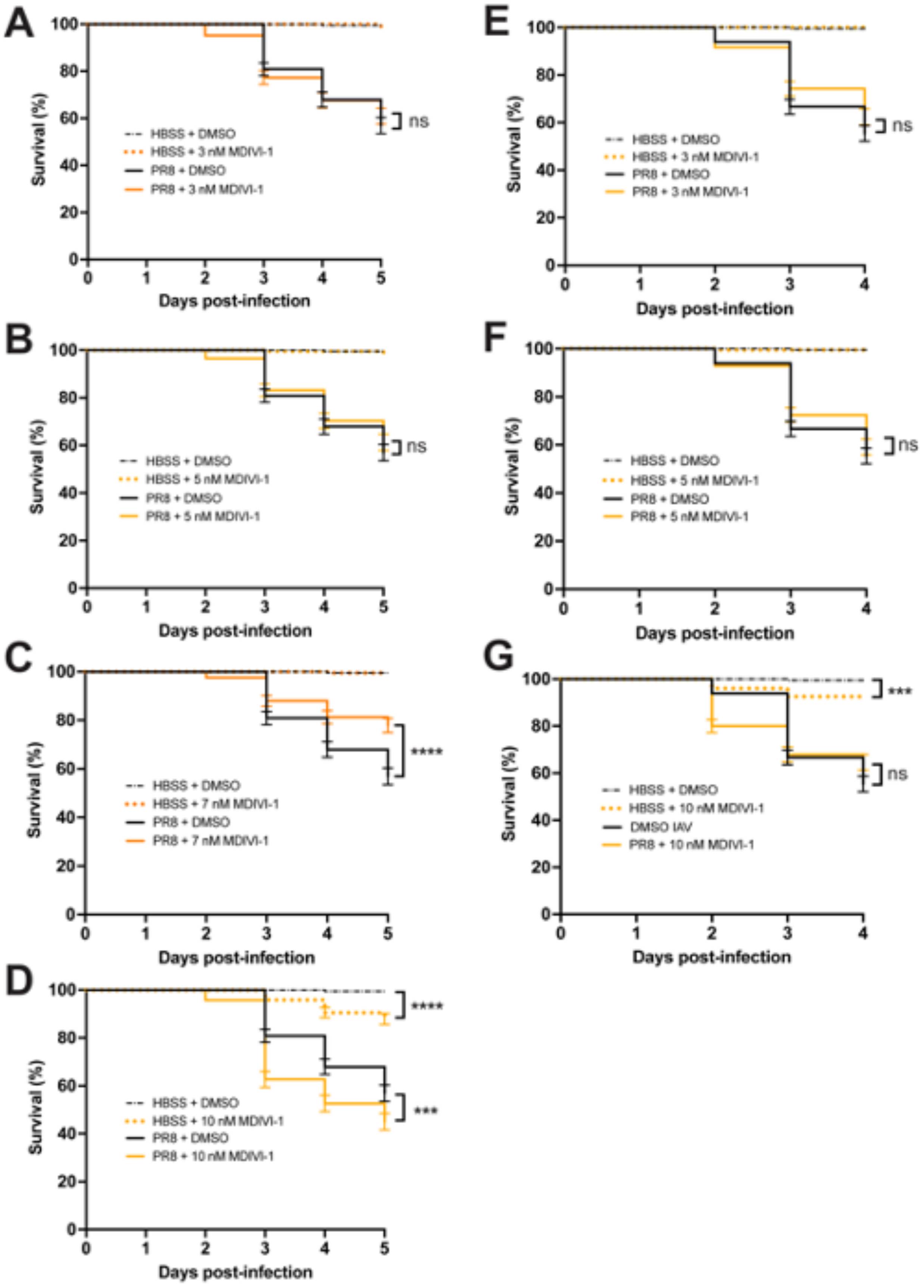
A
Survival (%)
Days post-infection
HBSS + DMSO
HBSS + 3 nM MDIVI-1
PR8 + DMSO
PR8 + 3 nM MDIVI-1
ns
B
Survival (%)
Days post-infection
HBSS + DMSO
HBSS + 5 nM MDIVI-1
PR8 + DMSO
PR8 + 5 nM MDIVI-1
ns
C
Survival (%)
Days post-infection
HBSS + DMSO
HBSS + 7 nM MDIVI-1
PR8 + DMSO
PR8 + 7 nM MDIVI-1
****
D
Survival (%)
Days post-infection
HBSS + DMSO
HBSS + 10 nM MDIVI-1
PR8 + DMSO
PR8 + 10 nM MDIVI-1
****
***
E
Survival (%)
Days post-infection
HBSS + DMSO
HBSS + 3 nM MDIVI-1
PR8 + DMSO
PR8 + 3 nM MDIVI-1
ns
F
Survival (%)
Days post-infection
HBSS + DMSO
HBSS + 5 nM MDIVI-1
PR8 + DMSO
PR8 + 5 nM MDIVI-1
ns
G
Survival (%)
Days post-infection
HBSS + DMSO
HBSS + 10 nM MDIVI-1
DMSO IAV
PR8 + 10 nM MDIVI-1
***
ns

**Figure 3.9 MDIVI-1 concentrations at 2 dpf and 3 dpf are used to determine toxicity.** A-D) 2 dpf survival curves with increasing doses of MDIVI-1 A = 3 nM MDIVI-1, B = 5 nM MDIVI-1, C = 7 nM MDIVI-1, D = 10 nM MDIVI-1. 7 nM of ramipril was chosen as it significantly increased survival. 3 and 5 nM of MDIVI-1 were not selected as they did not change survival. 10 nM MDIVI-1 was not selected as it decreased survival. E-F) 3 dpf survival curves with increasing doses of MDIVI-1 E = 3 nM MDIVI-1, F = 5 nM MDIVI-1, and G = 10 nM MDIVI-1. 0.2 nM of ramipril was chosen as it significantly increased survival. 3, 5, and 10 nM of MDIVI-1 were not selected as they did not change survival. Not significant (ns), $p > 0.05$; * $p < 0.05$; ** $p < 0.01$; *** $p < 0.001$; **** $p < 0.0001$. Survival studies were conducted with $n = 4$ and 50 larvae per sample group.

The ramipril and MDIVI-1 treatments also reduced the viral burden in IAV-infected larvae by 24 h after treatment (Figure 3.10). In the larvae infected with PR8 at 2 and 3 dpf, the viral burden increased at 24 hpi when the larvae were treated with ramipril, MDIVI-1, or DMSO. By 48 hpi, the viral burden was reduced in ramipril- and MDIVI-1-treated larvae. In the 2 dpf larvae infected with ramipril and MDIVI-1 treatment, the viral burden at 72 hpi was reduced to levels measured at 0 hpi. A reduction in viral burden following ramipril and MDIVI-1 treatment was also observed at 48 hpi with mVenus-PR8 infection (Figure 3.10C).

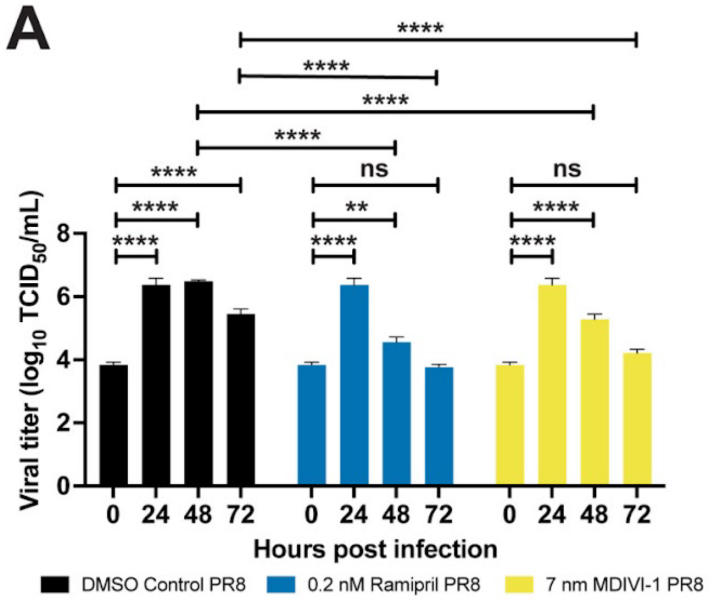
A
****
****
****
****
****
****
****
ns
**
****
ns
****
****
Viral titer (log10 TCID50/mL)
8
6
4
2
0
0 24 48 72
0 24 48 72
0 24 48 72
Hours post infection
DMSO Control PR8
0.2 nM Ramipril PR8
7 nm MDIVI-1 PR8

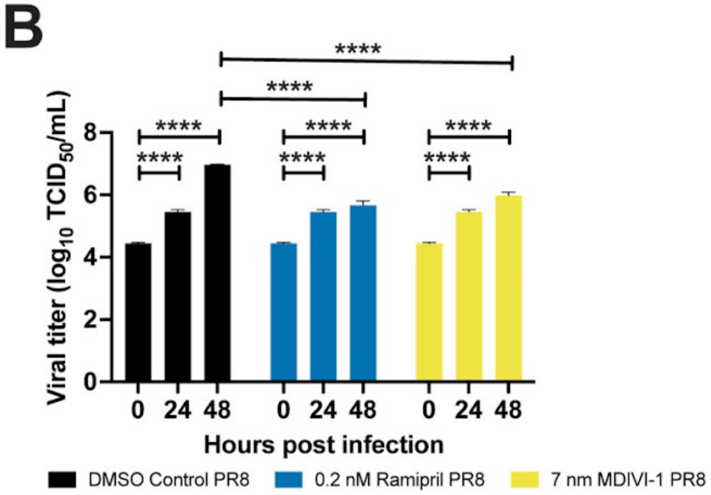
B
****
****
****
****
****
****
****
****
Viral titer (log10 TCID50/mL)
8
6
4
2
0
0 24 48
0 24 48
0 24 48
Hours post infection
DMSO Control PR8
0.2 nM Ramipril PR8
7 nm MDIVI-1 PR8

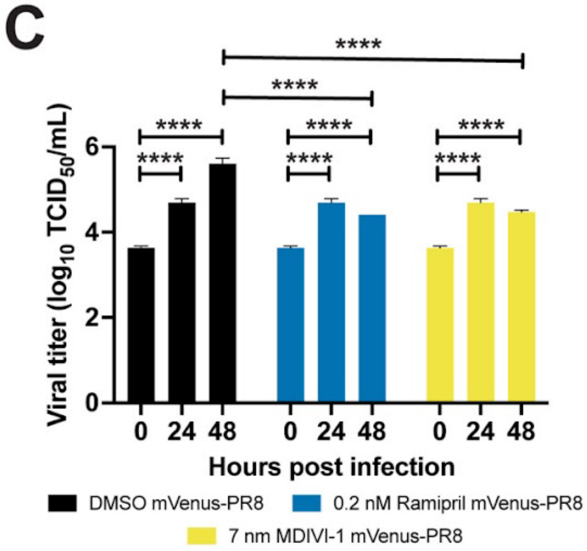
C
****
****
****
****
****
****
****
****
Viral titer (log10 TCID50/mL)
6
4
2
0
0 24 48
0 24 48
0 24 48
Hours post infection
DMSO mVenus-PR8
0.2 nM Ramipril mVenus-PR8
7 nm MDIVI-1 mVenus-PR8

**Figure 3.10 Ramipril and MDIVI-1 treatments lower viral burden in IAV-infected zebrafish.** (**A**) Viral titers for both ramipril (0.2 nM)- and MDIVI-1 (7 nM)-treated 2 dpf zebrafish infected with PR8 were significantly higher at 24 and 48 hpi when compared to 0 hpi, but not different at 72 hpi. For the DMSO-treated zebrafish, viral titers were significantly increased at 24, 48, and 72 hpi ($p < 0.0001$ for each comparison). For the ramipril-treated zebrafish, viral titers were significantly increased at 24 ($p < 0.0001$) and 48 hpi ($p = 0.0022$). For the MDIVI-1-treated zebrafish, viral titers were also significantly increased at 24 and 48 hpi ($p < 0.0001$ for each comparison). (**B**) Viral titers for ramipril- and MDIVI-1-treated 3 dpf zebrafish infected with PR8 were significantly lower by 48 hpi ($p < 0.0001$ for each comparison). (**C**) Viral titers for ramipril- and MDIVI-1-treated 3 dpf zebrafish infected with mVenus-PR8 were significantly lower at 48 hpi ($p < 0.0001$ for each comparison). TCID50 assays were conducted using $n = 3$ and 25 larvae per group for each time point. Not significant (ns), $p > 0.05$; ** $p < 0.01$; **** $p < 0.0001$.

Next, the level of ROS generated by the larvae following infection was quantified in order to characterize the capacity of the immune system to mount a respiratory burst response. In PR8- and mVenus-PR8-infected larvae, the respiratory burst response was reduced compared to uninfected controls (Figure 3.11). Ramipril and MDIVI-1 treatment rescued the response, such that the level of induction was the same or higher than that of the uninfected controls.

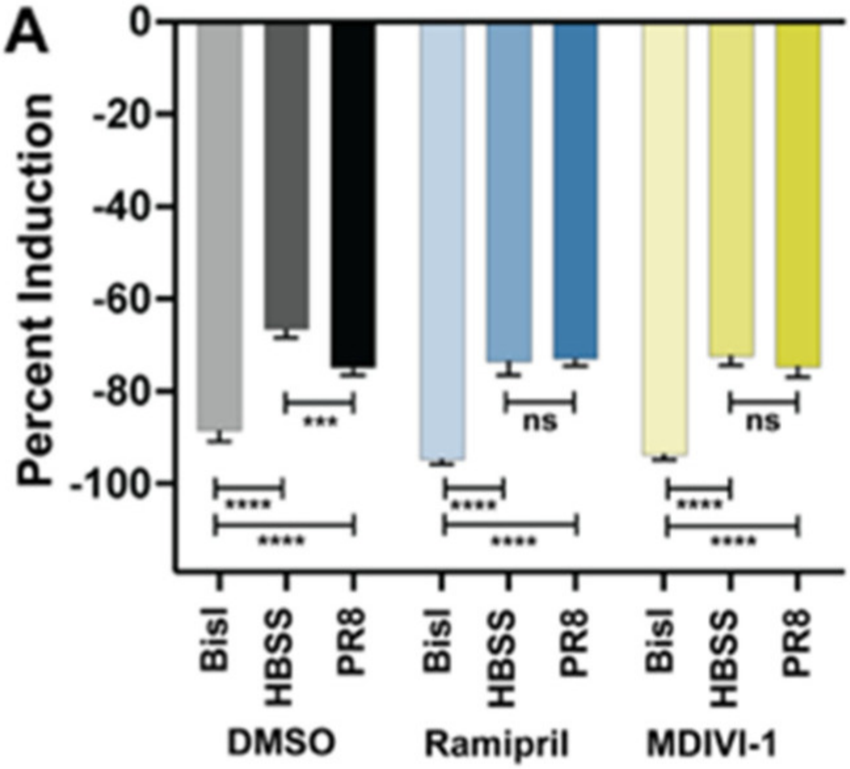
A
Percent Induction
0
-20
-40
-60
-80
-100
***
ns
ns
****
****
****
****
****
****
Bisl
HBSS
PR8
Bisl
HBSS
PR8
Bisl
HBSS
PR8
DMSO
Ramipril
MDIVI-1

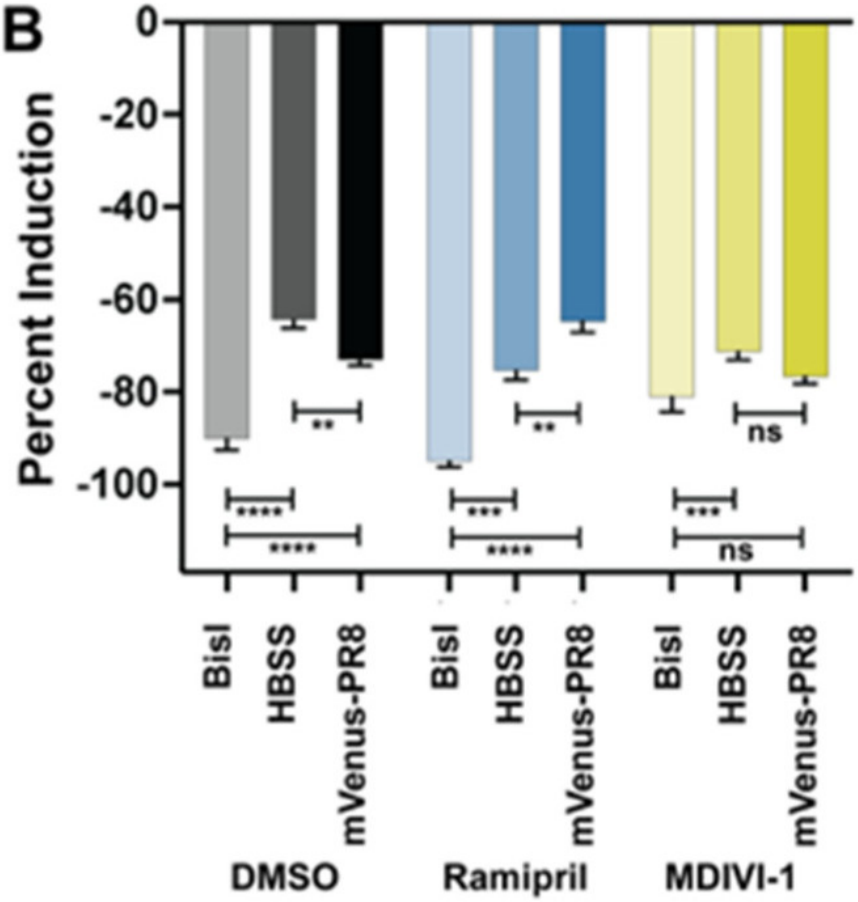
B
Percent Induction
0
-20
-40
-60
-80
-100
**
**
ns
****
****
***
****
***
ns
Bisl
HBSS
mVenus-PR8
Bisl
HBSS
mVenus-PR8
Bisl
HBSS
mVenus-PR8
DMSO
Ramipril
MDIVI-1

**Figure 3.11 Ramipril and MDIVI-1 treatment alters the respiratory burst response in IAV systemically infected zebrafish at 48 hpi.** (A) Respiratory burst response in larvae treated with DMSO, ramipril (0.2 nM), and MDIVI-1 (7 nM) at 48 hpi following systemic injection at 3 dpf with PR8 or HBSS. PR8 infection decreased the response over HBSS in DMSO-treated controls (adjusted $p = 0.0008$). Both ramipril and MDIVI-1 treatment remedied the reduction in respiratory burst response, as the PR8-infected larvae had the same response as HBSS-injected controls (comparisons were not significant (ns)). The protein kinase C inhibitor bisindolylmaleimide I (BisI) was used as a positive control as it suppresses the respiratory burst response (adj. $p < 0.0001$ for all comparisons). (B) Respiratory burst response in larvae treated with DMSO, ramipril (0.2 nM), and MDIVI-1 (7 nM) at 48 hpi following systemic injection at 3 dpf with mVenus-PR8 or HBSS. Similar to the PR8-infected larvae, mVenus-PR8 infection decreased the response over HBSS in DMSO-treated controls (adj. $p = 0.0040$). Ramipril treatment resulted in a higher respiratory burst response with mVenus-PR8 infection than HBSS controls (adj. $p = 0.0049$). MDIVI-1 treatment remedied the reduction in respiratory burst response as the mVenus-PR8-infected larvae had the same response as HBSS injected controls. The BisI controls were different to the DMSO (adj. $p < 0.0001$ for both), ramipril (adj. $p = 0.0003$ for HBSS, and adj. $p < 0.0001$ for mVenus-PR8), and MDIVI-1 (adj. $p = 0.0006$ for HBSS, ns for mVenus-PR8) groups. Not significant (ns), $p > 0.05$; ** $p < 0.01$; *** $p < 0.001$; **** $p < 0.0001$.

We then characterized the abundance of neutrophils and macrophages and the level of viral infection using fluorescent confocal imaging of Tg(*mpeg1*:eGFP;*lyz*:dsRed) larvae infected with eCFP-PR8. In DMSO-treated larvae, we observed higher numbers of neutrophils and viral infection, but lower numbers of macrophages at 48 hpi (Figure 3.12). Ramipril increased the number of neutrophils in infected larvae compared to uninfected controls, a difference not observed with the macrophages. With eCFP-PR8 infection, the number of macrophages increased with MDIVI-1 treatment over DMSO controls. The level of eCFP-PR8 infection was reduced with ramipril and MDIVI-1 treatment compared to DMSO controls.

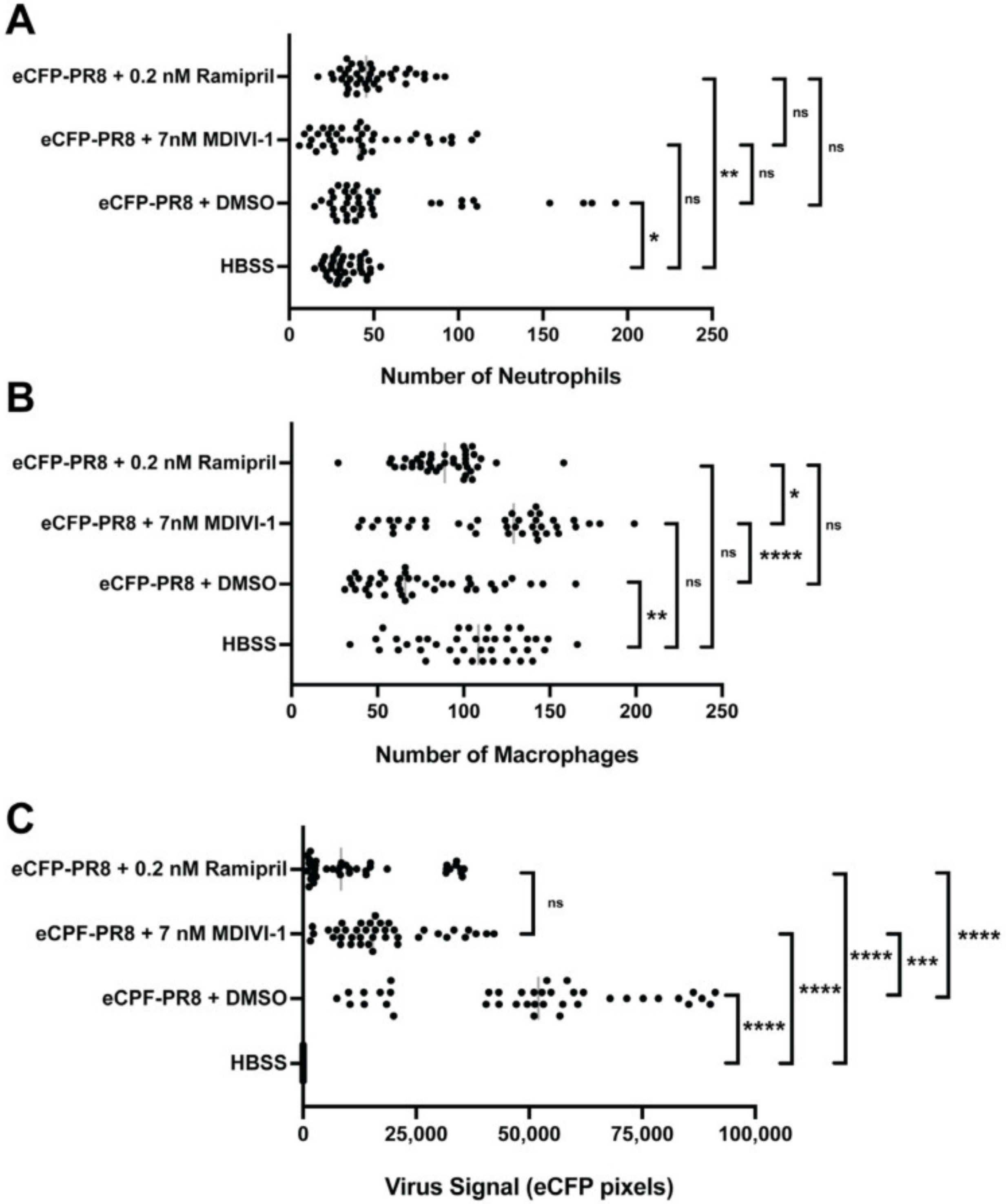

**Figure 3.12 Quantification of the number of neutrophils.** (A), macrophages (B), and the relative abundance of virus infected cells (C) via fluorescent confocal imaging of Tg(*mpeg1*:eGFP;*lyz*:dsRed) larvae at 48 h post injection by eCFP-PR8 or HBSS following

treatment with DMSO, ramipril, and MDIVI-1 per optical cross section. For each larva, 10 five-micron optical cross sections were analyzed, which together totaled 50 microns (*n* = 4 representative larvae). (A) The number of neutrophils increased with eCFP-PR8 infection following DMSO treatment over HBSS controls (adjusted *p*-value = 0.0145), and with ramipril treatment (adj. *p*-value = 0.0010), but not with MDIVI-1 treatment. (B) The number of macrophages decreased in eCFP-PR8-infected larvae treated with DMSO over HBSS controls (adj. *p*-value = 0.0020), but was not different with ramipril or MDIVI-1 treatment. MDIVI-1 treatment increased the number of macrophages compared to the DMSO controls (adj. *p*-value < 0.0001), and ramipril-treated larvae (adj. *p*-value = 0.0126). (C) The extent of viral infection was higher in eCFP-PR8-infected larvae treated with DMSO, ramipril, and MDIVI-1 (adj. *p*-value < 0.0001 for all comparisons). The level of virus infection was lower with ramipril (adj. *p*-value < 0.0001) and MDIVI-1 (adj. *p*-value = 0.0008) treatment compared to the DMSO-treated controls. Not significant (ns), $p > 0.05$; * $p < 0.05$; ** $p < 0.01$; *** $p < 0.001$; **** $p < 0.0001$.

Time-lapse in vivo confocal imaging allows cells to be tracked in these transgenic lines injected with Color-flu and then exposed to small molecules. Time-lapse imaging showed circulating neutrophils and macrophages over the course of 30 min in 5 dpf larvae that were injected with HBSS at 3 dpf (data not shown). In 5 dpf larvae infected with eCFP-PR8 at 3 dpf and then exposed to DMSO at 24 hpi for one hour, we observed viral infection in several tissues (data not shown). We observed macrophages and neutrophils near the highest density of viral infection, and more circulating macrophages over the course of 30 min. In eCFP-PR8-infected larvae exposed to ramipril, we observed lower viral infection, more neutrophils, and fewer macrophages over 30 min (data not shown). The number of macrophages was increased in eCFP-

PR8-infected larvae exposed to MDIVI-1 over 30 min (data not shown). A representative image used to generate Figure 3.12 is shown in Figure 3.13.

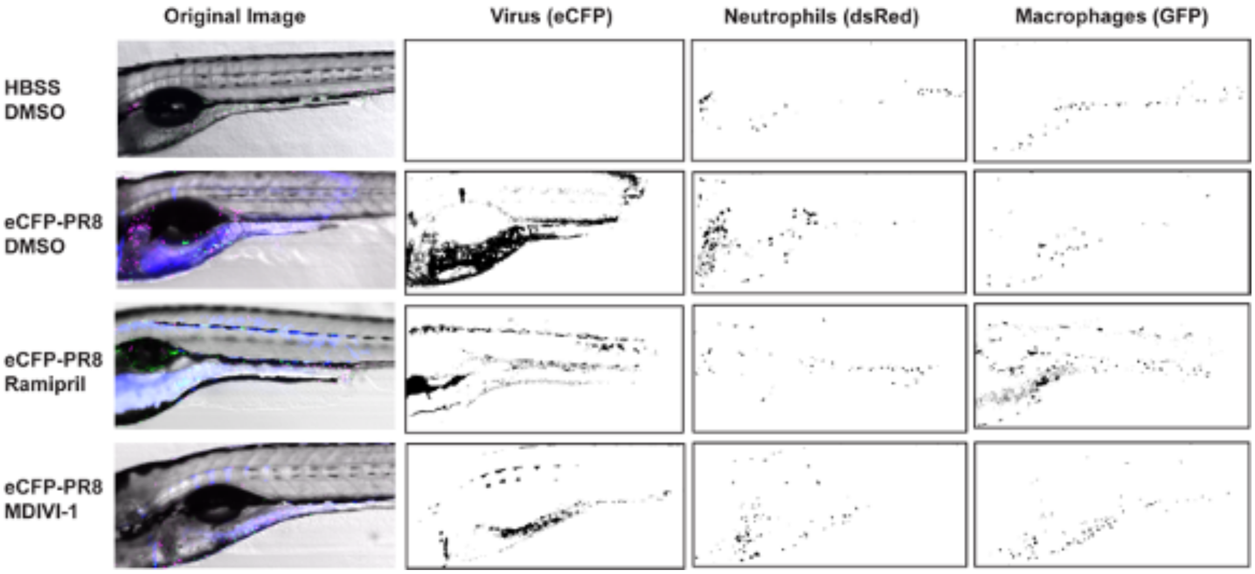
Original Image
Virus (eCFP)
Neutrophils (dsRed)
Macrophages (GFP)
HBSS
DMSO
eCFP-PR8
DMSO
eCFP-PR8
Ramipril
eCFP-PR8
MDIVI-1

**Figure 3.13. Quantification of virus, neutrophils, and macrophages by fluorescent confocal imaging of Tg*(mpeg1:*eGF*P;lyz:*dsRed*)* larvae at 48 hours post injection by eCFP-PR8 or HBSS following treatment by DMSO, ramipril, and MDIVI-1.** Representative images and masks were used to quantitate the level of eCFP-PR8 virus by pixel intensities in the cyan (emission at 476 nm) channel, the number of neutrophils estimated from pixel intensities in the red channel (emission at 583 nm), and number of macrophages estimated from pixel intensities in the green (emission at 510 nm) channel.

### 3.5. Discussion

Here, we demonstrate that Color-flu can be used to model the innate immune response to IAV infection in zebrafish larvae, and that both ramipril and MDIVI-1 treatment improve survival and reduce viral burden following IAV infection. There is an urgent need to develop new antiviral therapies for IAV due to the threat that new IAV strains will pose in the future. The IAV strains that caused the last four influenza pandemics since 1900 were derived from the viral transmission of strains from avian and non-human mammalian hosts and their subsequent recombination with human strains (Morens, 2013). Furthermore, antiviral therapies can become ineffective when the right combination of mutations occur in the virus. For example, a single amino acid substitution (H274Y) in neuraminidase was reported in H5N1 isolates that conferred resistance to oseltamivir (de Jong, 2005). The zebrafish model of IAV infection is complementary to other animal and cell line models used to evaluate antiviral therapies. We show how the model can be used to evaluate differences in survival, viral burden, respiratory burst, gene expression, and the dynamics of the neutrophil and macrophage response. This zebrafish Color-flu model of IAV infection is unique as it is the only model where innate immune and virus-infected cells can be visualized in a transparent host in vivo. As zebrafish larvae only have innate immune cells at this stage of development, the model can be used to study the roles of neutrophils and macrophages during IAV infection. Studies of the innate immune response to IAV are needed as the virus can evade the innate response through interactions of viral proteins (PB1, PB1-F2, PB2, PA, and NS1) with the host (Fernandez-Sesma, 2006; Graef, 2010; Hsu, 2015; Iwai,2010; Liedman, 2014; Varga, 2011).

We demonstrate that zebrafish larvae are a robust model for analyzing the innate immune response to IAV infection by evaluating multiple lots of PR8 viruses and multiple zebrafish lines. The landmark paper that first established the zebrafish larvae as a model for IAV infection (Gabor, 2014) had studied the AB line. Here, we demonstrate infection in two "wild-type" lines, AB and EK, along with the pigmentation mutant *casper*. When the same amount of virus is injected in larvae from these strains, *casper* had the lowest level of survival and highest viral burden. As is carried out in other model organisms, comparing strains with varying phenotypes can be a powerful way to understand disease mechanisms (Feng, 2005). Whole genome sequencing of *casper*, a related pigmentation mutant, *roy*, and AB zebrafish revealed 4.3 million single-nucleotide polymorphisms between strains, including mutations in the *mpv7* and *mitfa* genes in the *casper* line (Bian, 2020). In addition to cataloging sequence variants, the authors characterized gene expression in skin and skeletal muscle of adult *casper* and *roy* mutants compared to wild-type AB zebrafish (Bian, 2020). The interferon response stimulator *sting1* was consistently upregulated in the skin and skeletal muscle of *casper* mutants (Bian, 2020). The higher expression of *sting1*, along with any of the 11,583 non-synonymous variants found in *casper* (Bian, 2020), could potentially explain the difference in response to IAV infection.

The capability to simultaneously visualize both virus-infected cells and fluorescently tagged host cells, such as innate immune cells, in transparent living larvae makes the zebrafish Color-flu model unique. Zebrafish larvae from fluorescent reporter strains that label neutrophils and/or macrophages with green or red fluorescent reporters have enabled studies of host–pathogen interactions, such as those during bacterial and fungal infections. However, many of these studies have often included the use of a green or red fluorescently labeled pathogen, thereby preventing the simultaneous imaging of this pathogen with both host immune cell types. As we demonstrate here, the four Color-flu strains developed by the Kawaoka laboratory make it possible to image virus-infected cells along with neutrophils and macrophages using distinguishable color combinations. Furthermore, the Color-flu strains retained their virulence despite the introduction of the fluorescent transgene, as we demonstrate by showing the decreased survival and increased viral burden of infected AB, EK, and *casper* larvae.

We describe the response to both systemic and localized IAV infections. To study the systemic response, IAV was directly injected into the duct of Cuvier so that the virus could spread throughout the larvae via the circulatory system. Confocal imaging of Color-flu-infected larvae showed viral infection throughout different tissues of the larvae. The highest density of infected cells was in the yolk sac and yolk sac extension. The yolk sac accumulation of compounds has been noted in toxicological studies using zebrafish larvae (Halbach, 2020). In one study on the toxicity of nanoplastics, embryos were exposed to 70 nm diameter fluorescent polystyrene nanoparticles in embryo water (Pitt, 2018). By 1 dpf, fluorescence was detected in the yolk sac and yolk sac extension of 1 and 10 ppm exposed embryos, which persisted until 5 dpf, when the yolk sac is reabsorbed after the gastrointestinal system becomes active. As the diameter of nanoparticles is slightly smaller than IAV particles (80–120 nm), it is plausible that the virus particles accumulate in the yolk sac and yolk sac extension like these nanoparticles, thus resulting in an increase in the level of infection in these tissues.

We applied the zebrafish Color-flu model to evaluate whether the ACE inhibitor, ramipril, or the autophagy inhibitor MDIVI-1 would alter the response to IAV infection. Both small molecules improved the response to infection, as the treated larvae had increased survival, lower viral burden, and a respiratory burst response that was the same or higher than that of the uninfected controls. Quantification of fluorescent confocal images of Tg(*mpeg1*:eGFP;*lyz*:dsRed) larvae infected with Color-flu showed lower levels of viral infection in ramipril- and MDVI-1-treated larvae. Ramipril treatment increased the relative number of neutrophils in the infected larvae, whereas MDIVI-1 increased the relative number of macrophages.

Ramipril is an ACE inhibitor that is frequently prescribed for hypertension, as ACE produces angiotensin II, which, in turn, elevates blood pressure (Cushman, 1991). ACE has also been associated with innate immune function (Bernstein, 2018). Angiotensin II mediates proinflammatory responses, including the production of reactive oxygen species (ROS) by

NADPH oxidase and the subsequent activation of nuclear factor-κB (NF-κB) and activator protein 1 (AP1) (Montezano, 2014). An overexpression of ACE in mouse neutrophils increased superoxide production and enhanced the clearance of bacteria in mice infected with methicillin-resistant *Staphylococcus aureus* (MRSA), *Pseudomonas aeruginosa*, or *Klebsiella pneumoniae* (Khan, 2017). ACE overexpression in mouse macrophages also lowered the bacterial burden in mice infected with MRSA or *Listeria monocytogenes* (Okwan-Duodu, 2010). While ACE overexpression in myeloid cells benefit immune responses, ACE deficiency can also be beneficial. A study on mouse models of acute respiratory distress syndrome showed that ACE-deficient mice exhibit less lung damage (Imai, 2005). Interestingly, a study of electronic health records of patients in the Clinical Practice Research Datalink in the United Kingdom showed a lower risk of influenza infection depending on the duration of ACE inhibitor use (Chung, 2020). Our study of ramipril treatment in our zebrafish IAV model demonstrated an improved response to viral infection.

Mitochondria have important roles in immune function, including regulating inflammation (Nakahira, 2011). Mitophagy maintains mitochondrial function by clearing mitochondria when they become damaged (Youle, 2012). A myriad of biological processes is altered when mitochondrial function is disrupted, including the overproduction of mitochondrial ROS, which can activate the nucleotide oligomerization domain (NOD)-like receptor family pyrin domain-containing 3 (NLRP3) inflammasome (Zhou, 2010). IAV infection has been shown to induce mitophagy, thereby altering inflammasome activation (Lupfer, 2013; Wang, 2021). The IAV nucleoprotein (NP) has been shown to induce mitophagy through the toll interacting protein (TOLLIP) and mitochondria antiviral signaling protein (MAVS) (Zhang, 2023). In that study, the mitophagy inhibitor MDIVI-1 was found to reduce NP-induced degradation of mitochondrial proteins. The mitochondrial fission inhibitor MDIVI-1 was also shown to reduce NLRP3 inflammasome activation in transmitochondrial cybrid cells with diminished mitochondrial function (Chang, 2020). In our studies of IAV-infected zebrafish larvae, we show that inhibiting mitophagy using MDIVI-1 treatment increases survival and decreases viral burden. We can therefore hypothesize that MDVI-1 counters IAV-induced mitophagy and NLRP3 inflammasome activation.

Zebrafish embryos and larvae have been used to screen small molecule drugs where the response of separate larvae to different treatments can be monitored in multi-well plates (Garcia, 2016). Large-scale screening of small molecules that alter the innate immune response to IAV infection is feasible using our Color-flu model. Color-flu-infected larvae would be exposed to small molecules within wells, and then characterized using fluorescent confocal imaging to determine their relative levels of infection. In these studies, small molecules could be evaluated using different concentrations as well as in different combinations.

### 3.5. Conclusion

We demonstrate that Color-flu can be used to study the innate immune response to IAV infection in zebrafish larvae. This model is complementary to other models of IAV infection. Our model is the only IAV model where the dynamics of infection and the response of innate immune cells can be visualized in a transparent host in vivo. The roles of neutrophils and macrophages during IAV infection can also be readily characterized using this model. Using Color-flu, we characterize how ACE inhibition by ramipril and mitophagy inhibition by MDIVI-1 both improve the response to IAV infection by limiting inflammation through distinct mechanisms. These studies demonstrate how larger small molecule screens are possible using this zebrafish Color-flu model of IAV infection. Such screening studies are needed in order to find small molecules that could be developed into novel antiviral therapies for influenza viruses.

# CHAPTER 4

# NEUTROPHIL TRAFFICKING REGULATION IS ESSENTIAL FOR SURVIVAL IN A ZEBRAFISH MODEL OF INFLUENZA A INFECTION

## 4.1 Abstract

The World Health Organization has estimated that up to 650,000 deaths occur annually due to respiratory diseases associated with seasonal influenza infections. Influenza A virus (IAV) causes severe illness in older adults and individuals with chronic health conditions. While neutrophils play crucial roles in innate immunity against bacterial and fungal infections, their roles in antiviral responses are poorly understood. Zebrafish serve as valuable vertebrate models for studying infection and innate immunity. Our current research focuses on investigating the functions of neutrophils in controlling IAV infection and understanding how over-activation during infection leads to harmful hyperinflammatory responses. Several studies have suggested that regulating neutrophil numbers could be a potential therapeutic strategy. In our experiments, survival rates of IAV-infected zebrafish with genetically or pharmacologically controlled neutrophil levels were lower compared to control groups, highlighting the importance of neutrophils in combating the virus. These findings could have significant implications for the development of new therapeutic approaches. Furthermore, we explored the mechanisms underlying hyperinflammation during the innate immune response to IAV infection in order to identify new targets that can enhance antiviral responses while limiting inflammation.

## 4.2 Introduction

The function of neutrophils in the immune system is well-documented during bacterial and fungal infections (Sullivan, 2021). However, evidence also suggests the presence of neutrophils in the lungs and bronchoalveolar lavage (BAL) of mice, rats, and humans following infection with influenza A virus (IAV) (McNamara, 2003). The exact function of these resident lung neutrophils is not completely understood, but it is theorized that they position themselves in the pulmonary vasculature to quickly respond to pulmonary pathogens (Johannson, 2021). It is believed that these neutrophils are actively maintained in the lung through the upregulation of the chemokine receptor CXCR4, which binds to CXCL12, a ligand produced by certain lung endothelial cells (Walters, 2010). The CXCR4 receptor, a G protein–coupled chemokine receptor, has been linked to the development of primary immunodeficiency disorders (Devi, 2013). Truncations in CXCR4 result in gain-of-function (Walters, 2010). These truncations are inherited in an autosomal dominant manner and have been identified in individuals with (WHIM) syndrome. Warts, Hypogammaglobulinemia, Infections, and Myelokathexis (WHIM) syndrome (Murphy, 2014). This syndrome is characterized by neutropenia and recurrent infections, making it a primary immunodeficiency disorder (Johannson, 2021; Murphy, 2014).

In addition to combating bacterial infections, it has been noted that neutrophils play a role in controlling viral infections, including influenza (Tate, 2011). The inflammatory environment within the lung is responsible for recruiting neutrophils. Once these neutrophils have reached the lungs, they aid in viral clearance. Studies have shown that young mice depleted of neutrophils during infection experienced accelerated mortality and difficulty in clearing the virus (Tate, 2011). Neutrophils help clear IAV by creating extracellular traps, engulfing viral particles, and activating the inflammasome. However, excessive neutrophil activity can lead to hyperinflammation and subsequent tissue damage (Brandes, 2013; Papayannopoulos, 2017). To prevent such problems during infection, resident macrophages remove the neutrophils (Fullerton, 2016; Webster, 2013).

A previous study in young mice revealed that only partial depletion of neutrophils improved survival during influenza infection, while complete depletion led to faster mortality (Tate, 2011).

To further elucidate the role of neutrophils in response to IAV we utilize several zebrafish (*Danio rerio*) models related to neutrophil motility regulation. These zebrafish models are: zebrafish treated with AT7519, a pharmacological neutrophil inhibitor of multiple cyclin-dependent kinases that induces neutropenia, Cxcl8b morphants, a WHIM model that overexpresses a truncated CXCR4b protein specifically in neutrophils (Walters, 2010), and miR-199 and miR-722 overexpression lines that were shown to haveneutrophil motility defects in response to bacteria (Hsu, 2019).. With the optical clarity of the zebrafish and the recently developed Color-flu model (Fukuyama, 2015; Soos, 2024) we can ascertain *in vivo* what role, if any neutrophils have in IAV infection.

## 4.3. Materials and Methods

### 4.3.1. Zebrafish care and maintenance

The zebrafish utilized in this research were responsibly housed and maintained at the Zebrafish Facility located at the University of Maine, in compliance with the recommendations outlined in the Guide for the Care and Use of Laboratory Animals by the National Institutes of Health and the University of Maine's Institutional Animal Care and Use Committee (IACUC). All protocols adhered to in this study were officially approved by the IACUC at the University of Maine under Protocol Number A2021-02-02. The zebrafish were accommodated in recirculating tanks following the standard procedures of a 14-hour light, 10-hour dark cycle at a temperature of 28 °C. The zebrafish lines used in this study were AB, *WHIM* (*zCXCR4b: Whim: GFP* ) (Walters, 2010), miR-199 (Tg(lyz:dre-miR-199Dendra2)), miR-722 (Tg(lyz:dre-miR-722-Dendra2)), and Tg(*mpeg1*:eGFP;*lyz*:dsRed). The lines miR-199 (Tg(lyz:dre-miR-199Dendra2)), miR-722

(Tg(lyz:dre-miR-722-Dendra2)) were made by adding 20 ng transposase to 10 ng of the plasmid. They were injected into high one cell zebrafish that were collected every 15 minutes. They were screened for mortality six times over the first 48 hpf before screening to confirm the presence of GFP neutrophils. The Cxcl8b morphants were generated by injecting 20 ng of Cxcl8b morpholino (MO), as previously described (Zuñiga-Traslaviña, 2017). The Tg(*mpeg1*:eGFP;*lyz*:dsRed) line was created by crossing the Tg(*mpeg1*:eGFP) (Renshaw, 2006) and Tg(*lyz*:dsRed) (Hall, 2007) zebrafish lines. Embryos were obtained by breeding adult zebrafish using varying sets of females. Embryos were kept at 33 °C in 50 mL of sterilized egg water (60 μg/mL Instant Ocean Sea Salts; Aquarium Systems, Mentor, OH, USA) in 10 cm × 2.5 cm Petri dishes, with water changes every 2 days.

### 4.3.2. MDCK/ London cell culture

Madin–Dardy canine kidney/London (MDCK/London; Influenza Reagent Resource) cells (passage 4) were cultured using Dulbecco's Modified Eagle Medium (DMEM). Cells were grown at 37 °C with 5% CO2 in T-175 flasks in DMEM high glucose, GlutaMAX supplement (10% heat-inactivated fetal bovine serum, and 1% antibiotic–antimycotic). The cells were maintained by washing twice with 1× Dulbecco's phosphate-buffered saline (PBS, pH 7.4), trypsinized with 0.25% trypsin-EDTA with phenol red, and passaged in a 1:30 dilution every 3–4 days up to passage eight. Virus-infected cells were grown in Opti-MEM-BSA-TPCK media, containing Opti-MEM, 1% antibiotic–antimycotic, 1 μg/mL Tosyl phenylalanyl chloromethyl ketone (TPCK) trypsin and Bovine Albumin Fraction V.

### 4.3.3. Influenza virus

PR8 influenza virus (A/PR/8/34 (H1N1) and Color-flu (Fukuyama, 2015) influenza virus strains MA-mVenus-PR8 (mVenus-PR8), MA-eCFP-PR8 (eCFP-PR8), MA-eGFP-PR8 (eGFP-PR8), and MA-mCherry-PR8 (mCherry-PR8) were prepared as described in Chapter 3.3.3.

### 4.3.4. Microinjection

Microinjections were performed as described in (Soos, 2024) with the exception of Color-flu microinjection. Before microinjection, approximately 3 nL of 3% methyl cellulose prepared in egg water is added to the Color-flu aliquot and mixed. This allows for 4 nL of any Color-flu strain to be injected at 2 days post fertilization (dpf).

### 4.3.5. Drug exposures

For all of our small molecule drug studies, larvae were exposed to either dimethyl sulfoxide (DMSO), DMSO-solubilized ramipril, or DMSO-solubilized MDIVI-1 by adding these solutions into the embryo water at 24 hpi. The larvae were exposed to DMSO, ramipril, or MDIVI-1 for one hour at 33 °C in a dark incubator. For AT7519, DMSO-solubilized AT7519 was added for two hours at 33 °C in a dark incubator either as a pre-treatment for injection or a treatment at 24 hpi. After exposure, zebrafish were transferred to 50 mL of fresh embryo water twice to rinse away the DMSO or DMSO-solubilized drugs. The final concentrations used were 0.2 nM for ramipril (Vishnolia, 2020),  7 nM for MDIVI-1 (Vargo, 2017) and 50 nM for AT7519.

### 4.3.6. Survival studies

Survival studies were performed as described in Soos, et. al 2024. The exceptions are that the WHIM, miR-199, and miR-722 groups only have 35-45 zebrafish per group but the pharmacologically inhibited AT7519 groups have between 50-65 zebrafish per group.

### 4.3.7. Viral burden assays

Tissue culture infectious dose 50 (TCID50) end-point dilution assays using MDCK/London cells were used to measure the viral burden of influenza virus in zebrafish. Viral burden assays were performed as described in Soos, et. al 2024.

### 4.3.8. Respiratory burst assays

Respiratory burst assays were performed as described in Soos, et. al 2024.

### 4.3.9. Confocal imaging

Zebrafish were imaged as described in Soos, et. al 2024.

### 4.3.10. Statistical analysis

GraphPad Prism 10.2.3 (GraphPad Software, Boston, MA, USA) was used to generate and analyze survival curves and graphs. Analysis was performed as described in Soos, et. al 2024.

## 4.4 Results

### 4.4.1. AT7519 recapitulates neutropenia and decreases survival in IAV infection.

AT7519 is a pharmacological inhibitor of multiple cyclin-dependent kinases and has been used to induce neutropenia in zebrafish (Peterson, 2024). Survival assays following infection by

PR8 showed a decrease in survival of zebrafish 70 nM AT7519 by 11% compared to DMSO treated controls from a survival rate of 54% to 43% (Figure 4.1C). Other concentrations that were used for comparison are shown in Figure 4.1A and 4.1B. There was no significant change in viral burden (Figure 4.2A) between treated and untreated samples. Although not shown, imaging showed fewer neutrophils that were smaller in size compared to DMSO treatment indicating a complete ablation of neutrophils at one time. In fact, the respiratory burst, 24 hours post treatment, still demonstrated reduced neutrophil function, Figure 4.2B. There was a significant difference in ability to induce a respiratory burst response with 50 nM AT7519 treated zebrafish compared to controls.

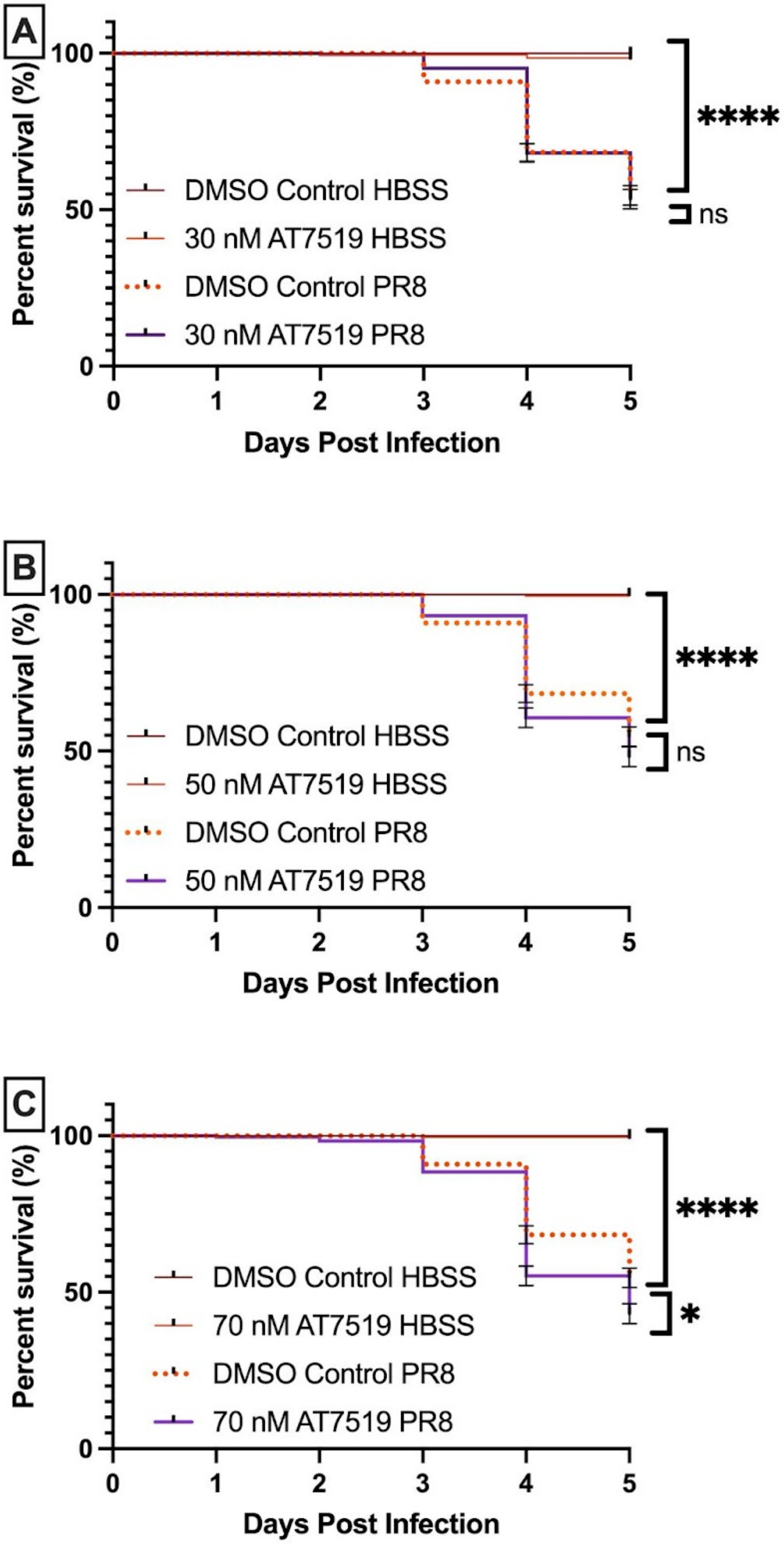
A
Percent survival (%)
100
50
0
Days Post Infection
0
1
2
3
4
5
DMSO Control HBSS
30 nM AT7519 HBSS
DMSO Control PR8
30 nM AT7519 PR8
****
ns
B
Percent survival (%)
100
50
0
Days Post Infection
0
1
2
3
4
5
DMSO Control HBSS
50 nM AT7519 HBSS
DMSO Control PR8
50 nM AT7519 PR8
****
ns
C
Percent survival (%)
100
50
0
Days Post Infection
0
1
2
3
4
5
DMSO Control HBSS
70 nM AT7519 HBSS
DMSO Control PR8
70 nM AT7519 PR8
****
*

**Figure 4.1. Survival rates of AT7519-treated zebrafish infected with PR8 compared to DMSO control.** A) Decreased survival of AB zebrafish systemically infected with PR8 IAV at 2 dpf compared to vehicle (HBSS) controls ($p < 0.0001$ for each lot comparison). Zebrafish were pre-treated with either A) 30 nM AT7519 or DMSO, B) 50 nM AT7519 or DMSO, or C) 70 nM AT7519 or DMSO for two hours before injections. There is decreased survival in both IAV sample groups compared to HBSS controls, with a slighter increase in mortality observed in the 70 nM AT7519 sample. (*$p = 0.0121$, ****$p = > 0.0001$). Experimental results were conducted with 4 replicates comprised of 60 fish per group.

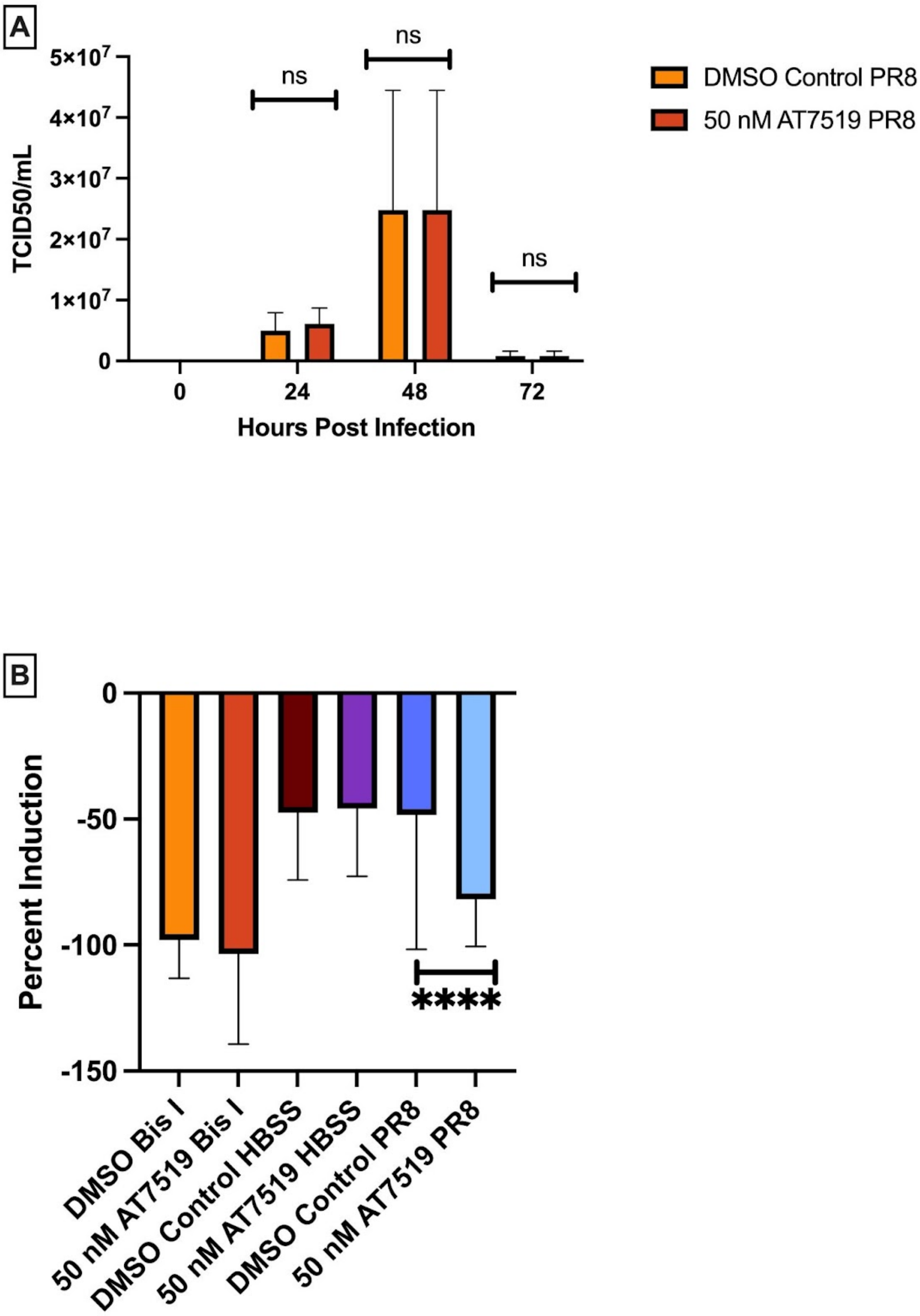
A
5×10^7
4×10^7
3×10^7
2×10^7
1×10^7
0
TCID50/mL
ns
ns
ns
0
24
48
72
Hours Post Infection
DMSO Control PR8
50 nM AT7519 PR8
B
0
-50
-100
-150
Percent Induction
****
DMSO Bis I
50 nM AT7519 Bis I
DMSO Control HBSS
50 nM AT7519 HBSS
DMSO Control PR8
50 nM AT7519 PR8

**Figure 4.2. Functional changes in antiviral response of AT7519 treated zebrafish infected with PR8 compared to DMSO control.** A) There was no significant change in $TCID_{50}$ viral titer between DMSO control and AT7519 treated zebrafish. Experimental results were conducted with 3 replicates comprised of 25 fish per replicate. B) There was no significant change in 50 nM AT7519 treated zebrafish when compared to DMSO control in Bis I or HBSS vehicle controls. There was a significant change between the two groups when infected with PR8. Experimental results were conducted with 3 replicates comprised of 24 zebrafish per group.

### 4.3.2. Cxcl8b morphants display decreased survival after IAV infection.

The chemokine, Cxcl8b, has been shown to regulate neutrophil migration along with its receptor, Cxcr2 (Zuñiga-Traslaviña, 2017). Survival assays of Cxcl8b morphants showed a decrease in survival of Cxcl8b morpholino injected zebrafish compared to controls. The Cxcl8b morphants survived at 35.8% compared to 45.6% for control morphants (Figure 4.3A). B) In the respiratory burst measured at 24 hours post treatment, Cxcl8b morphants and control morphants displayed no significant difference in the respiratory burst response in either HBSS or PR8 groups. However, when comparing PR8 to the corresponding Bis I groups, Cxcl8b morphants demonstrated reduced neutrophil function showing no significant change compared to a slight change when comparing control morphants to Bis I, (Figure 4.3B).

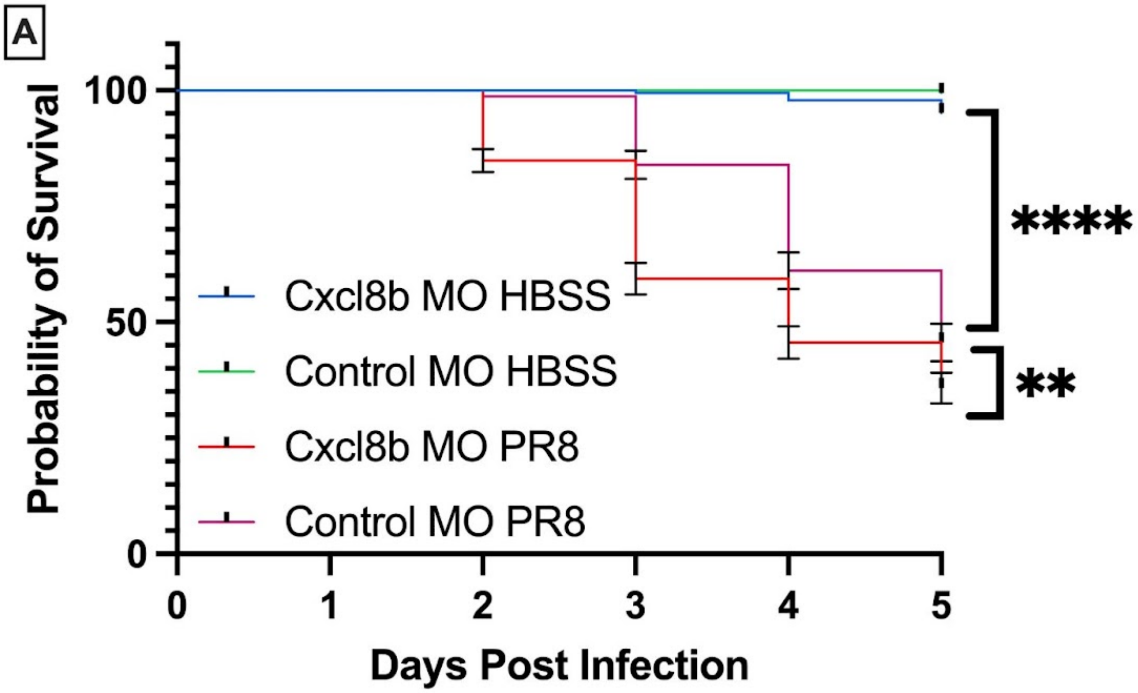
A
Probability of Survival
100
50
0
Days Post Infection
0
1
2
3
4
5
Cxcl8b MO HBSS
Control MO HBSS
Cxcl8b MO PR8
Control MO PR8
****
**

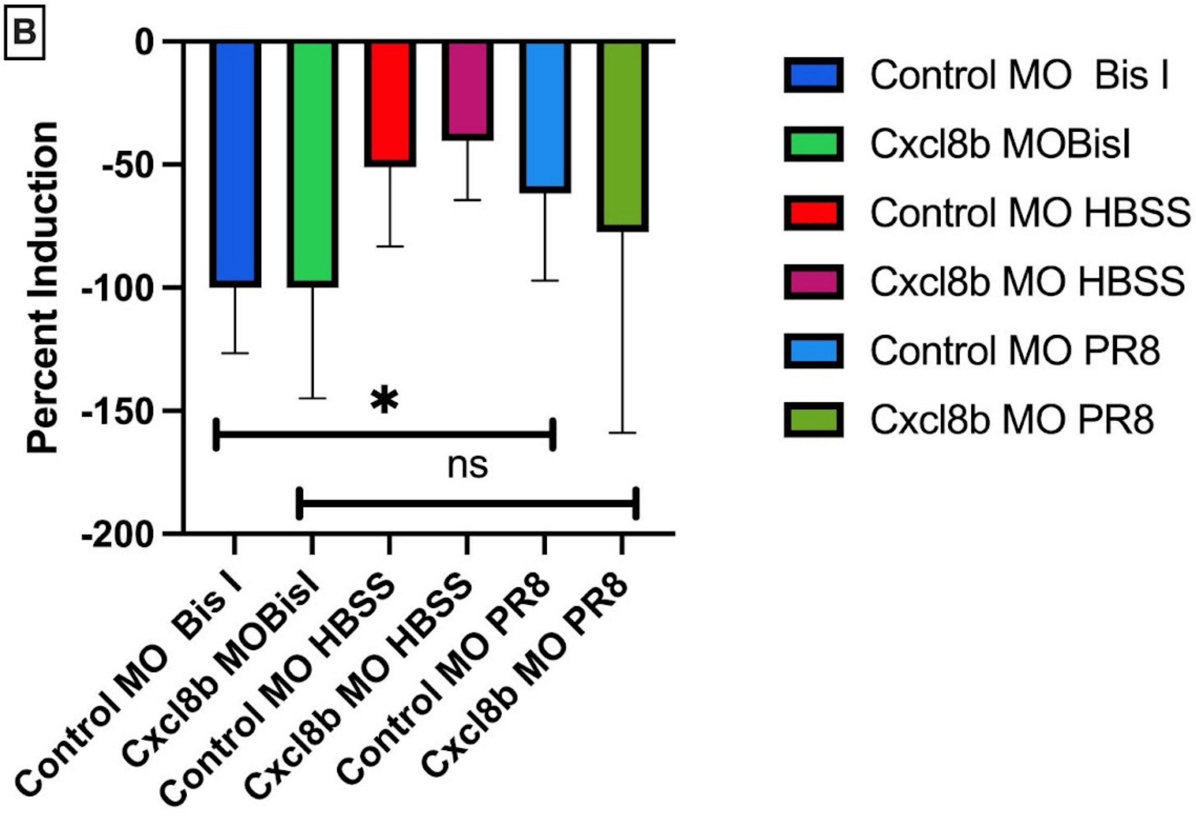
B
Percent Induction
0
-50
-100
-150
-200
*
ns
Control MO Bis I
Cxcl8b MOBisI
Control MO HBSS
Cxcl8b MO HBSS
Control MO PR8
Cxcl8b MO PR8

**Figure 4.3. Survival rates of Cxcl8b morphants compared to control morphants.** A) Decreased survival of Cxcl8b morphant zebrafish systemically infected with PR8 IAV at 2 dpf compared to the control morphant. PR8 infected groups had significantly decreased survival compared to HBSS vehicle controls (*****p* = >0.0001). There was a moderate difference between Cxcl8b and control morphants (***p* = >0.0022). Experimental results were conducted with 4 replicates comprised of 40 fish per replicate. B) The only significance that occurred was between control morphants treated with BisI and control morphants infected with PR8 (**p* = >0.0100). Experimental results were conducted with 3 replicates comprised of 24 fish per replicate.

### 4.3.3. Cxcr4b WHIM mutants decrease survival in IAV infection.

Survival assays showed a decrease in survival of WHIM mutant zebrafish compared to WHIM siblings with 35% for the WHIM mutant compared to 72% for sibling controls (Figure 4.4A). Survival assays of WHIM heterozygotes showed a decrease in survival of WHIM heterozygous mutant zebrafish compared to homozygous WHIM mutant zebrafish with 35% for the WHIM homozygous mutants compared to 46% for the heterozygous controls (Figure 4.4B). There was no significant change in viral burden (Figure 4.5A) between WHIM mutants and WHIM siblings. The respiratory burst, 24 hours post injection, also demonstrated reduced neutrophil function, Figure 4.5B. There was a significant difference in ability to induce a respiratory burst response with WHIM mutants when compared to WHIM siblings.

To see whether the phenotype could be rescued through pharmacological intervention, we tested previously identified small molecule therapeutics mitochondrial division inhibitor (MDIVI-1) and ramipril. The WHIM mutant and the WHIM sibling were both rescued by the treatment of 7 nM MDIVI-1 and 0.2 nM ramipril. For WHIM mutants, treatment with MDIVI-1 resulted in an increase of 44.3% in survival (80%) from an original survival of 35.7%. (Figure

4.6A) The WHIM siblings had a 28.3% increase from 54.7% to 83%. For WHIM mutants, treatment with ramipril resulted in an increase of 54.3% in survival (80%) from an original survival of 35.7%. The WHIM siblings had a 29% increase from 54.7% to 83%. From a survival rate of 54% to 43% (Figure 4.6B).

**A**

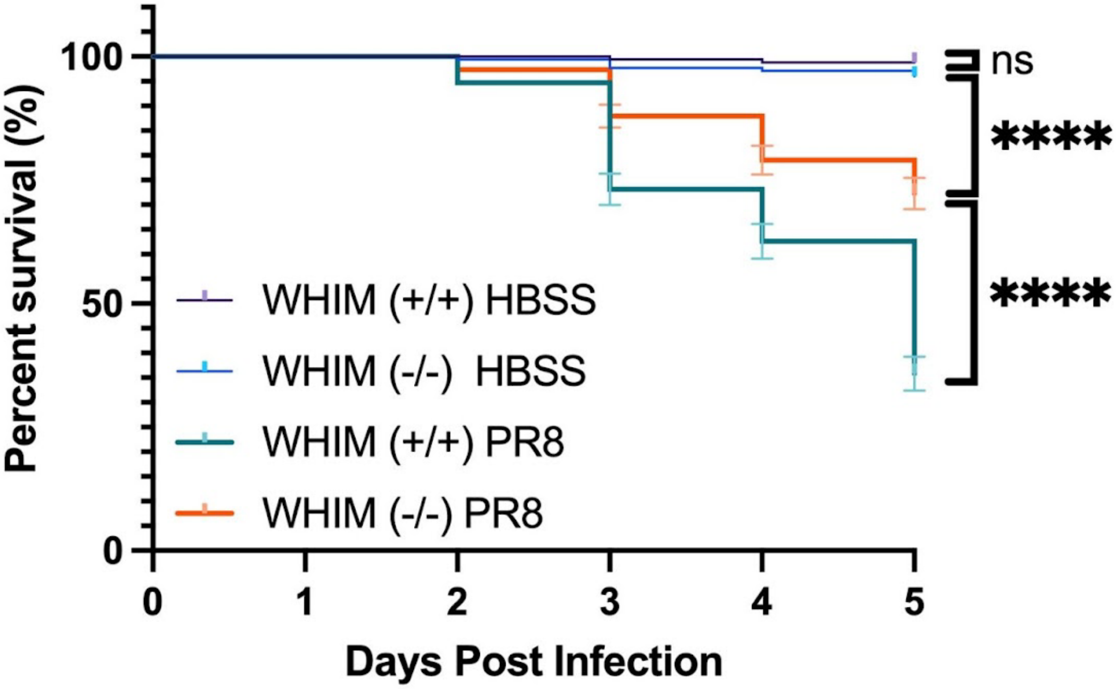

Percent survival (%)
100
50
0
0
1
2
3
4
5
Days Post Infection
ns
****
****
WHIM (+/+) HBSS
WHIM (-/-) HBSS
WHIM (+/+) PR8
WHIM (-/-) PR8

**B**

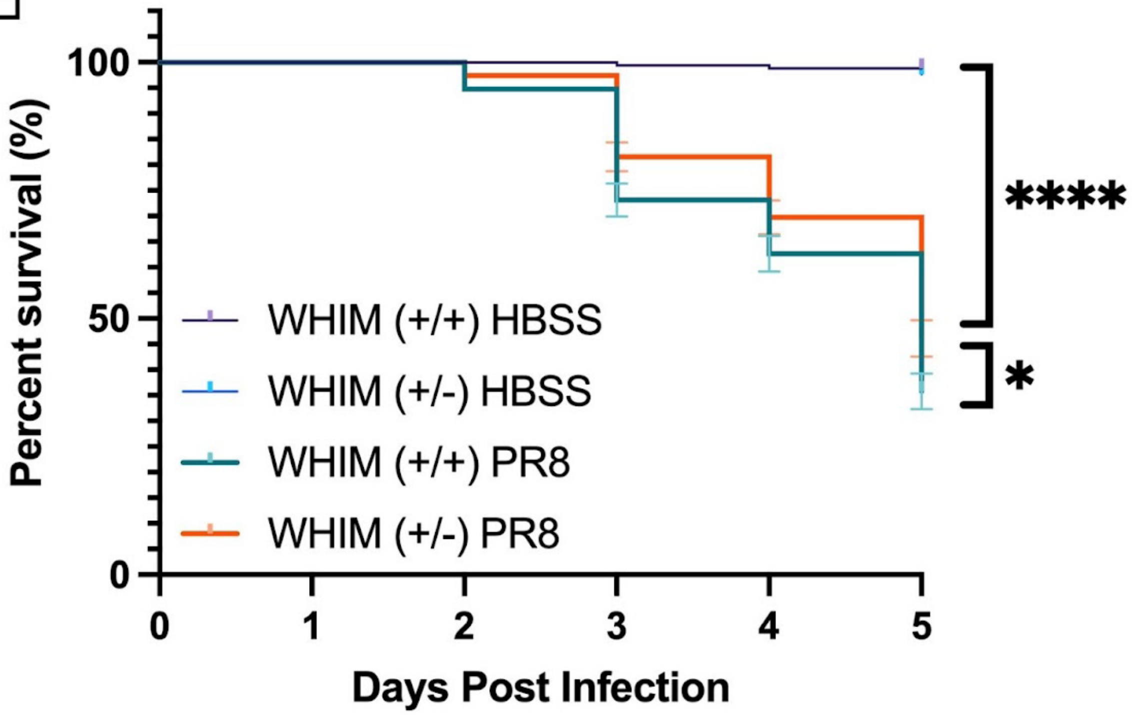

Percent survival (%)
100
50
0
0
1
2
3
4
5
Days Post Infection
****
*
WHIM (+/+) HBSS
WHIM (+/-) HBSS
WHIM (+/+) PR8
WHIM (+/-) PR8

**Figure 4.4. Survival rates of WHIM compared to WHIM hets and WHIM control.** A) Decreased survival of WHIM mutant zebrafish systemically infected with PR8 IAV at 2 dpf compared to the WHIM sibling PR8 IAV. HBSS controls (*p* < 0.0001 for each strain comparison). There was a significant difference between WHIM mutants (*mpx*$^{(+/+)}$) and WHIM sibling (*****p* = >0.0001). Experimental results were conducted with 4 replicates comprised of 40 fish per replicate. B) Moderately decreased survival of WHIM mutant zebrafish systemically infected with PR8 IAV at 2 dpf compared to WHIM heterozygous mutants PR8 IAV. HBSS controls (*p* < 0.0001 for each strain comparison). There was a considerable difference between WHIM mutants and WHIM heterozygous mutants (***p* = 0.0286, *****p* = > 0.0001). Experimental results were conducted with 4 replicates comprised of 40 fish per replicate.

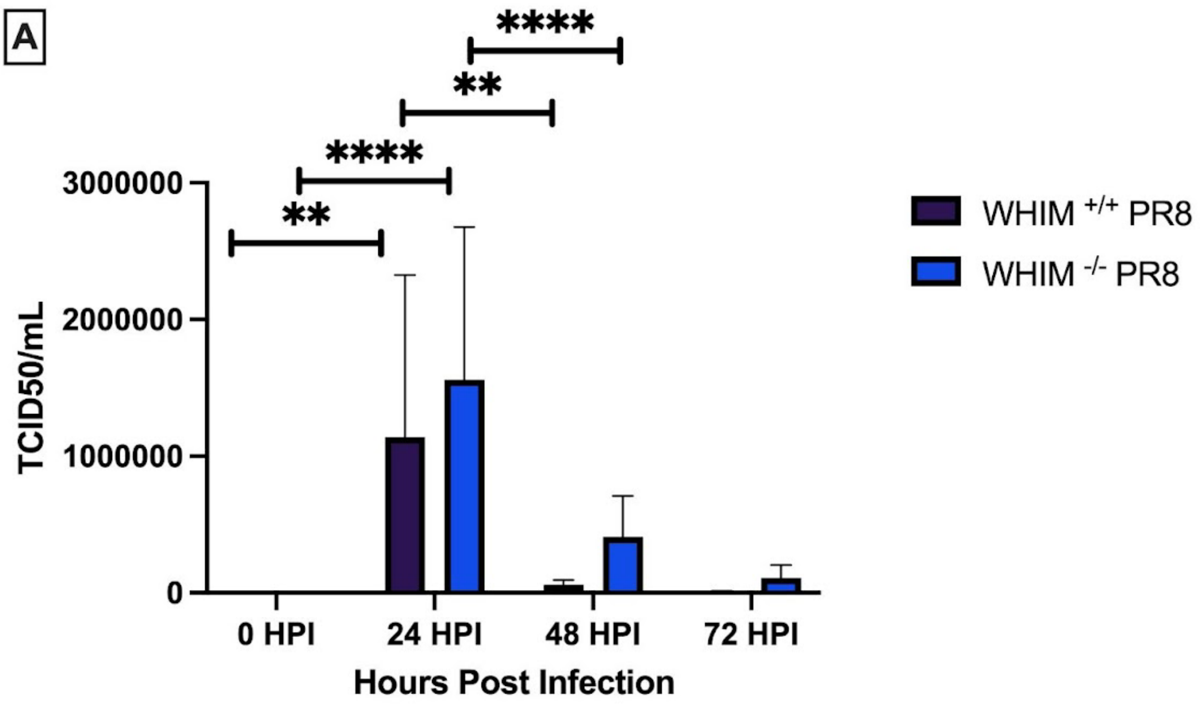
A
****
**
****
**
3000000
2000000
1000000
0
TCID50/mL
0 HPI
24 HPI
48 HPI
72 HPI
Hours Post Infection
WHIM +/+ PR8
WHIM -/- PR8

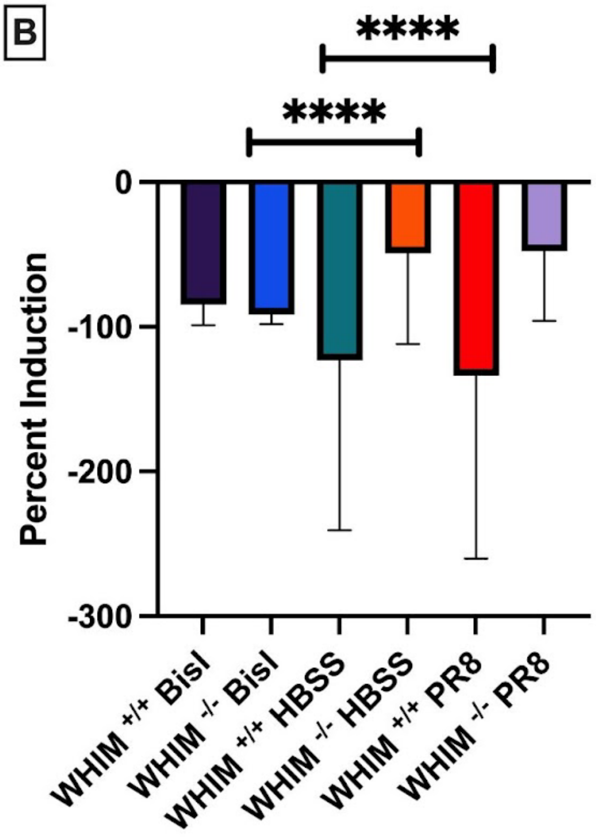
B
****
****
0
-100
-200
-300
Percent Induction
WHIM +/+ Bisl
WHIM -/- Bisl
WHIM +/+ HBSS
WHIM -/- HBSS
WHIM +/+ PR8
WHIM -/- PR8

**Figure 4.5. Functional assessment of antiviral response of WHIM mutants compared to WHIM sibling control.** A)There was no significant change in $TCID_{50}$ viral titer between WHIM mutant and WHIM sibling zebrafish. However, between timepoints 0 to 24 hpi showed increases for both groups and 24 to 48 showed significant decreases for both groups as well. n= 3 of 3 replicates with 25 fish per replicate. (***p* = > 0.0028, *****p* = >0.0001). B) There was a significant difference between WHIM mutants and WHIM siblings, with WHIM mutants having a lower respiratory burst response than the Bis I inhibited zebrafish. (*****p* = >0.0001) n = 3 of 24 fish per group.

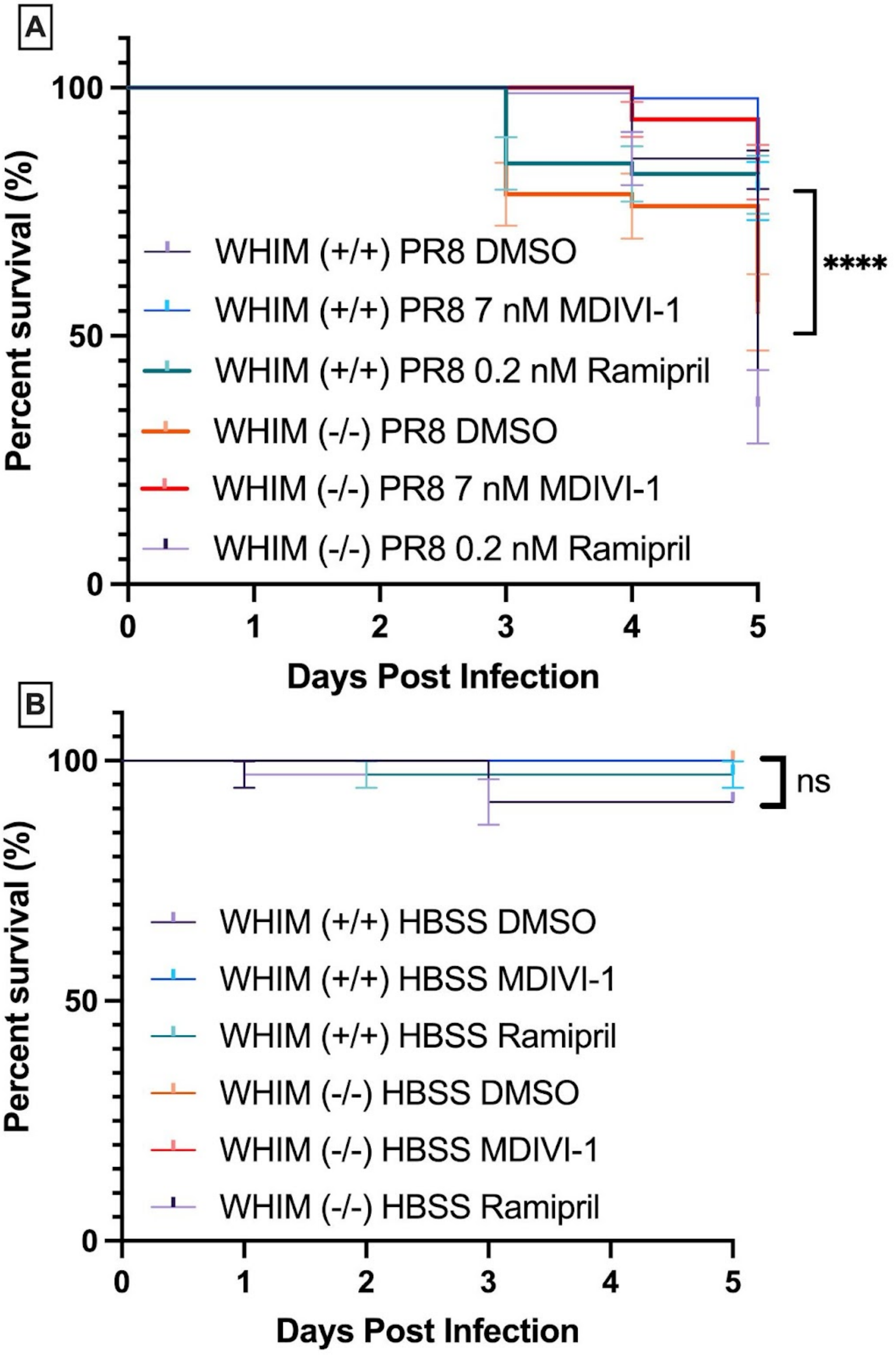
A
Percent survival (%)
100
50
0
0
1
2
3
4
5
Days Post Infection
WHIM (+/+) PR8 DMSO
WHIM (+/+) PR8 7 nM MDIVI-1
WHIM (+/+) PR8 0.2 nM Ramipril
WHIM (-/-) PR8 DMSO
WHIM (-/-) PR8 7 nM MDIVI-1
WHIM (-/-) PR8 0.2 nM Ramipril
****
B
Percent survival (%)
100
50
0
0
1
2
3
4
5
Days Post Infection
WHIM (+/+) HBSS DMSO
WHIM (+/+) HBSS MDIVI-1
WHIM (+/+) HBSS Ramipril
WHIM (-/-) HBSS DMSO
WHIM (-/-) HBSS MDIVI-1
WHIM (-/-) HBSS Ramipril
ns

**Figure 4.6. Survival rates of WHIM$^{(+/+)}$ compared to WHIM$^{(-/-)}$ with therapeutic rescue.** A) Increased survival of WHIM mutant (WHIM$^{(+/+)}$) zebrafish systemically infected with PR8 IAV at 2 dpf and the WHIM sibling (*WHIM*$^{(-/-)}$) PR8 IAV. Both lines were treated with either DMSO, 7 nM MDIVI-1, or 0.2 nM ramipril. There was a significant difference between MDIVI-1 treated and WHIM mutants and untreated WHIM sibling , (**$p$ = 0.0027, ****$p$ = >0.0001). When comparing ramipril treated and untreated groups, there was a significant difference between treated and untreated WHIM mutants and WHIM sibling (***$p$ = 0.0005, ****$p$ = >0.0001). n= 4 of 35 fish per group. B) The HBSS treated controls (****$p$ < 0.0001 for each strain comparison). n= 4 of 35 fish per group.

### 4.4.4. miR-199 overexpression mutants decrease survival in IAV infection.

The microRNA, miR-199, was shown to negatively regulate neutrophil migration through cyclin-dependent kinase 2 (Cdk2). The expression of miR-199 was shown to decrease following bacterial infection in zebrafish and a transgenic line, Tg(*lyz:dre-miR-199Dendra2*), was created to overexpress miR-199 which exhibited neutrophil migration defects (Hsu, 2019). Survival assays showed a decrease in survival of mmiR-199 overexpressed zebrafish compared controls. miR-199 overexpression line zebrafish infected with PR8 survived at 42% compared with a control survival of 80% (Figure 4.6A). There was no significant change in viral burden (Figure 4.6B) between miR-199 overexpressed zebrafish and the control. There were significant changes between timepoints such as for 0 and 24 and 24 to 48, but between groups there was not any significance. Additionally, the respiratory burst, 24 hours post injection, showed no significant difference between miR-199 overexpressed zebrafish and the control, Figure 4.6C.

The miR-199 overexpression zebrafish and the control were both rescued by the treatment of 7 nM MDIVI-1 and 0.2 nM ramipril (Figure 4.7). For miR-199 overexpression zebrafish treatment with MDIVI-1 resulted in an increase of 32% in survival (77%) from an original survival of 44.8%. The control had a 28.3% increase from 62% to 80%. For miR-199 overexpressed zebrafish treatment with ramipril resulted in an increase of 35% in survival (80%) from an original survival of 44.8%. The control had a 28.3% increase from 62% to 85%.

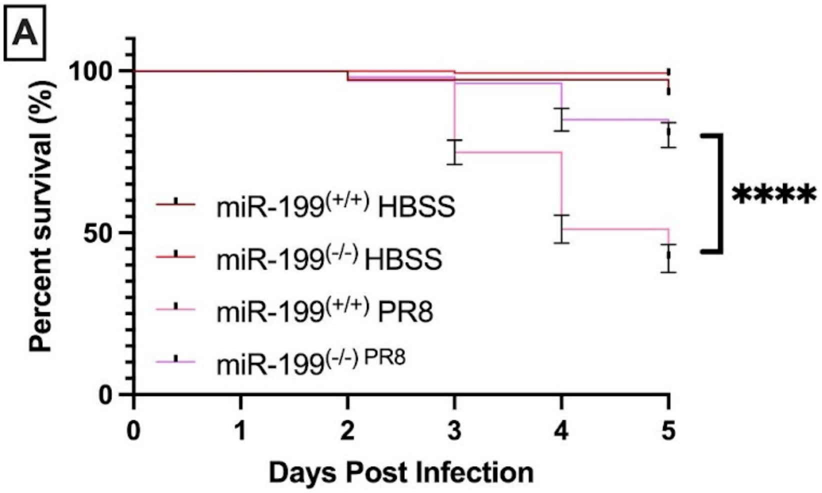
A
Percent survival (%)
100
50
0
Days Post Infection
0
1
2
3
4
5
miR-199(+/+) HBSS
miR-199(-/-) HBSS
miR-199(+/+) PR8
miR-199(-/-) PR8
****

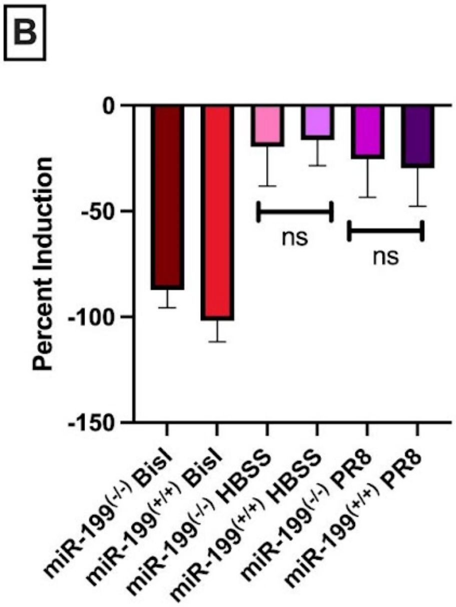
B
Percent Induction
0
-50
-100
-150
ns
ns
miR-199(-/-) Bisl
miR-199(+/+) Bisl
miR-199(-/-) HBSS
miR-199(+/+) HBSS
miR-199(-/-) PR8
miR-199(+/+) PR8

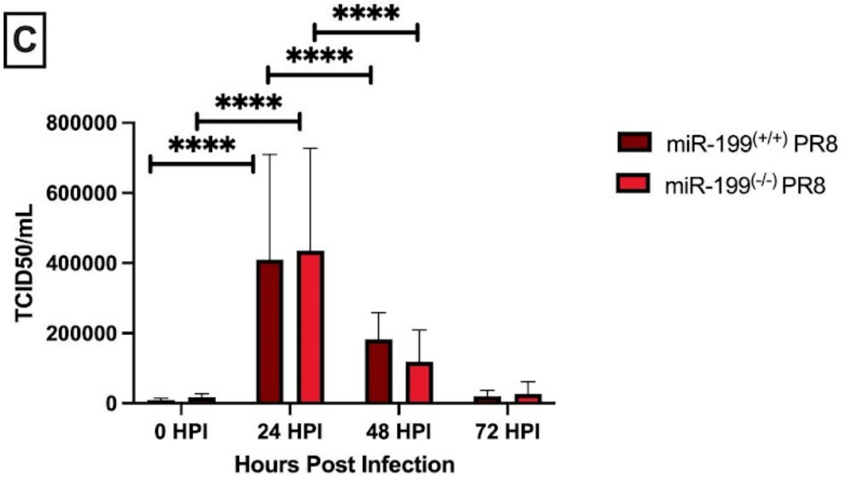
C
TCID50/mL
800000
600000
400000
200000
0
****
****
****
****
0 HPI
24 HPI
48 HPI
72 HPI
Hours Post Infection
miR-199(+/+) PR8
miR-199(-/-) PR8

**Figure 4.7. Survival and antiviral response assessment in miR-199 overexpression mutants (Tg(*lyz:dre-miR-199Dendra2*)) compared to controls.** A) MiR-199 overexpression zebrafish had an average survival of 42% when compared to the control at 80%. There was a significant difference between the two groups. (*****p* = >0.0001). n= 4 of 40 fish per group. There are HBSS controls ($p < 0.0001$ for each strain comparison). B) There was no significant change in $TCID_{50}$ viral titer miR-199 overexpression zebrafish systemically infected with PR8 IAV at 2 dpf and the control PR8 IAV zebrafish. However, between timepoints 0 to 24 hpi showed increases for both groups and 24 to 48 showed significant decreases for both groups as well. n= 3 of 3 replicates with 25 fish per replicate. (*****p* = >0.0001). C) There was not a significant difference for respiratory burst response between miR-199 mutants and miR-199 siblings (n = 3 of 24 fish per group).

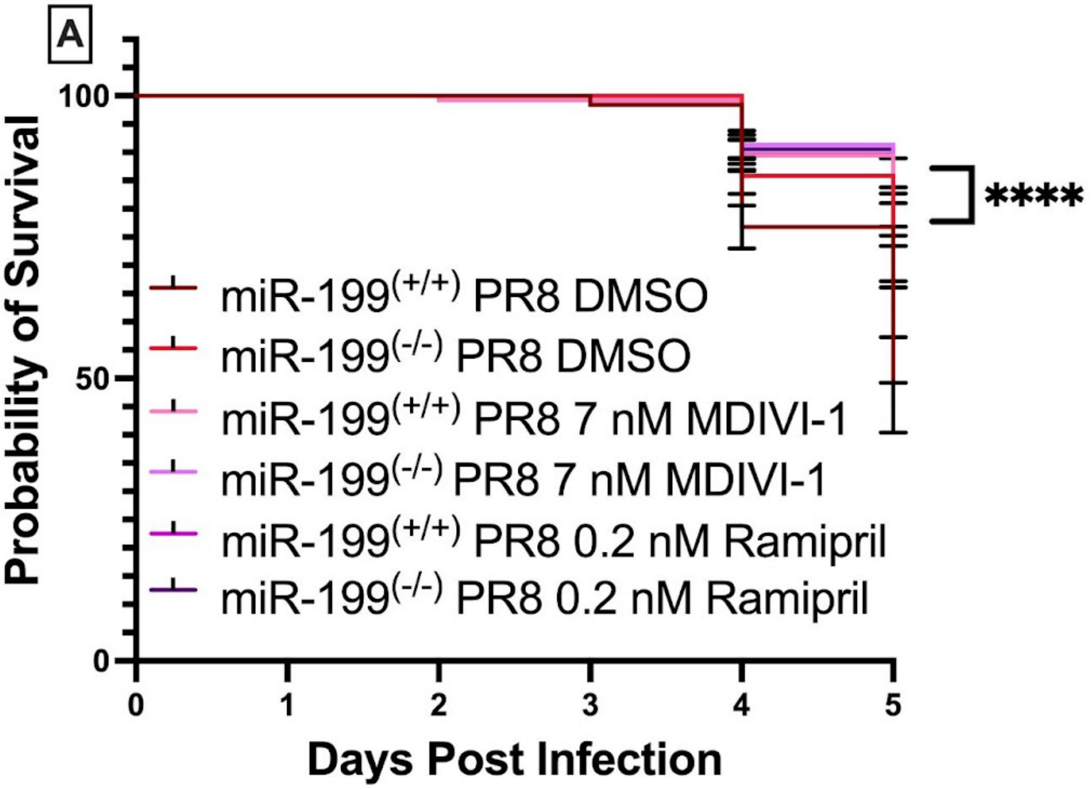
A
Probability of Survival
100
50
0
Days Post Infection
0
1
2
3
4
5
****
miR-199$^{(+/+)}$ PR8 DMSO
miR-199$^{(-/-)}$ PR8 DMSO
miR-199$^{(+/+)}$ PR8 7 nM MDIVI-1
miR-199$^{(-/-)}$ PR8 7 nM MDIVI-1
miR-199$^{(+/+)}$ PR8 0.2 nM Ramipril
miR-199$^{(-/-)}$ PR8 0.2 nM Ramipril

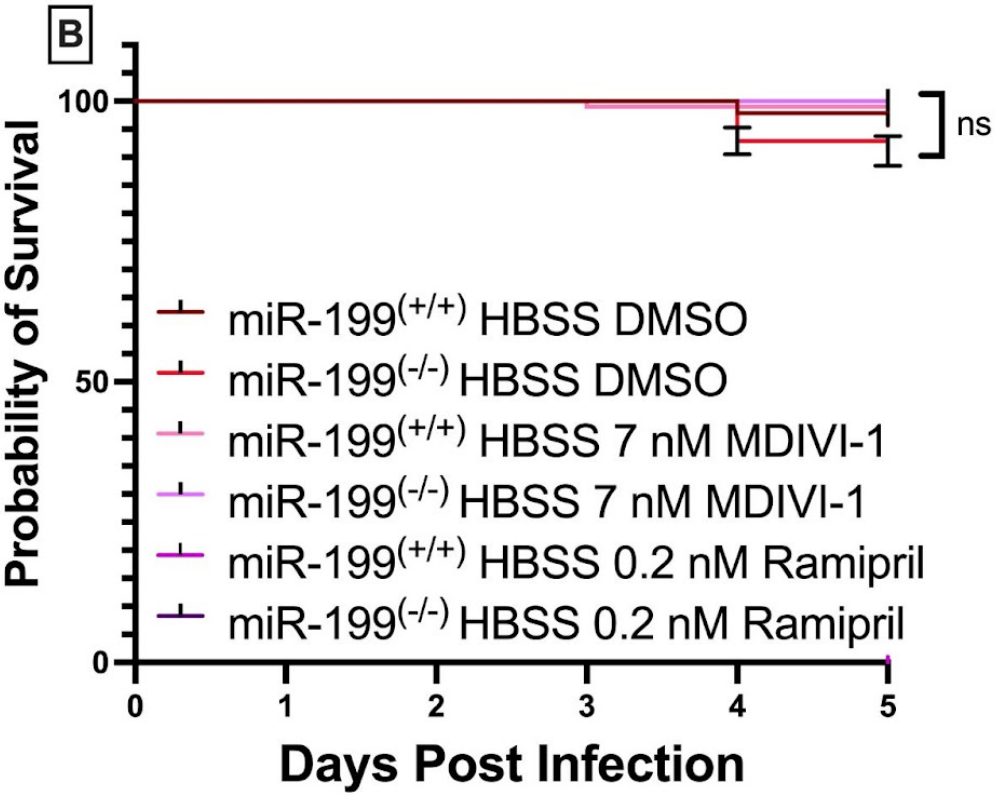
B
Probability of Survival
100
50
0
Days Post Infection
0
1
2
3
4
5
ns
miR-199$^{(+/+)}$ HBSS DMSO
miR-199$^{(-/-)}$ HBSS DMSO
miR-199$^{(+/+)}$ HBSS 7 nM MDIVI-1
miR-199$^{(-/-)}$ HBSS 7 nM MDIVI-1
miR-199$^{(+/+)}$ HBSS 0.2 nM Ramipril
miR-199$^{(-/-)}$ HBSS 0.2 nM Ramipril

**Figure 4.8. Survival rates of Tg(*lyz:dre-miR-199Dendra2*) compared to control with therapeutic rescue.** A) Increased survival of miR-199 overexpressing line zebrafish systemically infected with PR8 at 2 dpf and the control PR8 zebrafish. Both lines were treated with either DMSO, 7 nM MDIVI-1, or 0.2 nM ramipril. miR-199 overexpressed zebrafish treated with MDIVI-1 had an increase in survival from 44.8% to 77%. Control zebrafish had an increase in survival with MDIVI-1 treatment of 62% to 80%. (****$p$ = >0.0001). MiRr-199 overexpressed zebrafish treated with ramipril had an increase in survival from 44.8% to 80%. Control zebrafish had an increase in survival with ramipril treatment of 62% to 85%. (****$p$ = >0.0001). B) There are HBSS controls ($p < 0.0001$ for each strain comparison). n= 4 of 35 fish per group.

### 4.4.5. miR-722 overexpression mutants decrease survival and in IAV infection.

The microRNA, miR-722, was shown to negatively regulate neutrophil migration through Rac family small GTPase 2 (Rac2) (Hsu et al, 2019). Like miR-199, the expression of miR-722 was shown to decrease following bacterial infection in zebrafish. The transgenic line, Tg(*lyz:dre-miR-722Dendra2*), was created to overexpress miR-722 and exhibited neutrophil migration defects (Hsu et al, 2019). Survival assays showed a decrease in survival of miR-722 overexpressed zebrafish compared controls. miR-722 overexpression line zebrafish infected with PR8 survived at 46.3% compared with a control survival of 58.5% (Figure 4.8A). B) There were minor changes in the respiratory burst at 24 hours post infection. HBSS groups showed a slight difference between miR-722 overexpressed zebrafish and the control group, however they were not statistically relevant, Figure 4.8B.

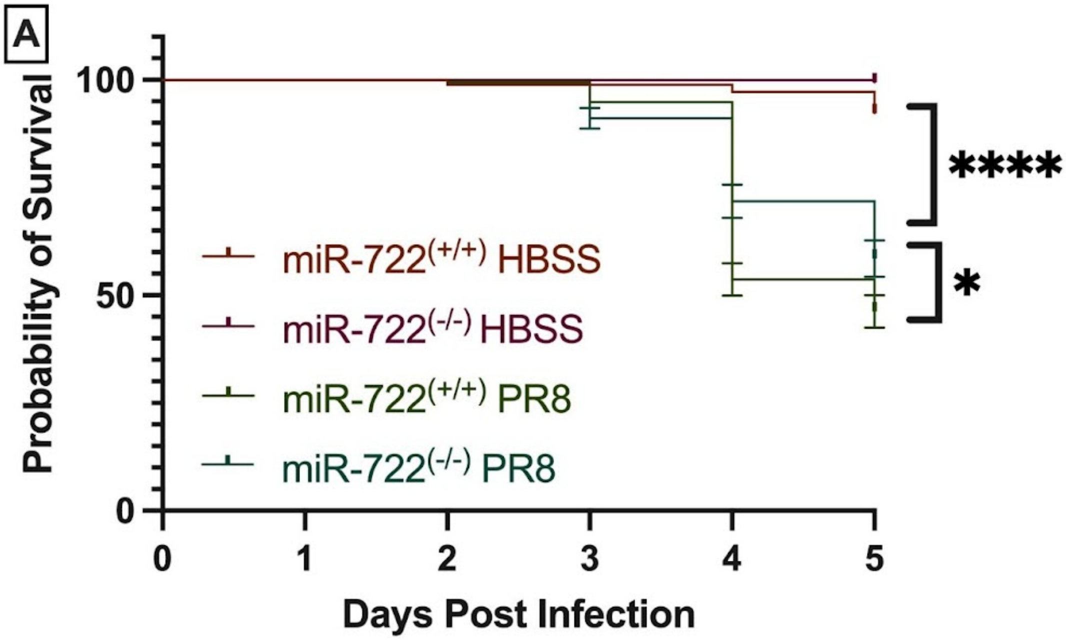
A
Probability of Survival
100
50
0
0
1
2
3
4
5
Days Post Infection
miR-722(+/+) HBSS
miR-722(-/-) HBSS
miR-722(+/+) PR8
miR-722(-/-) PR8
****
*

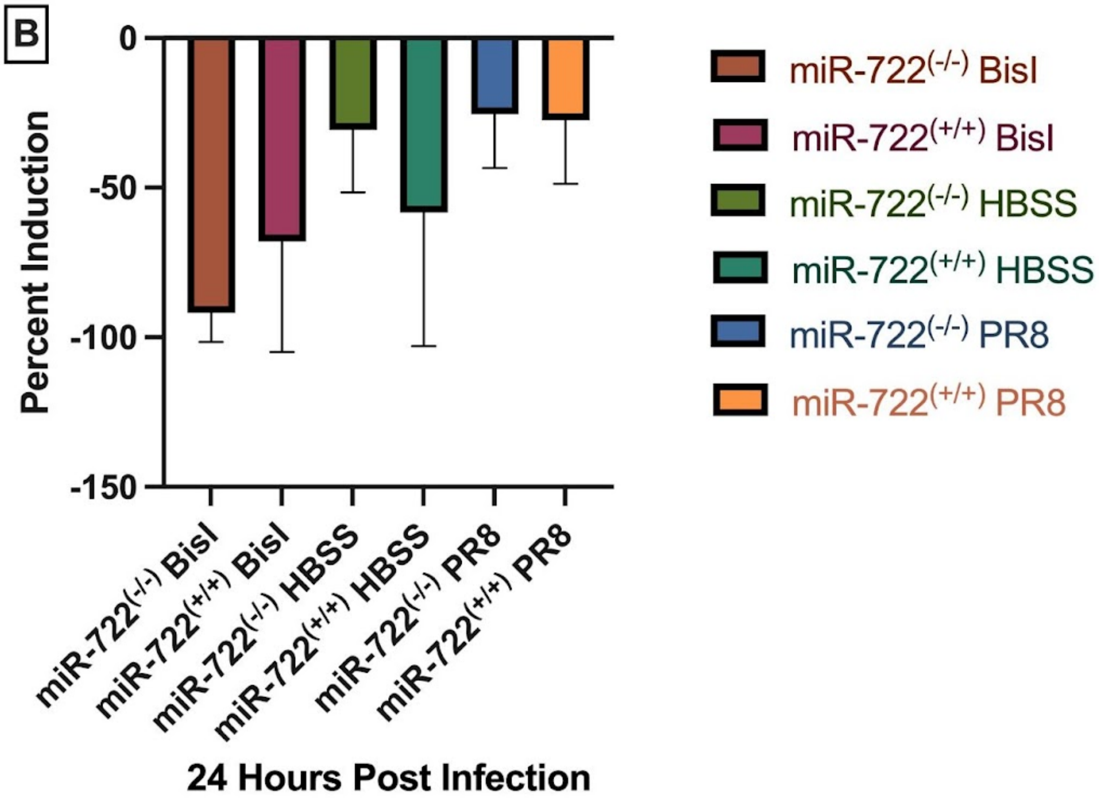
B
Percent Induction
0
-50
-100
-150
miR-722(-/-) BisI
miR-722(+/+) BisI
miR-722(-/-) HBSS
miR-722(+/+) HBSS
miR-722(-/-) PR8
miR-722(+/+) PR8
24 Hours Post Infection
miR-722(-/-) BisI
miR-722(+/+) BisI
miR-722(-/-) HBSS
miR-722(+/+) HBSS
miR-722(-/-) PR8
miR-722(+/+) PR8

**Figure 4.9. Survival and antiviral response assessment of overexpressed *Tg*(*lyz:dre-miR-722Dendra2*) compared to control.** A) miR-722 overexpressed zebrafish had an average survival of 46.3% when compared to the control at 58.5%. There was a slight difference between the two groups. (**p* = >0.0419). n= 4 of 40 fish per group. There are HBSS controls (*p* < 0.0001 for each strain comparison). B) There was not a significant difference for respiratory burst response between miR-199 mutants and miR-199 siblings (n = 3 of 24 fish per group).

### 4.4.6. miR-199 and WHIM mutants display different neutrophil profiles.

Confocal imaging of miR-199 zebrafish and WHIM zebrafish display vastly different numbers of neutrophils when compared to each other and Tg*(mpx:GFP)* controls (Figure 4.9A). A brief analysis of one slice from three individual zebrafish showed differences in B) neutrophils and C) the surface area of cells infected with eCFP-PR8.

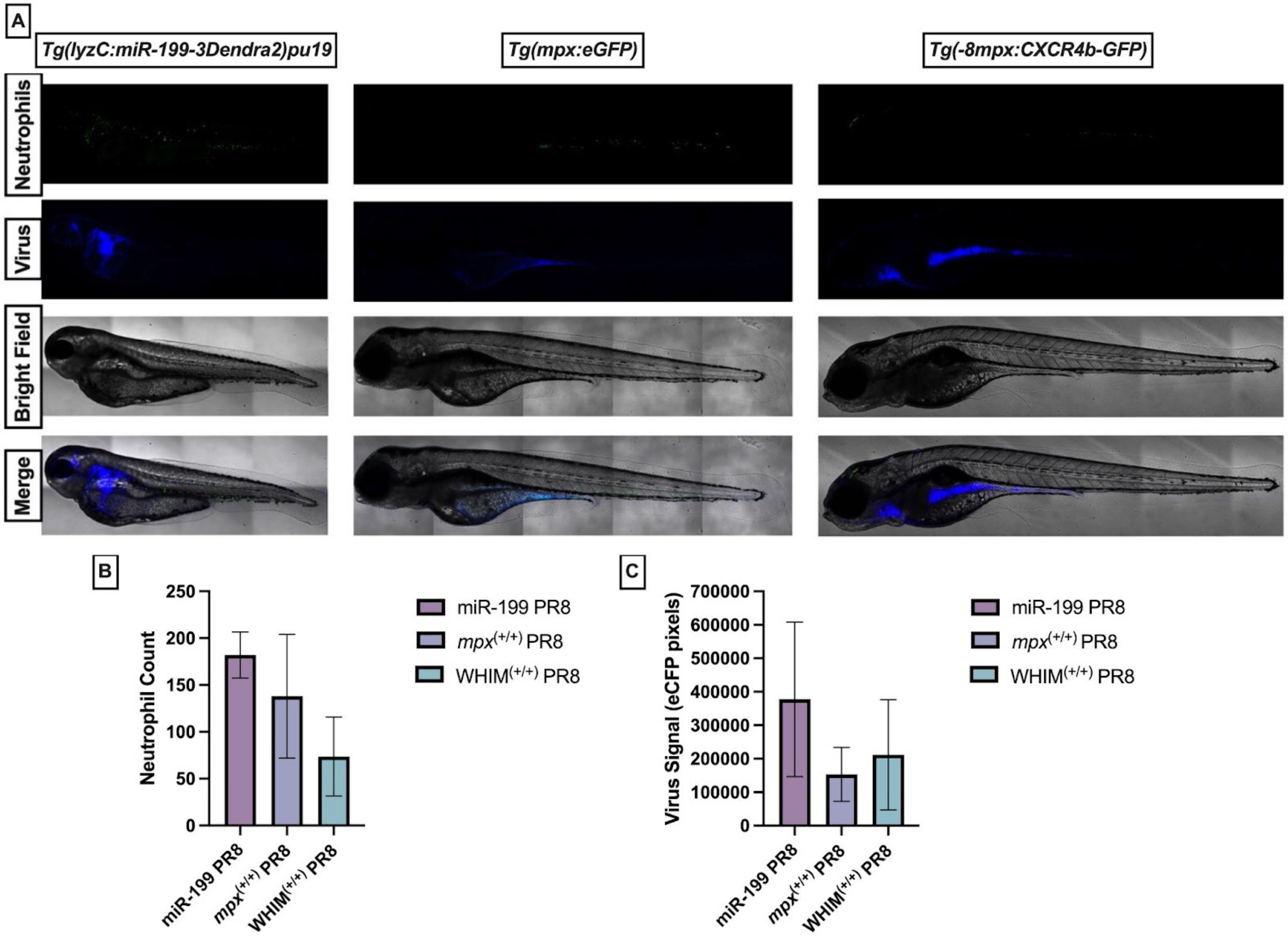
A
Tg(lyzC:miR-199-3Dendra2)pu19
Tg(mpx:eGFP)
Tg(-8mpx:CXCR4b-GFP)
Neutrophils
Virus
Bright Field
Merge
B
Neutrophil Count
250
200
150
100
50
0
miR-199 PR8
mpx(+/+) PR8
WHIM(+/+) PR8
miR-199 PR8
mpx(+/+) PR8
WHIM(+/+) PR8
C
Virus Signal (eCFP pixels)
700000
600000
500000
400000
300000
200000
100000
0
miR-199 PR8
mpx(+/+) PR8
WHIM(+/+) PR8
miR-199 PR8
mpx(+/+) PR8
WHIM(+/+) PR8

**Figure 4.10. miR-199 and WHIM mutants display different neutrophil profiles following infection by eCFP-PR8.** A) Confocal images of Tg(*lyz:dre-miR-199Dendra2*)left column, *Tg(mpx:GFP)* middle column, and WHIM mutants right column. Neutrophils are displayed in green, eCFP-PR8 in blue, and the bright field is in the gray channel. B) Analysis of neutrophils show a pattern of decreased neutrophils in the WHIM mutants compared to *mpx* controls and increased neutrophils in the Tg(*lyz:dre-miR-199Dendra2*) compared to *mpx* controls. C) B) Analysis of viral burden shows a slight increase in viral burden in the WHIM mutants and an increased viral burden in the Tg(*lyz:dre-miR-199Dendra2*) compared to *mpx* controls.

### 4.5. Discussion

Previous clinical studies have shown that neutrophils are the most abundant immune cell following IAV infection (Brandes, 2013). Although neutrophils have a crucial role in clearing influenza virus during infection (Tate, 2009), they also have a potential to cause lung tissue damage when actively invading the lung with other phagocytes (Brandes, 2013; Papayannopoulos, 2017). The precise cellular mechanisms that regulate neutrophil forward migration, activation and reverse migration are not fully understood. Understanding these regulatory mechanisms would help inform the development of therapies that could help patients combat IAV infection. For example, suppressing neutrophil activity in patients with severe infections may be beneficial. Furthermore, individuals with neutropenia are more susceptible to infection and increasing neutrophil activity may be beneficial.

We chose the zebrafish model for its optical clarity and reliance solely on an innate immune system. This reliance makes it a useful representation of vulnerable populations such as older adults with compromised adaptive immune systems, immune-compromised individuals, and younger individuals who have not yet developed a full adaptive immune response (Kulkarni, 2019;

Thompson, 2003). We used Cxcl8b morphants to establish a baseline of neutrophil alterations as previous work (Zuñiga-Traslaviña, 2017) established *cxcl8b* as a necessary gene for neutrophil trafficking response. Since miR-722 is not conserved in humans, we focused our studies on miR-199.

Our findings revealed that any modulation of neutrophil numbers, either genetically or pharmacologically, altered the innate immune response and resulted in increased mortality. Interestingly, we observed no significant differences in viral burdens between mutant neutrophil groups and control groups, suggesting that the mortality was likely due to impaired neutrophil functionality through either neutropenia, neutrophilia, or ablation. Survival was rescued in both mmiR-199 and WHIM mutants after treatment with ramilpril and MDIVI-1. Ramipril is a commonly prescribed medication classified as an angiotensin-converting enzyme (ACE) inhibitor, often used to treat hypertension (Chahaun, 2023). ACE has been linked to the body's natural immune response (Bernstein, 2018). Angiotensin II plays a role in triggering proinflammatory reactions, such as the generation of reactive oxygen species (ROS) by NADPH oxidase, as well as the activation of nuclear factor-κB (NF-κB) and activator protein 1 (AP1) (de Queiroz, 2013). Mitochondria play a considerable role in immune function, specifically in the regulation of inflammation (Nakahira, 2011). Research has demonstrated that infection with IAV can induce mitophagy, which in turn alters the activation of the inflammasome nucleotide oligomerization domain (NOD)-like receptor family pyrin domain-containing 3 (NLRP3) by producing excessive ROS (Lupfer, 2013; Wang, 2021; Zhou, 2010). Previous work by our lab showed it was effective at reducing pathogenesis of IAV infections (Soos, 2024). Extensive image quantification needs to be finalized before conclusive patterns can be identified.

Neutrophils play a critical role in pathogen clearing by producing extracellular traps, reactive oxidative species, enzymes (e.g., myeloperoxidase and elastase), and antimicrobial peptides (Mayadas, 2014). While detailed data was not presented, it is important to note that the miR-199 mutants exhibited increased reactive oxidative species production and displayed edema and severe tissue damage, potentially attributed to the high levels of neutrophils in these fish. Our study validates potential targets for antiviral treatment and opens the possibility of using similar targets for treating immune-compromised individuals.

## 4.6. Conclusion

In summary, our research highlights the critical role of neutrophils in combating IAV infections. Altering neutrophil counts has been shown to diminish the efficacy of the immune response necessary for clearing IAV infection. Mutants with either reduced or increased neutrophil levels did not exhibit a significant increase in viral load, yet experienced higher mortality rates compared to controls. WHIM mutants suffer from neutropenia, which reduces their ability to fight off infection. AT7519 pre-treatment removed enough neutrophils to simulate a brief duration of neutropenia and prevent hyperinflammation. However, they had slightly higher rates of mortality, although it was not significant like the WHIM mutants. miR-199 mutants suffered from neutrophilia and had too many neutrophils, subsequently causing tissue damage and increased mortality. Therefore, our findings suggest that manipulating neutrophil counts may not be favorable, prompting us to explore alternative strategies. Neutrophils serve various functions beyond pathogen defense, including the production of specialized reactive oxygen species (ROS) and NETosis. Moving forward, our focus will be on investigating ROS production, as NETosis is considered an extreme response to infections and is less common and sustained than ROS production.

# CHAPTER 5

# ROS MODULATION IMPROVES OUTCOME IN A ZEBRAFISH MODEL OF INFLUENZA A INFECTION

## 5.1 Abstract

Influenza virus infections can lead to significant respiratory illnesses, with estimates indicating that they result in between 9 million and 41 million cases annually in the United States. Our research endeavors to elucidate the mechanisms by which the innate immune system reacts to influenza virus infection, ultimately contributing to the advancement of novel therapeutic strategies. Zebrafish embryos provide an exceptional model for examining innate immunity in response to IAV infection, as their adaptive immune response is not fully developed until several weeks post-embryogenesis. While the functions of immune cells can be explored in vivo using fluorescent reporter lines, a notable limitation has been the challenge of visualizing the viral agent itself. To address this challenge, we have engineered innovative methodologies for studying IAV infection in zebrafish (Soos, 2024), employing four distinct fluorescent IAV strains, collectively referred to as Color-flu, which were originally developed for murine models by the Kawaoka laboratory. Through our Color-flu zebrafish infection model, we are able to monitor IAV infections and the subsequent innate immune responses in real time. While neutrophils are recognized for their critical roles in innate immunity against bacterial and fungal pathogens, their specific contributions to antiviral responses remain inadequately understood.

Zebrafish represent a valuable vertebrate model for investigating infection and innate immunity. Our current research is centered on exploring the functions of neutrophils in the regulation of IAV infection, as well as examining how their over-activation during infection may precipitate detrimental hyperinflammatory responses. Several studies have proposed that the

regulation of neutrophil populations could be a viable therapeutic approach. In our experimental evaluations, we observed that the survival rates of IAV-infected zebrafish, characterized by genetically or pharmacologically manipulated neutrophil levels, were significantly lower in comparison to control groups, underscoring the pivotal role of neutrophils in combating the virus. Additionally, we have leveraged this model to investigate the generation and release of ROS by neutrophils in response to infection. ROS have the capacity to directly degrade pathogens through oxidative mechanisms; however, dysregulation of ROS production may lead to tissue damage and mortality, attributed to hyperinflammation. We hypothesize that the modulation of neutrophil ROS production is governed by gene networks comprising both coding and noncoding genes. To explore this hypothesis, we are examined the influence of reducing ROS levels on survival rates, viral load, and neutrophil migration through the use of zebrafish mutants and pharmacological ROS inhibitors along with the Color-flu model. Overall, the Color-flu zebrafish model of IAV infection represents a robust and novel framework for visualizing the effects of genetic and pharmacological interventions on influenza virus infections.

## 5.2 Introduction

Influenza virus infections significantly impact public health globally, causing considerable illness, mortality, and **societal** consequences. In the United States, seasonal flu is linked to an estimated 95,000-172,000 hospitalizations and 21,000-41,000 deaths, resulting in substantial healthcare costs annually (CDC, 2024). Influenza A virus infections begin in the respiratory tract's epithelial cells and have the potential to spread throughout the body, leading to organ failure and death (Tate, 2008). The body's innate antiviral immune response is activated upon infection, recruiting additional neutrophils (Oslund, 2011). While the presence of neutrophils is essential in clearing the virus, it can trigger an aggressive inflammatory response, causing disruptions in interferon expression and the production of ROS (Nguyen, 2017; Tate, 2008 Tumpey, 2005).

ROS plays a critical role in numerous essential physiological functions at controlled levels. They contribute to various signaling pathways that respond to growth factor activation and regulate inflammatory reactions. The main sources of ROS production during viral infections are mitochondria and neutrophils (D'Autreaux, 2007). Mitochondrial ROS is largely produced due to oxidative phosphorylation, a necessary biological process for energy conversion (Brieger, 2012). However, mitochondria have innate immune activity partly due to the interactions with inflammasomes and autophagy. The production of mitochondrial reactive oxygen species (mROS) takes place through the electron transport chain (ETC) in response to changes in substrate availability, hypoxia, or other irregular mitochondrial or cellular conditions (Balaban, 2005). The leakage of electrons from the ETC at complex I-III combines with oxygen to create superoxide radicals (Kroller-Schon, 2014). It was previously believed that these reactive molecules enhance the immune system by targeting intracellular pathogens, but it is now understood that their role in the immune response is much broader (Banoth, 2018). mROS can directly and indirectly alter innate cellular responses (Brieger, 2012). Recent studies have revealed that mROS can directly impact cellular functions by influencing key transcription factors such as HIF-1α (hypoxia-inducible factor-1α) and NF-κB (Banoth, 2018). By eliminating damaged mitochondria that produce mROS through mitophagy, levels of mROS decrease, and innate immune responses diminish. Conversely, inhibiting mitophagy leads to heightened inflammation (Lupfer, 2013).

The other larger ROS producer NADPH oxidase, specifically, NADPH oxidase 2 is found on neutrophils. NADPH oxidases (NOX) are proteins located on cell membranes that facilitate the transfer of electrons across membranes, leading to the generation of superoxide when oxygen acts as the final electron acceptor (Tlili, 2011). These enzymes are involved in a wide range of cellular processes, such as differentiation, growth, proliferation, programmed cell death, cytoskeletal organization, cell movement, and muscle contractions (Paclet, 2022). The cellular components of the flavocytochrome b 558 include the gp91phox (Nox2) and p22phox subunits (Vermot, 2012). In inactive cells, the cytosolic components consist of p47phox, p40phox, and p67phox subunits that form a complex (Vermot, 2012). Upon the initiation of phagocytosis, the NADPH oxidase becomes active and generates superoxide anions ($O_2^-$) within the phagosome shortly after its formation (Paclet, 2022). The superoxide anions dismutate within the phagosome into hydrogen peroxide ($H_2O_2$) (Winterbourn, 2016). In neutrophils, myeloperoxidase (MPX) released from granules catalyzes the production of hypochlorous acid (HOCl) from chloride ions and $H_2O_2$ (Winterbourn, 2016). Significant amounts of $O_2^-$ are generated within the phagosome (Paclet, 2022). The specific chemical reactions and toxic effects of these reactive oxygen species within the unique environment of the phagosome have not been fully elucidated (Winterbourn, 2016).

The connection between viral infections and neutrophils remains primarily ambiguous in the scientific community. ROS produced by cells infected with viruses may trigger neutrophil chemotaxis towards infected areas during an IAV infection (Mugoni, 2014). By attracting neutrophils to sites of viral-induced tissue damage through the creation of gradients of $H_2O_2$, these neutrophils can then be retained at the location due to the inhibitory effects of high ROS levels on cell movement (Vangeti, 2018). ROS plays pivotal roles in the innate immune response, functioning both as indicators of immune dysregulation and as mediators of various immune processes (Brieger, 2012). Nonetheless, the connections between the factors involved in ROS production, such as NADPH oxidase and myeloperoxidase, and the mechanisms through which signaling suppresses neutrophil chemotaxis remain unknown, with the specific roles of ROS in viral infections even less specified (Mugoni, 2014; Nguyen, 2017; Tate, 2008; To, 2017; Tumpey, 2005; Warnatsch, 2017).

We have recently developed a groundbreaking zebrafish model for studying IAV infection (Soos, 2024). Zebrafish are an excellent choice for this type of research due to their rapid reproduction, genetic manipulability, and the presence of an innate immune system within 24-48 hours post fertilization (hpf). Our infection model has shown promising results, with a significant decrease in survivability (43% - 52%) compared to control groups in multiple IAV lots under the same experimental conditions. We have successfully demonstrated live infection using Color-flu (Fukiyama, 2015) in this model (Soos, 2024). Furthermore, zebrafish are an ideal model for studying innate immune function as they have not yet differentiated into male or female genders within the first 12 days post-fertilization (dpf) allowing for a non-gender biased approach to our studies (Yoo, 2011). Despite some differences, zebrafish share 85% gene synteny with the human genome, particularly in the orthologous functioning of the innate immune system (Howe, 2013). This model provides researchers with a unique opportunity to visually assess the innate immune response to influenza infection and examine the genetic factors involved.

## 5.3. Materials and Methods

### 5.3.1. Zebrafish care and maintenance

The zebrafish utilized in this research were responsibly housed and maintained as described in 4.3.1. under Protocol Number A2021-02-02. The zebrafish were accommodated in recirculating tanks following the standard procedures of a 14-hour light, 10-hour dark cycle at a temperature of 28 °C. The zebrafish lines used in this study were AB, Spotless (*mpx*$^{NL144}$) (Buchan, 2019), *Tg (actb2:HyPer3)* (Bilans, 2013; Niethammer, 2009), and MitoROS (*ROS: GFP + HM x AB)*. The *Tg (actb2:HyPer3)* line was created by injecting AB wild-type zebrafish lines using the Tol2 system (Kawakami, 2007) at the high one-cell stage. Embryos were obtained and kept as described in 4.3.1.

### 5.3.2. MDCK/ London cell culture

Cells were grown and passaged as discussed in Chapter 4.3.2.

### 5.3.3. Influenza virus

PR8 (A/PR/8/34 H1N1) and Color-flu (Fukuyama, 2015) IAV virus strains MA-mVenus-PR8 (mVenus-PR8), MA-eCFP-PR8 (eCFP-PR8), MA-eGFP-PR8 (eGFP-PR8), and MA-mCherry-PR8 (mCherry-PR8) were prepared as described in Chapter 3.3.3.

### 5.3.4. Microinjection

Microinjections were performed as described in (Soos, 2024).

### 5.3.5. Drug exposures

For all of our small molecule drug studies, larvae were exposed to either dimethyl sulfoxide (DMSO), DMSO-solubilized GSK279539 (NOX2), DMSO-solubilized N-acetyl cysteine (NAC), or DMSO-solubilized Urolithin A (UA) by adding these solutions into the embryo water at 24 hpi. The larvae were exposed to DMSO, NAC, NOX2, or UA for one hour at 33 °C in a dark incubator. After exposure, zebrafish were rinsed twice and transferred to 50 mL of fresh embryo to remove the traces of the DMSO or DMSO-solubilized drugs. The final concentrations used were 25 nM for NAC (Dowling, 2012; Formella, 2018; Liu, 2015; Wu, 2020), 5 nM for NOX2, and 20 nM for UA.

### 5.3.6. Survival studies

Survival studies were performed as described in Soos, et. al 2024.

### 5.3.7. Viral burden assays

Tissue culture infectious dose 50 ($TCID_{50}$) end-point dilution assays were performed as described in 4.3.7.

### 5.3.8. Respiratory burst assays

Respiratory burst assays were performed as described in Soos, et. al 2024.

### 5.3.9. Reactive oxygen species staining

ROS was stained using different stains and protocols. CellROX Orange (probe for hydrogen peroxide [$H_2O_2$]) and MitoSOX (probe for superoxide [$O_2^-$]) were stained as described in Rissone and Condotti (Rissone, 2016), with the exception that CellROX was increased to 5 μM, MitoSOX was increased to 10 μM, CellROX samples were also incubated in Hank's balanced salt solution supplemented with calcium and magnesium (HBSS/Ca/Mg), and samples were stained in 250 μL of HBSS/Ca/Mg at 33 °C in a dark incubator. Daf2da (diaminofluorescein probe for nitric oxide [NO]) samples were stained as previously described (Lepiller, 2007) for 2 hours at 33 °C in a dark incubator. DHE (dihydroethidium probe for $O_2^-$) samples were stained as previously described (Morash, 2011), except the zebrafish were placed in 1 mL HBSS/Ca/Mg at 33 °C in a dark incubator.

### 5.3.10. Confocal imaging

Zebrafish were imaged as described in Soos, et. al 2024.

### 5.3.11. Statistical analysis

GraphPad Prism 10.2.3 (GraphPad Software, Boston, MA, USA) was used to generate and analyze survival curves and graphs. Analysis was performed as described in Soos, et. al 2024.

## 5.4 Results

### 5.4.1. Spotless mutants exhibit improved survival, reduced viral burden, and altered ROS profiles compared to wild-type controls.

The survival assay between Spotless *(mpx*$^{NL144}$*)* zebrafish and AB wild-type controls showed an increase in survival of 8.5%, from a survival rate of 54.5% to 63% (Figure 5.1A). The survival assay between Spotless *(mpx*$^{NL144}$*)* zebrafish and Spotless heterozygotes *(mpx*$^{+/NL144}$*)* indicated an increase in survival of 19.5%, from a survival rate of 63% to 43.5% (Figure 5.1B). The survival assay between Spotless heterozygotes *(mpx*$^{+/NL144}$*)* zebrafish and AB wild-type controls revealed a decrease in survival of 11%, from a survival rate of 54.5% to 43.5% (Figure 5.1C). ROS-reducing drugs ramipril and the NOX2 inhibitor (GSK279539) were used to treat Spotless zebrafish. Interestingly, despite a lack of significance, there was a slight increase (2.3%) in the survival of Spotless zebrafish after treatment with the NOX2 inhibitor (Figure 5.2A). Conversely, Figure 5.2B depicts a very different scenario. Ramipril increases mortality by 27%. The survival of the Spotless zebrafish is more understandable when the viral burden between Spotless and AB wild types is compared. At the start, there is no significant difference in viral injection between the groups, but by 24-72 hours, there is a large difference, with 24 and 48 hours showing statistically significant differences (Figure 5.3A). Even the respiratory burst at 24 hpi, demonstrated reduced neutrophil function in Spotless mutants injected with HBSS and PR8 compared to wild-type. The Spotless HBSS and PR8 groups had lower activation than Bis I treated controls, Figure 5.3B. CellROX Orange stain for hydrogen peroxide showed different profiles between Spotless and control infected PR8 zebrafish.

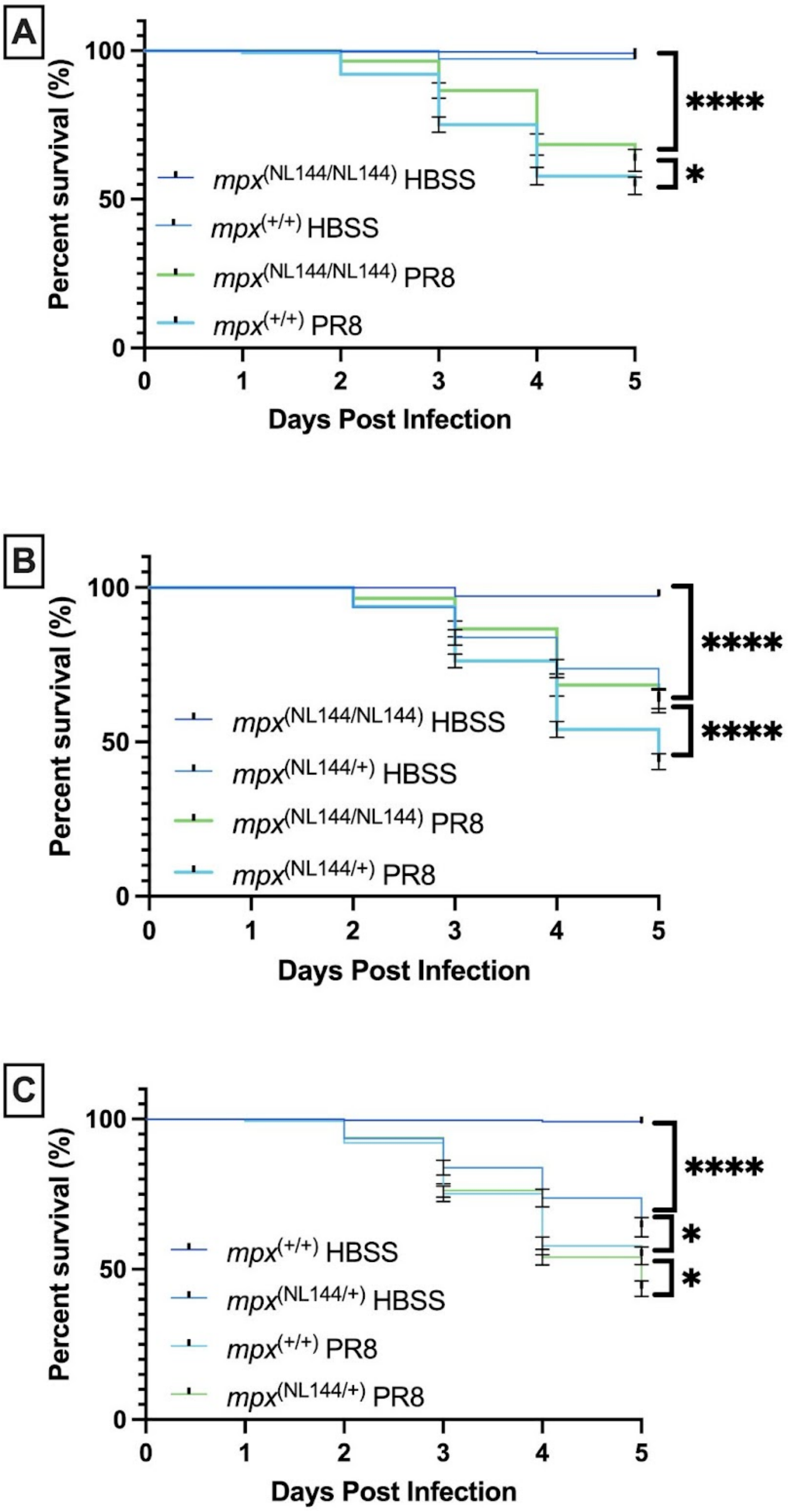
A
Percent survival (%)
100
50
0
Days Post Infection
0
1
2
3
4
5
$mpx^{(NL144/NL144)}$ HBSS
$mpx^{(+/+)}$ HBSS
$mpx^{(NL144/NL144)}$ PR8
$mpx^{(+/+)}$ PR8
****
*
B
Percent survival (%)
100
50
0
Days Post Infection
0
1
2
3
4
5
$mpx^{(NL144/NL144)}$ HBSS
$mpx^{(NL144/+)}$ HBSS
$mpx^{(NL144/NL144)}$ PR8
$mpx^{(NL144/+)}$ PR8
****
****
C
Percent survival (%)
100
50
0
Days Post Infection
0
1
2
3
4
5
$mpx^{(+/+)}$ HBSS
$mpx^{(NL144/+)}$ HBSS
$mpx^{(+/+)}$ PR8
$mpx^{(NL144/+)}$ PR8
****
*
*

**Figure 5.1. Survival rates of Spotless $(mpx^{NL144/NL144})$ zebrafish compared to Spotless heterozygotes and AB wild-type controls.** A) Decreased survival of AB wild-type zebrafish systemically infected with PR8 IAV at 2 dpf compared to Spotless $(mpx^{NL144})$ zebrafish. PR8-infected groups also survived worse when compared to vehicle (HBSS) controls. Survival of the Spotless $(mpx^{NL144})$ zebrafish increased by 9.5% when compared to controls (*$p$ = 0.0314, ****$p$ = > 0.0001). B) Decreased survival of Spotless heterozygote zebrafish systemically infected with PR8 IAV at 2 dpf compared to Spotless $(mpx^{NL144})$ zebrafish, 43.5% to 63%. PR8-infected groups also survived worse when compared to Spotless $(mpx^{NL144})$ zebrafish HBSS controls, 63% to 97%. However, heterozygotes HBSS controls only fared slightly better than PR8-infected Spotless $(mpx^{NL144})$ zebrafish, 64% to 63% (****$p$ = > 0.0001). C) Increased survival of AB wild-type zebrafish systemically infected with PR8 IAV at 2 dpf compared to Spotless heterozygote zebrafish, 54.5% to 43.5%. PR8-infected groups also survived worse when compared to HBSS controls. Survival of Spotless heterozygote HBSS controls survived slightly better than PR8-infected AB zebrafish, 64% to 54.5% (*$p$ = >0.0178, ****$p$ = > 0.0001). For each graph, n = 4 with 45 zebrafish per group.

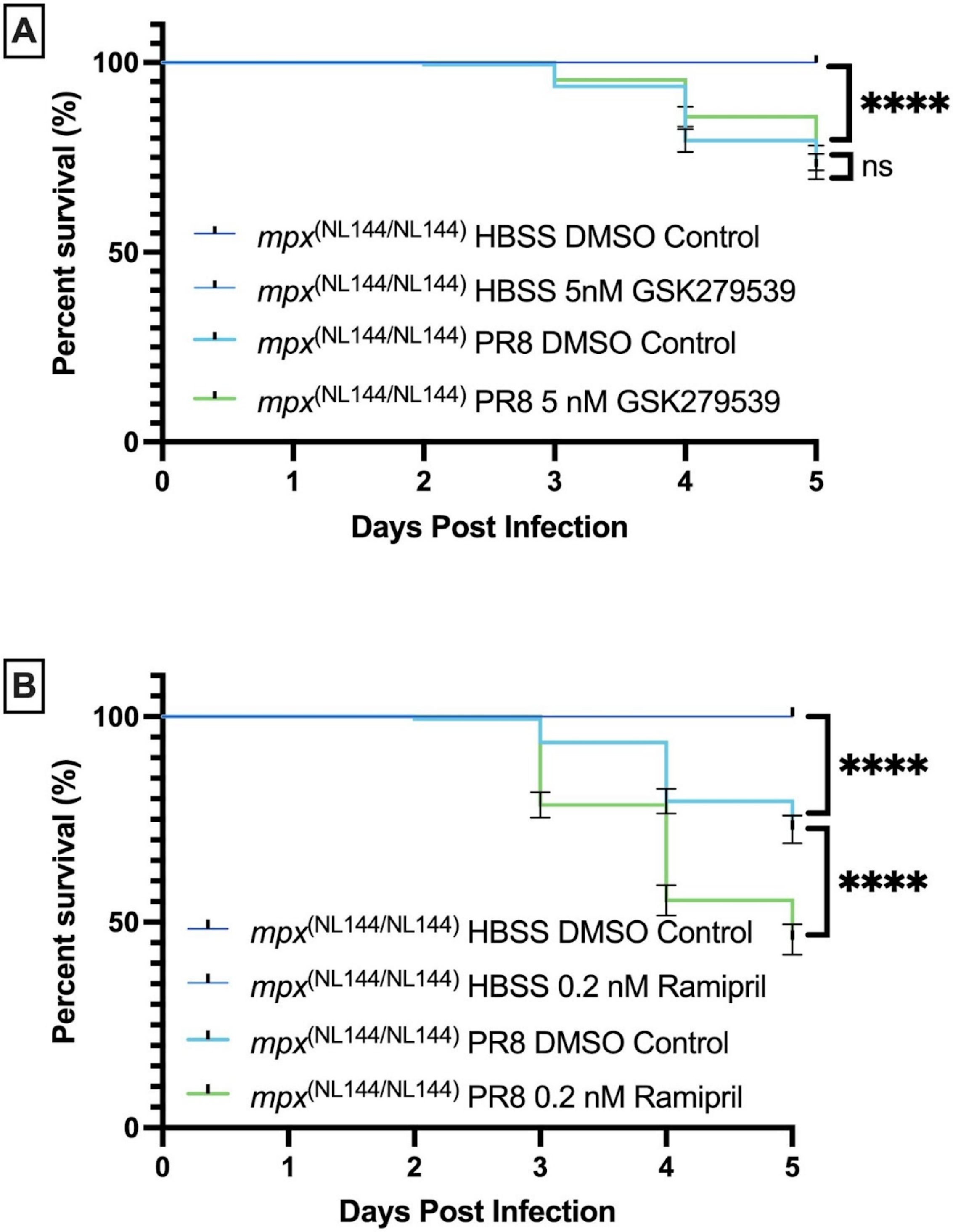

**Figure 5.2. Survival rates of Spotless *(mpx$^{NL144?NL144}$)* zebrafish treated with ROS inhibitors.** A) A negligible improvement in survival is displayed after treatment with NOX2 inhibitor at 24 hpi.

72.6% for DMSO controls compared to 74.9% NOX2 treated Spotless *(mpx*$^{NL144}$*)* zebrafish injected at 2 dpf. HBSS controls survived at 100% (*****p* = >0.0001). B) DMSO Spotless *(mpx*$^{NL144}$*)* zebrafish survived significantly better than ramipril Spotless *(mpx*$^{NL144}$*)* zebrafish infected at 2dpf, 72.6% compared to 45.8%. There was no significant difference in treatment conditions in the HBSS control groups (*****p* = >0.0001). For each graph, n = 4 with 40 zebrafish per group.

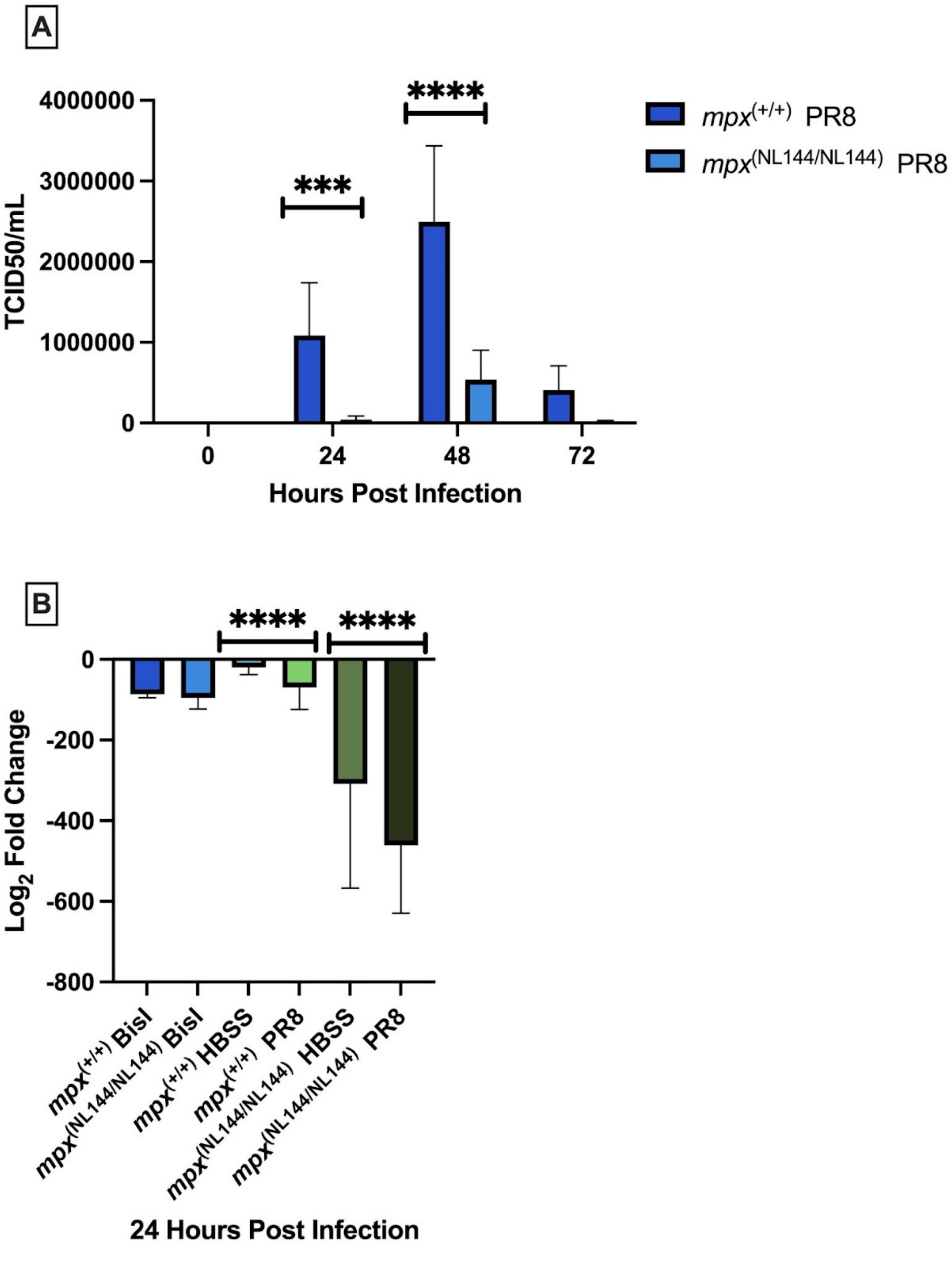
A
4000000
3000000
2000000
1000000
0
TCID50/mL
***
****
0
24
48
72
Hours Post Infection
mpx(+/+) PR8
mpx(NL144/NL144) PR8
B
0
-200
-400
-600
-800
Log2 Fold Change
****
****
mpx(+/+) Bisl
mpx(NL144/NL144) Bisl
mpx(+/+) HBSS
mpx(+/+) PR8
mpx(NL144/NL144) HBSS
mpx(NL144/NL144) PR8
24 Hours Post Infection

**Figure 5.3. Spotless $(mpx^{NL144})$ zebrafish reveal decreased viral burden and neutrophil respiratory fitness.** A) There was a significant change in TCID$_{50}$ viral titer between Spotless $(mpx^{NL144})$ and AB zebrafish. At time point zero, there is no significant difference between initial injection amounts between the two groups. At 24 and 48 hpi, there are significant decreases in viral burden for Spotless $(mpx^{NL144})$ zebrafish compared to AB zebrafish. There is still a noticeable decrease at 72 hpi, but it is not significant. n= 3 of 3 replicates with 25 fish per group (***$p$ = 0.0001, ****$p$ = >0.0001). B) There was a significant difference between Spotless $(mpx^{NL144})$ zebrafish compared to AB zebrafish, with HBSS and PR8 injected Spotless $(mpx^{NL144})$ mutants having a lower respiratory burst response than even the Bis I inhibited zebrafish. (****$p$ = >0.0001) n = 3 of 24 fish per group.

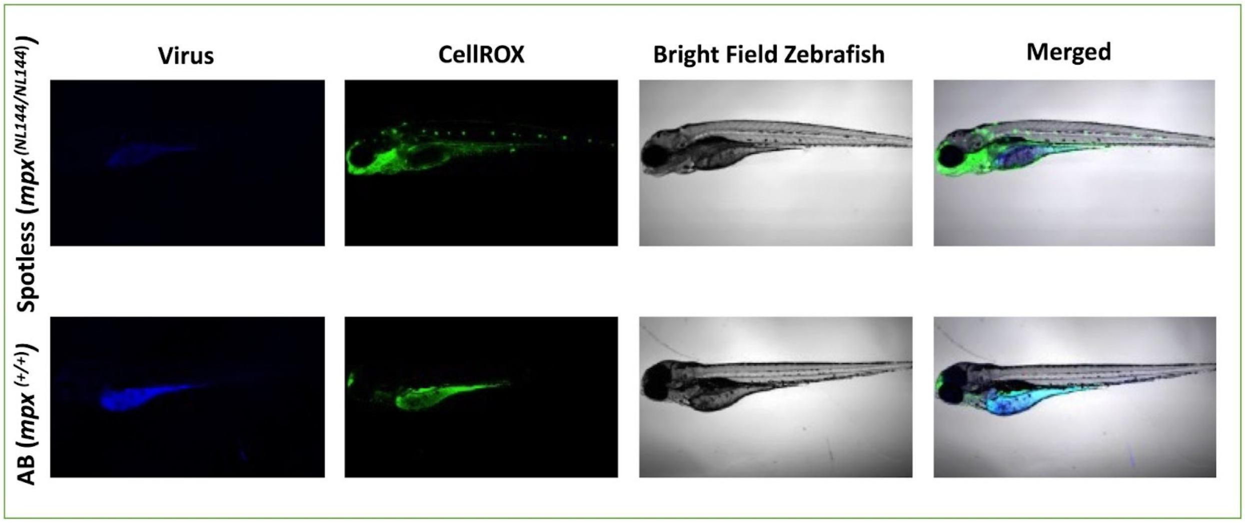

**Figure 5.4. Spotless $(mpx^{NL144})$ alters the profile of ROS species.** Confocal images of spotless $(mpx^{NL144})$ mutants compared to AB wild-type mutants. n = 4, after 12 zebrafish screened for CellROX. Images were taken at 18 hpi and show a distinct difference in growth, viral burden, and ROS profiles.

### 5.4.2. Diverse ROS inhibitors alter IAV infection response and rescue IAV infection.

The survival assay between the various ROS inhibitors all show an increase in survival compared to control-treated zebrafish. The broadscale ROS inhibitor NAC improved survival by 21.7% when compared to DMSO-treated zebrafish (Figure 5.5A). The NOX2 inhibitor (GSK279539), improved survival by 32.4%. The mitophagy activator UA, which inhibits mitochondrial ROS, improved survival by 27.7% when compared to DMSO-treated zebrafish (Figure 5.5C). Interestingly, despite the small molecules all inhibiting various types of ROS, the most effective at rescuing mortality after IAV infection was the NOX2 inhibitor (Figure 5.5D). Contrarily, Figure 5.6 illustrates how difficult ROS modulation can be. The incorrect doses of NAC can have no effect (20 nM, Figure 5.6A) or induce toxicity (30 nM, Figure 5.6B). The data indicate that NOX2 exhibits greater toxicity compared to NAC or UA, presenting an exceptionally narrow margin of safety. Specifically, treatment with 4 nM of GSK279539 demonstrated no observable effect (refer to Figure 5.6C), whereas an increase to 6 nM resulted in heightened mortality rates (see Figure 5.6D). Furthermore, as illustrated in Figure 5.6E, exposure to 25 nM of UA did not yield significant outcomes, while a concentration of 30 nM was associated with a slight improvement in survival rates (as shown in Figure 5.6F). Notably, concentrations of 40, 45, and 50 nM of UA were found to induce toxicity in IAV-infected zebrafish, with the 40 nM concentration exhibiting a mortality rate comparable to that of zebrafish treated with DMSO. Additionally, the 45 nM and 50 nM concentrations resulted in even greater mortality rates (data not provided). The application of all ROS inhibitors resulted in a notable decrease in viral burden when compared to the control-infected AB zebrafish. Specifically, NAC demonstrated a statistically significant reduction in viral levels as early as the 24-hour mark, shortly following the initiation of treatment (Figure 5.7A). Similarly, the NOX2 inhibitor also indicated decreased viral burden levels beginning at the 24-hour interval (Figure 5.7B); however, the results were not as statistically significant as those observed with NAC. The UA compound exhibited a significant reduction solely at the 48-hour time point (Figure 5.7C). It is important to note that there were no significant changes observed in neutrophil respiratory burst response as a result of treatment with the ROS inhibitors (Figure 5.8). Even the profile of how the ROS responses change via CellROX imaging is different with the NAC showing the highest levels of $H_2O_2$ and DMSO having the highest viral burden (Figure 5.9).

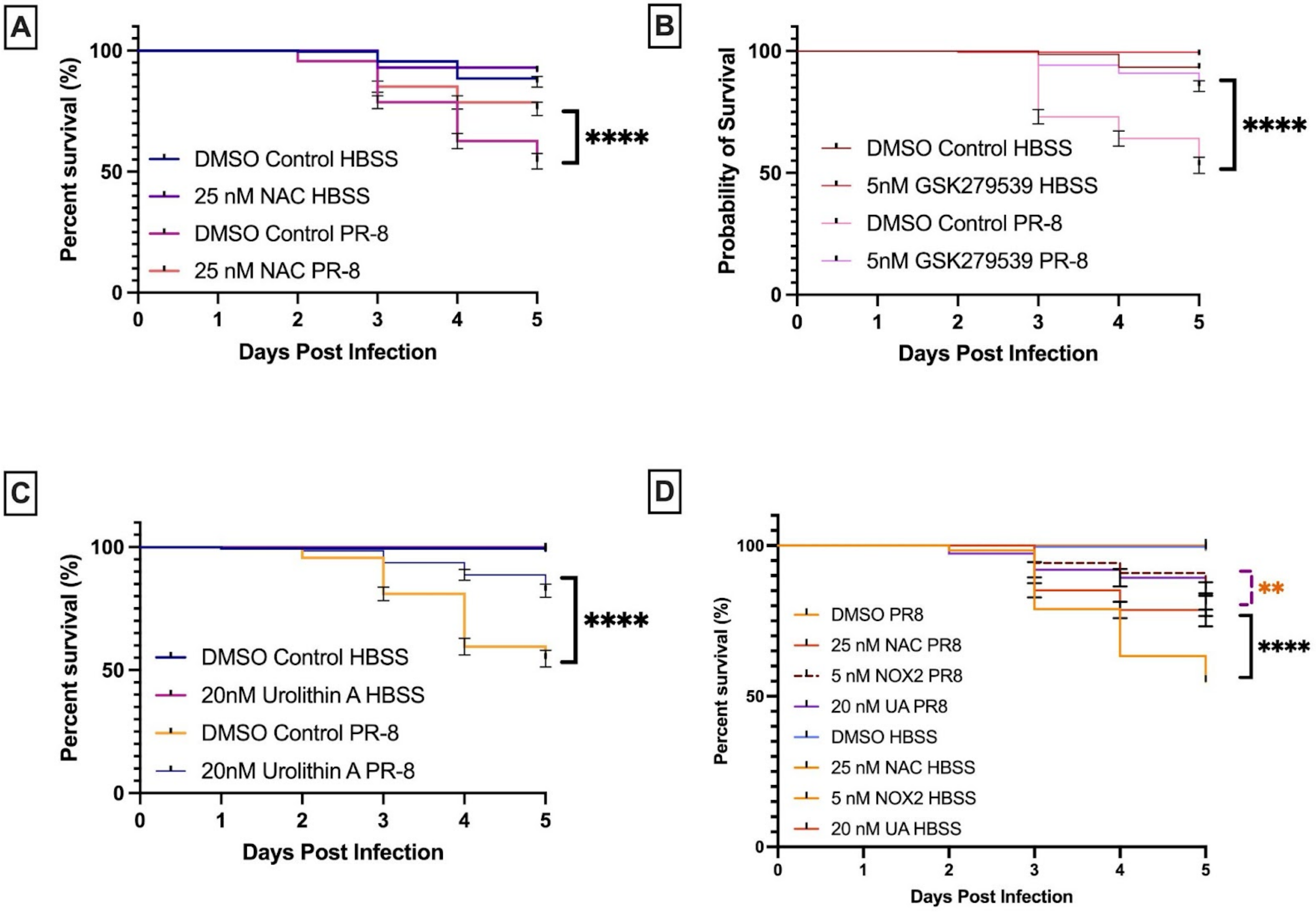
A
Percent survival (%)
100
50
0
DMSO Control HBSS
25 nM NAC HBSS
DMSO Control PR-8
25 nM NAC PR-8
****
0
1
2
3
4
5
Days Post Infection
B
Probability of Survival
100
50
0
DMSO Control HBSS
5nM GSK279539 HBSS
DMSO Control PR-8
5nM GSK279539 PR-8
****
0
1
2
3
4
5
Days Post Infection
C
Percent survival (%)
100
50
0
DMSO Control HBSS
20nM Urolithin A HBSS
DMSO Control PR-8
20nM Urolithin A PR-8
****
0
1
2
3
4
5
Days Post Infection
D
Percent survival (%)
100
50
0
DMSO PR8
25 nM NAC PR8
5 nM NOX2 PR8
20 nM UA PR8
DMSO HBSS
25 nM NAC HBSS
5 nM NOX2 HBSS
20 nM UA HBSS
**
****
0
1
2
3
4
5
Days Post Infection

**Figure 5.5. Survival rates of AB zebrafish treated with various ROS inhibitors.** A) After treatment with NAC, improvement in survival is shown. 54.3% for DMSO controls compared to 76% NAC treated zebrafish injected at 2 dpf. HBSS controls survived better, with a gain of 4.4% survival compared to DMSO-treated HBSS zebrafish. (*****p* = >0.0001). B) After treatment with NOX2, a decline in mortality is shown. 53.1% for DMSO controls compared to 85.5% NOX2-treated zebrafish injected with PR8 at 2 dpf. NOX2-treated HBSS controls survived better, with a gain of 5.5% survival compared to DMSO-treated HBSS zebrafish. (*****p* = >0.0001). C) UA treatment improves survival in 2 dpf PR8 IAV-infected zebrafish. 54.6% for DMSO controls compared to 82.2% for UA-treated zebrafish. UA-treated HBSS controls survived better, with a gain of 1% survival compared to DMSO-treated HBSS zebrafish. D) Compares the different types of ROS inhibitors. There was a considerable difference between DMSO-treated zebrafish and the least effective ROS inhibitor, NAC 54.8% for DMSO controls and 76% for NAC-treated zebrafish. There was not a significant difference between NAC and UA, 76% to 80%. Between UA and NOX2, there was also no discernible distinction, with 80% to 85.5%. However, there was a detectable difference between NAC and NOX2, with NOX2 improving survival by 9.5% compared to NAC. (***p* = 0.0060, *****p* = > 0.0001). For each graph, n= 4 of 60 fish per group.

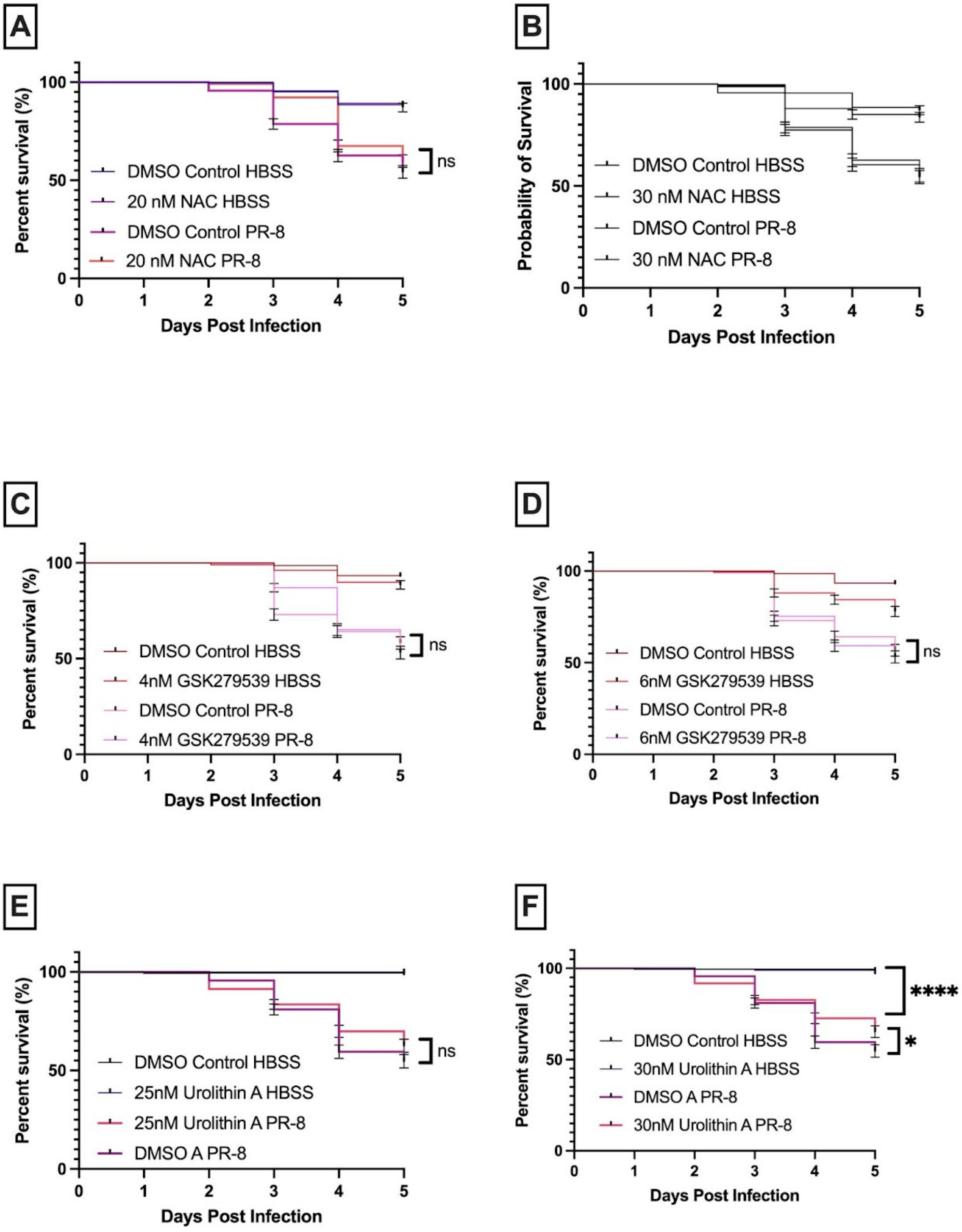
A
Percent survival (%)
Days Post Infection
DMSO Control HBSS
20 nM NAC HBSS
DMSO Control PR-8
20 nM NAC PR-8
ns
B
Probability of Survival
Days Post Infection
DMSO Control HBSS
30 nM NAC HBSS
DMSO Control PR-8
30 nM NAC PR-8
C
Percent survival (%)
Days Post Infection
DMSO Control HBSS
4nM GSK279539 HBSS
DMSO Control PR-8
4nM GSK279539 PR-8
ns
D
Percent survival (%)
Days Post Infection
DMSO Control HBSS
6nM GSK279539 HBSS
DMSO Control PR-8
6nM GSK279539 PR-8
ns
E
Percent survival (%)
Days Post Infection
DMSO Control HBSS
25nM Urolithin A HBSS
25nM Urolithin A PR-8
DMSO A PR-8
ns
F
Percent survival (%)
Days Post Infection
DMSO Control HBSS
30nM Urolithin A HBSS
DMSO A PR-8
30nM Urolithin A PR-8
****
*
0
50
100
0
1
2
3
4
5

**Figure 5.6. Survival rates of AB zebrafish treated with unsuccessful concentrations of the various ROS inhibitors.** A) 20 nM NAC, displayed no special improvement in survival. 54.3% for DMSO controls compared to 59.8% NAC-treated zebrafish injected at 2 dpf. B) 30 nM NAC appears to induce toxicity due to a precipitous decrease in survival compared to 25 nM NAC. 54.3% for DMSO controls compared to 55.2% for NAC-treated zebrafish. C) 4 nM NOX2, displayed no striking improvement in survival. 53.1% for DMSO controls compared to 58.2% NOX2-treated zebrafish injected at 2 dpf. D) 6 nM NAC appears to induce toxicity due to a precipitous decrease in survival compared to 5 nM NOX2. 53.1% for DMSO controls compared to 56.8% for NOX2-treated zebrafish. E) 25 nM UA, displayed no special improvement in survival. 54.6% for DMSO controls compared to 62.6% UA-treated zebrafish injected at 2 dpf. F) 30 nM UA appears to slightly increase survival compared to DMSO controls. 54.6% for DMSO controls compared to 65.3% for NAC-treated zebrafish. (*$p = 0.0401$). For each graph, n= 4 of 60 fish per group.

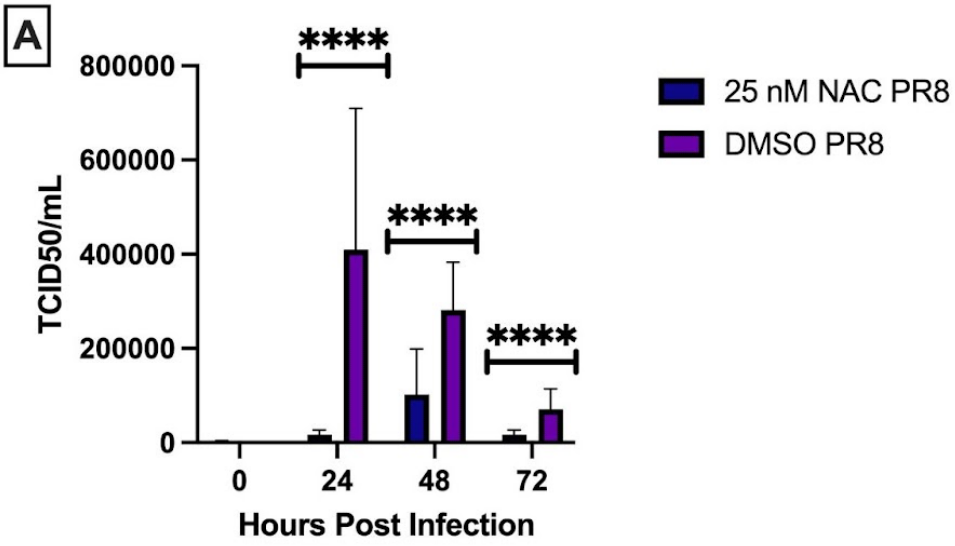
A
25 nM NAC PR8
DMSO PR8
TCID50/mL
800000
600000
400000
200000
0
****
****
****
0
24
48
72
Hours Post Infection

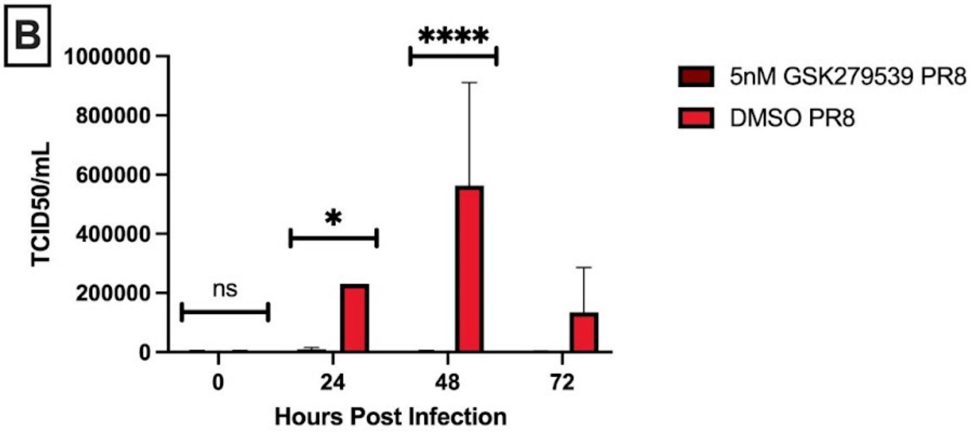
B
5nM GSK279539 PR8
DMSO PR8
TCID50/mL
1000000
800000
600000
400000
200000
0
ns
*
****
0
24
48
72
Hours Post Infection

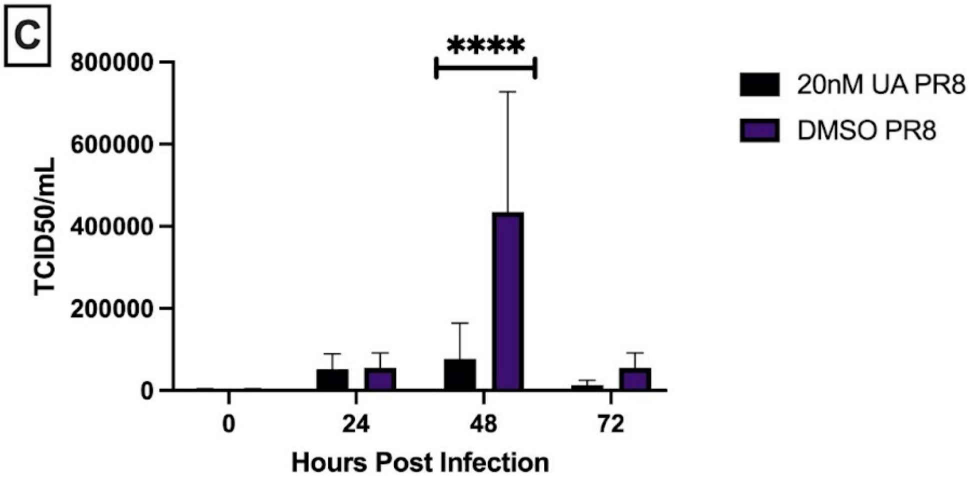
C
20nM UA PR8
DMSO PR8
TCID50/mL
800000
600000
400000
200000
0
****
0
24
48
72
Hours Post Infection

**Figure 5.7. The viral burden of ROS inhibitor treatments compared to DMSO controls.** There was a significant change in all of the ROS-inhibited samples of $TCID_{50}$ viral titers compared to DMSO controls. A) NAC showed a significant reduction in viral burden starting at the 24-hour time point until the 72-hour time point. B) The NOX2 inhibitor also produced reduced viral burden levels starting at the 24-hour time point. However, only the 24 and 48-hour time points are statistically relevant. C) UA shows a significant reduction at the 48-hour time point. n= 3 of 3 replicates with 25 fish per replicate. (**p* = > 0.0192, *****p* = >0.0001).

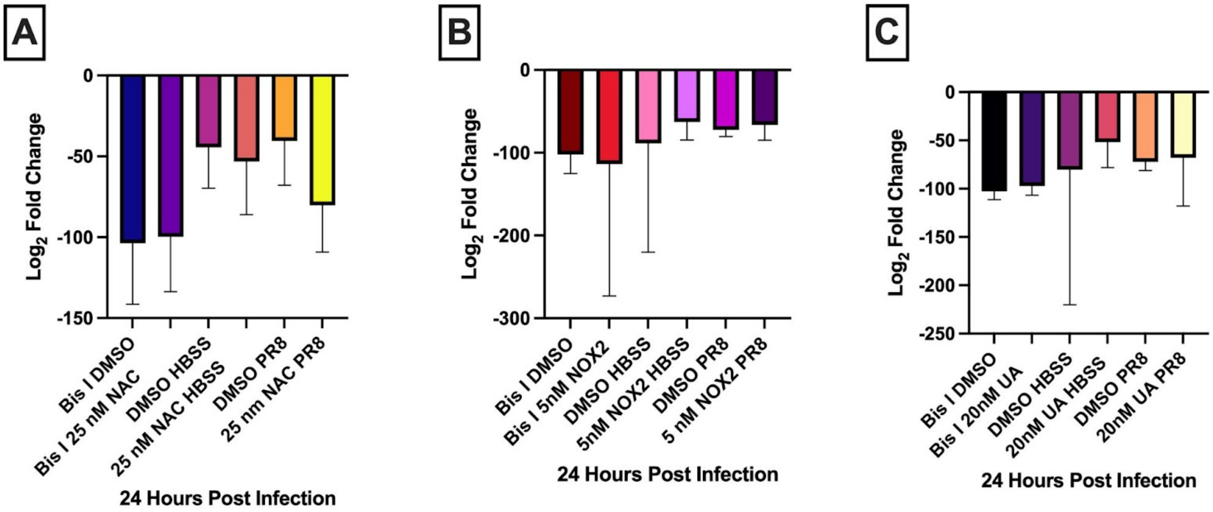

**Figure 5.8. Respiratory burst assay of ROS inhibitor treatments compared to DMSO control zebrafish.** There was no significant difference in the neutrophil respiratory burst response immediately after treatment with NAC, NOX2, or UA. n = 3 of 24 fish per group.

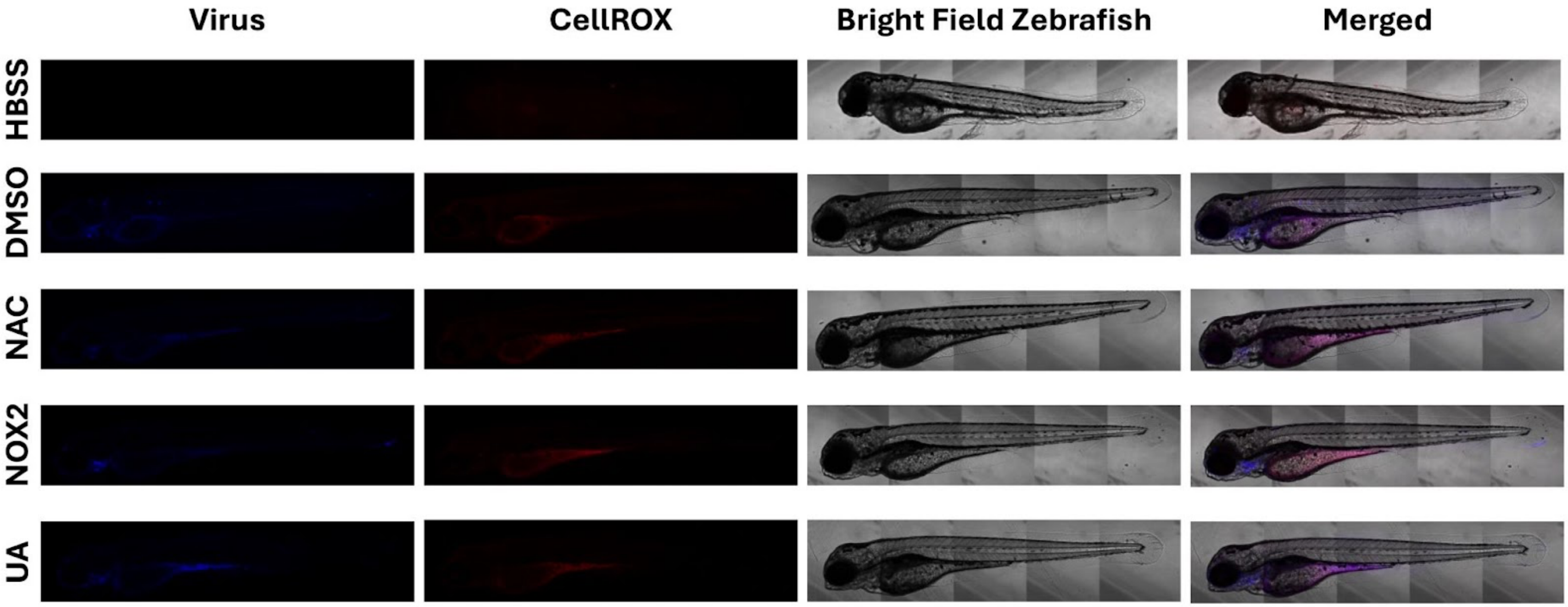
Virus
CellROX
Bright Field Zebrafish
Merged
HBSS
DMSO
NAC
NOX2
UA

**Figure 5.9. CellROX profiles of ROS therapeutic targets.** Confocal images of AB wild-type mutants after small molecule inhibitor treatment and CellROX Orange staining. Representative images of the 4 zebrafish screened for CellROX. Images were taken at ~24 hpi and show a distinct difference in growth, viral burden, and CellROX profiles.

## 5.4. Discussion

To date, extensive research has been conducted on neutrophils in the context of influenza, COVID-19, and RSV-associated bronchiolitis. Neutrophils contribute to antiviral defense through phagocytosis and NETosis and play a detrimental role in tissue and organ damage in certain viral infections. However, the precise mechanisms by which neutrophils operate in antiviral immunity remain unclear. This lack of understanding hinders the ability to effectively implement clinical interventions to modulate the body's antiviral immune response. Neutrophils, the most abundant type of white blood cell, have been implicated in both infectious and noninfectious diseases. A comprehensive investigation of neutrophil populations and how they respond to IAV infection could enhance viral disease treatments and advance knowledge in other disease areas.

Striking a delicate balance between ROS generation and detoxification by the host during IAV infection necessitates further investigation. Insights gained from studying IAV may pave the way for exploring oxidative stress modulation in other viral infections and autoimmune conditions. Once these mechanisms are elucidated, they could offer new perspectives on viral pathogenesis and the development of innovative therapeutics. ROS, which consists of various substances such as superoxide, hydrogen peroxide, and singlet oxygen, impacts numerous cellular functions, including immunity. Endogenous sources of ROS include NADPH oxidases, the mitochondrial respiratory chain, and cyclooxygenases, among others. ROS exert their effects by interacting at the atomic and molecular levels with various cellular targets. The regulation of ROS production involves multiple enzymatic pathways and molecules, including antioxidants and metabolic intermediates. ROS plays crucial roles in the immune system beyond cellular destruction, contributing to immune signaling and cell recruitment processes.

Here we demonstrate for the first time an *in vivo* way to visualize and quantify different ROS profiles in response to infection. We also identify the novel usage of several small molecules as antiviral treatments for IAV infection. The use of N-acetyl cysteine has demonstrated efficacy in managing ROS levels during antiviral therapy. While not as potent as mitophagy activators or NOX2 inhibitors, N-acetyl cysteine has shown promise in improving survival rates and reducing viral loads. Therefore, our work demonstrates that targeting ROS directly, even broadly, produced ROS and could serve as a viable strategy for antiviral interventions.

The antioxidant N-acetyl-l-cysteine (NAC) has demonstrated a capacity to inhibit the replication of seasonal human influenza A viruses (Garozzo, 2007). In this study, we investigated NAC's effects on various parameters, including virus replication, virus-induced mortality, and viral burden in zebrafish larvae infected with the PR8-H1N1 strain. Administration of NAC at a concentration of 25 nM resulted in a notable reduction in PR8-induced mortality, inflammation induced by the virus, and tissue damage observed at 24 hours post-infection. Additionally, NAC was associated with decreased ROS production and reduced viral load.

The mechanisms by which NAC exerts its antiviral and anti-inflammatory effects include the inhibition of oxidant-sensitive pathway activation, particularly concerning the transcription factor NF-κB and the mitogen-activated protein kinase p38 (MAPK p38) (Ludwig, 2008; Nencioni, 2009). Our findings present substantial evidence that NAC treatment effectively mitigates PR8 influenza A virus replication and significantly prevents cell death induced by PR8. Furthermore, the administration of NAC resulted in a marked decrease in mortality rates among the zebrafish larvae subjected to PR8 infection.

NAC acts as a potent antioxidant by enhancing the intracellular sulfhydryl pool, serving as a reduced glutathione (GSH) precursor (de Flora, 1997). The protective effects of NAC against seasonal influenza A infection have been substantiated through animal studies, which revealed a decrease in mortality among mice infected with the influenza A strain A/PR/8 H1N1 (Ungheri, 2000). Clinical observations in humans also support the efficacy of NAC, indicating a significant reduction in the incidence of clinically apparent A/H1N1 disease (de Flora, 1997). In vitro studies have shown that NAC effectively prevents oxidative stress, cell death, inflammatory gene expression, and NF-κB activity induced by influenza A (H3N2) virus (Knobil, 1998).

It is hypothesized that NAC's antiviral activity against the H5N1 virus arises from its capacity to inhibit the activation of intracellular signaling molecules and transcription factors that are sensitive to oxidative stress generated during influenza A infection (Geiler, 2010). Consistent with this, NAC treatment was observed to reduce ROS formation in PR8-infected zebrafish, likely inhibiting the activation of two components of redox-sensitive signaling pathways: NF-κB and MAPK p38. Both pathways are recognized for their involvement in the pathogenesis of influenza A viruses (Ludwig, 2008; Nencioni, 2009). Several compounds that inhibit NF-κB, such as the radical scavenger pyrrolidine dithiocarbamate (PDTC), the proteasome inhibitor MG132, the cyclooxygenase (COX) inhibitor acetylsalicylic acid, and the specific NF-κB inhibitor BAY 11-7085, have been demonstrated to impede IAV replication (Geiler, 2010). These findings emphasize that the efficacy of drugs may be context-conditional and may vary across different cell types and viral strains. Further research into the impact of NAC on inflammatory cytokines will be essential in validating its potential as a therapeutic option.

In a recent study by Denk, et al (Denk, 2024), the safety and tolerability of Urolithin A (UA) intake were assessed in a cohort of 25 participants, yielding positive results on immune cell profiles and inflammatory markers. UA intake led to immune remodeling characterized by changes in immune cell phenotypes and mitochondrial function. This suggests a potential role for UA in regulating immune responses, particularly in the context of hyperinflammation and viral infections.

In our current body of work, along with our prior research on Color-flu, we examine the critical function of mitophagy in mitigating IAV-induced mortality. Initially, we demonstrated that MDIVI-1 activates mitophagy and inhibits mitochondrial fusion and fission (Soos, 2024). Additionally, UA has been identified as a well-established mitophagy activator that facilitates the removal of older mitochondria, which are less efficient in producing significant levels of mitochondrial reactive oxygen species (mtROS) (Andreux, 2019).

Autophagy serves as a vital homeostatic mechanism responsible for the degradation of damaged organelles, denatured proteins, and pathogenic invaders via lysosomal pathways (Wang, 2011). Recent evidence underscores its significant roles in both innate and adaptive immune responses, thereby impacting the pathogenesis of various inflammatory diseases (Zhou, 2014). The identification of autophagy-related machinery has enabled the assessment of autophagic activity in both physiological and pathological contexts (Qian, 2017). Autophagy's potential to regulate inflammation by influencing the development, homeostasis, and survival of inflammatory cells such as macrophages, neutrophils, and lymphocytes, as well as affecting the transcription, processing, and secretion of numerous cytokines, offers a promising development, in engaging autophagy to regulate hyperinflammation (Qian, 2017).

A complex interplay between autophagy and inflammation has been established (Zhong, 2016). Specifically, autophagy affects inflammatory cells' development, homeostasis, and survival, which are integral to the development and pathogenesis of inflammatory conditions (Zhong, 2016). Furthermore, recent investigations have revealed that autophagy plays a role in facilitating caspase-independent cell death in activated macrophages (Lai, 2015). These studies identified elevated poly (ADP-ribose) polymerase activation and increased ROS production in macrophages treated with lipopolysaccharide plus Z-VAD (a pan-caspase inhibitor). This was followed by the formation of autophagic bodies, culminating in macrophage cell death, which may help regulate inflammation levels (Lai, 2015). Evidence suggests that autophagy also occurs in neutrophils, both independently and dependently of phagocytosis, similar to macrophages (Qian, 2017). Recent studies indicate that adhesion molecules initiate autophagy-associated caspase-independent cell death in neutrophils, characterized by significant cytoplasmic vacuolization and organelle fusion. Such vacuolated neutrophils have been observed in conditions including septic shock, cystic fibrosis, rheumatoid arthritis, and various dermatoses, indicating that autophagy induction in these cells is a widespread phenomenon associated with neutrophilic inflammatory responses (Itoh, 2015; Mihalache, 2011). Further, neutrophil extracellular trap (NET) cell death, also called NETosis, constitutes another form of programmed cell death in neutrophils involving NADPH oxidase activity (Qian, 2017). Recent research findings have demonstrated that inhibiting autophagy hampers NETosis by obstructing intracellular chromatin decondensation, leading to deficits in cell death typically marked by apoptotic characteristics (Tang, 2015).

Autophagic proteins play integral roles in regulating inflammatory mediators, thereby influencing cytokine production in macrophages (Hosogi, 2014). It is well-documented that Th1 cytokines, such as IFN-γ, TNF-α, IL-1, IL-2, IL-6, and TGF-β, promote autophagy, whereas classical Th2 cytokines, including IL-4, IL-10, and IL-13, exert inhibitory effects (Shi, 2016). Nonetheless, the regulatory role of neutrophils on inflammatory cytokines remains less understood. Although evidence indicates that autophagy occurs in neutrophils comparably to macrophages, the intricacies of the underlying mechanisms require further exploration. The importance of future studies aimed at elucidating this area, particularly through manipulating or modulating key components such as Atg5 or p62, should be highlighted as a key component for further research.

GSK2795039, an inhibitor that targets ROS production through NOX2, has shown promise as a potential antiviral agent. Research by Hirano et al. (2015) demonstrated GSK2795039's ability to inhibit ROS formation and enzyme-substrate utilization in preclinical models. By targeting NOX2 specifically, this inhibitor holds the potential to mitigate neutrophil-driven hyperinflammation and tissue damage in viral infections. IAV is known to induce severe respiratory tract infections, leading to significant lung inflammation, excessive ROS production due to NOX2 oxidase activity, and detrimental lung pathology (To, 2019). In our zebrafish model, we observed a decrease in mortality, tissue damage, viral load, and subsequent oxidative stress. The current study employed a high dose of the highly pathogenic IAV strain PR8 to investigate whether targeting the NOX2 oxidase could mitigate IAV pathogenesis. The infection with PR8 was associated with pronounced disruptions in tissue homeostasis, exemplified by extensive edema, hyperinflammatory responses, recruitment of inflammatory cells, and elevated viral burden. Notably, treatment with GSK279539 significantly alleviated these critical parameters, leading to substantial reductions in edema, hyperinflammation, and viral burden. These findings suggest that ROS plays a pivotal role in the harmful inflammation observed during infections with highly pathogenic IAV.

Neutrophil recruitment is a defining characteristic of the host's innate immune response to influenza virus infections; however, there exists conflicting evidence regarding the ultimate role of these cells (Hai, 2013). For example, neutrophil-depleted mice exhibited heightened pulmonary inflammation and respiratory dysfunction during influenza infection, indicating that these cells are essential for alleviating virus-induced pathology (Vlahos, 2014). Conversely, partial suppression of neutrophil infiltration at 24 hpi with AT7519 was associated with milder pathology and improved morbidity, although the relevant data was not presented in this study.

Variability may arise from unintentional discrepancies in virus dosages used across different studies, potentially leading to diverse inflammatory responses. In this study, a high dose of the PR8 virus led to a significant increase in neutrophil accumulation in the yolk sac of zebrafish beginning at 24 hpi. In contrast, treatment with GSK279539 immediately reduced viral load, suggesting a near-complete rescue following PR8 infection. While the role of neutrophils in influenza virus infections remains a subject of debate, our data indicate that neutrophil ROS inhibition leads to decreased IAV pathology and enhanced viral clearance. Future investigations aimed at elucidating the individual components of the NOX2 complex may offer greater insights into the function of neutrophil-specific ROS and the potential targeting of NOX2 components for ROS inhibition.

Spotless zebrafish represent a meritorious initial approach to exploring the potential impact of neutrophil-specific ROS. However, in comparison to the consistently favorable outcomes observed with the NOX2 inhibitor—particularly with respect to the reduction of viral load and mortality—the findings from the Spotless studies appear comparatively less compelling. Several factors could contribute to this discrepancy. Firstly, the precise role of the *mpx* gene during developmental stages remains uncertain; this is particularly noteworthy given that Spotless zebrafish exhibit a higher mortality rate as they transition from larvae to adults. Secondly, it is important to note that the Spotless phenotype arises from a genetic mutation that pre-existed at the onset of infection. In contrast, the NOX2 inhibitor, GSK279539, was administered 24 hours post-infection. These observations prompt several critical inquiries: would pre-treatment of zebrafish with the NOX2 inhibitor yield results comparable to those observed in spotless zebrafish? Is neutrophil-specific ROS essential for combating IAV infections within a specific temporal period? If so, what is the duration of this critical period? Additionally, is the *mpx* gene integral to larval development? If affirmative, what is the timeline for such involvement?

This manuscript endeavors to propose a novel approach to modulating the neutrophil response, aiming to sustain an effective immune response to clear infections while concurrently mitigating the propensity of neutrophils to induce a hyper-inflammatory and potentially deleterious tissue response. Prior investigations have indicated that adjusting neutrophil populations can be a viable strategy (Nasajaru, 2011); conversely, other research has demonstrated that alterations in neutrophil numbers may result in more adverse outcomes than leaving neutrophil levels unmodified (Tate, 2011). We align ourselves with the latter perspective. Our findings indicate that while a limited modification using AT7519 for a duration of one hour at 24 hours post-infection (hpi) provided some advantages when compared to control groups, extending the treatment to two hours with identical concentrations at 24 hpi yielded minimal to no benefits. Furthermore, pre-treating with AT7519 for two hours was associated with a slight increase in mortality at concentrations of 30 and 50 nM and a more pronounced rise in mortality at 70 nM. These observations imply that the modulation of neutrophils requires a nuanced approach that is contingent on the timing, specific circumstances, and dosage. Conversely, targeting broader ROS, mitochondrial ROS, or neutrophil-mediated ROS may yield more significant benefits with reduced associated risks.

## 5.5. Conclusion

In conclusion, our work has shown the importance of ROS modulation in maintaining a balance between fighting IAV infections and leaning toward a tissue-damaging cytokine storm. When you start to parse out the importance of regulating different types of ROS, the balance swings towards preventing hyperinflammation. Broadscale ROS inhibition is moderately effective in preventing hyperinflammatory-induced death. Mitochondrial ROS inhibition through activating mitophagy is more effective than NAC, but the most effective is targeting NOX2-specific ROS.

Our previous work has shown that modifying neutrophil numbers appears to reduce the robustness of the response needed to clear IAV infection. The neutrophil-depleted zebrafish did not lead to a significant increase in viral burden, yet the mutants still die at much higher rates compared to controls. However, that story changes when you allow the neutrophils to function for a brief period of time and then modulate neutrophil-specific ROS. Our work shows neutrophils are necessary for clearing IAV infections, but they should be regulated through ROS modulation to prevent a cytokine storm.

# CHAPTER 6

# CONCLUSION

## 6.1. Color-Flu Zebrafish Is A Tool For The Influenza Community To Study

We present findings that showcase how Color-flu technology can be harnessed to analyze the natural immune response to IAV infection in zebrafish larvae. This particular model serves as a valuable addition to existing IAV infection models. Notably, our model stands out as the sole IAV model that allows for real-time visualization of infection dynamics and innate immune cell reactions within a transparent host. A recent study by the Fukishima Lab demonstrated the use of Color-flu IAV by infecting mice, anesthetizing them, slicing open their chest to expose their lungs, and using confocal microscopy to study IAV and innate immunity interactions (Fukishima, 2018). While this is a unique approach, it would not be the best approach to understanding the immune system response to IAV, as the mice were clearly under duress. However, the same can be said about the zebrafish model, where we trap them in agarose and egg water. Additionally, we try to limit the time and duration as to reduce the stress and shock on our model, but the zebrafish have not had any more invasive procedures since the initial injections. The functions of innate immune cells, such as neutrophils and macrophages in the context of IAV infection and inflammation, can be effectively examined using this model with minimal stress from the zebrafish

Our utilization of Color-flu technology has facilitated an investigation into the potential applications of ACE inhibition via ramipril and the inhibition of mitophagy through MDIVI-1 to alleviate inflammation resulting from IAV infection. These studies, implemented using the zebrafish Color-flu model, illustrate the model's capacity for conducting extensive screenings of small molecules. Such screening efforts are essential for the identification of promising small molecules or targeted pathways that may be further refined into innovative antiviral therapies for influenza viruses and related inflammatory responses.

The insights derived from these small-molecule investigations could have significant implications, particularly for diseases that activate comparable pathways or are induced by hyperinflammatory reactions. Understanding these underlying mechanisms is increasingly critical in light of findings regarding "long flu," a term introduced by researchers at Washington University, who monitored patients over an 18-month period. Their findings revealed that, akin to "long COVID" patients, individuals affected by "long flu" exhibited an elevated risk of adverse health outcomes. Furthermore, they noted that these patients experienced reduced lung capacity during the study period (Xie, 2023).

One limitation of our current model is its capacity to focus solely on the innate immune response. Multiple factors contribute to the immune response, particularly in the context of infections from viruses that can penetrate the cell nucleus for replication, such as IAV. Research indicates that zebrafish harbor antigen-presenting cells analogous to dendritic cells (Lugo-Villarino, 2011), which serve as a critical connection between the innate and adaptive immune systems. Observing this process in vivo could provide valuable answers to several inquiries, including: Which adaptive immune cells demonstrate a rapid response to IAV infection? How do the innate and adaptive immune systems collaboratively combat infections? Do neutrophils directly influence the regulation of cytotoxic T-cells?

### 6.2. Neutrophils Are Required To Clear IAV Infection

Our research findings indicate that any alterations in neutrophil populations, whether through genetic or pharmacological means, significantly impacted the innate immune response and corresponded with elevated mortality rates. Notably, we found no substantial differences in viral loads between the neutrophil mutant groups and the control groups, implying that the observed mortality is likely attributable to compromised neutrophil functionality caused by conditions such as neutropenia, neutrophilia, or ablation. In both mmiR-199 and WHIM mutant zebrafish, we noted an increase in survival following treatment with MDIVI-1 and ramipril. Previous studies have demonstrated that IAV infection can induce mitophagy, consequently affecting the activation of the NLRP3 inflammasome through excessive ROS production (Lupfer, 2013; Wang, 2021; Zhou, 2010). Prior work from our own laboratory has shown effective mitigation of IAV pathogenesis with the use of a mitophagy activator MDIVI-1 (Soos, 2024) by potentially hijacking the mitophagy pathway and thus reducing the levels of ROS and NLRP3 activation. Before establishing definitive conclusions, comprehensive qRT-PCR and image quantification must be performed.

Neutrophils are integral to pathogen elimination, executing functions such as the generation of extracellular traps, reactive oxygen species, various enzymes (e.g., myeloperoxidase and elastase), and antimicrobial peptides (Mayadas, 2014). While detailed findings were not included in this report, it is pertinent to acknowledge the miR-199 overexpression line likely returns the expression of mmiR-199 to normal levels as we have observed that IAV decreases the expression of mmiR-199. Furthermore, the miR-199 overexpression line demonstrated an increase in ROS production following IAV infection. The increase in ROS coupled with edema and considerable tissue damage are outcomes likely related to the heightened levels of neutrophils in these subjects. This part of the study underscores potential targets for antiviral treatment and suggests the feasibility of employing similar strategies for managing immune-compromised individuals or patients with septicemia who may be suffering from neutrophilia.

A potential limitation of our model lies in the imaging of WHIM mutants. The expression levels of neutrophils in these mutants are notably low, resulting in challenges related to their visualization. Furthermore, these neutrophils exhibit a shorter lifespan compared to control zebrafish, leading to a significant decline in their numbers by 72 hpi, which limits imaging opportunities. To facilitate comparisons among the various lines, WHIM mutants were utilized as a baseline for GFP expression levels, which inadvertently resulted in the neutrophils from the mpx and miR-199 zebrafish appearing excessively bright. To address this issue, we propose employing a therapeutic pre-treatment with a CXCR4 inhibitor on the more discernible lyzC line, which may be analyzed to investigate the underlying mechanisms of WHIM neutropenia.

Our research highlights the pivotal role of neutrophils in the defense against IAV infections. Although previous studies utilizing mouse models have yielded conflicting results, our investigations in a zebrafish model affirm that neutrophils are indispensable components of the innate immune system required for effectively combating IAV infections. We observed that manipulating neutrophil populations compromises the immune response's efficacy in clearing IAV infections. Our experimental design included two groups subjected to neutropenia and one group exhibiting neutrophilia. In comparison to control zebrafish with standard neutrophil counts, the mutants did not present a significant increase in viral load; however, they exhibited markedly higher mortality rates. Our research conclusively indicates that neutrophils are critical to the antiviral response, as supported by $TCID_{50}$ analysis and visual quantitative assessments of neutrophil and viral levels in zebrafish. Thus, our findings suggest that alterations to neutrophil populations may not be advisable, prompting the need to explore alternative research pathways.

### 6.3. Not All ROS Are Created Equal In Influenza Infections

IAV is known to cause severe respiratory tract infections, which are characterized by lung inflammation, excessive production of ROS from the NOX2 oxidase pathway, and substantial lung pathology. The influx of neutrophils represents a prominent feature of the host's innate immune response to IAV infections; however, the precise role of neutrophils remains a matter of debate. Notably, neutrophil-depleted murine models have shown increased pulmonary inflammation and respiratory dysfunction in response to IAV, indicating that neutrophils are crucial in mitigating pathology induced by the virus. Our research in neutrophil management supports this concept, as WHIM mutant zebrafish, which exhibit neutropenia, demonstrated poorer survival outcomes compared to their counterparts with fully functional neutrophils. Interestingly, our findings also revealed that elevated levels of neutrophils were similarly detrimental, with zebrafish overexpressing miR-199 had lower survival than control groups. Both scenarios consistently resulted in significant changes in the ROS profile, prompting us to investigate whether regulating different types of ROS could enable a complete neutrophil response to infection while simultaneously preventing the onset of hyperinflammation.

To gain a deeper understanding of the role of ROS in the context of IAV infection, we employed targeted genetic and pharmacological approaches. We hypothesized that the antiviral properties of NAC against the H5N1 virus stemmed from its ability to inhibit the activation of intracellular signaling molecules and transcription factors that are sensitive to oxidative stress influenced by IAV infection (Geiler, 2010). Supporting this hypothesis, NAC treatment resulted in reduced ROS formation in PR8-infected zebrafish, potentially by inhibiting two key components of redox-sensitive signaling pathways: NF-κB and MAPK p38, both of which are implicated in the pathogenesis of influenza A viruses (Ludwig, 2008; Nencioni, 2009). Several agents that inhibit NF-κB have been demonstrated to restrict IAV replication (Geiler, 2010).

In our ongoing research, alongside our previous studies on Color-flu, we assess mitophagy's vital role in reducing mortality associated with IAV infections. Our initial findings indicated that MDIVI-1 promotes mitophagy while inhibiting mitochondrial fusion and fission processes (Soos, 2024). Furthermore, there is growing evidence that autophagy occurs in neutrophils, independent of or concurrently with phagocytosis, akin to macrophage behavior (Qian, 2017). Recent investigations suggest that adhesion molecules can initiate autophagy-associated, caspase-independent cell death in neutrophils, characterized by significant cytoplasmic vacuolization and organelle fusion. These vacuolated neutrophils have been observed in a variety of conditions, including septic shock, cystic fibrosis, rheumatoid arthritis, and various dermatoses, suggesting that autophagy induction in neutrophils is a widespread phenomenon linked to inflammatory responses.

GSK2795039, an inhibitor targeting ROS production through NOX2, shows promise as a potential antiviral therapy. Research by Hirano et al. (2015) demonstrated that GSK2795039 effectively inhibits ROS formation and enzymatic substrate utilization in preclinical models. By specifically targeting NOX2, this inhibitor may help alleviate hyperinflammation and tissue damage driven by neutrophils during viral infections. Our work supports this as the zebrafish treated with GSK2795039 predominantly recovered from infection, a 2-log fold decrease in viral burden, and neutrophils that appear more active in movies taken (data not shown). This suggests pharmacological targets of NOX2 complex of other NOX complexes may be a potentially beneficial therapeutic target in various diseases with hyperinflammatory associated pathologies.

Our findings indicate that the effectiveness of ROS targets varies, with broad targets proving less effective, whereas targeting mitochondrial and neutrophil-specific ROS appears to be the most effective strategy. This likely results from the collaborative role of mitochondria in supplying hydrogen peroxide (H2O2) to neutrophils, enhancing their ROS release. However, this dynamic complicates neutrophil self-regulation and may lead to increased tissue damage through hyperinflammatory responses. This research emphasizes the importance of ROS regulation in achieving a balance between effectively combating IAV infections and preventing tissue-damaging cytokine storms. By elucidating the significance of regulating distinct ROS types, we can advance strategies to mitigate excessive inflammation.

The implications of our research extend beyond IAV infections, as neutrophil dysfunction is associated with several conditions, including Type 1 and Type 2 diabetes mellitus, obesity-related disorders such as atherosclerosis and nonalcoholic fatty liver disease, as well as autoimmune diseases like chronic obstructive pulmonary disease and inflammatory bowel disease (Herrero-Cevara, 2022). Additionally, neutrophil involvement in blood-brain barrier damage may play a role in neurodegenerative disorders such as Alzheimer's disease, frontotemporal dementia, Huntington's disease, multiple sclerosis, Parkinson's disease, and stroke (Chakraborty, 2023; Santos-Lima, 2022). Targeting various ROS types could potentially yield therapeutic benefits in addressing these diverse health challenges. The cumulative findings of the research documented in this thesis are encapsulated in Figure 6.1.

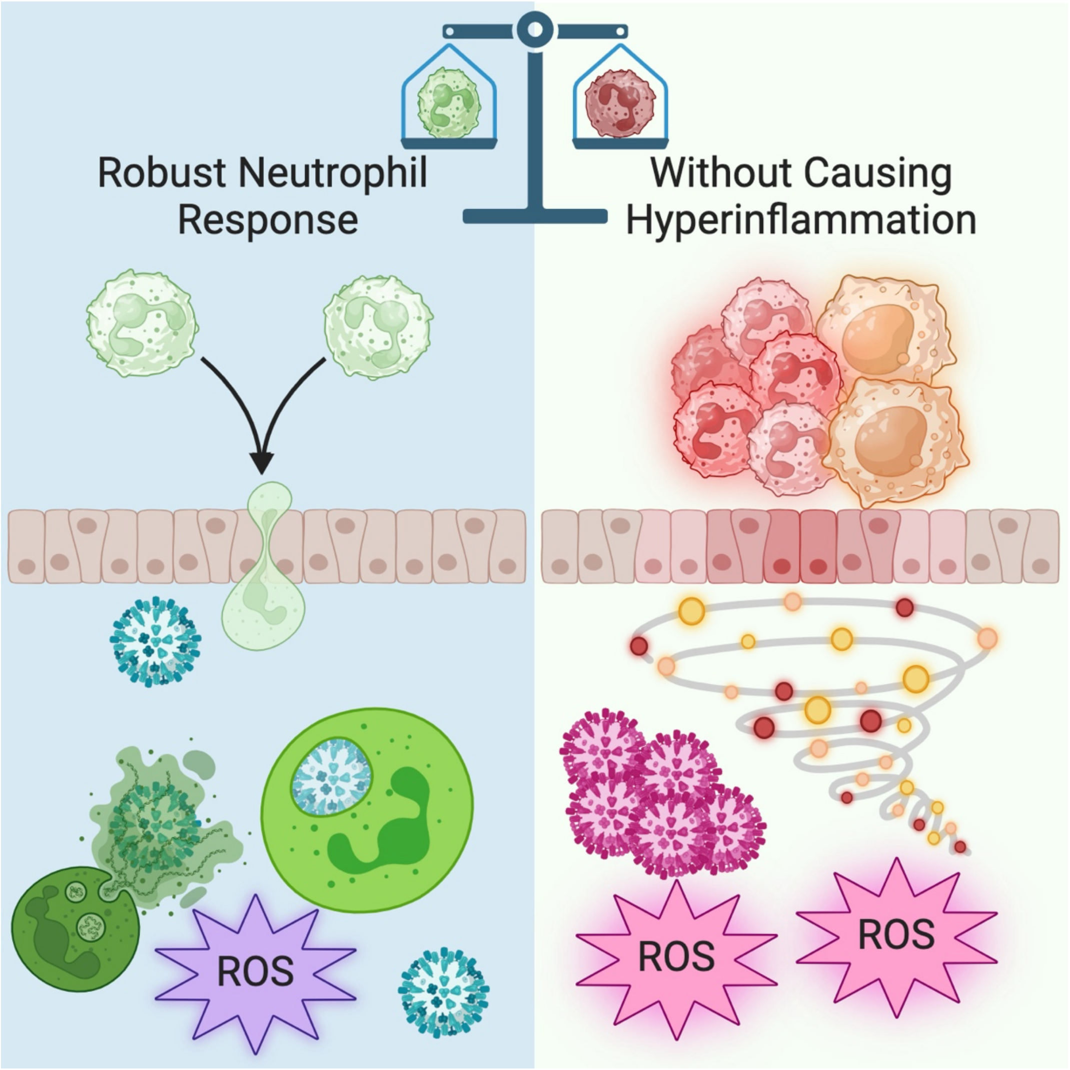
Robust Neutrophil Response
Without Causing Hyperinflammation
ROS
ROS
ROS

**Figure 6.1. Neutrophils robustly clear infection while preventing tissue-damaging hyperinflammation from excessive ROS levels.** Neutrophils must possess sufficient resilience to effectively eliminate infections while simultaneously mitigating the risk of hyperinflammation associated with excessive ROS production.

### 6.4. Color-Flu’s Future Resides In Small Molecules, Toxicology, Autophagy, And Neuromuscular Development

We are pleased to present our research findings demonstrating the application of Color-flu to analyze the natural immune response to IAV infection in zebrafish larvae. This innovative model represents a significant enhancement to current IAV infection methodologies. Importantly, our model uniquely facilitates real-time visualization of infection dynamics and the innate immune cell responses within a transparent organism. It effectively investigates the roles of innate immune cells, such as neutrophils and macrophages, in the context of IAV infection and associated inflammation.

Utilizing Color-flu has allowed us to explore the beneficial effects of ACE inhibition with ramipril and mitophagy inhibition with MDIVI-1 on the IAV infection response, specifically in terms of inflammation reduction through distinct biological pathways. These insightful studies underscore the potential for comprehensive small molecule screening initiatives employing the zebrafish Color-flu IAV model, essential for identifying promising small molecules or targeted pathways that could be further developed into novel antiviral therapies for influenza viruses and related inflammatory responses. This knowledge may also extend to other diseases that activate similar biological pathways or experience similar pathologies.

As previously mentioned, a recent study by Xie et al. (Xie, 2023) illustrated the long-term effects of severe IAV infections on lung damage, potentially lasting over 18 months. This finding emphasizes the necessity for ongoing influenza research. The visualization capabilities offered by Color-flu open up numerous avenues for exploration in zebrafish, which are renowned for their rapid generation and utility as models for genetic and toxicological research. In Table 6.1, we provide a compilation of small molecules warranting further investigation in relation to IAV infection. Some of these targets have been identified through RNA-Seq analyses, including findings from our own RNA-Seq study. By elucidating the impact of these pathways and protein targets on IAV outcomes, we can gain insight into their significance as influenza evolves.

**Table 6.1 Compounds to study in IAV infections.**

| **Compound name** | **Primary Target*** | **Primary Action** | **Brief Description** |
|---|---|---|---|
| Etoposide | DNA Topoisomerase | Inhibitor | Topoisomerase II inhibitor |
| PPT | Estrogen and Related Receptors | Agonist | Subtype-selective ERα agonist |
| ODQ | Other Nitric Oxide | Inhibitor | Selective inhibitor of NO-sensitive guanylyl cyclase |
| Taxol | Microtubules | Other | Promotes assembly and inhibits disassembly of microtubules |
| Bay 11-7085 | NF-kB/IkB | Inhibitor | Irreversible inhibitor of TNF-α-induced IκBα phosphorylation |
| L-755,507 | Adrenergic Beta-3 Receptors | Agonist | Very potent and selective β3 partial agonist |
| SB 328437 | Chemokine CC Receptors | Antagonist | Potent and selective CCR3 antagonist |
| Maraviroc | Chemokine CC Receptors | Antagonist | Selective CCR5 antagonist |
| R 568 hydrochloride | Calcium-Sensing Receptor | Modulator | Positive allosteric modulator of human calcium-sensing receptor (CaSR) |
| Olmesartan | Angiotensin AT1 Receptors | Antagonist | Potent AT1 antagonist |
| BHPI | Estrogen (GPER) Receptors | Antagonist | ERα antagonist; also activates unfolded protein response; active in vivo |
| FTY 720 | Sphingosine-1-phosphate Receptors | Agonist | Potent S1P receptor agonist; also immunosuppressant |
| Trazodone hydrochloride | 5-HT2A Receptors | Antagonist | 5-HT2A and α1 adrenoceptor antagonist; also enhances neural differentiation; antidepressant and neuroprotectant |
| Phentolamine Mesylate | Non-selective Adrenergic Alpha Receptors | Antagonist | Adrenergic α receptor antagonist; antihypertensive |
| AZD 2098 | Chemokine CC Receptors | Antagonist | Potent and selective CCR4 antagonist |

table continued

| | | | |
|---|---|---|---|
| Argatroban | Other Proteases | Inhibitor | Potent thrombin inhibitor |
| Lonidamine | Hexokinases | Inhibitor | Mitochondrial hexokinase inhibitor |
| BTS | Myosin | Inhibitor | Selective inhibitor of skeletal muscle myosin II ATPase activity |
| Ro 31-8220 mesylate | Broad Spectrum Protein Kinase Inhibitors | Inhibitor | Protein kinase inhibitor |
| Paxilline | Ca2+-ATPase | Blocker | SERCA ATPase blocker. Also potent BKCa channel blocker |
| Necrostatin-1 | RIP Kinases | Inhibitor | RIP1 kinase inhibitor; inhibits necroptosis |
| Acyclovir | RNA/DNA Polymerase | Inhibitor | Inhibits viral DNA polymerase; antiherpetic agent |
| Hesperadin hydrochloride | Aurora Kinases | Inhibitor | Potent Aurora kinase B inhibitor |
| PP 242 | mTOR | Inhibitor | Dual mTORC1/mTORC2 inhibitor |
| Rasagiline mesylate | Monoamine Oxidase | Inhibitor | Selective and irreversible MAO-B inhibitor |
| Axitinib | VEGFR | Inhibitor | Potent VEGFR-1, -2 and -3 inhibitor |
| TC-F 2 | Fatty Acid Amide Hydrolase (FAAH) | Inhibitor | Potent, reversible and selective FAAH inhibitor |
| Bosutinib | Src Kinases | Inhibitor | Dual Src-Abl inhibitor; antiproliferative |
| Letrozole | Cytochrome P450 | Inhibitor | Potent, reversible non-steroidal aromatase inhibitor |
| CHIR 99021 | Glycogen Synthase Kinase 3 | Inhibitor | Highly selective GSK-3 inhibitor |
| TCS ERK 11e | ERK | Inhibitor | Potent and selective ERK2 inhibitor |
| KB SRC 4 | Src Kinases | Inhibitor | Potent and selective c-Src inhibitor |
| U 104 | Carbonic anhydrases | Inhibitor | Potent carbonic anhydrase (CA) IX and XII inhibitor |
| SGC 0946 | Other Lysine Methyltransferases | Inhibitor | Highly potent and selective DOT1L inhibitor; cell permeable |
| SD 2590 hydrochloride | Matrix Metalloprotease | Inhibitor | Potent MMP inhibitor |
| SUN 11602 | FGFR | Other | Basic fibroblast growth factor (bFGF) mimetic; neuroprotective |
| AZD 6482 | PI 3-Kinase | Inhibitor | Potent and selective PI 3-Kβ inhibitor |

table continued

| | | | |
|---|---|---|---|
| BIX 02189 | MEK | Inhibitor | Selective MEK5 and ERK5 inhibitor |
| Amlexanox | TANK binding kinase (TBK) | Inhibitor | Selective inhibitor of TBK |
| Spautin 1 | Deubiquitinating Enzymes | Inhibitor | USP10 and USP13 inhibitor; inhibits autophagy |
| NHI 2 | Lactate Dehydrogenase A | Inhibitor | LDHA inhibitor |
| SM 324405 | Toll-like Receptors | Agonist | Potent TLR7 agonist |
| Balicatib | Cathepsin | Inhibitor | Potent and selective cathepsin K inhibitor |
| AZD 3147 | mTOR | Inhibitor | Potent and selective dual mTORC1 and 2 inhibitor; orally bioavailable |
| AZD 1480 | JAK Kinase | Inhibitor | Potent and selective JAK2 inhibitor; antiangiogenic |
| MSC 2032964A | ASK1 | Inhibitor | Potent and selective ASK1 inhibitor; orally bioavailable |
| GSK 319347A | IkB Kinase | Inhibitor | Potent and selective IKKε inhibitor |
| PF 543 hydrochloride | Sphingosine Kinase | Inhibitor | Potent and selective SphK1 inhibitor |
| MLi-2 | LRRK2 | Inhibitor | Potent and selective LRRK2 inhibitor |
| CDN 1163 | Ca2+-ATPase | Activator | SERCA2 allosteric activator |
| pCPA methyl ester hydrochloride | Hydroxylases | Inhibitor | Tryptophan hydroxylase inhibitor |
| Imatinib mesylate | Abl Kinase | Inhibitor | Potent and selective v-Abl tyrosine kinase inhibitor; also inhibits PDGFR and c-kit |
| PF 04449613 | Phosphodiesterases | Inhibitor | Potent PDE9 inhibitor; brain penetrant |
| B I09 | IRE1 | Inhibitor | IRE1 endonuclease inhibitor; cell permeable |
| Nexinhib20 | Other Small Monomeric GTPases | Inhibitor | Rab27 inhibitor; inhibits neutrophil exocytosis; active in vivo |
| Rucaparib camsylate | Poly(ADP-ribose) Polymerase | Inhibitor | PARP inhibitor |
| SLM 6031434 hydrochloride | Sphingosine Kinase | Inhibitor | Selective sphingosine kinase 2 (Sphk2) inhibitor |
| AZ 5704 | ATM & ATR Kinase | Inhibitor | Potent and selective ATM kinase inhibitor; orally bioavailable |

table continued

| | | | |
|---|---|---|---|
| GSK'872 | RIP Kinases | Inhibitor | Potent and selective RIP3 kinase inhibitor |
| VAS 2870 | NADPH Oxidase | Inhibitor | NADPH oxidase (Nox) inhibitor |
| Idasanutlin | Ubiquitin E3 Ligases | Inhibitor | Potent MDM2 inhibitor; inhibits MDM2-p53 interaction |
| TR 14035 | Integrins | Antagonist | Potent integrin α4β7 and α4β1 (VLA-4) antagonist; orally bioavailable |
| AZD 5363 | Akt (Protein Kinase B) | Inhibitor | Potent pan-AKT inhibitor |
| Ruxolitinib | JAK | Inhibitor | Potent and selective JAK1/JAK2 inhibitor; orally bioavailable |
| MRK 740 | Other Lysine Methyltransferases | Inhibitor | Potent PRDM9 inhibitor |
| Remdesivir | RNA Polymerase | Inhibitor | Viral RNA-dependent RNA polymerase (RdRP) inhibitor; broad spectrum antiviral nucelotide prodrug |
| Kynurenic acid | Non-selective Ionotropic Glutamate | Antagonist | Broad spectrum glutamatergic antagonist |
| 5,7-Dichlorokynurenic acid | NMDA Receptors | Antagonist | Potent NMDA antagonist; acts at glycine site |
| DNQX | AMPA Receptors | Antagonist | Selective non-NMDA iGluR antagonist |
| A 803467 | Voltage-gated Sodium Channels | Blocker | Selective NaV1.8 channel blocker |
| NS 1643 | Voltage-Gated Potassium Channels | Activator | KV11.1 (hERG) channel activator; antiarrhythmic |
| DS2 | GABAA Receptors | Modulator | Positive allosteric modulator of GABAA receptors; displays subunit selectivity |
| Ch 55 | Retinoic Acid Receptors | Agonist | Potent RAR agonist |
| Hydrocortisone | Glucocorticoid Receptor | Other | Adrenal glucocorticoid; immunosuppressant |
| AC 186 | Estrogen and Related Receptors | Agonist | Potent and selective ERβ agonist; neuroprotective |
| Megestrol Acetate | Progesterone Receptor | Agonist | Synthetic progesterone analog |
| Nomifensine | Dopamine Transporters | Inhibitor | Potent noradrenalin and dopamine uptake inhibitor. Antidepressant |
| SR 16832 | PPARgamma Receptors | Antagonist | Dual site PPARγ inhibitor |
| KF 38789 | Cell Adhesion Molecules | Other | Selective inhibitor of P-selectin-mediated cell adhesion |
| Levetiracetam | Translocation, Exocytosis & Endocytosis | Other | Antiepileptic; binds SV2A |

table continued

| | | | |
|---|---|---|---|
| GIT 27 | Cytokines | Other | Immunomodulator; reduces production of pro-inflammatory cytokines |
| Trovafloxacin mesylate | DNA, RNA and Protein Synthesis | Inhibitor | Antibiotic; inhibits bacterial DNA synthesis |
| ISO 1 | Cytokines | Inhibitor | Macrophage migration inhibitory factor (MIF) inhibitor |
| BIIB 021 | Hsp90 | Inhibitor | Selective Hsp90 inhibitor |
| JTE 607 dihydrochloride | Cytokines | Other | Cytokine release inhibitor; anti-inflammatory |
| ML 334 | Nrf2 | Activator | Inhibitor of Keap1- Nrf2 interaction |
| Liproxstatin-1 hydrochloride | Ferroptosis | Inhibitor | Potent ferroptosis inhibitor |
| 16673-34-0 NLRP3i | Inflammasomes | Inhibitor | NLRP3 inflammasome inhibitor |
| W-7 hydrochloride | Calcium Binding Protein | Antagonist | Calmodulin antagonist. Inhibits myosin light chain kinase |
| SANT-1 | Hedgehog Signaling | Inhibitor | Inhibitor of hedgehog (Hh) signaling; antagonizes smoothened activity |
| Bax channel blocker | Bcl-2 Family | Inhibitor | Allosteric inhibitor of Bax channel activation |
| NSC 146109 hydrochloride | p53 | Activator | Cell-permeable, genotype-selective antitumor agent; activates p53-dependent transcription |
| PNU 74654 | Beta-catenin | Other | β-catenin binder; inhibits Wnt signaling |
| I-BET 151 dihydrochloride | Bromodomains | Inhibitor | BET bromodomain inhibitor; also promotes differentiation of hiPSCs into megakaryocytes |
| NSC 74859 | STAT | Inhibitor | Selective STAT3 inhibitor |
| Ro 5-3335 | Other Transcription Factors | Inhibitor | Core binding factor inhibitor; attenuates hematopoiesis |
| PFI 3 | Bromodomains | Inhibitor | Potent and selective SMARCA2/4 and polybromo 1 inhibitor |
| J 147 | Amyloid Beta Peptides | Other | Neuroprotective and neurotrophic compound; reduces Aβ40 and Aβ42 levels |
| GN 44028 | Hypoxia Inducible Factors | Inhibitor | Potent HIF-1α inhibitor |
| H 151 | STING-Dependent Signaling | Antagonist | STING antagonist |

As the demand for new synthetic compounds rises, environmental health disciplines and toxicant exposure's effects have emerged as critical public health issues. Naturally occurring environmental chemicals, such as metals, significantly impact human and animal health. Substances like lead, arsenic, and per- and poly-fluoroalkyl substances have garnered public attention for their detrimental effects on wildlife and human health in recent years (Bambino, 2017). Despite the recognized dangers posed by environmental toxins, there remains a limited understanding of their mechanisms underlying disease causation and a lack of engagement from the business sector. The field of environmental health presents numerous unanswered questions, necessitating increased research efforts (Landrigan, 2016). Key inquiries include the effects of low-dose, cumulative exposures and interactions with multiple toxicants and the developmental processes that such exposures alter (Bambino, 2017).

Zebrafish are at the forefront of toxicology research, widely used for detecting toxins in water samples and exploring the mechanisms of action of environmental toxins. Preliminary studies conducted in our laboratory have identified arsenic as a potential inhibitor of the antiviral response to IAV infection, correlated with decreased survival and increased viral load. Further detailed investigation through confocal imaging of phagocytes and reactive oxygen species (ROS) staining is warranted to reinforce these findings. Additionally, assessing the potential of small molecules to moderate the exacerbating effects of arsenic would be beneficial. Furthermore, conducting RNA sequencing of genes at selected time points could yield new insights into arsenic-related disruptions. Once arsenic's role is confirmed, there are numerous other toxic compounds, including persistent chemicals and heavy metals, that could be investigated, as referenced in Babich et al. (Babich, 2024).

Autophagy represents a fundamental cellular process responsible for the degradation of cellular components, which is essential for the maintenance of cellular homeostasis and the turnover of exhausted organelles and aggregated proteins. Importantly, research has elucidated that autophagy contributes significantly to host-virus interactions, with its roles varying according to the type of virus and host cell involved (Jassey, 2024). This process is instrumental in the degradation of viral components, viral particles, and even host factors necessary for viral replication, thus positioning autophagy as a critical component of the innate antiviral response (Choi et al., 2018; Ismayil et al., 2020; Yang et al., 2020). Numerous studies have established that autophagy serves a defensive function against viral infection by silencing or mutating autophagy-related genes (ATGs) (Liu et al., 2005; Yordy et al., 2013).

Over the past two decades, advancements in the understanding of autophagy-virus interactions have underscored the importance of this conserved catabolic pathway in antiviral immunity, particularly through its role in the selective elimination of viral proteins and particles. Nevertheless, in the ongoing evolutionary conflict between viruses and their hosts, pathogens have developed various mechanisms to inhibit and exploit the autophagy pathway, thereby diminishing the host's antiviral capabilities and potentially utilizing autophagy to facilitate their own infection.

In our investigations, the evaluation of several small molecules has indicated that the modulation of specific autophagic processes can enhance the host's ability to combat infection. Notably, the LC3 zebrafish model developed by Daniel Klionsky has exhibited a remarkable consistency of autophagic activity during prolonged IAV infection. This observation raises pertinent inquiries: Is autophagy functioning as a protector or an impediment against IAV in our model? Do systematic pharmacological interventions that disrupt specific autophagic pathways ultimately aid or hinder the host's response? Can the activation or inhibition of macroautophagy mitigate viral spread and/or alleviate hyperinflammatory responses? Furthermore, does influenza infection prompt host cells to engage in specialized autophagic processes, such as reticulophagy or nucleophagy?

Additionally, an important investigation avenue involves examining tissue and DNA damage. Previous research by Goody et al. (Goody, 2016) demonstrated the utility of Evan's blue dye, a known DNA-binding agent indicative of necrotic cells, in zebrafish models, revealing that IAV-infected zebrafish experience exacerbated muscle damage. Preliminary findings in our laboratory suggest significant muscle damage in PR8-infected wild-type zebrafish compared to controls injected with a diluent. Future research should prioritize the identification of genes correlated with this phenomenon, including non-coding RNAs. Furthermore, investigating the roles of neutrophils, hyperinflammation, ROS in contributing to tissue damage would be of considerable interest. Our laboratory possesses several validated small molecules that modulate ROS production and neutrophil activity, as well as multiple genetic zebrafish lines, facilitating the execution of these assays. As IAV severity peaks between 72 and 96 hpi, focusing our efforts on these critical time points may optimize outcomes while minimizing undue stress and suffering in the zebrafish models.

As was mentioned earlier, Color-flu opens up a realm of possible inquiries further heightened by the utility and flexibility of the zebrafish model. So many things can be investigated using this model starting with these projects.

## REFERENCES

1. Aakanksha Jain, Chandrashekhar Pasare; Innate Control of Adaptive Immunity: Beyond the Three-Signal Paradigm. *J Immunol* 15 May 2017; 198 (10): 3791–3800.

2. Abbas, A.K., Lichtman, A.H. and Pillai, S. (2022) *Cellular and molecular immunology*. 10th edn. Philadelphia, Pennsylvania: Elsevier Inc.

3. Abdulnour, R. E. *et al.* Maresin 1 biosynthesis during platelet–neutrophil interactions is organ-protective. *Proc. Natl Acad. Sci. USA* 111, 16526–16531 (2014).

4. Abe G, Suster ML, Kawakami K. Tol2-mediated transgenesis, gene trapping, enhancer trapping, and the Gal4-UAS system. Methods Cell Biol. 2011;104:23-49. doi: 10.1016/B978-0-12-374814-0.00002-1.

5. Abouhashem, A. S., Singh, K., Azzazy, H. M. E. & Sen, C. K. Is low alveolar type II cell SOD3 in the lungs of elderly linked to the observed severity of COVID-19? *Antioxid. Redox Signal* 33, 59–65 (2020).

6. Acuna UM, Wittwer J, Ayers S, Pearce CJ, Oberlies NH, De Blanco EJ. Effects of (5Z)-7-Oxozeaenol on the Oxidative pathway of cancer cells. *Anticancer Res.* 2012;32(7):2665–2671.

7. Agostini, L.; Martinon, F.; Burns, K.; McDermott, M.F.; Hawkins, P.N.; Tschopp, J. NALP3 Forms an IL-1β-Processing Inflammasome with Increased Activity in Muckle-Wells Autoinflammatory Disorder. *Immunity* 2004, *20*, 319–325.

8. Agraz-Cibrian JM, Giraldo DM, Mary FM, Urcuqui-Inchima S. Understanding the molecular mechanisms of NETs and their role in antiviral innate immunity. *Virus Res.* 2017;228:124-133.

9. Alberts B, Johnson A, Lewis J, et al. Molecular Biology of the Cell. 4th edition. New York: Garland Science; 2002. Chapter 24, The Adaptive Immune System. Available from: https://www.ncbi.nlm.nih.gov/books/NBK21070/.

10. Allen, I.C.; Scull, M.A.; Moore, C.B.; Holl, E.K.; McElvania-TeKippe, E.; Taxman, D.J.; Guthrie, E.H.; Pickles, R.J.; Ting, J.P.Y. The NLRP3 Inflammasome Mediates In Vivo Innate Immunity to Influenza A Virus through Recognition of Viral RNA. *Immunity* 2009, *30*, 556–565.

11. Anchi Wu, Valia T Mihaylova, Marie L Landry, Ellen F Foxman. Interference between rhinovirus and influenza A virus: a clinical data analysis and experimental infection study. The Lancet Microbe, Volume 1, Issue 6, 2020, Pages e254-e262, https://doi.org/10.1016/S2666-5247(20)30114-2.

12. Au, L., Boos, L., Swerdlow, A., Byrne, F., Shepherd, S., Fendler, A. and Turajlic, S., 2020. Cancer, COVID-19, and Antiviral Immunity: The CAPTURE Study. *Cell*, 183(1), pp.4-10.

13. Babac B.D., Milton Dulay R.R., Arwen Calpito R.S., Domingo M.A., Grace Macamos M.M., Mangabat A.R., Zhyra Zoberiaga N.L. In-vitro activity of ethanolic extract of Lentinus strigosus mycelia in N2 wild strain Caenorhabditis elegans-An animal model for obesity and its chemical composition. *J. Appl. Biol. Biotech.* 2021;9:41–46. doi: 10.7324/JABB.2021.9106.

14. Babu YS, Chand P, Bantia S, Kotian P, Dehghani A, El-Kattan Y, Lin TH, Hutchison TL, Elliott AJ, Parker CD, Ananth SL, Horn LL, Laver GW, Montgomery JA. 2000. BCX-1812 (RWJ-270201): discovery of a novel, highly potent, orally active, and selective influenza neuraminidase inhibitor through structure-based drug design. *J Med Chem* 43:3482–3486. doi: 10.1021/jm0002679

15. Bambino K, Chu J. Zebrafish in Toxicology and Environmental Health. Curr Top Dev Biol. 2017;124:331-367. doi: 10.1016/bs.ctdb.2016.10.007.

16. Barnes, B. J. et al. Targeting potential drivers of COVID-19: neutrophil extracellular traps. *J. Exp. Med.* 217, e20200652 (2020).

17. Bachelerie F, Ben-Baruch A, Burkhardt AM, Combadière C, Farber JM, Graham GJ, Horuk R, Sparre-Ulrich AH, Locati M, Luster AD *et al* (2014) International Union of Pharmacology. LXXXIX. Update on the extended family of chemokine receptors and introducing a new nomenclature for atypical chemokine receptors. *Pharmacol Rev* 66, 1–79.

18. Bajrami, B. *et al.* G-CSF maintains controlled neutrophil mobilization during acute inflammation by negatively regulating CXCR2 signaling. *J. Exp. Med.* 213, 1999–2018 (2016).

19. Banoth B, Cassel SL. Mitochondria in innate immune signaling. Transl Res. 2018 Dec;202:52-68. doi: 10.1016/j.trsl.2018.07.014. Epub 2018 Aug 7.

20. Barlan, A.U.; Griffin, T.M.; Mcguire, K.A.; Wiethoff, C.M. Adenovirus Membrane Penetration Activates the NLRP3 Inflammasome. *J. Virol.* 2011, *85*, 146–155.

21. Barlan, A.U.; Danthi, P.; Wiethoff, C.M. Lysosomal Localization and Mechanism of Membrane Penetration Influence Nonenveloped Virus Activation of the NLRP3 Inflammasome. *Virology* 2011, *412*, 306–314.

22. Berkhoff E.G., Geelhoed-Mieras M.M., Verschuren E.J., van Baalen C.A., Gruters R.A., Fouchier R.A., Osterhaus A.D., Rimmelzwaan G.F. The loss of immunodominant epitopes affects interferon-gamma production and lytic activity of the human influenza virus-specific cytotoxic T lymphocyte response *in vitro*. *Clin. Exp. Immunol.* 2007;148:296–306. (2007a).

23. Berkhoff E.G., Geelhoed-Mieras M.M., Fouchier R.A., Osterhaus A.D., Rimmelzwaan G.F. Assessment of the extent of variation in influenza A virus cytotoxic T-lymphocyte epitopes by using virus-specific CD8+ T-cell clones. *J. Gen. Virol.* 2007;88:530–535. doi: 10.1099/vir.0.82120-0. (2007b).

24. Bernstein K.E., Khan Z., Giani J.F., Cao D.Y., Bernstein E.A., Shen X.Z. Angiotensin-converting enzyme in innate and adaptive immunity. *Nat. Rev. Nephrol.* 2018;14:325–336. doi: 10.1038/nrneph.2018.15.

25. Bian C., Chen W., Ruan Z., Hu Z., Huang Y., Lv Y., Xu T., Li J., Shi Q., Ge W. Genome and Transcriptome Sequencing of casper and roy Zebrafish Mutants Provides Novel Genetic Clues for Iridophore Loss. *Int. J. Mol. Sci.* 2020;21:2385. doi: 10.3390/ijms21072385.

26. Bhattacharyya A, Chattopadhyay R, Mitra S, Crowe SE. Oxidative stress: an essential factor in the pathogenesis of gastrointestinal mucosal diseases. Physiol Rev. 2014 Apr;94(2):329-54. doi: 10.1152/physrev.00040.2012.

27. Björkström, N.K., Strunz, B. & Ljunggren, HG. Natural killer cells in antiviral immunity. *Nat Rev Immunol* 22, 112–123 (2022). https://doi.org/10.1038/s41577-021-00558-3.

28. Boliar S., Chambers T.M. A new strategy of immune evasion by influenza A virus: Inhibition of monocyte differentiation into dendritic cells. *Vet. Immunol. Immunopathol.* 2010;136:201–210. doi: 10.1016/j.vetimm.2010.03.004.

29. Bolton JL, Trush MA, Penning TM, Dryhurst G, Monks TJ. Role of quinones in toxicology. *Chem Res Toxicol* 13: 135–160, 2000.

30. Borregaard N, Cowland JB. Granules of the human neutrophilic polymorphonuclear leukocyte. *Blood* (1997) 89(10):3503–21.

31. Bousfiha A, Jeddane L, Al-Herz W, Ailal F, Casanova JL, Chatila T, et al. The 2015 IUIS phenotypic classification for primary immunodeficiencies. *J Clin Immunol* (2015) 35(8):727–38. 10.1007/s10875-015-0198-5.

32. Bowie JU. Solving the membrane protein folding problem. *Nature* (2005) 438:581–9. doi:10.1038/nature04395.

33. Boztug K, Rosenberg PS, Dorda M, Banka S, Moulton T, Curtin J, et al. Extended spectrum of human glucose-6-phosphatase catalytic subunit 3 deficiency: novel genotypes and phenotypic variability in severe congenital neutropenia. *J Pediatr* (2012) 160(4):679–83.e2. 10.1016/j.jpeds.2011.09.019.

34. Bradley LM, Douglass MF, Chatterjee D, Akira S, Baaten BJ. Matrix metalloprotease 9 mediates neutrophil migration into the airways in response to influenza virus-induced toll-like receptor signaling. *PLoS Pathog*. 2012;8(4):e1002641.

35. Brandes M., Klauschen F., Kuchen S., Germain R.N. A systems analysis identifies a feedforward inflammatory circuit leading to lethal influenza infection. *Cell.* 2013;154:197–212. doi: 10.1016/j.cell.2013.06.013.

36. Bravo Garcia-Morato M., Calvo Apalategi A., Bravo-Gallego L.Y., Blazquez Moreno A., Simon-Fuentes M., Garmendia J.V., Mendez Echevarria A., Del Rosal Rabes T., Dominguez-Soto A., Lopez-Granados E., et al. Impaired control of multiple viral infections in a family with complete IRF9 deficiency. *J. Allergy Clin. Immunol.* 2019;144:309–312.e10. doi: 10.1016/j.jaci.2019.02.019.

37. Brieger, K., Schiavone, S., Miller, Jr. and Krause, K. (2012). Reactive oxygen species: from health to disease. *Swiss Medical Weekly*. doi:https://doi.org/10.4414/smw.2012.13659.

38. Brothers K.M., Newman Z.R., Wheeler R.T. Live imaging of disseminated candidiasis in zebrafish reveals role of phagocyte oxidase in limiting filamentous growth. *Eukaryot. Cell.* 2011;10:932–944. doi: 10.1128/EC.05005-11.

39. Buchbinder D, Nugent DJ, Fillipovich AH. Wiskott-Aldrich syndrome: diagnosis, current management, and emerging treatments. *Appl Clin Genet* (2014) 7:55–66. 10.2147/TACG.S58444.

40. Bui M, Whittaker G, Helenius A. Effect of M1 protein and low pH on nuclear transport of influenza virus ribonucleoproteins. *J Virol* (1996) 70:8391–401.

41. Bullido R., Gomez-Puertas P., Saiz M.J., Portela A. Influenza A virus NEP (NS2 protein) downregulates RNA synthesis of model template RNAs. *J. Virol.* 2001;75:4912–4917. doi: 10.1128/JVI.75.10.4912-4917.2001.

42. Burgui I., Aragon T., Ortin J., Nieto A. PABP1 and eIF4GI associate with influenza virus NS1 protein in viral mRNA translation initiation complexes. *J. Gen. Virol.* 2003;84:3263–3274. doi: 10.1099/vir.0.19487-0.

43. Butterfield DA, Perluigi M, Sultana R. Oxidative stress in Alzheimer's disease brain: new insights from redox proteomics. *Eur J Pharmacol.* 2006;545(1):39–50.

44. Caceres CJ, Seibert B, Cargnin Faccin F, Cardenas-Garcia S, Rajao DS, Perez DR. Influenza antivirals and animal models. FEBS Open Bio. 2022 Jun;12(6):1142-1165. doi: 10.1002/2211-5463.13416.

45. Cai Z, Deng X, Jia J, Wang D, Yuan G. Ectodysplasin A/Ectodysplasin A Receptor System and Their Roles in Multiple Diseases. Front Physiol. 2021 Dec 6;12:788411. doi: 10.3389/fphys.2021.788411. PMID: 34938205; PMCID: PMC8685516.

46. Canton M, Sánchez-Rodríguez R, Spera I, Venegas FC, Favia M, Viola A, et al. Reactive oxygen species in macrophages: sources and targets. *Front Immunol*. (2021) 12:734229. doi: 10.3389/fimmu.2021.734229.

47. Cao X. Self-regulation and cross-regulation of pattern-recognition receptor signaling in health and disease. *Nat Rev Immunol* (2016) 16(1):35. 10.1038/nri.2015.8

48. Carlin, L. E., Hemann, E. A., Zacharias, Z. R., Heusel, J. W. & Legge, K. L. Natural killer cell recruitment to the lung during influenza a virus infection is dependent on CXCR3, CCR5, and virus exposure dose. *Front. Immunol.* 9, 781 (2018).

49. Carninci P, Kasukawa T, Katayama S, et al. FANTOM Consortium; RIKEN Genome Exploration Research Group and Genome Science Group (Genome Network Project Core Group)The transcriptional landscape of the mammalian genome., Science, 2005, vol. 309 5740(pg. 1559-1563).

50. Cassidy-Stone A., Chipuk J.E., Ingerman E., Song C., Yoo C., Kuwana T., Kurth M.J., Shaw J.T., Hinshaw J.E., Green D.R., et al. Chemical inhibition of the mitochondrial division dynamin reveals its role in Bax/Bak-dependent mitochondrial outer membrane permeabilization. *Dev. Cell.* 2008;14:193–204. doi: 10.1016/j.devcel.2007.11.019.

51. Castro SM, Guerrero-Plata A, Suarez-Real G et al (2006) Antioxidant treatment ameliorates respiratory syncytial virus-induced disease and lung inflammation. Am J Respir Crit Care Med 174:1361–1369.

52. CDC. 2024. Interim guidance on the use of antiviral medications for treatment of human infections with novel influenza a viruses associated with severe human disease. Available from:https://www.cdc.gov/bird-flu/hcp/novel-av-treatment-guidance/index.html.

53. Cerato JA, da Silva EF, Porto BN. Breaking Bad: Inflammasome Activation by Respiratory Viruses. Biology (Basel). 2023 Jul 1;12(7):943. doi: 10.3390/biology12070943.Chemokine. Br J Pharmacol. 2009 Nov;158(Suppl 1):S35–7. doi: 10.1111/j.1476-5381.2009.00501_19.x. PMCID: PMC2884550.

54. Chakraborty S, Tabrizi Z, Bhatt NN, Franciosa SA, Bracko O. A Brief Overview of Neutrophils in Neurological Diseases. Biomolecules. 2023 Apr 25;13(5):743. doi: 10.3390/biom13050743. PMID: 37238612; PMCID: PMC10216532.

55. Chang Y.H., Lin H.Y., Shen F.C., Su Y.J., Chuang J.H., Lin T.K., Liou C.W., Lin C.Y., Weng S.W., Wang P.W. The Causal Role of Mitochondrial Dynamics in Regulating Innate Immunity in Diabetes. *Front. Endocrinol.* 2020;11:445. doi: 10.3389/fendo.2020.00445.

56. Channappanavar, R. & Perlman, S. Pathogenic human coronavirus infections: causes and consequences of cytokine storm and immunopathology. *Semin. Immunopathol.* 39, 529–539 (2017).

57. Chen BJ, Leser GP, Morita E, Lamb RA. Influenza virus hemagglutinin and neuraminidase, but not the matrix protein, are required for assembly and budding of plasmid-derived virus-like particles. *J Virol* (2007) 81:7111–23. doi:10.1128/JVI.00361-07.

58. Chen C, Zhuang X. Epsin 1 is a cargo-specific adaptor for the clathrin-mediated endocytosis of the influenza virus. *Proc Natl Acad Sci U S A* (2008) 105:11790–5. doi:10.1073/pnas.0803711105.

59. Chen X, Liu S, Goraya MU, Maarouf M, Huang S, Chen JL. Host Immune Response to Influenza A Virus Infection. Front Immunol. 2018 Mar 5;9:320. doi: 10.3389/fimmu.2018.00320. PMID: 29556226; PMCID: PMC5845129.

60. Cheeseman KH, Slater TF. An introduction to free radical biochemistry. *Br Med Bull.* 1993;49(3):481–493.Cheeseman KH, Slater TF. An introduction to free radical biochemistry. *Br Med Bull.* 1993;49(3):481–493.

61. Chen LF, Dailey NJ, Rao AK, Fleischauer AT, Greenwald I, Deyde VM, Moore ZS, Anderson DJ, Duffy J, Gubareva LV, Sexton DJ, Fry AM, Srinivasan A, Wolfe CR. Cluster of oseltamivir-resistant 2009 pandemic influenza A (H1N1) virus infections on a hospital ward among immunocompromised patients--North Carolina, 2009. J Infect Dis. 2011 Mar 15;203(6):838-46. doi: 10.1093/infdis/jiq124.

62. Chi, H., Pepper, M. and Thomas, P.G. (2024) 'Principles and therapeutic applications of adaptive immunity,' *Cell*, 187(9), pp. 2052–2078. doi:10.1016/j.cell.2024.03.037.

63. Choi, Y., Bowman, J. W., Jung, J. U. (2018). Autophagy During Viral Infection - a Double-Edged Sword. *Nat. Rev. Microbiol.* 16 (6), 341–354. doi: 10.1038/s41579-018-0003-6.

64. Chou YY, Heaton NS, Gao Q, Palese P, Singer RH, Lionnet T. Colocalization of different influenza viral RNA segments in the cytoplasm before viral budding as shown by single-molecule sensitivity FISH analysis. *PLoS Pathog* (2013) 9:e1003358. doi:10.1371/journal.ppat.1003358.

65. Chistiakov DA, Bobryshev YV, Orekhov AN. Neutrophil's weapons in atherosclerosis. *Exp Mol Pathol* 2015;99:663–71.

66. Chung S.C., Providencia R., Sofat R. Association between Angiotensin Blockade and Incidence of Influenza in the United Kingdom. *N. Engl. J. Med.* 2020;383:397–400. doi: 10.1056/NEJMc2005396.

67. Conenello G.M., Tisoncik J.R., Rosenzweig E., Varga Z.T., Palese P., Katze M.G. A single N66S mutation in the PB1-F2 protein of influenza A virus increases virulence by inhibiting the early interferon response *in vivo*. *J. Virol.* 2011;85:652–662.

68. Cortjens B, de Jong R, Bonsing JG, van Woensel JBM, Antonis AFG, Bem RA. Local dornase alfa treatment reduces NETs-induced airway obstruction during severe RSV infection. *Thorax*. 2018;73(6):578-580.

69. Cushman D.W., Ondetti M.A. History of the design of captopril and related inhibitors of angiotensin converting enzyme. *Hypertension.* 1991;17:589–592. doi: 10.1161/01.HYP.17.4.589.

70. Cyster J.G, Allen C.D.C. B cell responses: cell interaction dynamics and decisions. Cell. 2019;177:524–540.

71. D'Agati G., Beltre R., Sessa A., Burger A., Zhou Y., Mosimann C., White R.M. A defect in the mitochondrial protein Mpv17 underlies the transparent casper zebrafish. *Dev. Biol.* 2017;430:11–17. doi: 10.1016/j.ydbio.2017.07.017.

72. Dale DC, Person RE, Bolyard AA, Aprikyan AG, Bos C, Bonilla MA, et al. Mutations in the gene encoding neutrophil elastase in congenital and cyclic neutropenia. *Blood* (2000) 96(7):2317–22.

73. Dancey, J. T., Deubelbeiss, K. A., Harker, L. A. & Finch, C. A. Neutrophil kinetics in man. *J. Clin. Invest.* 58, 705–715 (1976).

74. Daniels R, Kurowski B, Johnson AE, Hebert DN. N-linked glycans direct the cotranslational folding pathway of influenza hemagglutinin. *Mol Cell* (2003) 11:79–90. doi:10.1016/S1097-2765(02)00821-3.

75. de Almeida, L.; da Silva, A.L.N.; Rodrigues, T.S.; Oliveira, S.; Ishimoto, A.Y.; Seribelli, A.A.; Becerra, A.; Andrade, W.A.; Ataide, M.A.; Caetano, C.C.S.; et al. Identification of Immunomodulatory Drugs That Inhibit Multiple Inflammasomes and Impair SARS-CoV-2 Infection. *Sci. Adv.* 2022, *8*, 5400.

76. De Duve C, Bauduhuin P. peroxisomes (microbodies and related particles) *Physiol Rev.* 1966;46:323–357.

77. De Jong J.C., Rimmelzwaan G.F., Fouchier R.A., Osterhaus A.D. Influenza virus: A master of metamorphosis. *J. Infect.* 2000;40:218–228. doi: 10.1053/jinf.2000.0652.

78. de Jong M.D., Tran T.T., Truong H.K., Vo M.H., Smith G.J., Nguyen V.C., Bach V.C., Phan T.Q., Do Q.H., Guan Y., et al. Oseltamivir resistance during treatment of influenza A (H5N1) infection. *N. Engl. J. Med.* 2005;353:2667–2672. doi: 10.1056/NEJMoa054512.

79. De La Fuente M, Miquel J, Catalan MP et al (2002) The amount of thiolic antioxidant ingestion related to improve several immune functions is higher in aged than in adult mice. Free Radic Res 36:119–126.

80. Dembic, Z. (2015) *The cytokines of the immune system: The role of cytokines in disease related to immune response*. London, United Kingdom: Academic Press is an imprint of Elsevier.

81. Desmet E.A., Bussey K.A., Stone R., Takimoto T. Identification of the N-terminal domain of the influenza virus PA responsible for the suppression of host protein synthesis. *J. Virol.* 2013;87:3108–3118. doi: 10.1128/JVI.02826-12.

82. de Vries E, Tscherne DM, Wienholts MJ, Cobos-Jimenez V, Scholte F, Garcia-Sastre A, et al. Dissection of the influenza A virus endocytic routes reveals macropinocytosis as an alternative entry pathway. *PLoS Pathog* (2011) 7:e1001329. doi:10.1371/journal.ppat.1001329.

83. Deng, X.; Yan, Z.; Luo, Y.; Xu, J.; Cheng, F.; Li, Y.; Engelhardt, J.F.; Qiu, J. In Vitro Modeling of Human Bocavirus 1 Infection of Polarized Primary Human Airway Epithelia. *J. Virol.* 2013, *87*, 4097–4102.

84. Deng, X.; Zou, W.; Xiong, M.; Wang, Z.; Engelhardt, J.F.; Ye, S.Q.; Yan, Z.; Qiu, J. Human Parvovirus Infection of Human Airway Epithelia Induces Pyroptotic Cell Death by Inhibiting Apoptosis. *J. Virol.* 2017, *91*, e01533-17.

85. Denk, D., Singh, A., Kasler, H., Lucia Alcober Boquet, Davide D'Amico, Gorol, J. and Greten, F. (2024). Impact of urolithin A supplementation, a mitophagy activator on mitochondrial health of immune cells (MitoIMMUNE): A randomized, double-blind, placebo-controlled trial in healthy adults. *Journal of clinical oncology*, 42(16_suppl), pp.e14562–e14562. doi:https://doi.org/10.1200/jco.2024.42.16_suppl.e14562.

86. Devi, S. *et al.* Neutrophil mobilization via plerixafor- mediated CXCR4 inhibition arises from lung demargination and blockade of neutrophil homing to the bone marrow. *J. Exp. Med.* 210, 2321–2336 (2013).

87. Dhanwani R, Khan M, Alam SI et al (2011) Differential proteome analysis of Chikungunya virus infected new-born mice tissues reveal implication of stress, inflammatory and apoptotic pathways in disease pathogenesis. Proteomics 11:1936–1951.

88. Dhanwani R, Khan M, Bhaskar AS et al (2012) Characterization of Chikungunya virus infection in human neuroblastoma SH-SY5Y cells: role of apoptosis in neuronal cell death. Virus Res 163(2012):563–572.

89. Dias A., Bouvier D., Crepin T., McCarthy A.A., Hart D.J., Baudin F., Cusack S., Ruigrok R.W. The cap-snatching endonuclease of influenza virus polymerase resides in the PA subunit. *Nature.* 2009;458:914–918.

90. Dienz O, Rud JG, Eaton SM, et al. Essential role of IL-6 in protection against H1N1 influenza virus by promoting neutrophil survival in the lung. *Mucosal Immunol.* 2012;5(3):258-266.

91. Dijkman, R.; Koekkoek, S.M.; Molenkamp, R.; Schildgen, O.; van der Hoek, L. Human Bocavirus Can Be Cultured in Differentiated Human Airway Epithelial Cells. *J. Virol.* 2009, *83*, 7739–7748.

92. do Amaral MA, Paredes LC, Padovani BN, Mendonça-Gomes JM, Montes LF, Câmara NOS, Morales Fénero C. Mitochondrial connections with immune system in Zebrafish. Fish Shellfish Immunol Rep. 2021 Aug 14;2:100019. doi: 10.1016/j.fsirep.2021.100019. PMID: 36420514; PMCID: PMC9680083.

93. Domínguez-Oliva A, Hernández-Ávalos I, Martínez-Burnes J, Olmos-Hernández A, Verduzco-Mendoza A, Mota-Rojas D. The Importance of Animal Models in Biomedical Research: Current Insights and Applications. Animals (Basel). 2023 Mar 31;13(7):1223. doi: 10.3390/ani13071223.

94. Dou D, da Silva DV, Nordholm J, Wang H, Daniels R. Type II transmembrane domain hydrophobicity dictates the cotranslational dependence for inver- sion. *Mol Biol Cell* (2014) 25:3363–74. doi:10.1091/mbc.E14-04-0874.

95. Dou D, Revol R, Östbye H, Wang H and Daniels R (2018) Influenza A Virus Cell Entry, Replication, Virion Assembly and Movement. Front. Immunol. 9:1581. doi: 10.3389/fimmu.2018.01581.

96. Dreher D, Junod AF. Role of oxygen free radicals in cancer development. *Eur J Cancer.* 1996;32A(1):30–38.

97. Dröge W, Eck HP, Mihm S (1994) Oxidant-antioxidant status in human immunodeficiency virus infection. Oxygen Radic Biol Syst Methods Enzymol 233:594–601.

98. Dröge W. Free radicals in the physiological control of cell function. Review. *Physiol. Rev.* 2002;82:47–95.

99. Dyer DP, Salanga CL, Volkman BF, Kawamura T & Handel TM (2016) The dependence of chemokine-glycosaminoglycan interactions on chemokine oligomerization. *Glycobiology* 26, 312–326.

100. Eash KJ, Greenbaum AM, Gopalan PK & Link DC (2010) CXCR2 and CXCR4 antagonistically regulate neutrophil trafficking from murine bone marrow. *J Clin Invest* 120, 2423–2431.

101. Eichholz, K.; Bru, T.; Thu, T.; Tran, P.; Fernandes, P.; Welles, H.; Mennechet, F.J.D.; Manel, N.; Alves, P.; Perreau, M.; et al. Immune-Complexed Adenovirus Induce AIM2-Mediated Pyroptosis in Human Dendritic Cells. *PLoS Pathog.* 2016, *12*, e1005871.

102. Eisfeld AJ, Kawakami E, Watanabe T, Neumann G, Kawaoka Y. RAB11A is essential for transport of the influenza virus genome to the plasma mem- brane. *J Virol* (2011) 85:6117–26. doi:10.1128/JVI.00378-11.

103. Eisfeld A.J., Neumann G., Kawaoka Y. Influenza A virus isolation, culture and identification. *Nat. Protoc.* 2014;9:2663–2681. doi: 10.1038/nprot.2014.180.

104. Escada-Rebelo S, Mora FG, Sousa AP, Almeida-Santos T, Paiva A, Ramalho-Santos J. Fluorescent probes for the detection of reactive oxygen species in human spermatozoa. Asian J Androl. 2020 Sep-Oct;22(5):465-471. doi: 10.4103/aja.aja_132_19.

105. Favier A, Sappey C, Leclerc P et al (1994) Antioxidant status and lipid peroxidation in patients infected with HIV. Chem-Biol Interact 91(2–3):165–180.

106. Feng M., Deerhake M.E., Keating R., Thaisz J., Xu L., Tsaih S.W., Smith R., Ishige T., Sugiyama F., Churchill G.A., et al. Genetic analysis of blood pressure in 8 mouse intercross populations. *Hypertension.* 2009;54:802–809. doi: 10.1161/HYPERTENSIONAHA.109.134569.

107. Feng S., Yang Y., Mei Y., Ma L., Zhu D.E., Hoti N., Castanares M., Wu M. Cleavage of RIP3 inactivates its caspase-independent apoptosis pathway by removal of kinase domain. *Cell Signal.* 2007;19:2056–2067.

108. Ferko, B., J. Stasakova, J. Romanova, C. Kittel, S. Sereinig, H. Katinger, and A. Egorov. 2004. Immunogenicity and protection efficacy of replication-deficient influenza A viruses with altered NS1 genes. J. Virol. 78:13037-13045.

109. Fernandez-Sesma A, Marukian S, Ebersole BJ, Kaminski D, Park MS, Yuen T, Sealfon SC, García-Sastre A, Moran TM. Influenza virus evades innate and adaptive immunity via the NS1 protein. J Virol. 2006 Jul;80(13):6295-304. doi: 10.1128/JVI.02381-05.

110. Fitzgerald K.A, Kagan J.C. Toll-like receptors and the control of immunity. Cell. 2020;180:1044–1066.

111. Fodor E. The RNA polymerase of influenza a virus: mechanisms of viral transcription and replication. *Acta Virol* (2013) 57:113–22. doi:10.4149/ av_2013_02_113.

112. Fox, T.G.; Christenson, J.C. Influenza and Parainfluenza Viral Infections in Children. *Pediatr. Rev.* 2014, *35*, 217–228.

113. Francis T Jr. On the doctrine of original antigenic sin. Proc Am Philosoph Soc. 1960;104:572–8.

114. Fu, J. et al. The clinical implication of dynamic neutrophil to lymphocyte ratio and D-dimer in COVID-19: a retrospective study in Suzhou China. *Thromb. Res.* 192, 3–8 (2020).

115. Fuchs J, Emerit I, Levy A et al (1995) Clastogenic factors in plasma of HIV-1 infected patients. Free Radic Biol Med 19:843–848.

116. Fukuyama S., Katsura H., Zhao D., Ozawa M., Ando T., Shoemaker J.E., Ishikawa I., Yamada S., Neumann G., Watanabe S., et al. Multi-spectral fluorescent reporter influenza viruses (Color-flu) as powerful tools for in vivo studies. *Nat. Commun.* 2015;6:6600. doi: 10.1038/ncomms7600.

117. Gabor K.A., Goody M.F., Mowel W.K., Breitbach M.E., Gratacap R.L., Witten P.E., Kim C.H. Influenza A virus infection in zebrafish recapitulates mammalian infection and sensitivity to anti-influenza drug treatment. *Dis. Model. Mech.* 2014;7:1227–1237. doi: 10.1242/dmm.014746.

118. Gack M.U., Albrecht R.A., Urano T., Inn K.S., Huang I.C., Carnero E., Farzan M., Inoue S., Jung J.U., Garcia-Sastre A. Influenza A virus NS1 targets the ubiquitin ligase TRIM25 to evade recognition by the host viral RNA sensor RIG-I. *Cell Host Microbe.* 2009;5:439–449. doi: 10.1016/j.chom.2009.04.006.

119. Galani, IE., Rovina, N., Lampropoulou, V. *et al.* Untuned antiviral immunity in COVID-19 revealed by temporal type I/III interferon patterns and flu comparison. *Nat Immunol* 22, 32–40 (2021). https://doi.org/10.1038/s41590-020-00840-x.

120. Gao S., Song L., Li J., Zhang Z., Peng H., Jiang W., Wang Q., Kang T., Chen S., Huang W. Influenza A virus-encoded NS1 virulence factor protein inhibits innate immune response by targeting IKK. *Cell Microbiol.* 2012;14:1849–1866. doi: 10.1111/cmi.12005.

121. Garcia G.R., Noyes P.D., Tanguay R.L. Advancements in zebrafish applications for 21st century toxicology. *Pharmacol. Ther.* 2016;161:11–21. doi: 10.1016/j.pharmthera.2016.03.009.

122. Garcia M.A., Gil J., Ventoso I., Guerra S., Domingo E., Rivas C., Esteban M. Impact of protein kinase PKR in cell biology: From antiviral to antiproliferative action. *Microbiol. Mol. Biol. Rev.* 2006;70:1032–1060.

123. Garcia-Sastre A., Egorov A., Matassov D., Brandt S., Levy D.E., Durbin J.E., Palese P., Muster T. Influenza A virus lacking the NS1 gene replicates in interferon-deficient systems. *Virology.* 1998;252:324–330. doi: 10.1006/viro.1998.9508.

124. García-Sastre A. Induction and evasion of type I interferon responses by influenza viruses. Virus Res. 2011 Dec;162(1-2):12-8. doi: 10.1016/j.virusres.2011.10.017.

125. Garozzo A, Tempera G, Ungheri D, Timpanaro R, Castro A. N-acetylcysteine synergizes with oseltamivir in protecting mice from lethal influenza infection. Int J Immunopathol Pharmacol. 2007 Apr-Jun;20(2):349-54. doi: 10.1177/039463200702000215.

126. Geiler J, Michaelis M, Naczk P, Leutz A, Langer K, Doerr HW, Cinatl J Jr. N-acetyl-L-cysteine (NAC) inhibits virus replication and expression of pro-inflammatory molecules in A549 cells infected with highly pathogenic H5N1 influenza A virus. Biochem Pharmacol. 2010 Feb 1;79(3):413-20. doi: 10.1016/j.bcp.2009.08.025.

127. Genestra M. Oxyl radicals, redox-sensitive signalling cascades and antioxidants. Review. *Cell Signal.* 2007;19:1807–1819.

128. Golonka, R. M. et al. Harnessing innate immunity to eliminate SARS-CoV-2 and ameliorate COVID-19 disease. *Physiol. Genomics* 52, 217–221 (2020).

129. Gonsette RE. Neurodegeneration in multiple sclerosis: the role of oxidative stress and excitotoxicity. *J Neurol Sci.* 2008;274(1–2):48–53.

130. Goody M., Jurczyszak D., Kim C., Henry C. Influenza A Virus Infection Damages Zebrafish Skeletal Muscle and Exacerbates Disease in Zebrafish Modeling Duchenne Muscular Dystrophy. *PLoS Curr.* 2017;9 doi: 10.1371/currents.md.8a7e35c50fa2b48156799d3c39788175.

131. Gorlino, C. V. *et al.* Neutrophils exhibit differential requirements for homing molecules in their lymphatic and blood trafficking into draining lymph nodes. *J. Immunol.* 193, 1966–1974 (2014).

132. Goubau D, Schlee M, Deddouche S, Pruijssers AJ, Zillinger T, Goldeck M, et al. Antiviral immunity via RIG-I-mediated recognition of RNA bearing 5’-diphosphates. *Nature* (2014) 514(7522):372–5. 10.1038/nature13590.

133. Graef K.M., Vreede F.T., Lau Y.F., McCall A.W., Carr S.M., Subbarao K., Fodor E. The PB2 subunit of the influenza virus RNA polymerase affects virulence by interacting with the mitochondrial antiviral signaling protein and inhibiting expression of beta interferon. *J. Virol.* 2010;84:8433–8445. doi: 10.1128/JVI.00879-10.

134. Grant EJ, Quinones-Parra SM, Clemens EB, Kedzierska K. Human influenza viruses and CD8(+) T cell responses. *Curr Opin Virol* (2016) 16:132–42. 10.1016/j.coviro.2016.01.016.

135. Gregg MB, Hinman AR, Craven RB. The Russian flu. Its history and implications for this year’s influenza season. JAMA. 1978;240:2260–3.

136. Griffith JW, Sokol CL & Luster AD (2014) Chemokines and chemokine receptors: positioning cells for host defense and immunity. *Annu Rev Immunol* 32, 659–702.

137. Gross E, Sevier CS, Heldman N, Vitu E, Bentzur M, Kaiser CA, et al. Generating disulfides enzymatically: reaction products and electron acceptors of the endoplasmic reticulum thiol oxidase Ero1p. *Proc Nat Acad Sci USA.* 2006;103(2):299–304.

138. Guan, W.-J. et al. Clinical characteristics of coronavirus disease 2019 in China. *N. Engl. J. Med.* https://doi.org/10.1056/NEJMoa2002032 (2020).

139. Guan Z., Liu D., Mi S., Zhang J., Ye Q., Wang M., Gao G.F., Yan J. Interaction of Hsp40 with influenza virus M2 protein: Implications for PKR signaling pathway. *Protein Cell.* 2010;1:944–955. doi: 10.1007/s13238-010-0115-x.

140. Guilligay D, Tarendeau F, Resa-Infante P, Coloma R, Crepin T, Sehr P, et al. The structural basis for cap binding by influenza virus polymerase subunit PB2. *Nat Struct Mol Biol* (2008) 15:500–6. doi:10.1038/nsmb.1421.

141. Gupta K., Phan N., Wang Q., Liu B. Necroptosis in cardiovascular disease - a new therapeutic target. *J Mol Cell Cardiol.* 2018;118:26–35.

142. Hadjadj, J. et al. Impaired type I interferon activity and exacerbated inflammatory responses in severe COVID-19 patients. Preprint at *medRxiv* https://doi.org/10.1101/2020.04.19.20068015 (2020).

143. Halbach K., Ulrich N., Goss K.U., Seiwert B., Wagner S., Scholz S., Luckenbach T., Bauer C., Schweiger N., Reemtsma T. Yolk Sac of Zebrafish Embryos as Backpack for Chemicals? *Environ. Sci. Technol.* 2020;54:10159–10169. doi: 10.1021/acs.est.0c02068.

144. Hall C., Flores M.V., Storm T., Crosier K., Crosier P. The zebrafish lysozyme C promoter drives myeloid-specific expression in transgenic fish. *BMC Dev. Biol.* 2007;7:42. doi: 10.1186/1471-213X-7-42.

145. Halliwell B. Antioxidants in human health and disease. *Annu Rev Nutr.* 1996;16:33–50. doi: 10.1146/annurev.nu.16.070196.000341.

146. Halliwell B, Gutteridge JMC. *Free radicals in biology and medicine.* 4th. Oxford, UK: Clarendon Press; 2007.

147. Hampton, H. R. & Chtanova, T. The lymph node neutrophil. *Semin. Immunol.* 28, 129–136 (2016).

148. Han, M.; Ishikawa, T.; Bermick, J.R.; Rajput, C.; Lei, J.; Goldsmith, A.M.; Jarman, C.R.; Lee, J.; Bentley, J.K.; Hershenson, M.B. IL-1β Prevents ILC2 Expansion, Type 2 Cytokine Secretion, and Mucus Metaplasia in Response to Early-Life Rhinovirus Infection in Mice. *Allergy* 2020, *75*, 2001–2015.

149. Han, M.; Bentley, J.K.; Rajput, C.; Lei, J.; Ishikawa, T.; Jarman, C.R.; Lee, J.; Goldsmith, A.M.; Jackson, W.T.; Hoenerhoff, M.J.; et al. Inflammasome Activation Is Required for Human Rhinovirus-Induced Airway Inflammation in Naive and Allergen-Sensitized Mice. *Soc. Mucosal Immunol.* 2019, *12*, 958–968.

150. Hanna S, Etzioni A. Leukocyte adhesion deficiencies. *Ann N Y Acad Sci* (2012) 1250:50–5. 10.1111/j.1749-6632.2011.06389.x.

151. Haney, J., Vijayakrishnan, S., Streetley, J. *et al.* Coinfection by influenza A virus and respiratory syncytial virus produces hybrid virus particles. *Nat Microbiol* 7, 1879–1890 (2022). https://doi.org/10.1038/s41564-022-01242-5.

152. Hao W, Wang L, Li S. Roles of the Non-Structural Proteins of Influenza A Virus. Pathogens. 2020 Oct 3;9(10):812. doi: 10.3390/pathogens9100812. PMID: 33023047; PMCID: PMC7600879.

153. Hause BM, Collin EA, Liu R, Huang B, Sheng Z, Lu W, et al. Characterization of a novel influenza virus in cattle and swine: proposal for a new genus in the Orthomyxoviridae family. MBio (2014) 5:e31–14. doi:10.1128/mBio. 00031-14.

154. He L, He T, Farrar S, Ji L, Liu T, Ma X. Antioxidants Maintain Cellular Redox Homeostasis by Elimination of Reactive Oxygen Species. Cell Physiol Biochem. 2017;44(2):532-553. doi: 10.1159/000485089.

155. Henn BC, Coull BA, Wright RO. Chemical mixtures and children's health. *Current Opinion in Pediatrics.* 2014;26:223–229.

156. Hernandez N., Melki I., Jing H., Habib T., Huang S.S.Y., Danielson J., Kula T., Drutman S., Belkaya S., Rattina V., et al. Life-threatening influenza pneumonitis in a child with inherited IRF9 deficiency. *J. Exp. Med.* 2018;215:2567–2585. doi: 10.1084/jem.20180628.

157. Herrero-Cervera, A., Soehnlein, O. & Kenne, E. Neutrophils in chronic inflammatory diseases. *Cell Mol Immunol* 19, 177–191 (2022). https://doi.org/10.1038/s41423-021-00832-3.

158. Herrmann JM, Dick TP. Redox biology on the rise. *Biol Chem*. 2012;393(9):999-1004.

159. Heusinkveld LE, Majumdar S, Gao JL, McDermott DH, Murphy PM. WHIM Syndrome: from Pathogenesis Towards Personalized Medicine and Cure. J Clin Immunol. 2019 Aug;39(6):532-556. doi: 10.1007/s10875-019-00665-w.

160. Hierholzer J.C., Killington R.A. Virus isolation and quantitation. In: Mahy B.W.J., Kangro H.O., editors. *Virology Methods Manual.* Academic Press; Cambridge, MA, USA: 1996. pp. 25–46.

161. Hirano K, Chen WS, Chueng AL, Dunne AA, Seredenina T, Filippova A, Ramachandran S, Bridges A, Chaudry L, Pettman G, Allan C, Duncan S, Lee KC, Lim J, Ma MT, Ong AB, Ye NY, Nasir S, Mulyanidewi S, Aw CC, Oon PP, Liao S, Li D, Johns DG, Miller ND, Davies CH, Browne ER, Matsuoka Y, Chen DW, Jaquet V, Rutter AR. Discovery of GSK2795039, a Novel Small Molecule NADPH Oxidase 2 Inhibitor. Antioxid Redox Signal. 2015 Aug 10;23(5):358-74. doi: 10.1089/ars.2014.6202.

162. Hiscott J, Lin R, Nakhaei P, Paz S. MasterCARD: a priceless link to innate immunity. *Trends Mol Med* (2006) 12(2):53–6. 10.1016/j.molmed.2005.12.003.

163. Ho AW, Prabhu N, Betts RJ, Ge MQ, Dai X, Hutchinson PE, et al. Lung CD103+ dendritic cells efficiently transport influenza virus to the lymph node and load viral antigen onto MHC class I for presentation to CD8 T cells. *J Immunol* (2011) 187(11):6011–21.

164. Hobson-West P., Davies A. Societal Sentience: Constructions of the public in animal research policy and practice. *Sci. Technol. Hum. Values.* 2018;43:671–693. doi: 10.1177/0162243917736138.

165. Hock H, Hamblen MJ, Rooke HM, Traver D, Bronson RT, Cameron S, et al. Intrinsic requirement for zinc finger transcription factor Gfi-1 in neutrophil differentiation. *Immunity* (2003) 18(1):109–20. 10.1016/S1074-7613(02)00501-0.

166. Hosakote YM, Liu T, Castro SM et al (2009) Respiratory syncytial virus induces oxidative stress by modulating antioxidant enzymes. Am J Respir Cell Mol Biol 41:348–357.

167. Hosakote YM, Jantzi PD, Esham DL et al (2011) Viral-mediated inhibition of antioxidant enzymes contributes to the pathogenesis of severe respiratory syncytial virus bronchiolitis. Am J Respir Crit Care Med 183:1550–1560.

168. Horst D., Verweij M.C., Davison A.J., Ressing M.E., Wiertz E.J. Viral evasion of T cell immunity: Ancient mechanisms offering new applications. *Curr. Opin. Immunol.* 2011;23:96–103.

169. Howe K, Clark MD, Torroja CF, et al. The zebrafish reference genome sequence and its relationship to the human genome. *Nature.* 2013 Apr;496(7446):498-503. https://doi.org/10.1038/nature12111.

170. Howley, Peter M., and David M. Knipe. Fields Virology: Emerging Viruses, Wolters Kluwer Health, 2020.

171. Hsu AY, Wang D, Liu S, Lu J, Syahirah R, Bennin DA, Huttenlocher A, Umulis DM, Wan J and Deng Q. Phenotypical microRNA screen reveals a noncanonical role of CDK2 in regulating neutrophil migration. *Proc Natl Acad Sci U S A*. 2019;116:18561-18570. (Hsu, 2019a)

172. Hsu AY, Liu S, Syahirah R, Brasseale KA, Wan J and Deng Q. Inducible overexpression of zebrafish microRNA-722 suppresses chemotaxis of human neutrophil like cells. *Mol Immunol*. 2019;112:206-214. (Hsu, 2019b)

173. Hsu S.F., Su W.C., Jeng K.S., Lai M.M. A host susceptibility gene, DR1, facilitates influenza A virus replication by suppressing host innate immunity and enhancing viral RNA replication. *J. Virol.* 2015;89:3671–3682. doi: 10.1128/JVI.03610-14..

174. Huang RT, Rott R, Klenk HD. Influenza viruses cause hemolysis and fusion of cells. *Virology* (1981) 110:243–7. doi:10.1016/0042-6822(81)90030-1.Hughes CE, Nibbs RJB. A guide to chemokines and their receptors. FEBS J. 2018 Aug;285(16):2944-2971. doi: 10.1111/febs.14466. Epub 2018 Apr 24. PMID: 29637711; PMCID: PMC6120486.

175. Huang SH, Cao XJ, Liu W et al (2010) Inhibitory effect of melatonin on lung oxidative stress induced by respiratory syncytial virus infection in mice. J Pineal Res 48(2):109–116. doi:10.1111/j.1600-079X.2009.00733.x.

176. Hussain M, Galvin HD, Haw TY, Nutsford AN, Husain M. Drug resistance in influenza A virus: the epidemiology and management. Infect Drug Resist. 2017 Apr 20;10:121-134. doi: 10.2147/IDR.S105473.

177. Imai Y., Kuba K., Rao S., Huan Y., Guo F., Guan B., Yang P., Sarao R., Wada T., Leong-Poi H., et al. Angiotensin-converting enzyme 2 protects from severe acute lung failure. *Nature.* 2005;436:112–116. doi: 10.1038/nature03712.

178. Introne WJ, Westbroek W, Golas GA, Adams D. Chediak-Higashi syndrome. In: Pagon RA, Adam MP, Ardinger HH, Wallace SE, Amemiya A, Bean LJH, et al., editors. *GeneReviews(R)*. Seattle, WA: University of Washington, Seattle; (1993).

179. Ireland A. S., Oliver T. G. (2020). Neutrophils create an ImpeNETrable shield between tumor and cytotoxic immune cells. *Immunity* 52, 729–731. 10.1016/j.immuni.2020.04.009.

180. Ismayil, A., Yang, M., Liu, Y. (2020). Role of Autophagy During Plant-Virus Interactions. *Semin. Cell Dev. Biol.* 101, 36–40. doi: 10.1016/j.semcdb.2019.07.001.

181. Iwai A., Shiozaki T., Kawai T., Akira S., Kawaoka Y., Takada A., Kida H., Miyazaki T. Influenza A virus polymerase inhibits type I interferon induction by binding to interferon beta promoter stimulator 1. *J. Biol. Chem.* 2010;285:32064–32074. doi: 10.1074/jbc.M110.112458.

182. Iwasaki A, Medzhitov R. Regulation of adaptive immunity by the innate immune system. Science. 2010 Jan 15;327(5963):291-5. doi: 10.1126/science.

183. Jackson, D.J.; Glanville, N.; Trujillo-Torralbo, M.B.; Shamji, B.W.H.; Del-Rosario, J.; Mallia, P.; Edwards, M.J.; Walton, R.P.; Edwards, M.R.; Johnston, S.L. Interleukin-18 Is Associated with Protection against Rhinovirus-Induced Colds and Asthma Exacerbations. *Clin. Infect. Dis.* 2015, *60*, 1528–1531.

184. Jagger BW, Wise HM, Kash JC, Walters KA, Wills NM, Xiao YL, et al. An overlapping protein-coding region in influenza A virus segment 3 modulates the host response. Science. 2012;337(6091):199–204.

185. Jassey, A., Jackson, W.T. Viruses and autophagy: bend, but don't break. *Nat Rev Microbiol* 22, 309–321 (2024). https://doi.org/10.1038/s41579-023-00995-y.

186. Ji ZX, Wang XQ, Liu XF. NS1: A Key Protein in the "Game" Between Influenza A Virus and Host in Innate Immunity. Front Cell Infect Microbiol. 2021 Jul 13;11:670177. doi: 10.3389/fcimb.2021.670177.

187. Jia X, Chua BY, Loh L, Koutsakos M, Kedzierski L, Olshansky M, Heath WR, Chang SY, Xu J, Wang Z, Kedzierska K. High expression of CD38 and MHC class II on CD8+ T cells during severe influenza disease reflects bystander activation and trogocytosis. Clin Transl Immunology. 2021 Sep 8;10(9):e1336. doi: 10.1002/cti2.1336.

188. Jiang T, Wang Y, Chen X, Xia W, Xue S, Gu L, Guo L, Lin H. Neutrophil extracellular traps (NETs)-related lncRNAs signature for predicting prognosis and the immune microenvironment in breast cancer. Front Cell Dev Biol. 2023 Feb 2;11:1117637. doi: 10.3389/fcell.2023.1117637.

189. Jing X, Ma C, Ohigashi Y, Oliveira FA, Jardetzky TS, Pinto LH, Lamb RA. 2008. Functional studies indicate amantadine binds to the pore of the influenza A virus M2 proton-selective ion channel. *Proc Natl Acad Sci U S A* 105:10967–10972. doi: 10.1073/pnas.0804958105.

190. Johnston, S.L.; Pattemore, P.K.; Sanderson, G.; Smith, S.; Lampe, F.; Josephs, L.; Symington, P.; Toole, S.O.; Myint, S.H.; Tyrrell, D.A.J.; et al. Community Study of Role of Viral Infections in Exacerbations of Asthma in 9-11 Year Old Children. *BMJ* 1995, *310*, 1225–1229.

191. Jordan EO. Epidemic Influenza: A Survey. Chicago: American Medical Association; 1927.

192.

193. Jota Baptista C.V., Faustino-Rocha A.I., Oliveira P.A. Animal models in pharmacology: A brief history awarding the nobel prizes for physiology or medicine. *Pharmacology.* 2021;106:356–368. doi: 10.1159/000516240.

194. Joubert PE, Werneke SW, de la Calle C et al (2012) Chikungunya virus-induced autophagy delays caspase-dependent cell death. J Exp Med 209(5):1029–1047.

195. Junqueira, C.; Crespo, Â.; Ranjbar, S.; de Lacerda, L.B.; Lewandrowski, M.; Ingber, J.; Parry, B.; Ravid, S.; Clark, S.; Schrimpf, M.R.; et al. FcγR-Mediated SARS-CoV-2 Infection of Monocytes Activates Inflammation. *Nature* 2022, *606*, 576–584.

196. Kallikourdis M, Trovato AE, Anselmi F, Sarukhan A, Roselli G, Tassone L, Badolato R, Viola A. The CXCR4 mutations in WHIM syndrome impair the stability of the T-cell immunologic synapse. Blood. 2013 Aug 1;122(5):666-73. doi: 10.1182/blood-2012-10-461830. Epub 2013 Jun 21.

197. Kanneganti, T.-D.; Body-Malapel, M.; Amer, A.; Park, J.-H.; Whitfield, J.; Franchi, L.; Taraporewala, Z.F.; Miller, D.; Patton, J.T.; Inohara, N.; et al. Critical Role for Cryopyrin/Nalp3 in Activation of Caspase-1 in Response to Viral Infection and Double-Stranded RNA. *J. Biol. Chem.* 2006, *281*, 36560–36568.

198. Kapoor, A.; Slikas, E.; Simmonds, P.; Chieochansin, T.; Naeem, A.; Shaukat, S.; Alam, M.M.; Sharif, S.; Angez, M.; Zaidi, S.; et al. A Newly Identified Bocavirus Species in Human Stool. *J. Infect. Dis.* 2009, *199*, 196–200.

199. Kawai T, Takahashi K, Sato S, Coban C, Kumar H, Kato H, Ishii KJ, Takeuchi O, Akira S. IPS-1, an adaptor triggering RIG-I- and Mda5-mediated type I interferon induction. Nat Immunol. 2005 Oct;6(10):981-8. doi: 10.1038/ni1243. Epub 2005 Aug 28. PMID: 16127453.

200. Kawai T, Akira S. The role of pattern-recognition receptors in innate immunity: update on toll-like receptors. *Nat Immunol* (2010) 11(5):373. 10.1038/ni.1863.

201. Kawai T, Malech HL. WHIM syndrome: congenital immune deficiency disease. *Curr Opin Hematol* 2009;16:20–6.

202. Kawaoka Y, Krauss S, Webster RG. Avian-to-human transmission of the PB1 gene of influenza A viruses in the 1957 and 1968 pandemics. J Virol. 1989;63: 4603–8.

203. Kemler I, Whittaker G, Helenius A. Nuclear import of microinjected influenza virus ribonucleoproteins. *Virology* (1994) 202:1028–33. doi:10.1006/viro.1994.1432.

204. Khan Z., Shen X.Z., Bernstein E.A., Giani J.F., Eriguchi M., Zhao T.V., Gonzalez-Villalobos R.A., Fuchs S., Liu G.Y., Bernstein K.E. Angiotensin-converting enzyme enhances the oxidative response and bactericidal activity of neutrophils. *Blood.* 2017;130:328–339. doi: 10.1182/blood-2016-11-752006.

205. Khoury MK, Gupta K, Franco SR, Liu B. Necroptosis in the Pathophysiology of Disease. Am J Pathol. 2020 Feb;190(2):272-285. doi: 10.1016/j.ajpath.2019.10.012. Epub 2019 Nov 26.

206. Kilbourne ED, Smith C, Brett I, Pokorny BA, Johansson B, Cox N. The total influenza vaccine failure of 1947 revisited: major intrasubtypic antigenic change can

explain failure of vaccine in a post-World War II epidemic. Proc Natl Acad Sci U S A. 2002;99:10748–52.

207. Kim HJ, Jeong MS, Jang SB. Structure and Activities of the NS1 Influenza Protein and Progress in the Development of Small-Molecule Drugs. *International Journal of Molecular Sciences*. 2021; 22(8):4242. https://doi.org/10.3390/ijms22084242.

208. Kittel C., Sereinig S., Ferko B., Stasakova J., Romanova J., Wolkerstorfer A., Katinger H., Egorov A. Rescue of influenza virus expressing GFP from the NS1 reading frame. *Virology.* 2004;324:67–73. doi: 10.1016/j.virol.2004.03.035.

209. Klein C, Grudzien M, Appaswamy G, Germeshausen M, Sandrock I, Schaffer AA, et al. HAX1 deficiency causes autosomal recessive severe congenital neutropenia (Kostmann disease). *Nat Genet* (2007) 39(1):86–92. 10.1038/ng1940.

210. Köhler, A. *et al.* G-CSF-mediated thrombopoietin release triggers neutrophil motility and mobilization from bone marrow via induction of Cxcr2 ligands. *Blood* 117, 4349–4357 (2011).

211. Kohlmeier JE, Cookenham T, Roberts AD, Miller SC, Woodland DL. Type I interferons regulate cytolytic activity of memory CD8(+) T cells in the lung airways during respiratory virus challenge. Immunity. 2010 Jul 23;33(1):96-105. doi: 10.1016/j.immuni.2010.06.016.

212. Komaravelli, N. & Casola, A. Respiratory viral infections and subversion of cellular antioxidant defenses. *J. Pharmacogenomics Pharmacoproteomics* 5, 1000141 (2014).

213. Krammer F, García-Sastre A, Palese P. Is It Possible to Develop a "Universal" Influenza Virus Vaccine? Potential Target Antigens and Critical Aspects for a Universal Influenza Vaccine. Cold Spring Harb Perspect Biol. 2018 Jul 2;10(7):a028845. doi: 10.1101/cshperspect.a028845. (Krammer, 2018a)

214. Krammer, F., Smith, G. J. D., Fouchier, R. A. M., Peiris, M., Kedzierska, K., Doherty, P. C., Palese, P., Shaw, M. L., Treanor, J., Webster, R. G., & García-Sastre, A. (2018). Influenza. Nature Reviews Disease Primers, 4(1), 3. https://doi.org/10.1038/s41572-018-0002-y. (Krammer, 2018b)

215. Kreijtz JH, Fouchier RA, Rimmelzwaan GF. Immune responses to influenza virus infection. *Virus Res* (2011) 162(1–2):19–30. 10.1016/j.virusres.2011.09.022.

216. Kufareva I, Salanga CL & Handel TM (2015) Chemokine and chemokine receptor structure and interactions: implications for therapeutic strategies. *Immunol Cell Biol* 93, 372–383.

217. Kuhns DB, Alvord WG, Heller T, Feld JJ, Pike KM, Marciano BE, et al. Residual NADPH oxidase and survival in chronic granulomatous disease. *N Engl J Med* (2010) 363(27):2600–10. 10.1056/NEJMoa1007097.

218. Kuiken T, Taubenberger JK. Pathology of human influenza revisited. Vaccine. 2008;26(Suppl. 4):D59–66. Matrosovich MN, Gambaryan AS, Klenk HD. Receptor specificity of influenza viruses and its alteration during interspecies transmission. In: Klenk HD, Matrosovich M, Stech J, editors. Avian Influenza. Basel: Karger; 2008. p. 134–55.

219. Kumar B.V, Connors T.J, Farber D.L. Human T cell development, localization, and function throughout Life. Immunity . 2018;48:202–213.

220. Kumar H, Kawai T, Akira S. Pathogen recognition by the innate immune system. *Int Rev Immunol* (2011) 30(1):16–34. 10.3109/08830185.2010.529976

221. Lamb JR, Eckels DD, Lake P, Johnson AH, Hartzman RJ, Woody JN. Antigen-specific human T lymphocyte clones: induction, antigen specificity, and MHC restriction of influenza virus-immune clones. *J Immunol* (1982) 128(1):233–8.

222. Lampejo T. Influenza and antiviral resistance: an overview. Eur J Clin Microbiol Infect Dis. 2020 Jul;39(7):1201-1208. doi: 10.1007/s10096-020-03840-9. Epub 2020 Feb 13.

223. Lander ES, Linton LM, Birren B, et al. International Human Genome Sequencing ConsortiumInitial sequencing and analysis of the human genome., Nature, 2001, vol. 409 6822(pg. 860-921).

224. Landrigan PJ, Sly JL, Ruchirawat M, Silva ER, Huo X, Diaz-Barriga F, et al. Health consequences of environmental exposures: Changing global patterns of exposure and disease. *Annals of Global Health.* 2016;82:10–19.

225. Lasko P., Lüthy K. Investigating rare and ultrarare epilepsy syndromes with Drosophila models. *Fac. Rev.* 2021;10:10. doi: 10.12703/r/10-10.

226. Lê, V.B.; Dubois, J.; Couture, C.; Cavanagh, M.-H.; Uyar, O.; Pizzorno, A.; Rosa-Calatrava, M.; Hamelin, M.-È.; Boivin, G. Human Metapneumovirus Activates NOD-like Receptor Protein 3 Inflammasome via Its Small Hydrophobic Protein Which Plays a Detrimental Role during Infection in Mice. *PLoS Pathog.* 2019, *15*, e1007689.

227. Leff JA, Oppegard MA, Curiel TJ et al (1992) Progressive increases in serum catalase activity in advancing human immunodeficiency virus infection. Free Radic Biol Med 13(2):143–149.

228. Leiding JW, Holland SM. Chronic granulomatous disease. In: Pagon RA, Adam MP, Ardinger HH, Wallace SE, Amemiya A, Bean LJH, et al., editors. *GeneReviews(R).* Seattle, WA: University of Washington, Seattle; (1993).

229. Leiding JW. Neutrophil Evolution and Their Diseases in Humans. Front Immunol. 2017 Aug 28;8:1009. doi: 10.3389/fimmu.2017.01009.

230. Li M, Zhao L, Page-McCaw PS, Chen W. Zebrafish Genome Engineering Using the CRISPR-Cas9 System. Trends Genet. 2016 Dec;32(12):815-827. doi: 10.1016/j.tig.2016.10.005. Epub 2016 Nov 8. PMID: 27836208; PMCID: PMC5127170.

231. Li Y, Huo S, Yin Z, Tian Z, Huang F, Liu P, Liu Y, Yu F. Retracted and republished from: "The current state of research on influenza antiviral drug development: drugs in clinical trial and licensed drugs". mBio. 2024 May 8;15(5):e0017524. doi: 10.1128/mbio.00175-24.

232. Liedmann S., Hrincius E.R., Guy C., Anhlan D., Dierkes R., Carter R., Wu G., Staeheli P., Green D.R., Wolff T., et al. Viral suppressors of the RIG-I-mediated interferon response are pre-packaged in influenza virions. *Nat. Commun.* 2014;5:5645. doi: 10.1038/ncomms6645.

233. Lin X, Wang R, Zou W et al (2016) The influenza virus H5N1 infection can induce ROS production for viral replication and host cell death in A549 cells modulated by human Cu/Zn superoxide dismutase (SOD1) overexpression. Viruses 8:13. doi:10.3390/v8010013.

234. Liu H, Zhang J, Zhang S, Yang F, Thacker PA, Zhang G, Qiao S, Ma X: Oral administration of Lactobacillus fermentum I5007 favors intestinal development and alters the intestinal microbiota in formula-fed piglets. J Agric Food Chem 2014; 62: 860-866.

235. Liu S., Yan R., Chen B., Pan Q., Chen Y., Hong J., Zhang L., Liu W., Wang S., Chen J.L. Influenza Virus-Induced Robust Expression of SOCS3 Contributes to Excessive Production of IL-6. *Front. Immunol.* 2019;10:1843. doi: 10.3389/fimmu.2019.01843.

236. Liu T, Zhang L, Joo D, Sun SC. NF-κB signaling in inflammation. Signal Transduct Target Ther. 2017;2:17023–. doi: 10.1038/sigtrans.2017.23. Epub 2017 Jul 14.

237. Liu, T.; Zhou, Y.T.; Wang, L.Q.; Li, L.Y.; Bao, Q.; Tian, S.; Chen, M.X.; Chen, H.X.; Cui, J.; Li, C.W. NOD-like Receptor Family, Pyrin Domain Containing 3 (NLRP3) Contributes to Inflammation, Pyroptosis, and Mucin Production in Human Airway Epithelium on Rhinovirus Infection. *J. Allergy Clin. Immunol.* 2019, *144*, 777–787.e9.

238. Liu, Y., Schiff, M., Czymmek, K., Talloczy, Z., Levine, B., Dinesh-Kumar, S. P. (2005). Autophagy Regulates Programmed Cell Death During the Plant Innate Immune Response. *Cell* 121 (4), 567–577. doi: 10.1016/j.cell.2005.03.007.

239. Lohmann N, Schirmer L, Atallah P, Wandel E, Ferrer RA, Werner C, Simon JC, Franz S & Freudenberg U (2017) Glycosaminoglycan-based hydrogels capture

inflammatory chemokines and rescue defective wound healing in mice. *Sci Transl Med* 9, eaai9044.

240. López, C. B., A. García-Sastre, B. R. G. Williams, and T. M. Moran. 2003. Type I interferon induction pathway, but not released interferon, participates in the maturation of dendritic cells induced by negative-strand RNA viruses. J. Infect. Dis. 187:1126-1136.

241. López-Cotarelo P, Gómez-Moreira C, Criado-García O, Sánchez L & Rodríguez-Fernández JL (2017) Beyond chemoattraction: multifunctionality of chemokine receptors in leukocytes. *Trends Immunol* 38, 927–941.

242. Lu J, Holmgren A: The thioredoxin antioxidant system. Free Radic Biol Med 2014; 66: 75-87.

243. Ludwig S, Planz O. Influenza viruses and the NF-kappaB signaling pathway - towards a novel concept of antiviral therapy. Biol Chem. 2008 Oct;389(10):1307-12. doi: 10.1515/BC.2008.148.

244. Lugo-Villarino G, Balla KM, Stachura DL, Bañuelos K, Werneck MB, Traver D. Identification of dendritic antigen-presenting cells in the zebrafish. Proc Natl Acad Sci U S A. 2010 Sep 7;107(36):15850-5. doi: 10.1073/pnas.1000494107.

245. Lukacs, N.W.; Smit, J.J.; Mukherjee, S.; Morris, S.B.; Nunez, G.; Lindell, D.M. Respiratory Virus-Induced TLR7 Activation Controls IL-17–Associated Increased Mucus via IL-23 Regulation. *J. Immunol.* 2010, *185*, 2231–2239.

246. Lund JM, Alexopoulou L, Sato A, Karow M, Adams NC, Gale NW, et al. Recognition of single-stranded RNA viruses by toll-like receptor 7. *Proc Natl Acad Sci U S A* (2004) 101(15):5598–603. 10.1073/pnas.0400937101.

247. Lupfer C., Thomas P.G., Anand P.K., Vogel P., Milasta S., Martinez J., Huang G., Green M., Kundu M., Chi H., et al. Receptor interacting protein kinase 2-mediated mitophagy regulates inflammasome activation during virus infection. *Nat. Immunol.* 2013;14:480–488. doi: 10.1038/ni.2563.

248. Lynch Iii, J.P.; Kajon, A.E.; Singh, S.K. Adenovirus: Epidemiology, Global Spread of Novel Serotypes, and Advances in Treatment and Prevention. *Semin. Respir. Crit. Care Med.* 2016, *37*, 586–602.

249. Ma, J.; Ramachandran, M.; Jin, C.; Quijano-Rubio, C.; Martikainen, M.; Yu, D.; Essand, M. Characterization of Virus-Mediated Immunogenic Cancer Cell Death and the Consequences for Oncolytic Virus-Based Immunotherapy of Cancer. *Cell Death Dis.* 2020, *11*, 48.

250. Ma Y, Zhang Y, Zhu L. Role of neutrophils in acute viral infection. Immun Inflamm Dis. 2021 Dec;9(4):1186-1196. doi: 10.1002/iid3.500. Epub 2021 Sep 2.

251. Malik G., Zhou Y. Innate Immune Sensing of Influenza A Virus. *Viruses.* 2020;12:755. doi: 10.3390/v12070755.

252. Malinczak, C.A.; Schuler, C.F.; Duran, A.J.; Rasky, A.J.; Mire, M.M.; Núñez, G.; Lukacs, N.W.; Fonseca, W. NLRP3-Inflammasome Inhibition during Respiratory Virus Infection Abrogates Lung Immunopathology and Long-Term Airway Disease Development. *Viruses* 2021, *13*, 692.

253. Malvy DJM, Richard M-J, Arnaud J et al. (1994) Relationship of plasma malondialdehyde, vitamin E and antioxidant micronutrients to human immunodeficiency virus-1 seropositivity. Clin Chim Acta 224:89–94.

254. Mandal P., Berger S.B., Pillay S., Moriwaki K., Huang C., Guo H., Lich J.D., Finger J., Kasparcova V., Votta B., Ouellette M., King B.W., Wisnoski D., Lakdawala A.S., DeMartino M.P., Casillas L.N., Haile P.A., Sehon C.A., Marquis R.W., Upton J., Daley-Bauer L.P., Roback L., Ramia N., Dovey C.M., Carette J.E., Chan F.K., Bertin J., Gough P.J., Mocarski E.S., Kaiser W.J. RIP3 induces apoptosis independent of pronecrotic kinase activity. *Mol Cell.* 2014;56:481–495.

255. Manicassamy B., Manicassamy S., Belicha-Villanueva A., Pisanelli G., Pulendran B., Garcia-Sastre A. Analysis of in vivo dynamics of influenza virus infection in mice using a GFP reporter virus. *Proc. Natl. Acad. Sci. USA.* 2010;107:11531–11536. doi: 10.1073/pnas.0914994107.

256. Manoharan RR, Prasad A, Pospíšil P, Kzhyshkowska J. ROS signaling in innate immunity via oxidative protein modifications. Front Immunol. 2024 Mar 7;15:1359600. doi: 10.3389/fimmu.2024.1359600.

257. Mantovani A, Cassatella MA, Costantini C, Jaillon S. Neutrophils in the activation and regulation of innate and adaptive immunity. *Nat Rev Immunol*. 2011;11(8):519-531.

258. Mao H., Tu W., Qin G., Law H.K., Sia S.F., Chan P.L., Liu Y., Lam K.T., Zheng J., Peiris M., et al. Influenza virus directly infects human natural killer cells and induces cell apoptosis. *J. Virol.* 2009;83:9215–9222.

259. Mariathasan, S.; Newton, K.; Monack, D.M.; Vucic, D.; French, D.M.; Lee, W.P.; Roose-Girma, M.; Erickson, S.; Dixit, V.M. Differential Activation of the Inflammasome by Caspase-1 Adaptors ASC and Ipaf. *Nature* 2004, *430*, 213–218.

260. Mariscal A., Caldarone L., Tikkanen J., Nakajima D., Chen M., Yeung J., Cypel M., Liu M., Keshavjee S. Pig lung transplant survival model. *Nat. Protoc.* 2018;13:1814–1828. doi: 10.1038/s41596-018-0019-4.

261. Marquardt, N. et al. The human NK cell response to yellow fever virus 17D is primarily governed by NK cell differentiation independently of NK cell education. *J. Immunol.* 195, 3262–3272 (2015).

262. Martin K, Helenius A. Nuclear transport of influenza virus ribonucleoproteins: the viral matrix protein (M1) promotes export and inhibits import. *Cell* (1991) 67:117–30. doi:10.1016/0092-8674(91)90576-K.

263. Masurel N, Marine WM. Recycling of Asian and HongKong influenza A virus hemagglutinins in man. Am J Epidemiol. 1973;97:44–9.

264. McAuley J.L., Chipuk J.E., Boyd K.L., Van De Velde N., Green D.R., McCullers J.A. PB1-F2 proteins from H5N1 and 20-century pandemic influenza viruses cause immunopathology. *PLoS Pathog.* 2010;6:e1001014. doi: 10.1371/journal.ppat.1001014.

265. McGeoch D, Fellner P, Newton C. Influenza virus genome consists of eight distinct RNA species. Proc Natl Acad Sci U S A (1976) 73:3045–9. doi:10.1073/ pnas.73.9.3045.

266. McIlwaine L, Parker A, Sandilands G, Gallipoli P, Leach M. Neutrophil-specific granule deficiency. *Br J Haematol* (2013) 160(6):735. 10.1111/bjh.12207.

267. Menon M.P., Hua K.-F. The Long Non-Coding RNAs: Paramount Regulators of the NLRP3 Inflammasome. *Front. Immunol.* 2020;11:569524. doi: 10.3389/fimmu.2020.569524.

268. Merad, M., Martin, J.C. Pathological inflammation in patients with COVID-19: a key role for monocytes and macrophages. *Nat Rev Immunol* 20, 355–362 (2020). https://doi.org/10.1038/s41577-020-0331-4.

269. Metzemaekers M, Van Damme J, Mortier A & Proost P (2016) Regulation of chemokine activity – a focus on the role of dipeptidyl peptidase IV/CD26. *Front Immunol* 7, 483.

270. Mochizuki H, Todokoro M, Arakawa H (2009) RS virus-induced inflammation and the intracellular glutathione redox state in cultured human airway epithelial cells. Inflammation 32(4):252–264. doi:10.1007/s10753-009-9128-0.

271. Mokhtari V, Afsharian P, Shahhoseini M, Kalantar SM, Moini A. A Review on Various Uses of N-Acetyl Cysteine. Cell J. 2017 Apr-Jun;19(1):11-17. doi: 10.22074/cellj.2016.4872. Epub 2016 Dec 21. PMID: 28367412; PMCID: PMC5241507.

272. Monneau Y, Arenzana-Seisdedos F & Lortat-Jacob H (2016) The sweet spot: how GAGs help chemokines guide migrating cells. *J Leukoc Biol* 99, 935–953.

273. Montezano A.C., Nguyen Dinh Cat A., Rios F.J., Touyz R.M. Angiotensin II and vascular injury. *Curr. Hypertens. Rep.* 2014;16:431. doi: 10.1007/s11906-014-0431-2.

274. Morash MG, Douglas SE, Robotham A, Ridley CM, Gallant JW, Soanes KH. The zebrafish embryo as a tool for screening and characterizing pleurocidin host-defense peptides as anti-cancer agents. Dis Model Mech. 2011 Sep;4(5):622-33. doi: 10.1242/dmm.007310. Epub 2011 Jul 4. PMID: 21729875; PMCID: PMC3177944.

275. Moreno-Solís G, de la Torre-Aguilar MJ, Torres-Borrego J et al (2015) Oxidative stress and inflamatory plasma biomarkers in respiratory syncytial virus bronchiolitis. Clin Respir J. doi:10.1111/crj.12425.

276. Morens DM, Taubenberger JK, Fauci AS. Predominant role of bacterial pneumonia as a cause of death in pan- demic influenza: implications for pandemic influenza preparedness. J Infect Dis. 2008;198:962–70.

277. Morens D.M., Taubenberger J.K., Fauci A.S. Pandemic influenza viruses—Hoping for the road not taken. *N. Engl. J. Med.* 2013;368:2345–2348. doi: 10.1056/NEJMp1307009.

278. Mueller S.N, Mackay L.K. Tissue-resident memory T cells: local specialists in immune defence. Nat Rev Immunol . 2016;16:79–89.

279. Mugoni V, Camporeale A, Santoro MM. Analysis of oxidative stress in zebrafish embryos. J Vis Exp. 2014 Jul 7;(89):51328. doi: 10.3791/51328. PMID: 25046434; PMCID: PMC4212721.

280. Mullen L, Mengozzi M, Hanschmann E-M, Alberts B, Ghezzi P. How the redox state regulates immunity. *Free Radical Biol Med*. (2020) 157:3–14. doi: 10.1016/j.freeradbiomed.2019.12.022.

281. Munir M. TRIM proteins: another class of viral victims. *Sci Signal* (2010) 3(118):jc2. 10.1126/scisignal.3118jc2.

282. Munster V.J., Feldmann F., Williamson B.N., van Doremalen N., Pérez-Pérez L., Schulz J., Meade-White K., Okumura A., Callison J., Brumbaugh B., et al. Respiratory disease in rhesus macaques inoculated with SARS-CoV-2. *Nature.* 2020;585:268–272. doi: 10.1038/s41586-020-2324-7.

283. Muramoto Y, Noda T, Kawakami E, Akkina R, Kawaoka Y 2013. Identification of Novel Influenza A Virus Proteins Translated from PA mRNA. J Virol 87:. https://doi.org/10.1128/jvi.02656-12.

283. Muri J, Thut H, Feng Q, Kopf M. Thioredoxin-1 distinctly promotes NF-κB target DNA binding and NLRP3 inflammasome activation independently of Txnip. *eLife*. (2020) 9:e53627. doi: 10.7554/eLife.53627.

284. Murphy, K. (2012) *Janeway's Immunobiology*. 8th edn. London, United Kingdom: Garland Science.

285. Nakahira K., Haspel J.A., Rathinam V.A., Lee S.J., Dolinay T., Lam H.C., Englert J.A., Rabinovitch M., Cernadas M., Kim H.P., et al. Autophagy proteins regulate innate immune responses by inhibiting the release of mitochondrial DNA mediated by the NALP3 inflammasome. *Nat. Immunol.* 2011;12:222–230. doi: 10.1038/ni.1980.

286. Nair, H.; Nokes, D.J.; Gessner, B.D.; Dherani, M.; Madhi, S.A.; Singleton, R.J.; O'Brien, K.L.; Roca, A.; Wright, P.F.; Bruce, N.; et al. Global Burden of Acute Lower Respiratory Infections Due to Respiratory Syncytial Virus in Young Children: A Systematic Review and Meta-Analysis. *Lancet* 2010, *375*, 1545–1555.

287. Narasaraju T, Yang E, Samy RP, et al. Excessive neutrophils and neutrophil extracellular traps contribute to acute lung injury of influenza pneumonitis. *Am J Pathol*. 2011;179(1):199-210.

288. Nencioni L, De Chiara G, Sgarbanti R, Amatore D, Aquilano K, Marcocci ME, Serafino A, Torcia M, Cozzolino F, Ciriolo MR, Garaci E, Palamara AT. Bcl-2 expression and p38MAPK activity in cells infected with influenza A virus: impact on virally induced apoptosis and viral replication. J Biol Chem. 2009 Jun 5;284(23):16004-15. doi: 10.1074/jbc.M900146200.

289. Newcomb LL, Kuo RL, Ye Q, Jiang Y, Tao YJ, Krug RM. Interaction of the influenza a virus nucleocapsid protein with the viral RNA polymerase poten- tiates unprimed viral RNA replication. *J Virol* (2009) 83:29–36. doi:10.1128/ JVI.02293-07.

290. Nguyen GT, Green ER, Mecsas J. Neutrophils to the ROScue: mechanisms of NADPH oxidase activation and bacterial resistance. *Front Cell Infect Microbiol*. (2017) 7:373.

291. Niture SK, Khatri R, Jaiswal AK: Regulation of Nrf2-an update. Free Radic Biol Med 2014; 66: 36-44.

292. Okwan-Duodu D., Datta V., Shen X.Z., Goodridge H.S., Bernstein E.A., Fuchs S., Liu G.Y., Bernstein K.E. Angiotensin-converting enzyme overexpression in mouse myelomonocytic cells augments resistance to Listeria and methicillin-resistant Staphylococcus aureus. *J. Biol. Chem.* 2010;285:39051–39060. doi: 10.1074/jbc.M110.163782.

293. O'Hanlon R, Shaw ML. 2019. Baloxavir marboxil: the new influenza drug on the market. *Curr Opin Virol* 35:14–18. doi: 10.1016/j.coviro.2019.01.006.

294. Olson DR, Simonsen L, Edelson PJ, Morse SS. Epidemiological evidence of an early wave of the 1918 influenza pandemic in New York City. Proc Natl Acad Sci U S A. 2005;102:11059–63.

295. O’Neill RE, Jaskunas R, Blobel G, Palese P, Moroianu J. Nuclear import of influenza virus RNA can be mediated by viral nucleoprotein and transport factors required for protein import. *JBiol Chem* (1995) 270:22701–4. doi:10.1074/jbc.270.39.22701.

296. Paclet MH, Laurans S, Dupré-Crochet S. Regulation of Neutrophil NADPH Oxidase, NOX2: A Crucial Effector in Neutrophil Phenotype and Function. Front Cell Dev Biol. 2022 Jul 14;10:945749. doi: 10.3389/fcell.2022.945749.

297. Palese P, Schulman JL. Mapping of the influenza virus genome: identification of the hemagglutinin and the neuraminidase genes. Proc Natl Acad Sci U S A (1976) 73:2142–6. doi:10.1073/pnas.73.6.2142.

298. Pang, L. L. et al. The suppression of innate immune response by human rhinovirus C. *Biochem. Biophys. Res. Commun.* 490, 22–28 (2017).

299. Papayannopoulos V, Metzler KD, Hakkim A, Zychlinsky A. Neutrophil elastase and myeloperoxidase regulate the formation of neutrophil extracellular traps. *J Cell Biol.* (2010) 191:677–91. doi: 10.1083/jcb.201006052.

300. Parvez S, Long MJC, Poganik JR, Aye Y. Redox signaling by reactive electrophiles and oxidants. *Chem Rev*. 2018;118(18):8798-8888.

301. Pasparakis M., Vandenabeele P. Necroptosis and its role in inflammation. *Nature.* 2015;517:311–320.

302. Patil DR, Hundekar SL, Arankalle VA (2012) Expression profile of immune response genes during acute myopathy induced by chikungunya virus in a mouse model. Institut Pasteur Microbes Infect 14:457–469.

303. Perrone LA, Plowden JK, García-Sastre A, Katz JM, Tumpey TM. H5N1 and 1918 pandemic influenza virus infection results in early and excessive infiltration of macrophages and neutrophils in the lungs of mice. PLoS Pathog. 2008 Aug 1;4(8):e1000115. doi: 10.1371/journal.ppat.1000115.

304. Peterson EA, Sun J, Chen X, Wang J. Neutrophils facilitate the epicardial regenerative response after zebrafish heart injury. Dev Biol. 2024 Apr;508:93-106. doi: 10.1016/j.ydbio.2024.01.011.

305. Pflug A, Lukarska M, Resa-Infante P, Reich S, Cusack S. Structural insights into RNA synthesis by the influenza virus transcription-replication machine. *Virus Res* (2017) 234:103–17. doi:10.1016/j.virusres.2017.01.013.

306. Pham-Huy LA, He H, Pham-Huy C. Free radicals, antioxidants in disease and health. Int J Biomed Sci. 2008 Jun;4(2):89-96.

307. Phaniendra A, Jestadi DB, Periyasamy L. Free radicals: properties, sources, targets, and their implication in various diseases. Indian J Clin Biochem. 2015 Jan;30(1):11-26. doi: 10.1007/s12291-014-0446-0. Epub 2014 Jul 15.

308. Pichlmair A, Schulz O, Tan CP, Näslund TI, Liljeström P, Weber F, et al. RIG-I-mediated antiviral responses to single-stranded RNA bearing 5'-phosphates. *Science* (2006) 314(5801):997–1001. 10.1126/science.1132998.

309. Pinto LH, Lamb RA. The M2 proton channels of influenza A and B viruses. *J Biol Chem* (2006) 281:8997–9000. doi:10.1074/jbc.R500020200.

310. Pipkin ME, Sacks JA, Cruz-Guilloty F, Lichtenheld MG, Bevan MJ, Rao A. Interleukin-2 and inflammation induce distinct transcriptional programs that promote the differentiation of effector cytolytic T cells. *Immunity* (2010) 32(1):79–90. 10.1016/j.immuni.2009.11.012.

311. Pitt J.A., Kozal J.S., Jayasundara N., Massarsky A., Trevisan R., Geitner N., Wiesner M., Levin E.D., Di Giulio R.T. Uptake, tissue distribution, and toxicity of polystyrene nanoparticles in developing zebrafish (*Danio rerio*) *Aquat. Toxicol.* 2018;194:185–194. doi: 10.1016/j.aquatox.2017.11.017.

312. Plotch S.J., Bouloy M., Ulmanen I., Krug R.M. A unique cap(m7GpppXm)-dependent influenza virion endonuclease cleaves capped RNAs to generate the primers that initiate viral RNA transcription. *Cell.* 1981;23:847–858. doi: 10.1016/0092-8674(81)90449-9.

313. Pollack M, Leeuwenburgh C. Molecular mechanisms of oxidative stress in aging: free radicals, aging, antioxidants and disease. Elsevier Science B.V. Handbook of Oxidants and Antioxidants in Exercise. 1999;881–923.

314. Poon LL, Pritlove DC, Fodor E, Brownlee GG. Direct evidence that the poly(A) tail of influenza A virus mRNA is synthesized by reiterative copying of a U track in the virion RNA template. *J Virol* (1999) 73:3473–6.

315. Poss K.D., Wilson L.G., Keating M.T. Heart regeneration in zebrafish. *Science.* 2002;298:2188–2190. doi: 10.1126/science.1077857.

316. Pothlichet J., Chignard M., Si-Tahar M. Cutting edge: Innate immune response triggered by influenza A virus is negatively regulated by SOCS1 and SOCS3 through a RIG-I/IFNAR1-dependent pathway. *J. Immunol.* 2008;180:2034–2038.

317. Pressley M.E., Phelan P.E., 3rd, Witten P.E., Mellon M.T., Kim C.H. Pathogenesis and inflammatory response to *Edwardsiella tarda* infection in the zebrafish. *Dev. Comp. Immunol.* 2005;29:501–513. doi: 10.1016/j.dci.2004.10.007.

318. Pribul, P.K.; Harker, J.; Wang, B.; Wang, H.; Tregoning, J.S.; Schwarze, J.; Openshaw, P.J.M. Alveolar Macrophages Are a Major Determinant of Early Responses to Viral Lung Infection but Do Not Influence Subsequent Disease Development. *J. Virol.* 2008, *82*, 4441–4448.

319. Proudfoot AEI, Handel TM, Johnson Z, Lau EK, LiWang P, Clark-Lewis I, Borlat F, Wells TNC & Kosco-Vilbois MH (2003) Glycosaminoglycan binding and oligomerization are essential for the in vivo activity of certain chemokines. *Proc Natl Acad Sci USA* 100, 1885–1890.

320. Qian M, Fang X, Wang X. Autophagy and inflammation. Clin Transl Med. 2017 Dec;6(1):24. doi: 10.1186/s40169-017-0154-5.

321. Qiao M, Moyes G, Zhu F, Li Y, Wang X. The prevalence of influenza bacterial co-infection and its role in disease severity: A systematic review and meta-analysis. J Glob Health. 2023 Jun 16;13:04063. doi: 10.7189/jogh.13.04063. PMID: 37319008; PMCID: PMC10270314.

322. Raftery MJ, Lalwani P, Krautkrämer E, et al. β2 integrin mediates hantavirus-induced release of neutrophil extracellular traps. *J Exp Med*. 2014;211(7):1485-1497.

323. Rajsbaum R., Albrecht R.A., Wang M.K., Maharaj N.P., Versteeg G.A., Nistal-Villan E., Garcia-Sastre A., Gack M.U. Species-specific inhibition of RIG-I ubiquitination and IFN induction by the influenza A virus NS1 protein. *PLoS Pathog.* 2012;8:e1003059. doi: 10.1371/journal.ppat.1003059.

324. Rambaut A., Pybus O.G., Nelson M.I., Viboud C., Taubenberger J.K., Holmes E.C. The genomic and epidemiological dynamics of human influenza A virus. *Nature.* 2008;453:615–619.

325. Rasolofonirina N. The history of flu in Madagascar. Arch Inst Pasteur Madagascar. 2003;69:6–11.

326. Raut P., Weller S.R., Obeng B., Soos B.L., West B.E., Potts C.M., Sangroula S., Kinney M.S., Burnell J.E., King B.L., et al. Cetylpyridinium chloride (CPC) reduces zebrafish mortality from influenza infection: Super-resolution microscopy reveals CPC interference with multiple protein interactions with phosphatidylinositol 4,5-bisphosphate in immune function. *Toxicol. Appl. Pharmacol.* 2022;440:115913. doi: 10.1016/j.taap.2022.115913.

327. Rawat S, Vrati S, Banerjee A. Neutrophils at the crossroads of acute viral infections and severity. Mol Aspects Med. 2021 Oct;81:100996. doi: 10.1016/j.mam.2021.100996. Epub 2021 Jul 18.

328. Reed C., Chaves S.S., Daily Kirley P., Emerson R., Aragon D., Hancock E.B., Butler L., Baumbach J., Hollick G., Bennett N.M., et al. Estimating influenza disease

burden from population-based surveillance data in the United States. *PLoS ONE.* 2015;10:e0118369. doi: 10.1371/journal.pone.0118369.

329.

330. Rehwinkel J, Tan CP, Goubau D, Schulz O, Pichlmair A, Bier K, et al. RIG-I detects viral genomic RNA during negative-strand RNA virus infection. Cell (2010) 140(3):397–408. 10.1016/j.cell.2010.01.020

331. Reich S, Guilligay D, Pflug A, Malet H, Berger I, Crepin T, et al. Structural insight into cap-snatching and RNA synthesis by influenza polymerase. Nature (2014) 516:361–6. doi:10.1038/nature14009.

332. Reich S, Guilligay D, Cusack S. An in vitro fluorescence based study of initiation of RNA synthesis by influenza B polymerase. *Nucleic Acids Res* (2017) 45:3353–68. doi:10.1093/nar/gkx043.

333. Renshaw S.A., Loynes C.A., Trushell D.M., Elworthy S., Ingham P.W., Whyte M.K. A transgenic zebrafish model of neutrophilic inflammation. *Blood.* 2006;108:3976–3978. doi: 10.1182/blood-2006-05-024075.

334. Reshi ML, Su Y-C, Hong J-R (2014) RNA viruses; ROS-mediated cell death. Int J Cell Biol 2014:467452-1–467452-16. doi:10.155/2014/467452.

335. Rimmelzwaan G.F., Boon A.C., Voeten J.T., Berkhoff E.G., Fouchier R.A., Osterhaus A.D. Sequence variation in the influenza A virus nucleoprotein associated with escape from cytotoxic T lymphocytes. *Virus Res.* 2004;103:97–100.

336. Rissone, A. and Candotti, F. (2016). Detection of Reactive Oxygen Species Using MitoSOX and CellROX in Zebrafish. *Bio-protocol* 6(19): e1941. DOI: 10.21769/BioProtoc.1941.

337. Robb N.C., Smith M., Vreede F.T., Fodor E. NS2/NEP protein regulates transcription and replication of the influenza virus RNA genome. *J. Gen. Virol.* 2009;90:1398–1407. doi: 10.1099/vir.0.009639-0.

338. Robb NC, Te Velthuis AJ, Wieneke R, Tampe R, Cordes T, Fodor E, et al. Single-molecule FRET reveals the pre-initiation and initiation conformations of influenza virus promoter RNA. *Nucleic Acids Res* (2016) 44:10304–15. doi:10.1093/nar/gkw884.

339. Robinson, K.S.; Teo, D.E.T.; Tan, K.S.; Toh, G.A.; Ong, H.H.; Lim, C.K.; Lay, K.; Au, B.V.; Lew, T.S.; Chu, J.J.H.; et al. Enteroviral 3C Protease Activates the Human NLRP1 Inflammasome in Airway Epithelia. *Science* 2020, *370*, eaay2002.

340. Robinson N.B., Krieger K., Khan F.M., Huffman W., Chang M., Naik A., Yongle R., Hameed I., Krieger K., Girardi L.N., et al. The current state of animal models in research: A review. *Int. J. Surg.* 2019;72:9–13. doi: 10.1016/j.ijsu.2019.10.015.

341. Rodrigues, T.S.; de Sá, K.S.G.; Ishimoto, A.Y.; Becerra, A.; Oliveira, S.; Almeida, L.; Gonçalves, A.V.; Perucello, D.B.; Andrade, W.A.; Castro, R.; et al. Inflammasomes Are Activated in Response to SARS-CoV-2 Infection and Are Associated with COVID-19 Severity in Patients. *J. Exp. Med.* 2021, *218*, e20201707.

342. Rosales C. Neutrophils at the crossroads of innate and adaptive immunity. J Leukoc Biol. 2020 Jul;108(1):377-396. doi: 10.1002/JLB.4MIR0220-574RR.

343. Rossaint, J. *et al.* Synchronized integrin engagement and chemokine activation is crucial in neutrophil extracellular trap-mediated sterile inflammation. *Blood* 123, 2573–2584 (2014).

344. Rossman JS, Lamb RA. Viral membrane scission. *Annu Rev Cell Dev Biol* (2013) 29:551–69. doi:10.1146/annurev-cellbio-101011-155838.

345. Rust MJ, Lakadamyali M, Zhang F, Zhuang X. Assembly of endocytic machinery around individual influenza viruses during viral entry. *Nat Struct Mol Biol* (2004) 11:567–73. doi:10.1038/nsmb769.

346. Saffarzadeh M, Juenemann C, Queisser MA, et al. Neutrophil extracellular traps directly induce epithelial and endothelial cell death: a predominant role of histones. *PLoS One*. 2012;7(2):e32366.

347. Salvatore F. Priore, Andrew D. Kauffmann, Jayson R. Baman, and Douglas H. Turner. The Influenza A PB1-F2 and N40 Start Codons Are Contained within an RNA Pseudoknot. Biochemistry 2015 *54* (22), 3413-3415 DOI: 10.1021/bi501564d.

348. Santiago-López JA, Bautista-Martínez CI, Reyes-Hernandez M, Aguilar-Martínez S, Rivas- Arancibia S. Oxidative stress, progressive damage in the substantia nigra and plasma dopamine oxidation, in rats chronically exposed to ozone. *Toxicol Lett.* 2010;197(3):193–200.

349. Santos-Lima B, Pietronigro EC, Terrabuio E, Zenaro E, Constantin G. The role of neutrophils in the dysfunction of central nervous system barriers. Front Aging Neurosci. 2022 Aug 11;14:965169. doi: 10.3389/fnagi.2022.965169.

350. Schieber M, Chandel NS: ROS Function in Redox Signaling and Oxidative Stress. Curr Biol 2014; 24:R453-R462.

351. Schneider, C.; Nobs, S.P.; Heer, A.K.; Kurrer, M.; Klinke, G.; van Rooijen, N.; Vogel, J.; Kopf, M. Alveolar Macrophages Are Essential for Protection from Respiratory Failure and Associated Morbidity Following Influenza Virus Infection. *PLoS Pathog.* 2014, *10*, e1004053.

352. Schönrich G, Raftery MJ. Neutrophil extracellular traps go viral. *Front Immunol.* 2016;7:366.

353. Schrader M, Fahimi HD. Review Peroxisomes and oxidative stress. *Biochim Biophys Acta.* 2006;1763(12):1755–1766.

354. Schuster, J.E.; Williams, J.V. Human Metapneumovirus. *Microbiol. Spectr.* 2014, *2*, 237–247.

355. Selders GS, Fetz AE, Radic MZ, Bowlin GL. An overview of the role of neutrophils in innate immunity, inflammation and host-biomaterial integration. Regen Biomater. 2017 Feb;4(1):55-68. doi: 10.1093/rb/rbw041.

356. Semerad, C. L., Liu, F., Gregory, A. D., Stumpf, K. & Link, D. C. G-CSF is an essential regulator of neutrophil trafficking from the bone marrow to the blood. *Immunity* 17, 413–423 (2002).

357. Sharma K., Tripathi S., Ranjan P., Kumar P., Garten R., Deyde V., Katz J.M., Cox N.J., Lal R.B., Sambhara S., et al. Influenza A virus nucleoprotein exploits Hsp40 to inhibit PKR activation. *PLoS One.* 2011;6:e20215.

358. Shil, N.K.; Pokharel, S.M.; Banerjee, A.K.; Hoffman, M.; Bose, S. Inflammasome Antagonism by Human Parainfluenza Virus Type 3 C Protein. *J. Virol.* 2018, *92*, e01776-17.

359. Shim CH, Cho S, Shin YM, Choi JM. Emerging role of bystander T cell activation in autoimmune diseases. BMB Rep. 2022 Feb;55(2):57-64. doi: 10.5483/BMBRep.2022.55.2.183.

360. Shinya K., Fujii Y., Ito H., Ito T., Kawaoka Y. Characterization of a neuraminidase-deficient influenza a virus as a potential gene delivery vector and a live vaccine. *J. Virol.* 2004;78:3083–3088. doi: 10.1128/JVI.78.6.3083-3088.2004.

361. Shope RE. Swine influenza. III. Filtration experiments and etiology. J Exp Med. 1931;54:373–80.

362. Shrestha S.S., Swerdlow D.L., Borse R.H., Prabhu V.S., Finelli L., Atkins C.Y., Owusu-Edusei K., Bell B., Mead P.S., Biggerstaff M., et al. Estimating the burden of 2009 pandemic influenza A (H1N1) in the United States (April 2009–April 2010) *Clin. Infect. Dis.* 2011;52((Suppl. 1)):S75–S82. doi: 10.1093/cid/ciq012.

363. Sies H. Hydrogen peroxide as a central redox signaling molecule in physiological oxidative stress: oxidative eustress. *Redox Biol*. 2017;11:613-619.

364. Sims A, Tornaletti LB, Jasim S, Pirillo C, Devlin R, Hirst JC, Loney C, Wojtus J, Sloan E, Thorley L, Boutell C, Roberts E, Hutchinson E. Superinfection exclusion creates spatially distinct influenza virus populations. PLoS Biol. 2023 Feb 9;21(2):e3001941. doi: 10.1371/journal.pbio.3001941.

365. Sies, H., Mailloux, R.J. & Jakob, U. Fundamentals of redox regulation in biology. *Nat Rev Mol Cell Biol* (2024). https://doi.org/10.1038/s41580-024-00730-2.

366. Singh, Natesh, et al. "Drug discovery and development: Introduction to the general public and patient groups." *Frontiers in Drug Discovery*, vol. 3, 24 May 2023, https://doi.org/10.3389/fddsv.2023.1201419.

367. Smith D.J., Lapedes A.S., de Jong J.C., Bestebroer T.M., Rimmelzwaan G.F., Osterhaus A.D., Fouchier R.A. Mapping the antigenic and genetic evolution of influenza virus. *Science.* 2004;305:371–376.

368. Smith GJ, Vijaykrishna D, Bahl J, Lycett SJ, Worobey M, Pybus OG, et al. Origins and evolutionary genomics of the 2009 swine-origin H1N1 influenza A epidemic. Nature. 2009;25, 459:1122–5.

369. Smith J.R., Bolton E.R., Dwinell M.R. The rat: A model used in biomedical research. In: Hayman T., Smith J.R., Dwinell M.R., Shimoyama M., editors. *Rat Genomics.* Springer; Hertfordshire, UK: 2019. pp. 1–41.

370. Smith W, Andrewes CH, Laidlaw PP. A virus obtained from influenza patients. Lancet. 1933;1:66–8.

371. Soehnlein O. Direct and alternative antimicrobial mechanisms of neutrophil-derived granule proteins. *J Mol Med (Berl)*. 2009; 87: 1157-1164.

372. Staal FJT, Roederer M, Herzenberg LA et al (1990) Intracellular thiols regulate activation of nuclear factor κB and transcription of human immunodeficiency virus. Proc Natl Acad Sci USA 87(24):9943–9947.

373. Stasakova, J., B. Ferko, C. Kittel, S. Sereinig, J. Romanova, H. Katinger, and A. Egorov. 2005. Influenza A mutant viruses with altered NS1 protein function provoke caspase-1 activation in primary human macrophages, resulting in fast apoptosis and release of high levels of interleukins 1β and 18. J. Gen. Virol. 86:185-195.

374. Steponavičienė A, Burokienė S, Ivaškevičienė I, Stacevičienė I, Vaičiūnienė D, Jankauskienė A. Influenza and respiratory syncytial virus infections in pediatric patients during the COVID-19 pandemic: a single-center experience. *Children (Basel).* 2023; 10 https://doi.org/10.3390/children10010126.

375. Stoppelenburg, A.J.; de Roock, S.; Hennus, M.P.; Bont, L.; Boes, M. Elevated Th17 Response in Infants Undergoing Respiratory Viral Infection. *Am. J. Pathol.* 2014, *184*, 1274–1279.

376. Sugiyama K., Obayashi E., Kawaguchi A., Suzuki Y., Tame J.R., Nagata K., Park S.Y. Structural insight into the essential PB1-PB2 subunit contact of the influenza virus RNA polymerase. *EMBO J.* 2009;28:1803–1811. doi: 10.1038/emboj.2009.138.

377. Sullivan C., Soos B.L., Millard P.J., Kim C.H., King B.L. Modeling Virus-Induced Inflammation in Zebrafish: A Balance Between Infection Control and Excessive Inflammation. *Front. Immunol.* 2021;12:636623. doi: 10.3389/fimmu.2021.636623.

378. Sun L., Wang H., Wang Z., He S., Chen S., Liao D., Wang L., Yan J., Liu W., Lei X., Wang X. Mixed lineage kinase domain-like protein mediates necrosis signaling downstream of RIP3 kinase. *Cell.* 2012;148:213–227.

379. Suratt BT, Petty JM, Young SK, Malcolm KC, Lieber JG, Nick JA, Gonzalo JA, Henson PM, Worthen GS. Role of the CXCR4/SDF-1 chemokine axis in circulating neutrophil homeostasis. Blood. 2004 Jul 15;104(2):565-71. doi: 10.1182/blood-2003-10-3638.

380. Swanson K.V, Deng M, Ting J.P. The NLRP3 inflammasome: molecular activation and regulation to therapeutics. Nat Rev Immunol . 2019;19:477–489.

381. Swearengen J.R. Choosing the right animal model for infectious disease research. *Anim. Model. Exp. Med.* 2018;1:100–108. doi: 10.1002/ame2.12020.

382. Swets MC, Russell CD, Harrison EM, Docherty AB, Lone N, Girvan M, et al. SARS-CoV-2 co-infection with influenza viruses, respiratory syncytial virus, or adenoviruses. *Lancet.* 2022; 399: 1463-1464 https://doi.org/10.1016/S0140-6736(22)00383-X.

383. Swirski, F. K. *et al.* Identification of splenic reservoir monocytes and their deployment to inflammatory sites. *Science* 325, 612–616 (2009).

384. Szabo SJ, Kim ST, Costa GL, Zhang X, Fathman CG, Glimcher LH. A novel transcription factor, T-bet, directs Th1 lineage commitment. *Cell* (2000) 100(6):655–69. 10.1016/S0092-8674(00)80702-3.

385. Tabarani, C.M.; Bonville, C.A.; Suryadevara, M.; Branigan, P.; Wang, D.; Huang, D.; Rosenberg, H.F.; Domachowske, J.B. Novel Inflammatory Markers, Clinical Risk Factors and Virus Type Associated with Severe Respiratory Syncytial Virus Infection. *Pediatr. Infect. Dis. J.* 2013, *32*, e437–e442.

386. Takeuchi O., Akira S. Innate immunity to virus infection. *Immunol. Rev.* 2009;227:75–86.

387. Tang JW, Kennedy M, Lackenby A, Ellis J, Lam T (2019) Transmitted and acquired oseltamivir resistance during the 2018-2019 influenza season. J Inf Secur. 10.1016/j.jinf.2019.10.020.

388. Tassone L, Notarangelo LD, Bonomi V, Savoldi G, Sensi A, Soresina A, et al. Clinical and genetic diagnosis of warts, hypogammaglobulinemia, infections, and myelokathexis syndrome in 10 patients. *Journal of Allergy and Clinical Immunology*. 2009;123:1170–1173.e3.

389. Tate, M.D.; Ong, J.D.H.; Dowling, J.K.; McAuley, J.L.; Robertson, A.B.; Latz, E.; Drummond, G.R.; Cooper, M.A.; Hertzog, P.J.; Mansell, A. Reassessing the Role of the NLRP3 Inflammasome during Pathogenic Influenza A Virus Infection via Temporal Inhibition. *Sci. Rep.* 2016, *6*, 27912.

390. Thomas, P.G.; Dash, P.; Aldridge, J.R.; Ellebedy, A.H.; Reynolds, C.; Funk, A.J.; Martin, W.J.; Lamkanfi, M.; Webby, R.J.; Boyd, K.L.; et al. The Intracellular Sensor NLRP3 Mediates Key Innate and Healing Responses to Influenza A Virus via the Regulation of Caspase-1. *Immunity* 2009, *30*, 566–575.

391. To EE, Luong R, Diao J, O' Leary JJ, Brooks DA, Vlahos R, Selemidis S. Novel endosomal NOX2 oxidase inhibitor ameliorates pandemic influenza A virus-induced lung inflammation in mice. Respirology. 2019 Oct;24(10):1011-1017. doi: 10.1111/resp.13524.

392. Tokars J.I., Olsen S.J., Reed C. Seasonal Incidence of Symptomatic Influenza in the United States. *Clin. Infect. Dis.* 2018;66:1511–1518. doi: 10.1093/cid/cix1060.

393. Tomashefski JF, Farver CF. Anatomy and histology of the lung. In: Tomashefski JF, editor. Dail and Hammar’s Pulmonary Pathology, 3rd ed. New York: Springer; 2008. p. 20–48.

394. Treanor J.J., Talbot H.K., Ohmit S.E., Coleman L.A., Thompson M.G., Cheng P.Y., Petrie J.G., Lofthus G., Meece J.K., Williams J.V., et al. Effectiveness of seasonal influenza vaccines in the United States during a season with circulation of all three vaccine strains. *Clin. Infect. Dis.* 2012;55:951–959. doi: 10.1093/cid/cis574.

395. Triantafilou, K.; Kar, S.; Van Kuppeveld, F.J.M.; Triantafilou, M. Rhinovirus-Induced Calcium Flux Triggers NLRP3 and NLRC5 Activation in Bronchial Cells. *Am. J. Respir. Cell Mol. Biol.* 2013, *49*, 923–934.

396. Tyrkalska, S.D., Candel, S., Pedoto, A., García-Moreno, D., Alcaraz-Pérez, F., Sánchez-Ferrer, Á., Cayuela, M.L. and Mulero, V. (2022). Zebrafish models of COVID-19. *FEMS Microbiology Reviews*, 47(1). doi:https://doi.org/10.1093/femsre/fuac042.

397. Tumpey TM, García-Sastre A, Taubenberger JK, Palese P, Swayne DE, Pantin-Jackwood MJ, Schultz-Cherry S, Solórzano A, Van Rooijen N, Katz JM, Basler CF. Pathogenicity of influenza viruses with genes from the 1918 pandemic virus: functional roles of alveolar macrophages and neutrophils in limiting virus replication and mortality in mice. J Virol. 2005 Dec;79(23):14933-44. doi: 10.1128/JVI.79.23.14933-14944.2005. PMID: 16282492; PMCID: PMC1287592.

398. Ueno T, Hara K, Willis MS, Malin MA, Höpken UE, Gray DHD, Matsushima K, Lipp M, Springer TA, Boyd RL *et al* (2002) Role for CCR7 ligands in the emigration of newly generated T lymphocytes from the neonatal thymus. *Immunity* 16, 205–218.

399. Uršič, T.; Steyer, A.; Kopriva, S.; Kalan, G.; Krivec, U.; Petrovec, M. Human Bocavirus as the Cause of a Life-Threatening Infection. *J. Clin. Microbiol.* 2011, *49*, 1179–1181.

400. Uttara B, Singh AV, Zamboni P, Mahajan RT. Oxidative stress and neurodegenerative diseases. A Review of upstream and downstream antioxidant therapeutic options. *Curr Neuropharmacol.* 2009;7(1):65–74.

401. Valko M, Izakovic M, Mazur M, Rhodes CJ, Telser J. Role of oxygen radicals in DNA damage and cancer incidence. *Mol Cell Biochem.* 2004;266(1–2):37–56.

402. van de Sandt CE, Kreijtz JH, Rimmelzwaan GF. Evasion of influenza A viruses from innate and adaptive immune responses. Viruses. 2012 Sep;4(9):1438-76. doi: 10.3390/v4091438. Epub 2012 Sep 3.

403. Varga Z.T., Ramos I., Hai R., Schmolke M., Garcia-Sastre A., Fernandez-Sesma A., Palese P. The influenza virus protein PB1-F2 inhibits the induction of type I interferon at the level of the MAVS adaptor protein. *PLoS Pathog.* 2011;7:e1002067. doi: 10.1371/journal.ppat.1002067.

404. Vargo J.W., Walker S.N., Gopal S.R., Deshmukh A.R., McDermott B.M., Jr., Alagramam K.N., Stepanyan R. Inhibition of Mitochondrial Division Attenuates Cisplatin-Induced Toxicity in the Neuromast Hair Cells. *Front. Cell Neurosci.* 2017;11:393. doi: 10.3389/fncel.2017.00393.

405. Vishnolia K.K., Hoene C., Tarhbalouti K., Revenstorff J., Aherrahrou Z., Erdmann J. Studies in Zebrafish Demonstrate That CNNM2 and NT5C2 Are Most Likely the Causal Genes at the Blood Pressure-Associated Locus on Human Chromosome 10q24.32. *Front. Cardiovasc. Med.* 2020;7:135. doi: 10.3389/fcvm.2020.00135.

406. Viola A, Munari F, Sánchez-Rodríguez R, Scolaro T, Castegna A. The metabolic signature of macrophage responses. *Front Immunol*. (2019) 10:1462. doi: 10.3389/fimmu.2019.01462.

407. von Hundelshausen P, Agten SM, Eckardt V, Blanchet X, Schmitt MM, Ippel H, Neideck C, Bidzhekov K, Leberzammer J, Wichapong K *et al* (2017) Chemokine interactome mapping enables tailored intervention in acute and chronic inflammation. *Sci Transl Med* 9, eaah6650.

408. Voeten J.T., Bestebroer T.M., Nieuwkoop N.J., Fouchier R.A., Osterhaus A.D., Rimmelzwaan G.F. Antigenic drift in the influenza A virus (H3N2) nucleoprotein and

escape from recognition by cytotoxic T lymphocytes. *J. Virol.* 2000;74:6800–6807. doi: 10.1128/JVI.74.15.6800-6807.2000.

409. Walters KB, Green JM, Surfus JC, Yoo SK, Huttenlocher A. Live imaging of neutrophil motility in a zebrafish model of WHIM syndrome. Blood. 2010 Oct 14;116(15):2803-11. doi: 10.1182/blood-2010-03-276972. Epub 2010 Jun 30.

410. Wang P, Palese P, O'Neill RE. The NPI-1/NPI-3 (karyopherin alpha) binding site on the influenza a virus nucleoprotein NP is a nonconventional nuclear localization signal. *J Virol* (1997) 71:1850–6.

411. Wang R., Zhu Y., Ren C., Yang S., Tian S., Chen H., Jin M., Zhou H. Influenza A virus protein PB1-F2 impairs innate immunity by inducing mitophagy. *Autophagy.* 2021;17:496–511. doi: 10.1080/15548627.2020.1725375.

412. Wang Y., Liu F., Chen L., Fang C., Li S., Yuan S., et al. (2022). Neutrophil extracellular traps (NETs) promote non-small cell lung cancer metastasis by suppressing lncRNA MIR503HG to activate the NF-κB/NLRP3 inflammasome pathway. *Front. Immunol.* 13, 867516. 10.3389/fimmu.2022.867516.

413. Wang Z, Zhu L, Nguyen THO, Wan Y, Sant S, Quiñones-Parra SM, Crawford JC, Eltahla AA, Rizzetto S, Bull RA, Qiu C, Koutsakos M, Clemens EB, Loh L, Chen T, Liu L, Cao P, Ren Y, Kedzierski L, Kotsimbos T, McCaw JM, La Gruta NL, Turner SJ, Cheng AC, Luciani F, Zhang X, Doherty PC, Thomas PG, Xu J, Kedzierska K. Clonally diverse CD38+HLA-DR+CD8+ T cells persist during fatal H7N9 disease. Nat Commun. 2018 Feb 26;9(1):824. doi: 10.1038/s41467-018-03243-7.

414. Watanabe T, Watanabe S, Kawaoka Y. Cellular networks involved in the influenza virus life cycle. Cell Host Microbe. 2010 Jun 25;7(6):427-39. doi: 10.1016/j.chom.2010.05.008. PMID: 20542247; PMCID: PMC3167038.

415. Webster, R.G. *et al.* (eds.) (2013) *Textbook of Influenza*. 2nd edn. Hoboken, NJ: John Wiley & Sons, Ltd.

416. Weis W, Brown JH, Cusack S, Paulson JC, Skehel JJ, Wiley DC. Structure of the influenza virus haemagglutinin complexed with its receptor, sialic acid. Nature (1988) 333:426–31. doi:10.1038/333426a0.

417. Westerfield M. *The Zebrafish Book: A Guide for the Laboratory Use of Zebrafish (Brachydanio Rerio)* M. Westerfield; Eugene, OR, USA: 1993.

418. Wherry E.J., Barouch D.H. T cell immunity to COVID-19 vaccines. *Science.* 2022; 377: 821-822.

419. White R.M., Sessa A., Burke C., Bowman T., LeBlanc J., Ceol C., Bourque C., Dovey M., Goessling W., Burns C.E., et al. Transparent adult zebrafish as a tool for in vivo

transplantation analysis. *Cell Stem Cell.* 2008;2:183–189. doi: 10.1016/j.stem.2007.11.002.

420. Whitmire JK, Tan JT, Whitton JL. Interferon-gamma acts directly on CD8+ T cells to increase their abundance during virus infection. *J Exp Med* (2005) 201(7):1053–9. 10.1084/jem.20041463.

421. WHO (World Health Organization) . 2023. Influenza (seasonal). Available from: https://www.who.int/health-topics/influenza-seasonal.

422. Wise H.M., Foeglein A., Sun J., Dalton R.M., Patel S., Howard W., Anderson E.C., Barclay W.S., Digard P. A complicated message: Identification of a novel PB1-related protein translated from influenza A virus segment 2 mRNA. *J. Virol.* 2009;83:8021–8031. doi: 10.1128/JVI.00826-09.

423. Witte P.U., Irmisch R., Hajdu P., Metzger H. Pharmacokinetics and pharmacodynamics of a novel orally active angiotensin converting enzyme inhibitor (HOE 498) in healthy subjects. *Eur. J. Clin. Pharmacol.* 1984;27:577–581. doi: 10.1007/BF00556895.

424. Wong SS, Webby RJ. Traditional and new influenza vaccines. Clin Microbiol Rev. 2013 Jul;26(3):476-92. doi: 10.1128/CMR.00097-12.

425. Wu W, Luo X, Ren M. Clearance or Hijack: Universal Interplay Mechanisms Between Viruses and Host Autophagy From Plants to Animals. Front Cell Infect Microbiol. 2022 Jan 3;11:786348. doi: 10.3389/fcimb.2021.786348.

426. Xian, H.; Liu, Y.; Rundberg Nilsson, A.; Gatchalian, R.; Crother, T.R.; Tourtellotte, W.G.; Zhang, Y.; Aleman-Muench, G.R.; Lewis, G.; Chen, W.; et al. Metformin Inhibition of Mitochondrial ATP and DNA Synthesis Abrogates NLRP3 Inflammasome Activation and Pulmonary Inflammation. *Immunity* 2021, *54*, 1463–1477.e11.

427. Xie M, Yunis J, Yao Y, Shi J, Yang Y, Zhou P, Liang K, Wan Y, Mehdi A, Chen Z, Wang N, Xu S, Zhou M, Yu M, Wang K, Tao Y, Zhou Y, Li X, Liu X, Yu X, Wei Y, Liu Z, Sprent J, Yu D. High levels of soluble CD25 in COVID-19 severity suggest a divergence between anti-viral and pro-inflammatory T-cell responses. Clin Transl Immunology. 2021 Feb 15;10(2):e1251. doi: 10.1002/cti2.1251.

428. Xie Y, Choi T, Al-Aly Z. Long-term outcomes following hospital admission for COVID-19 versus seasonal influenza: a cohort study. The Lancet Infectious Diseases. Dec. 14, 2023. DOI: https://doi.org/10.1016/S1473-3099(23)00684-9

429. Xu, Z. et al. Pathological findings of COVID-19 associated with acute respiratory distress syndrome. *Lancet Respir. Med.* 8, 420–422 (2020).

430. Yamamoto M, Kensler TW, Motohashi H. The KEAP1-NRF2 system: a thiol-based sensor-effector apparatus for maintaining redox homeostasis. *Physiol Rev*. 2018;98(3):1169-1203.

431. Yan, L.; Zhang, H.T.; Goncalves, J.; Xiao, Y.; Wang, M.; Guo, Y.; Sun, C.; Tang, X.; Jing, L.; Zhang, M.; et al. An Interpretable Mortality Prediction Model for COVID-19 Patients. *Nat. Mach. Intell.* 2020, *2*, 283–288.

432. Yan X, Li K, Lei Z, Luo J, Wang Q, Wei S. Prevalence and associated outcomes of coinfection between SARS-CoV-2 and influenza: a systematic review and meta-analysis. Int J Infect Dis. 2023 Nov;136:29-36. doi: 10.1016/j.ijid.2023.08.021.

433. Yang, M., Ismayil, A., Liu, Y. (2020). Autophagy in Plant-Virus Interactions. *Annu. Rev. Virol.* 7 (1), 403–419. doi: 10.1146/annurev-virology-010220-054709.

434. Yasui K, Baba A, Iwasaki Y, et al. Neutrophil-mediated inflammation in respiratory syncytial viral bronchiolitis. *Pediatr Int*. 2005;47(2):190-195.

435. Yildirim A, Mavi A, Oktay M, Kara AA, Algur OF, Bilaloglu V. Comparison of antioxidant and antimicrobial activities of tilia (*Tilia argentea* Desf ex DC), sage (*Salvia triloba* l.), and black tea (*Camellia sinensis*) extracts. *J Agric Food Chem* 48: 5030–5034, 2000.

436. Yin V.P., Thomson J.M., Thummel R., Hyde D.R., Hammond S.M., Poss K.D. FGF-dependent depletion of microRNA-133 promotes appendage regeneration in zebrafish. *Genes. Dev.* 2008;22:728–733. doi: 10.1101/gad.1641808.

437. Yoo, J.-K.; Kim, T.S.; Hufford, M.M.; Braciale, T.J. Viral Infection of the Lung: Host Response and Sequelae. *J. Allergy Clin. Immunol.* 2013, *132*, 1263–1276.

438. Yordy, B., Tal, M. C., Hayashi, K., Arojo, O., Iwasaki, A. (2013). Autophagy and Selective Deployment of Atg Proteins in Antiviral Defense. *Int. Immunol.* 25 (1), 1–10. doi: 10.1093/intimm/dxs101.

439. York A, Fodor E. Biogenesis, assembly, and export of viral messenger ribonucleoproteins in the influenza A virus infected cell. *RNA Biol* (2013) 10:1274–82. doi:10.4161/rna.25356. (2013a)

440. York A, Hengrung N, Vreede FT, Huiskonen JT, Fodor E. Isolation and characterization of the positive-sense replicative intermediate of a negative-strand RNA virus. *Proc Natl Acad Sci U S A* (2013) 110:E4238–45. doi:10.1073/pnas.1315068110 (2013b).

441. Yoshimura A, Ohnishi S. Uncoating of influenza virus in endosomes. *J Virol* (1984) 51:497–504.

442. Yoshimura T, Matsushima K, Tanaka S, Robinson EA, Appella E, Oppenheim JJ, et al. Purification of a human monocyte-derived neutrophil chemotactic factor that has peptide sequence similarity to other host defense cytokines. *Proc Natl Acad Sci U S A* (1987) 84:9233–7. doi:10.1073/pnas.84.24.9233.

443. Youle R.J., van der Bliek A.M. Mitochondrial fission, fusion, and stress. *Science.* 2012;337:1062–1065. doi: 10.1126/science.1219855.

444. Young I, Woodside J. Antioxidants in health and disease. *J. Clin. Pathol.* 2001;54:176–186.

445. Yu W.C., Chan R.W., Wang J., Travanty E.A., Nicholls J.M., Peiris J.S., Mason R.J., Chan M.C. Viral replication and innate host responses in primary human alveolar epithelial cells and alveolar macrophages infected with influenza H5N1 and H1N1 viruses. *J. Virol.* 2011;85:6844–6855. doi: 10.1128/JVI.02200-10.

446. Yuan J, Amin P, Ofengeim D. Necroptosis and RIPK1-mediated neuroinflammation in CNS diseases. Nat Rev Neurosci. 2019 Jan;20(1):19-33. doi: 10.1038/s41583-018-0093-1.

447. Yunis J, Short KR, Yu D. Severe respiratory viral infections: T-cell functions diverging from immunity to inflammation. Trends Microbiol. 2023 Jun;31(6):644-656. doi: 10.1016/j.tim.2022.12.008.

448. Zang L., Maddison L.A., Chen W. Zebrafish as a Model for Obesity and Diabetes. *Front. Cell Dev. Biol.* 2018;6:91. doi: 10.3389/fcell.2018.00091.

449. Zeng, J.; Xie, X.; Feng, X.L.; Xu, L.; Han, J.B.; Yu, D.; Zou, Q.C.; Liu, Q.; Li, X.; Ma, G.; et al. Specific Inhibition of the NLRP3 Inflammasome Suppresses Immune Overactivation and Alleviates COVID-19 like Pathology in Mice. *EBioMedicine* 2022, *75*, 103803.

450. Zeng L-Y, Yang J, Liu S. 2017. Investigational hemagglutinin-targeted influenza virus inhibitors. *Expert Opin Investig Drugs* 26:63–73. doi: 10.1080/13543784.2017.1269170.

451. Zhang B., Xu S., Liu M., Wei Y., Wang Q., Shen W., Lei C.Q., Zhu Q. The nucleoprotein of influenza A virus inhibits the innate immune response by inducing mitophagy. *Autophagy.* 2023;19:1916–1933. doi: 10.1080/15548627.2022.2162798.

452. Zhao M., Wang L., Li S. Influenza A Virus-Host Protein Interactions Control Viral Pathogenesis. *Int. J. Mol. Sci.* 2017:18. doi: 10.3390/ijms18081673.

453. Zhang, H.; Luo, J.; Alcorn, J.F.; Chen, K.; Fan, S.; Pilewski, J.; Liu, A.; Chen, W.; Kolls, J.K.; Wang, J. AIM2 Inflammasome Is Critical for Influenza-Induced Lung Injury and Mortality. *J. Immunol.* 2017, *198*, 4383–4393.

454. Zhang T, Yin C, Boyd DF, Quarato G, Ingram JP, Shubina M, Ragan KB, Ishizuka T, Crawford JC, Tummers B, Rodriguez DA, Xue J, Peri S, Kaiser WJ, López CB, Xu Y, Upton JW, Thomas PG, Green DR, Balachandran S. Influenza Virus Z-RNAs Induce ZBP1-Mediated Necroptosis. Cell. 2020 Mar 19;180(6):1115-1129.e13. doi: 10.1016/j.cell.2020.02.050.

455. Zhang X, Matsuda M, Yaegashi N, Nabe T, Kitatani K. Regulation of Necroptosis by Phospholipids and Sphingolipids. *Cells*. 2020; 9(3):627. https://doi.org/10.3390/cells9030627

456. Zhou R., Tardivel A., Thorens B., Choi I., Tschopp J. Thioredoxin-interacting protein links oxidative stress to inflammasome activation. *Nat. Immunol.* 2010;11:136–140. doi: 10.1038/ni.1831.

457. Zhou, Z. et al. Overly exuberant innate immune response SARS-CoV-2 infect. *Cell Host Microbe* https://doi.org/10.2139/ssrn.3551623 (2020).

458. Zimmer, C. L. et al. NK cells are activated and primed for skin-homing during acute dengue virus infection in humans. *Nat. Commun.* 10, 3897 (2019).

459. Zimmerman R.K., Nowalk M.P., Chung J., Jackson M.L., Jackson L.A., Petrie J.G., Monto A.S., McLean H.Q., Belongia E.A., Gaglani M., et al. 2014–2015 Influenza Vaccine Effectiveness in the United States by Vaccine Type. *Clin. Infect. Dis.* 2016;63:1564–1573. doi: 10.1093/cid/ciw635.

460. Zuo J, Zhang Z, Luo M, Zhou L, Nice EC, Zhang W, Wang C, Huang C. Redox signaling at the crossroads of human health and disease. MedComm (2020). 2022 Mar 31;3(2):e127. doi: 10.1002/mco2.127.

# APPENDICES

Table 6.1 Whim Genes to Investigate for Chapter 4

| Gene | Description | Log2 Fold Change | P-Value |
|---|---|---|---|
| **timp2b** | TIMP metallopeptidase inhibitor 2b [Source:ZFIN;Acc:ZDB-GENE-040426-2655] | -1.83 | 2.21E-50 |
| **cbx7a** | chromobox homolog 7a [Source:ZFIN;Acc:ZDB-GENE-050417-400] | -1.13 | 2.06E-18 |
| **socs3b** | suppressor of cytokine signaling 3b [Source:ZFIN;Acc:ZDB-GENE-040426-2528] | -1.12 | 2.04E-15 |
| **thbs1a** | thrombospondin 1a [Source:ZFIN;Acc:ZDB-GENE-120402-2] | -0.91 | 5.82E-15 |
| **clu** | clusterin [Source:ZFIN;Acc:ZDB-GENE-040426-1774] | -0.91 | 2.22E-14 |
| **tinagl1** | tubulointerstitial nephritis antigen-like 1 [Source:ZFIN;Acc:ZDB-GENE-060503-240] | -1.51 | 8.74E-14 |
| **mknk2b** | MAPK interacting serine/threonine kinase 2b [Source:ZFIN;Acc:ZDB-GENE-030829-2] | -0.83 | 1.21E-13 |
| **ptmab** | prothymosin alpha b [Source:NCBI gene;Acc:559194] | 0.76 | 3.20E-13 |
| **stm** | starmaker [Source:NCBI gene;Acc:386700] | 0.77 | 1.26E-11 |
| **tubb5** | tubulin, beta 5 [Source:ZFIN;Acc:ZDB-GENE-031110-4] | 0.74 | 2.02E-10 |
| **serpina1** | serpin peptidase inhibitor, clade A (alpha-1 antiproteinase, antitrypsin), member 1 | | |

■ Genes to be investigated with 24 hpi WHIM samples

# Appendix B

Table B.1 Spotless Genes to Investigate for Chapter 5

| **Gene** | **Full Name** |
|---|---|
| hbbe1.1 | hemoglobin beta embryonic 1.1 |
| klf9 | klf transcription factor 9 |
| fkbp5 | fkbp prolyl isomerase 5 |
| socs3b | suppressor of cytokine signaling 3 |
| nr1d1 | nuclear receptor subfamily 1 group d member 1 |

■ Genes to be investigated with 12, 24, and 36 hpi Spotless samples

# BIOGRAPHY

Brandy Soos is an avid science fanatic. Originally starting a degree in chemistry, she was soon bitten by a biology bug and began a new career path. She loves studying new viruses, developing new tools, and problem-solving. When she’s not in the lab, she like to hike, read, build terrariums, woodwork, explore new places, eat delicious food, and photograph things of interest. She was recruited to a lab at the Cleveland Clinic Lerner Research Institute, where she now lives with her husband, two dogs, and many geckos in Cleveland, Ohio. She is a candidate for the Doctor of Philosophy Degree in Biochemistry and Molecular Biology from the University of Maine in August 2024.